

THE UNIVERSITY OF SHEFFIELD

Department of Civil and Structural Engineering

**Dynamic Interaction of Walking Humans with
Pedestrian Structures in Vertical Direction**

Experimentally Based Probabilistic Modelling

Erfan Shahabpoor Ardakani

A thesis submitted for the Degree of Doctor of Philosophy in Engineering

August, 2014

Abstract

There is a lack of credible and usable knowledge, specifically related to human-structure interaction in the vertical direction despite of its importance and potentially huge economic impact. The research presented in this thesis addresses this problem via a systematic combined experimental and analytical study of the effects of people on dynamic properties of vibrating structures they excite by walking.

Series of extensive frequency response function based modal tests were performed on a full-scale test structure with more than one hundred test subjects walking in different loading scenarios. The experimental results were then used to identify the parameters of a single-degree-of-freedom (SDOF) mass-spring-damper (MSD) model of a walking human. Four different approaches, including agent-based modelling, were used to simulate measured scenarios of multi-pedestrian traffic. It was found that normal distributions with $\mu=2.864$ Hz and $\sigma=0.191$ Hz, and $\mu=0.295$ and $\sigma=0.023$ can describe the natural frequency and damping ratio of the SDOF MSD model of a *walking* human, respectively, when total mass of the human body is assumed as the mass of the SDOF system.

A new vibration serviceability assessment method was proposed that takes into account not only the *variability* of the human body MSD parameters and the forcing function but also their *interaction* with the structure. Application of this novel method on two full-scale structures under walking traffic load verified its excellent performance yielding a maximum 10% error in estimating the level of structural response compared to 200-500% error margins when key design guidelines currently used around the world were employed. This method is versatile and, being easy to apply in practice, has the potential to replace the existing methods for simulating single and multi-pedestrian traffic on footbridges and floors.

Acknowledgements

This PhD has been the most challenging and rewarding activity I have done so far in my life. However, all that I have achieved would have not been possible without the support, friendship and love of those close to me and I would like to thank here everyone who has helped me so much.

Firstly, I would like to thank my supervisors, Professor Aleksandar Pavic and Dr Vitomir Racic. Throughout my PhD, Alex has guided, challenged and inspired me to get the most out of my work. He was not only a technical supervisor, but a true mentor, and I spent each moment I had with him learning how to live life of a researcher to the fullest. Vito's kind, to the point and useful support has allowed this work to develop to its current state. Thank you both for believing in me and for your great care, help and support.

I also would like to thank Professor Paul Reynolds as without his help I would not get to where I am now.

Moreover, I would like to thank deeply my loving wife, Legha and my son Hami who deserve every bit of this PhD as much as I do. Without their limitless sacrifice, patience and encouragement, assuring comments, compliments and dedication to create loving family environment, this work would not have been possible. I am incredibly fortunate to have them by my side. I would like to dedicate this work to you and many more who supported me over the years.

Finally, would like to extend my gratefulness to all of my friends and family who have been incredibly kind and supportive throughout these years. My mother, Molouk, and father, Abbas, my sister, Banafsheh, and my brother, Rojhan, baba William, maman Nahid, Kambiz, Shahla whose pure affection always was heart-warming and Aziz and Darya who are fighting for their lives.

Memorandum

The accompanying thesis entitled “Interaction of Walking Human with Structure in Vertical Direction” is submitted for the degree of Doctor of Philosophy in the Faculty of Engineering at the University of Sheffield. The thesis is based entirely on the independent work carried out by the author in the University of Sheffield between November 2010 and August 2014 under the supervision of Professor Aleksandar Pavic and Dr Vitomir Racic. All the work and ideas recorded are original except where acknowledged in the text or by reference. The work contained in the thesis has not previously been submitted for a degree or diploma at this, or any other, University or Examining Body.

Erfan Shahabpoor Ardakani

August 2014

Table of Contents

Abstract	I
Acknowledgements	III
Memorandum	IV
Table of Contents	V
List of Figures	XI
List of Tables	XXII
1 Introduction	1
1.1 The research problem	3
1.2 Research Aim and Objectives	4
1.3 The research approach	4
1.4 Organization of thesis	5
2 Literature Review	8
2.1 Introduction	9
2.2 Effects of humans on modal properties of empty structures	10
2.3 Effects of structure on walking human	16
2.3.1 Lock-in	17
2.3.2 Modal properties of human model	19
2.4 Walking human models	20
2.4.1 Oscillator-based models	20
2.4.2 Inverted-pendulum models	27
2.4.3 Whole body models	31
2.5 Design guidelines/assessment methods	32

2.6	Conclusions	35
3	Evaluation of Existing Design Guidelines	36
3.1	Introduction	37
3.2	Design guidelines	37
3.2.1	Sétra guideline (2006)	37
3.2.2	UK National Annex to Eurocode 1 (2008)	38
3.3	Description of tested footbridges	40
3.3.1	The University of Sheffield post-tensioned slab strip	40
3.3.2	Podgorica footbridge	40
3.4	Methodology	41
3.5	Full scale measurements	42
3.5.1	Modal properties estimation	42
3.5.2	Pedestrian traffic parameters	46
3.5.3	Structural response	46
3.6	Results of design guidelines	49
3.7	Conclusion	53
4	Mass-Spring-Damper Model of Walking Pedestrian	54
4.1	Introduction	55
4.2	SDOF MSD model description	56
4.3	Analysis cases	58
4.4	Model parameters	58
4.4.1	Dynamic parameters of the structure model	58
4.4.2	Dynamic properties of the human model	59
4.5	Parametric studies results	60
4.5.1	Effects of human model natural frequency (Case 1)	60
4.5.2	Effects of human model damping (Case 2)	63

4.6	Conclusions	66
5	Mass-Spring-Damper Model of Walking Crowd	67
5.1	Introduction	68
5.2	SDOF MSD model description	68
5.3	Analysis Specifications	69
5.4	Model parameters	70
5.4.1	Dynamic parameters of structure model	70
5.4.2	Dynamic properties of crowd model	71
5.5	Results of the analysis	72
5.5.1	Parametric analysis	72
5.5.2	Sensitivity analysis	76
5.6	Conclusion	79
6	Effects of Multiple Pedestrian Traffic on Dynamic Properties of Structures	80
6.1	Introduction	81
6.2	Key assumptions	81
6.3	Modal properties of empty test structure	82
6.3.1	Non-linear behaviour of the empty structure	83
6.3.2	Modal testing using narrow band excitation	84
6.4	Tests with standing people	85
6.4.1	Experimental setup	85
6.4.2	Identification process	88
6.5	Tests with walking people	90
6.5.1	Experimental setup	90
6.5.2	Identification process	93
6.6	Comparison of Effects of Standing and Walking People	99

6.7	Analytical verification	102
6.7.1	2DOF crowd-structure model	102
6.7.2	Analysis specifications	104
6.7.3	Simulation results	106
6.8	Conclusion	109
7	Identification of Mass-Spring-Damper Model of Walking Human	111
7.1	Introduction	112
7.2	Experimental campaigns	113
7.2.1	Empty structure	114
7.2.2	Pedestrian data	114
7.2.3	Occupied structure tests	115
7.2.4	Mode shape changes	118
7.3	Identification of walking human model	119
7.3.1	Walking traffic – structure model	119
7.3.2	Identification process	123
7.3.3	Common ranges of human model parameters	131
7.3.4	Expected errors	132
7.4	Conclusions	133
8	Identification of Mass-Spring-Damper Model of Walking Human	135
8.1	Introduction	136
8.2	Agent-based Modelling	136
8.3	Experimental work	138
8.3.1	Empty structure	138
8.3.2	Occupied structure tests	139
8.4	Identification of walking human model	140
8.4.1	Agent-based model of discrete traffic – structure system	140

8.4.2	Identification process	145
8.5	Results	147
8.6	Conclusions	150
9	Assessment of Vibration Serviceability Due to Walking-Induced Vibrations Including Human-Structure Interaction	152
9.1	Introduction	153
9.2	Assessment method description	154
9.2.1	Input parameters	155
9.2.2	Step 1: Human-structure interaction	157
9.2.3	Step 2: Generating modal traffic walking force	161
9.2.4	Step 3: Calculating structural response	166
9.2.5	Step 4: Results interpretation	166
9.3	Challenges addressed	173
9.3.1	Human-structure interaction	173
9.3.2	Versatility	173
9.3.3	Practicality	174
9.3.4	Realistic simulation	174
9.3.5	Refined assessment tool	175
9.4	Sensitivity analysis	175
9.5	Technical recommendations for designers	178
9.5.1	Modelling unsteady traffic volume	178
9.5.2	Non-stabilized response assessment	180
9.6	Conclusions	181
10	Validation of Interaction-based Vibration Serviceability Assessment Method Using Full-scale Structures	183
10.1	Introduction	184
10.2	Empty structures	184

10.2.1	Sheffield footbridge	185
10.2.2	Podgorica footbridge	185
10.3	Monitoring tests	186
10.3.1	Sheffield footbridge tests	186
10.3.2	Podgorica footbridge tests	191
10.4	Vibration serviceability assessment	194
10.4.1	Input parameters	195
10.4.2	Step 1 implementation	196
10.4.3	Step 2 implementation	201
10.4.4	Steps 3 and 4 analysis	203
10.4.5	Comparison with design guidelines	207
10.5	Conclusions	210
11	Conclusions and Recommendations for Future Work	211
11.1	Conclusions	212
11.2	Recommendations for future work	216
	References	217
	Appendix I	234

List of Figures

Figure 2.1. The footbridge in the rapid transit railway terminus in Singapore (after Brownjohn, 2004)	12
Figure 2.2. FRF magnitude and phase graphs of Sheffield University test footbridge under standing/walking groups of people (after Zivanovic, et al., 2009)	13
Figure 2.3. Acceleration response of structure at anti-node of first vertical mode and the corresponding arrival rate of pedestrians. Olga footbridge (after Dong, et al., 2011)	14
Figure 2.4. The test footbridge built by Georgakis and Jorgensen (2013).....	15
Figure 2.5. Amplitude-dependent pedestrian damping coefficient for varying probability fractile (after Georgakis and Jorgensen, 2013)	16
Figure 2.10. Probability of synchronization as a function of the acceleration of the bridge (after Grundmann, et al., 1993).....	17
Figure 2.11. Simulated (orange) and measured modal responses due to free walking at resonance on a) footbridge 1 (slow pacing rate) at first mode natural frequency of 1.52 Hz and b) footbridge 2 (fast pacing rate) at first mode natural frequency of 2.04 Hz (after Zivanovic, et al., 2006)	19
Figure 2.12. Human body model (ISO, 1981)	21
Figure 2.13. Moving MSD model coupled with single harmonic walking force to represent walking human (after Caprani et al., 2011)	23
Figure 2.14. Ratio of interactive/force-only models responses for different human model	

parameters (after Caprani et al., 2011)	23
Figure 2.15. Pedestrian walking with accelerometer attached at waist level representing CoM (after Silva and Pimentel, 2011).....	24
Figure 2.16. Mean power spectra for a density of 0.3 pedestrians/m ² (after Silva, et al., 2013)	26
Figure 2.17. Mean power spectra for a density of 0.7 pedestrians/m ² (after Silva, et al., 2013)	26
Figure 2.18. Mean power spectra for a density of 0.9 pedestrians/m ² (after Silva, et al., 2013)	27
Figure 2.19. Inverted-pendulum walking human model on vertically vibrating structure (after Bocian, et al., 2011).....	28
Figure 2.20. The schematics of Qin, et al. (2013) biomechanical walking model (TD: touch down of leading leg; TO: toe off of the trailing leg)	29
Figure 2.21. The 2D walking human model comprised of 8 bodies / 9 DOFs (after Maca and Valasek, 2011).....	31
Figure 2.22. The 3D walking human model with 13 rigid bodies and 34 DOFs (after Maca and Valasek, 2011).....	31
Figure 2.23. Factors ψ (Setra) and 'k' (UK NA to EC1 and EC5) as a function of natural frequency and forcing harmonic (after Zivanovic, et al., 2010).....	33
Figure 2.25. The crowd model used by UK recommendations for design of permanent grandstands (2008) (after Jones, et al., 2005).....	35

Figure 3.1. Plan of the University of Sheffield footbridge and a typical support detail (after Nyawako and Reynolds, 2000)	40
Figure 3.2. Podgorica footbridge view (left) and General arrangement drawing (right) (after Zivanovic, et al., 2006)	41
Figure 3.3. Test setup photo (left) and Walking pattern of pedestrians (right).....	43
Figure 3.4. Experimentally acquired mode shapes of PT slab.....	44
Figure 3.5. Experimentally acquired FRFs of empty and occupied PT slab.....	45
Figure 3.6. CDFs of measured acceleration response at mid-span for Tests 1 (a), Test 2 (b) and Test 3 (c)	48
Figure 3.7. Comparison of acceleration response estimated by UK NA to EC1 (BSI, 2008) and French guideline (Setra, 2006) and experimental results	52
Figure 4.1: Conceptual 2DOF model of coupled system (stationary human).....	57
Figure 4.2: Physical representation of S-MSD model - a stationary human walking on the structure	57
Figure 4.3. FRF magnitude of coupled system for different natural frequencies of human model a) Empty structure, b) Occupied structure with $f_h > f_s$, c) Occupied structure with $f_h < f_s$	61
Figure 4.4. FRF phase of coupled system for different natural frequencies of human model a) Empty structure, b) Occupied structure with $f_h > f_s$, c) Occupied structure with $f_h < f_s$	62
Figure 4.5. Effects of the natural frequency of the human model on the modal frequency of the occupied structure	62

Figure 4.6. Effects of the natural frequency of the human model on the modal damping ratio of the occupied structure	63
Figure 4.7. Effects of damping of human model on modal damping ratio of occupied structure (Set 1)	64
Figure 4.8. FRF magnitude of occupied structure for different damping values of human model (Set 1) a) Empty structure, b) Occupied structure when $f_h < f_s$	65
Figure 4.9. Effects of damping of human model on modal damping ratio of occupied structure (Set 2)	65
Figure 4.10. FRF magnitude of occupied structure for different damping values of human model (Set 2) a) Empty structure, b) Occupied structure when $f_h > f_s$	66
Figure 5.1. Conceptual 2DOF model of coupled crowd-structure system (stationary walking people)	69
Figure 5.2. Effects of the m_c , k_c and c_c on f_{os} ($f_{si} = 4$ Hz)	73
Figure 5.3. Effects of the m_c , k_c and c_c on ζ_{os} ($f_{si} = 4$ Hz)	73
Figure 5.4. Maximum effects of the m_c , k_c and c_c on f_{os} for $f_{ci} = 3.05$ Hz and f_{si} varying from 2-4 Hz	75
Figure 5.5. Maximum effects of the m_c , k_c and c_c on ζ_{os} for $f_{ci} = 3.05$ Hz and f_{si} varying from 2-4 Hz	75
Figure 5.6. Sensitivity of f_{os} to m_c (red curves), k_c (blue curves) and c_c (green curves). Continues curves. $f_{si} = 2$ Hz, crossed curves: $f_{si} = 3$ Hz and dashed curves: $f_{si} = 4$ Hz.	76

Figure 5.7. Sensitivity of ζ_{os} to m_c (red curves), k_c (blue curves) and c_c (green curves). Continues curves: $f_{si} = 2$ Hz, crossed curves: $f_{si} = 3$ Hz and dashed curves: $f_{si} = 4$ Hz.	77
Figure 5.8. Maximum sensitivity of the f_{os} to m_c , k_c and c_c for $f_{ci} = 3.05$ Hz and f_{si} varying from 2-4 Hz.....	78
Figure 5.9. Maximum sensitivity of the ζ_{os} to m_c , k_c and c_c for $f_{ci} = 3.05$ Hz and f_{si} varying from 2-4 Hz.....	79
Figure 6.1. Nonlinear amplitude-dependent damping and natural frequency of structure (after Zivanovic, et al., (2009)).....	83
Figure 6.2. FRF-based modal test setup for standing still pedestrians tests (Mode 1).....	86
Figure 6.3. Time-domain and frequency-domain representation of excitation (a and b) and structural response (c and d) at mid-span.....	87
Figure 6.4. Over-plotted experimental FRF magnitude and phase diagrams of occupied structure with different number of standing people	88
Figure 6.5. Analytical (dashed red) and Experimental (blue) FRF magnitude and phase graphs for the test with 6 standing people.....	89
Figure 6.6. Change of occupied structure modal properties with different number of standing people at mid-span	89
Figure 6.7. A typical walking path and accelerometer (square) and shaker (triangle) placement layout of walking tests.....	91
Figure 6.8. Experimental FRF magnitude and phase curves of the 1 st and 2 nd vertical modes of the structure with different number of people walking along the structure (Scenario 1) ..	92

Figure 6.9. The point-mobility experimental FRF amplitude and phase curves (blue) and their analytical fit (red) – Mode 1 - 10 pedestrians walking along the structure (Scenario 1).
..... 93

Figure 6.10. The point-mobility FRF magnitude and phase graphs captured for 6 and 10 walking people repeated twice with different participants – Mode 1..... 94

Figure 6.11. Trends of occupied structure modal frequency f_{os} (a), stiffness k_{os} (b), damping ratio ζ_{os} (c) and damping c_{os} (d) against number of walking pedestrians – Mode 1 – (Red: Series A; Blue: Series B; Green: Circular walking around mid-span) 96

Figure 6.12. Trends of change of occupied structure modal frequency f_{os} (a), stiffness k_{os} (b), damping ratio ζ_{os} (c) and damping c_{os} (d) against number of walking pedestrians – Mode 2 – (Red: Series A; Blue: Series B; Green: Circular walking around 1/4-span) 98

Figure 6.13. Change of natural frequency f_{os} and damping ratio ζ_{os} of occupied structure against the location of 6 walking pedestrians on the structure – Mode 1..... 99

Figure 6.14. Over-plotted FRF magnitude and phase curves for groups of 3, 6 and 10 walking/standing people at mid-span – structural mode 1 100

Figure 6.15. Trends of changes in occupied structure modal frequency f_{os} and damping ratio ζ_{os} for varying number of standing and walking people on the structure (Red: Circular walking at mid-span; Green: standing at mid-span)..... 101

Figure 6.16. Conceptual 2DOF model of coupled crowd-structure system (crowd model parameters are shown generally by m_c , k_c and c_c 103

Figure 6.17. Trends of walking crowd SDOF model natural frequency f_{cw} , stiffness k_{cw} , damping ratio ζ_{cw} and damping c_{cw} against number of walking pedestrians (Red: S1-Series A; Blue: S1-Series B; Green: S2)..... 107

Figure 6.18. Comparison of changes in natural frequency f_c (a) and damping ratio ζ_c (b) of walking (green) and standing (Blue) crowd models against the number of pedestrians.....	109
Figure 7.1. Prediction of people location between each two consecutive crossing of laser pedestrian counter	114
Figure 7.2. A typical time-history of location of three pedestrians on the structure presented with three different colors	115
Figure 7.3. A typical walking path of designed loading scenarios	116
Figure 7.4. First mode shape of empty (blue trace) and occupied (red trace) Sheffield footbridge	118
Figure 7.5. A conceptual illustration of stationary walking people	120
Figure 7.6. MDOF Mass-spring-damper model of stationary walking traffic-structure system	121
Figure 7.7. A typical over plot of occupied structure FRF graphs resulted from accepted human model parameters (Grey curves) – Test No 1.1C – (3 pedestrians walking at mid-span – Empty structure: green; Experimental: Blue; Best analytical match: Red)	125
Figure 7.8. The illustration of pre-defined location patterns for the group of 4 pedestrians	127
Figure 7.9. A typical over plot of occupied structure FRF graphs for different location patterns and the average FRF– Test No. 1.2 – (Empty structure: Green; Curves corresponding to different patterns: Grey; Average analytical: Red; Experimental: Blue) .	128
Figure 7.10. A typical over plot of average occupied structure FRF graphs resulted from accepted human model parameters (Grey curves) – Test No 1.2– (Empty structure: Green;	

Average analytical: Red; Experimental: Blue).....	129
Figure 7.11. A typical time-history of f_{os} and ζ_{os} (blue), average value(red) and experimental value (cyan) resulted from a typical accepted human model parameter set – Test No 1.2 – (3 pedestrians).....	131
Figure 7.12. A typical over plot of empty (green), test-verified occupied structure FRF graphs (grey), analytical average FRF (red) and experimental FRF (blue) resulted from test-verified human model parameters – Test No 1.2 – (3 pedestrians).....	131
Figure 7.13. Test-verified ranges of f_h and ζ_h found in different tests and their common ranges	132
Figure 7.14. Expected errors in occupied structure natural frequency f_{os} , damping ratio ζ_{os} and peak FRF magnitude a_{FRF} for the common ranges of human model parameters –Mode 1	133
Figure 8.1. A typical walking path	139
Figure 8.2. The interaction force composed of modal walking force on stiff surface and human model response to structural vibrations	142
Figure 8.3. Mechanical model of walking people-structure system simulated by ABM	143
Figure 8.4. Taking into account the modal effects of each pedestrian based on their location on structure	144
Figure 8.5. A typical over plot of empty (green), experimental (red) and acceptable analytical occupied structure FRFs (grey) magnitude and phase – Test No. 1.5 – (6 pedestrians)	146
Figure 8.6. Test-verified ranges of f_h and ζ_h found in different tests and their common ranges	148

Figure 8.7. Expected errors in occupied structure natural frequency f_{os} , damping ratio ζ_{os} and peak FRF magnitude a_{FRF} for the common ranges of human model parameters –Mode 1 ..	149
Figure 8.8. Probability density function of human SDOF model natural frequency (a) and damping ratio (b).....	150
Figure 9.1. Input parameters of proposed assessment method.....	156
Figure 9.3. A conceptual illustration of ‘stationary’ walking people. Φ_{ab} represents ordinate of mode ‘a’ at the location of human ‘b’	158
Figure 9.4. Interaction-based VSA method step 1 procedure	159
Figure 9.5. Mass-spring-damper model of stationary walking traffic-structure system	160
Figure 9.6. A typical fluctuation of average occupied structure natural frequency f_{os} and damping ratio ζ_{os}	161
Figure 9.7. Interaction-based VSA method Step 2 procedure	162
Figure 9.8. A typical mode 1 modal walking force of an individual – Walking force (grey), modal walking force (blue) and mode shape (red).....	164
Figure 9.9. Superposition of modal walking of three pedestrians (a, b and c) to generate modal force of walking traffic (d) – walking force (grey), modal walking force (blue) and mode shape (red).....	165
Figure 9.10. Time-history of each pedestrian’s experience as they walk along the structure	168
Figure 9.11. Comparison of Time and Traffic domain CDFs.....	170

Figure 9.12. Typical fluctuation of acceleration response with 95%, 85%, 75% and 50% probability of non-exceedance (from top to bottom).....	172
Figure 9.13. Sensitivity of the interaction-based VSA method outputs f_{os} , ζ_{os} , $a_{95\%}$ and a_{rms} to input parameters (x/x_{base}): mean f_h (blue), m_h (red), ζ_h (pink), arrival rate r_a (green) and walking speed v_w (black).....	177
Figure 9.14. Possible methods to simulate time-varying traffic volumes	179
Figure 9.15. A typical over-plot of CDFs with t_s duration and their stabilized (blue) and envelope (dashed red) CDF curves.....	181
Figure 10.1. Mode shape of the first vertical mode of the Podgorica footbridge.....	186
Figure 10.2. A typical walking path	187
Figure 10.3. Prediction of people location between each two of the consecutive crossings of the PeCo laser pedestrian counter (arrow pointing to it).....	187
Figure 10.4. A typical statistical presentation of the traffic data - Sheffield footbridge Test 2	189
Figure 10.5. Statistical representation of Sheffield footbridge response - Tests 1 – 3	191
Figure 10.6. Statistical representation of Podgorica footbridge response - Tests 4 – 6	194
Figure 10.7. PDF of human SDOF model natural frequency f_h (a) and damping ratio ζ_h (b)	196
Figure 10.8. A conceptual illustration of stationary walking people. Φ_{ab} represents ordinate of mode ‘a’ at the location of human ‘b’	197
Figure 10.9. Mass-spring-damper model of stationary walking traffic-structure system.....	197

Figure 10.10. Fluctuation and stabilization of average occupied structure natural frequency f_{os} and damping ratio ζ_{os} – Test 5	198
Figure 10.11. FRF plots of Sheffield footbridge tests - Empty structure (green), occupied structure experimental (blue) and occupied structure analytical (red).....	200
Figure 10.12. FRF graphs of Podgorica footbridge tests - Empty structure (green) and occupied structure analytical (red).....	201
Figure 10.13. A typical mode 1 modal walking force.....	202
Figure 10.14. A typical total modal walking force (a) and its frequency domain content (Fourier transform)(b).....	203
Figure 10.15. Comparison of experimental and analytical CDFs. Experimental (blue), envelope of analytical CDFs (dashed red), stabilized analytical CDF (red) and stabilized CDF of non-interactive model (green).....	205
Figure 10.16. Typical fluctuation of acceleration response with 95%, 85%, 75% and 50% probability of non-exceedance (in order from top to bottom).....	207
Figure 10.17. Comparison of performance of the interaction-based VSA method with non-interactive, ISO, UK National Annex, Setra and Butz assessment methods	209

List of Tables

Table 3.1. Estimated modal properties of PT slab (empty structure) using both analytical and experimental methods.....	44
Table 3.2. Estimated modal properties of PT slab (occupied structure) using FRF-based methods	44
Table 3.3. Estimated modal properties of Podgorica footbridge using both analytical and experimental methods (after Zivanovic, et al., 2006).....	46
Table 3.4. Input parameters used in selected guidelines methods.....	50
Table 3.5. Estimated response of structure by design guidelines for Tests 1, 2 and 3	51
Table 4.1: Dynamic parameters of human and structure models used in different analysis cases	59
Table 5.1. Parameters of human and structure models used in different analysis cases	71
Table 6.1. Results of modal analysis of the empty structure.....	84
Table 6.2. Occupied structure modal properties with different number of standing people ..	89
Table 6.3. Identified modal properties of the first mode of the occupied structure for different number of pedestrians and walking Scenarios	95
Table 6.4. Identified modal properties of the second mode of the occupied structure for different number of pedestrians and walking Scenarios.....	97
Table 6.5. Walking crowd model properties obtained from simulation of 2DOF crowd-structure model	106

Table 6.6. Standing-still crowd model properties obtained from simulation of 2DOF crowd-structure model – standing at mid-span	106
Table 7.1. Modal properties of the occupied structure for different group sizes – walking around the tight circle tests	117
Table 7.2. Modal properties of the occupied structure for different group sizes – ‘walking along the structure’ tests	117
Table 7.3. Test-verified ranges of SDOF human model parameters – Scenario 1	125
Table 7.4. Test-verified ranges of SDOF human model parameters.....	129
Table 7.5. Test-verified ranges of SDOF human model parameters.....	130
Table 8.1. Modal properties of the occupied structure for different group sizes	140
Table 8.2. Test-verified ranges of SDOF human model parameters.....	147
Table 9.1. Base value of sensitivity analysis parameters	176
Table 10.1. Results of modal analysis of the empty structure	185
Table 10.2. Traffic statistics of Sheffield University footbridge tests	188
Table 10.3. Statistics of Sheffield University footbridge acceleration response	191
Table 10.4. Traffic statistics of Podgorica footbridge tests	192
Table 10.5. Statistics of Podgorica footbridge acceleration responses	194
Table 10.6. Input parameters of 6 tests used in the interaction-based VSA method	195
Table 10.7. Modal properties of occupied structure	198

Table 10.8. Statistical features of the ‘interactive’ and ‘non-interactive’ responses.....204

Chapter 1

Introduction

Vibration serviceability of structures under human activities has been the concern of engineers since the 19th century (Tredgold, 1828; Figueiredo, et al., 2008). Recent advances in structural materials and design trends towards more slender elements and longer spans have made structures more susceptible to vibration serviceability problems (Zivanovic, et al., 2005; Racic, et al., 2009, Ingólfsson, et al., 2012; Caprani, 2014). Investigation of several incidences of such problems in the last three decades (Pimentel, et al., 2001), both in the vertical and horizontal directions, have highlighted lack of ability of the current calculation models to predict accurately enough the structural vibration response due to walking. This lack of performance of the calculation models is mainly attributed to ignoring the natural inter- and intra- subject variability of people and their interaction with vibrating structure (Brownjohn, et al., 2004; Kasperski and Sahnaci, 2007; Zivanovic, et al., 2010; Shahabpoor and Pavic, 2012).

A significant move towards more realistic estimation of the structural response was made only recently by taking into account inter- and intra- subject variability of the walking people in the form of statistical models (Brownjohn, et al., 2004a; Racic and Brownjohn, 2011; Zivanovic, et al., 2007; Zivanovic and Pavic, 2009; Piccardo and Tubino, 2012; Krenk, 2012; Caprani, 2014). This has increased considerably the fidelity of the walking force models, but they are still unable to approximate reliably the structural response (Zivanovic, et al., 2010; Shahabpoor and Pavic, 2012). Although initially denied by Ellis and Ji (1997), researches subsequently showed that one of the main reasons for this has been ignoring the interaction of vibrating structure and walking people (Zivanovic, et al., 2009). The Millennium bridge excessive vibration in 2000 caused a wave of research on the interaction of people with pedestrian structures in the horizontal lateral direction (Fitzpatrick, et al., 2001). But, the interaction of walking people with pedestrian structures in the vertical direction, despite its much higher likelihood and potentially huge effects on the structural response, has almost not been explored to date.

1.1 The research problem

A literature review carried out identified key gaps in the knowledge and research challenges related to the interaction of walking humans with a structure in the vertical direction as follows:

- I. Scarcity of credible, sufficiently accurate and large experimental data on human-structure interaction (HSI). It includes lack of experimentally verified data on the effects of walking pedestrians on the dynamic properties (mass, stiffness and damping) of the supporting structure, as well as the effects of structural vibrations on the human body and its walking pattern.
- II. Unknown mechanisms of HSI. Different hypotheses exist about the nature of this interaction, vast majority supported only by theoretical modelling due to lack of sufficient and reliable experimental evidence.
- III. Lack of verified *walking human model* which takes into account HSI. Different types of models were proposed over the years to be used for simulating effects of walking humans on the vibrating structures they occupy, but they often lack experimental verification, have limited application and produce inconsistent and unreliable results. The type and parameters of these models were often adapted from biomechanics literature and were not validated for a rather specific application to vibration serviceability of civil engineering structures under walking excitation.
- IV. Despite its apparent significance, no design guidelines to date have taken into account the interaction of walking people with structures in the vertical direction. This is again mainly due to the lack of knowledge about the mechanisms of these interactions and the complexity of its modelling.

1.2 Research Aim and Objectives

The aim of this research is to develop a methodology to simulate dynamic interaction of single/multi- pedestrian walking traffic with supporting structures in an accurate yet practical way.

The key objectives of the research are:

1. Performing the most extensive and detailed set of experiments to date to capture parameters of walking traffic and vibrating structure as they interact in vertical direction.
2. Finding an appropriate mechanical model to simulate dynamics of walking human body in the vertical direction and to identify its parameters for vibration serviceability of civil structures application using the captured experimental data.
3. Developing a vibration serviceability assessment method that takes into account the inter- and intra- subject variability of walking human parameters and their individualized interaction with supporting structures in the vertical direction.

1.3 The research approach

This research is underpinned by probably the most comprehensive set of purposefully designed experiments carried out to date. There were two campaigns with over a hundred test participants to capture the effects of walking pedestrians on dynamic properties of the structure they occupy. Several different technologies, such as 3D wireless accelerometers, motion capturing system, laser pedestrian counting and video image processing were used simultaneously to collect data sets of sufficient detail and quality related to both pedestrian and structure behaviour. On top of this, a database of 1200 ground reaction forces (GRFs) due to walking measured on a treadmill was also utilised. To the best knowledge of the

author, this is the most complete information of this kind ever collected for the purpose of vibration serviceability research, all put to use in this doctoral research.

An SDOF MSD model was initially selected to simulate effects of a walking human on a structure. Performance of this model was first analysed by performing a set of parametric studies and sensitivity analysis and by comparing the results with experimental data to check the model's applicability. The collected experimental data were then used to identify the parameters of the SDOF MSD walking human model. Four different methods were used for identification and results were cross-checked and validated.

Finally, a novel, as realistic as possible, versatile and practically applicable vibration serviceability assessment method was developed. The method takes into account both *variability* of the human body and the forcing function as well as their *interaction* with the structure when calculating vibration response of structures under multi-pedestrian walking loading. The performance of the model was checked by applying it on two full-scale structures and the results were compared with responses estimated using a number of currently available design guidelines.

1.4 Organization of thesis

The thesis is organized in 11 chapters.

Chapter 2 presents a comprehensive literature review of the research on the interaction of walking people with structures in the vertical direction. It highlights gaps in knowledge and the key areas that need to be further investigated.

Chapter 3 analyses the performance of two of the current widely used design guidelines, UK National Annex (NA) to Eurocode 1 (2008) and French Sétra guideline (2006), in estimating structural response level under walking load. The potential sources of discrepancy in the

results of these two guidelines were discussed when compared with the experimental data (such as ignoring HSI effects, invalid ‘perfect periodicity’ assumption, limited applicability and unrealistic ‘people correlation’).

In Chapter 4 a classic SDOF MSD model was used to simulate the effects of a walking pedestrian on dynamic properties of a structure. A series of parametric studies were carried out to analyse the effects of the choice of the model’s parameters on the occupied structure response.

Chapter 5 extends the studies performed in Chapter 4 by investigating the sensitivity of the occupied structure natural frequency and damping ratio to properties of the SDOF MSD walking crowd model.

Chapter 6 describes the details of the two experimental campaigns performed to quantify the effects of different walking traffic sizes on modal properties of the supporting structure. The experimental results presented in this chapter provide concrete evidence and offer some clues on how the presence, number and location of the walking people change dynamic properties of a pedestrian structure in the vertical direction.

A selection of the experiments described in this chapter (not all of them) are used in each of Chapters 7 -10 for analysis. In each chapter, the selected tests are presented in a specific order to best suit the analysis presented in that chapter. The complete list of all the experiments and their reference number in each chapter are presented in Appendix I. The reader is encouraged to refer to the Appendix I to check the relation between tests presented in Chapters 6-10.

In Chapter 7, the occupied structure modal properties found in experiments are used in three different identification procedures where ‘reverse engineering’ is employed to find parameters of the walking individual’s SDOF MSD model. A discrete MDOF model of

human – structure system is then used to simulate independent interaction of each walking person with the structure.

Chapter 8, similar to Chapter 7, uses the occupied structure modal properties found in experiments to find parameters of walking individual's SDOF MSD model. However, it uses an agent-based model (ABM) to simulate discrete traffic structure interactions. Findings of Chapters 7 and 8 are compared and combined at the end and a set of statistical distributions are suggested for the natural frequency and damping ratio of SDOF MSD individual walking human model.

A novel serviceability assessment method for structures under multi-pedestrian walking traffic in the vertical direction is proposed in Chapter 9. It takes into account both variability of pedestrians and their individualized interaction with the structure. Extensive analysis was performed to examine the sensitivity of the proposed method to various modelling assumptions. The proposed method is validated in Chapter 10 by using it to predict response of the structure in six different vibration monitoring tests performed on two full-scale footbridges under different walking traffic. Key findings of this research are summarized in Chapter 11 where recommendations for future work are also presented.

Finally, as to the organisation and structure of this thesis, it should be mentioned here that the findings of this research were initially written in the form of conference and journal papers. This thesis is presented as a coherent and logically structured and sequenced set of those papers with standard introduction and conclusion sections. Therefore, because of this form of presentation some levels of repetition throughout the thesis is unavoidable. Each chapter was adapted from an already written paper and its contents were presented with the same organization as the source paper.

Chapter 2

Literature Review

The contents of this chapter are adapted with minor changes from the following journal paper in preparation to be submitted to the Journal of Sound and Vibration:

Shahabpoor, E., Pavić, A. & Racić, V. Interaction of Walking Humans with Structures in Vertical Direction: A Literature Review. Journal of Sound and Vibration.

2.1 Introduction

Interaction of a human body with a vibrating structure happens through several distinct mechanisms and in different directions (vertical, lateral and longitudinal horizontal). The interaction is dependent on the human body posture and the type of activity (standing, walking, jumping, running, etc.) (Zivanovic, et al., 2005). This literature review focuses on the interaction of the walking people with the vibrating structures they occupy in the *vertical* direction.

Based on the classification proposed by Sachse (2003) and assuming human body to be acting as a mechanical mass-spring-damper (MSD) system, human-structure interaction mechanisms can be divided into two categories. The first category comprises the effects of the structural vibrations on the forces induced by human occupants. For walking people, this includes effects of the structural vibration on the walking parameters, such as the pacing frequency and phase, stride length and walking speed.

The second category encompasses the effects which the human occupants have on the vibrating structure dynamic parameters: mass, stiffness and damping. Hence, the mass of the human body accelerates when exposed to structural vibration and applies interaction force on the structure through the contact of the human body and the structure, for example feet in the case of walking (Griffin, 1990). This way human – structure system acts more like a multiple degrees of freedom (MDOF) system in which human DOFs affect dynamics of the structure DOFs and vice versa. The effects of this phenomenon on the dynamics of structure manifest themselves as changes in the modal frequency (i.e. mass and/or stiffness) as well as damping of the empty (unoccupied) structure.

It must be mentioned that effects of the walking people on each other is not considered as HSI in this study although it may affect the walking pattern of people. Therefore, the cases

where synchronization of people is improved within a spatially restricted crowd or by a prompt (Ebrahimpour and Sack, 1992; Kasperski and Niemann, 1993) that can be provided by music or movements of other people (Fujino et al., 1993; van Staalduinen and Courage, 1994) or visual and audio contact between people (Haman, 1994; Ebrahimpour and Fitts; 1996; Sachse, 2003) are not considered here.

This chapter reviews key research specifically related to the HSI in vertical direction and highlights the key areas that need to be further investigated. Section 2.2 reviews the analytical and experimental evidence in the literature on the effects of walking humans on modal properties of the structure they occupy. Section 2.3 discusses the effects of the structural vibrations on human walking parameters such as the ‘lock-in’ effect. The suggested walking human models in the literature and their parameters are discussed in Section 2.4. The approach of the current design guidelines to take into account HSI is discussed in Section 2.5 and conclusions are presented in Section 2.6.

2.2 Effects of humans on modal properties of empty structures

The key mechanism of the HSI in the vertical direction is provided by a human body acting as a (bio)dynamic system. Such system has the potential to change the dynamics of the structure over which it moves. Several pieces of research exist on increase of damping and change of the natural frequency of unoccupied structures when occupied by standing, sitting or jumping people (Ellis and Ji, 1994; Sachse, et al., 2002; 2003; Willford, 2002; Brownjohn, et al., 2004a; Brownjohn, et al., 2004b; Brownjohn and Fu, 2005; Butz, et al., 2008; Reynolds, et al., 2004; Salyards and Firman, 2011; Harrison, et al., 2008; Dong, et al., 2011). However, research into similar changes of dynamic properties of structures specifically due to walking people in the vertical direction is rare (Barker and Mackenzie, 2008; Zivanovic, et al., 2009).

The first generation of models used to simulate the effects of human occupants on modal properties of the structure by simply adding more mass to an empty structure (Walley, 1959; Allen and Rainer, 1975; Ohlsson, 1982; Ebrahimpour et al., 1989). This normally resulted in decrease of the modal frequency of the structure. However, the procedure was unable to describe the occasional increase in the modal frequency and additional damping observed in occupied structures (Zivanovic, et al., 2009).

Ohlsson (1982) reported that the spectrum of a force measured on a rigid surface was different from that measured on a flexible timber floor. It showed a drop around the natural frequency of the structure where the response was prominent. He also observed that moving pedestrian increased both the mass and the damping of the structure. Baumann and Bachmann (1988) similarly reported dynamic load factors (DLFs) of walking up to 10% lower if measured on a flexible 19 m long pre-stressed beam. These observations were confirmed by Pimentel (1997) where he reported lower DLFs on moving footbridges in comparison with those measured on rigid surfaces. He also reported reduction in the natural frequency of a test footbridge under walking human load.

Ebrahimpour, et al. (1989), based on measurements performed on a purposefully built instrumented platform suggested that damping and mass of the platform were dependent on the number of walking people on the platform. Ebrahimpour and Sack (1996), in a different set of experiments on the same test structure, found that walking DLFs generally decreased as the number of simultaneously walking people increased. Investigations of Bishop et al. (1993) and Pimentel and Waldron (1996) also showed that moving human occupants add damping to structures they occupy. Similar trend was observed for standing people shortly afterwards by Ellis and Ji (1997) and Sachse, et al. (2002). However, contrary to all previous observations, Ellis and Ji (1997) claimed that moving people are a dynamic load only because neither a jumping occupant nor an occupant walking on the spot changed the

estimated natural frequency of the beam.

In 2002, Willford performed an extensive set of experiments on the Millennium Bridge and reported increase in the damping of the footbridge under walking load in the vertical direction. Later in 2004, Brownjohn reported results of a combination of forced vibration testing and human forcing on a 1,300-tonne footbridge in Singapore. The footbridge (Figure 2.1) was a steel skeleton clad with glass, spanning 140m between pin supports at platform level of a rapid transit railway terminus. During some of the tests, 150 pedestrians were walking on the footbridge for several minutes. Results of the analysis showed an increase of the vertical mode damping to somewhere between empty and full of stationary pedestrians cases.



Figure 2.1. The footbridge in the rapid transit railway terminus in Singapore (after Brownjohn, 2004)

Studies of Brownjohn, et al. (2005) on a 46 m long steel pedestrian bridge linking Teaching Block and Engineering Block in Singapore Polytechnic showed that the changes in the

modal properties of the structure with moving pedestrians were small compared to those with stationary pedestrians. They suggest that within limits, modal properties of the empty structure could be used in analysis.

Zivanovic, et al. (2009) did a systematic set of experiments on a full-scale pedestrian structure to quantify the effects of walking and standing people on modal properties of the structure. Groups of 2, 4, 6 and 10 people were asked to stand-still or walk along the Sheffield University post-tensioned simply-supported slab footbridge. For each loading scenario, an FRF-based modal test was done using an APS electro-dynamic shaker connected directly to the mid-span of the structure to excite the first mode.

Experimentally measured FRFs of the occupied structure under different loading scenarios (Figure 2.2) were curve-fitted to find modal properties of the occupied structure. It was found that the presence of humans on the structure, either in passive or active form, increased the damping of the structure. They also found that presence of standing people increase the natural frequency of the structure while the same people walking decrease it.

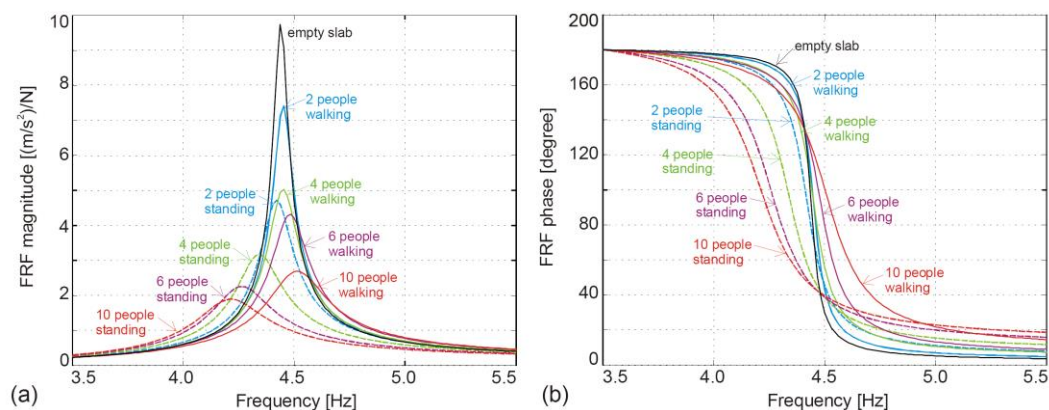


Figure 2.2. FRF magnitude and phase graphs of Sheffield University test footbridge under standing/walking groups of people (after Zivanovic, et al., 2009)

Zivanovic, et al. (2010) conducted an extensive set of monitoring tests on Podgorica

footbridge in Montenegro under normal daily walking pedestrian load. Their study showed a three-fold increase of effective damping of the first vertical mode of structure from 0.26% to 0.67% under walking traffic load. Similarly, the experimental and analytical studies of Fanning, et al. (2010) on vibration serviceability of Sean O’Casey Bridge in Dublin showed that the actual acceleration response of the structure was 20% less than the analytically estimated value. They concluded that this is due to the added damping of the walking people on structure.

Dong, et al. (2011) did a series of tests on the Olga footbridge at Oberhausen, Germany under a stream of walking pedestrians. Bridge had the total length of 66 m with two spans of 18m and 45m. First vertical mode with natural frequency of 1.8 Hz and damping ratio of 0.5% (empty structure) was found to be most sensitive to the walking pedestrian effects. The acceleration response of the structure at the anti-node of this mode (close to mid-span of the longer span) and the corresponding arrival rate of pedestrians are shown in Figure 2.3. It was found that during the largest arrival rate period, the natural frequency reduced to 1.72 Hz and damping ratio increased to 1.9%.

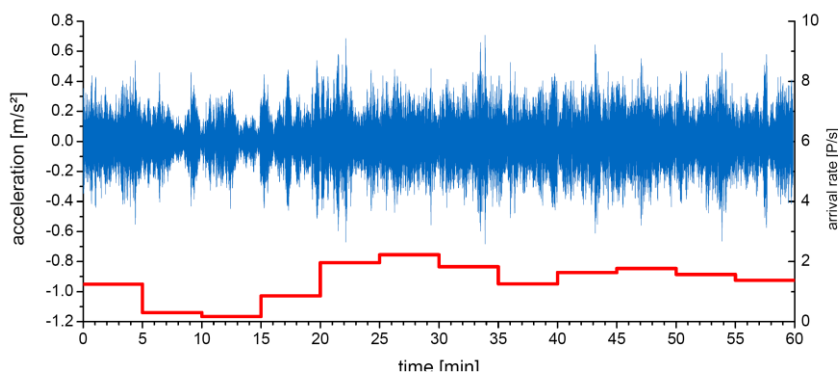


Figure 2.3. Acceleration response of structure at anti-node of first vertical mode and the corresponding arrival rate of pedestrians. Olga footbridge (after Dong, et al., 2011)

Georgakis and Jorgensen (2013) did a series of forced vibration tests on a test footbridge to quantify the effects of walking pedestrians on the mass and damping of structure. The footbridge (Figure 2.4) had a simply-supported 16m long steel double U-beam structure and

was located in the Department of Civil Engineering at Technical University of Denmark. The structure had a mass of 5,224 kg, natural frequency of 2.23Hz and amplitude dependent damping of 0.25-0.58%. Each test lasted 3 minutes and 4, 7 and 10 pedestrians representing 0.35, 0.62 and 0.88 peds/s flow rates participated in each test, respectively.



Figure 2.4. The test footbridge built by Georgakis and Jorgensen (2013)

Results of their analysis showed that the full mass of human body (and not a percentage of it) can be used in simulation to model each single pedestrian. They found that Weibull distribution can describe the probability distribution of the observed added damping values for each pedestrian. An exponential fit was then made to the data to find amplitude-dependent and flow-independent pedestrian damping coefficients, c_p , for varying probability (fractile) levels (Figure 2.5). They finally suggest that for design purposes, a pedestrian may

be treated as a moving point viscous damper with $c_p=500\text{kg/s}$ for moderate vertical vibrations of up to 5mm amplitude.

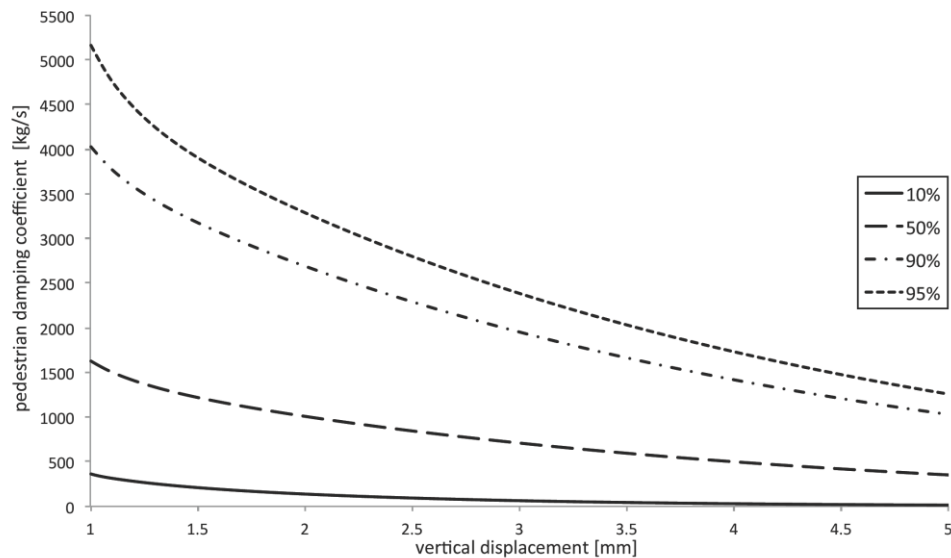


Figure 2.5. Amplitude-dependent pedestrian damping coefficient for varying probability fractile (after Georgakis and Jorgensen, 2013)

2.3 Effects of structure on walking human

Term ‘*Synchronization*’ in the context of pedestrian dynamic walking loads is normally taken to mean the tendency of pedestrians to walk with a same pacing frequency and is more the matter of human-human interaction. ‘*Lock-in*’, on the other hand, describes the tendency of pedestrians to synchronize their pacing rate with structural vibrations. In some cases, lock-in may trigger the synchronization (McRobie et al., 2003). Only the lock-in term is discussed in this study as a mechanism of human-structure interaction.

2.3.1 Lock-in

Bachmann and Ammann (1987) argued that vertical vibrations with amplitude higher than 10-20 mm can force walking pedestrians to adjust their pacing rate with the motion of the vibrating structure. Grundmann, et al. (1993) suggested a method to take into account the probability of synchronization of people with vertical vibration of a structure. They defined the probability of synchronization $P_s(a_g)$ as a function of the acceleration amplitude of the structure a_g (Figure 2.6). They proposed that the response to N walking people on a structure can be calculated from the following equation:

$$a_g = P_s(a_g) N_r a_{1rz} \quad (\text{Equation 2.1})$$

Where a_{1rz} is the response to a single pedestrian and $N_r = NK$ is the number of people reduced by factor $K < 1$ which takes into account that the location of the load moves along the structure.

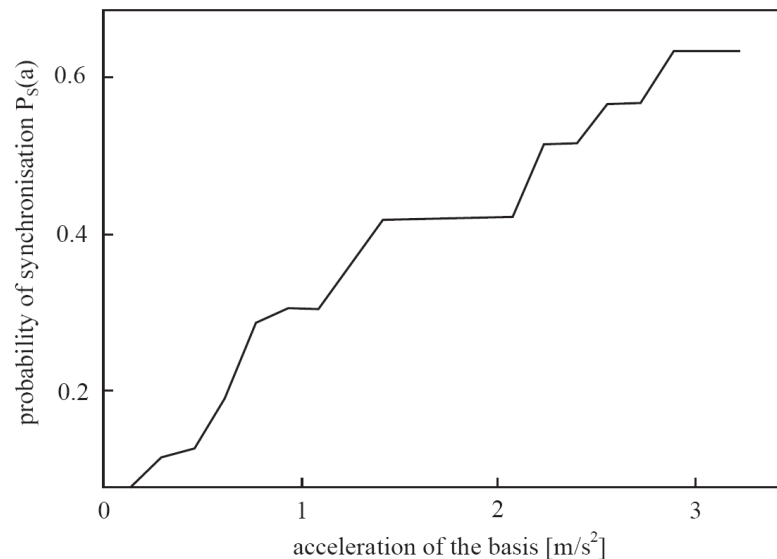


Figure 2.6. Probability of synchronization as a function of the acceleration of the bridge (after Grundmann, et al., 1993).

However, investigations on the Paris Solferino bridge (Setra, 2006) suggested that lock-in in the vertical direction is unlikely to happen as pedestrians would be disturbed by the excessive vibration and will not be able to maintain the pacing rate at resonant frequency. Findings of Zivanovic, et al. (2005) in single pedestrian testing on three footbridges support this claim. They analyzed the interaction of footbridge structures and a single pedestrian walking at or near resonant frequency. Test subjects were asked to walk on three real-world footbridges once with the aid of a metronome tuned to the natural frequency of structure and once without the metronome. A methodology was developed for systematic comparison of the measured and simulated structural response with a purpose of identifying vibration levels which disturb normal walking. It was argued that in the presence of strong vibration, a pedestrian cannot keep a steady step and this reduces the chance of a resonant build-up.

Figure 2.7 shows the simulated (orange) and measured modal responses from free walking at resonance on two footbridges. In both cases the test subject was asked to walk with resonance frequency without the aid of a metronome. It was found that at $t=35s$ and $26s$ from the beginning of tests, test subjects started losing their pacing rate. The perceived vibration level by test subjects at these points were found equal to 0.33 m/s^2 and 0.37 m/s^2 , respectively, based on their location at that time on structure. They suggested that 0.33 m/s^2 and 0.37 m/s^2 are the maximum acceleration magnitude that a pedestrian can endure without disturbing their established walking pattern. Zivanovic, et al. (2005) further argued that the observed reduction in the response of the structure can be simulated either as a disturbance in normal walking or increase of the damping of the structure. They found that for the case of increased damping method, the occupied structure damping ratio was up to 10 times higher than that of the empty structure.

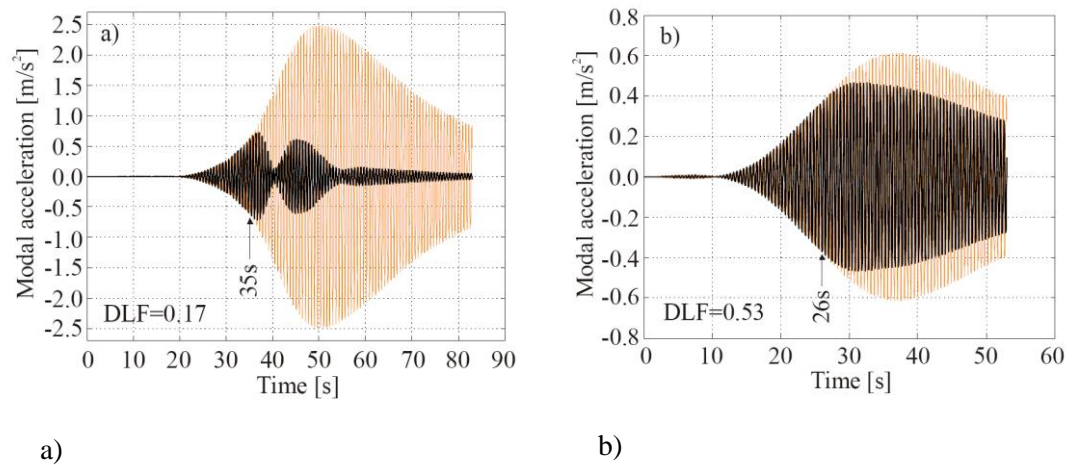


Figure 2.7. Simulated (orange) and measured modal responses due to free walking at resonance on a) footbridge 1 (slow pacing rate) at first mode natural frequency of 1.52 Hz and b) footbridge 2 (fast pacing rate) at first mode natural frequency of 2.04 Hz (after Zivanovic, et al., 2006)

The design guidelines for steel footbridges (EC, 2008) developed by European Commission suggests that synchronization of the human body center of mass with structural vibration is similar to walking with pacing rate equal to resonant frequency. Their experiments showed no stable synchronization behavior for vibration amplitudes with up to 10 mm amplitude. They argued that synchronization may occur at higher amplitudes but they will be outside acceptable limit for vibration serviceability of a footbridge and it is very probable for pedestrians to be disturbed or stop walking. They suggested that fast walking persons are almost not affected by the vibration of the deck as the contact time of the feet with structure is very short.

2.3.2 Modal properties of human model

Investigations of the effects of vibration level on dynamic properties of a human body are limited to standing and sitting people and mostly irrelevant in the context of civil structures vibration serviceability. The rare studies done on standing and sitting people showed that the

modal frequencies of the human model increase (stiffer model) as the level of vibration decrease (Hinz and Seidel, 1987; Matsumoto and Griffin, 1998; Mansfield and Griffin, 2000). For instance, Matsumoto and Griffin (1998) observed that modal frequency of standing people increased from 5 to 7 Hz when magnitude of the base acceleration root-mean-square (RMS) reduced from 2 m/s² to 0.125 m/s².

2.4 Walking human models

Several attempts were made in the last two decades to model walking human effects on vibrating structure in the vertical direction. As human body is a complex non-linear biodynamic system with time-varying parameters (Williams, et al., 1999), some level of simplification and approximation is necessary to be able to model its dynamics. These models can be divided here into three categories based on their type. The first category comprises the linear oscillator-based models which simulate a human with a single or multiple lumped masses connected together linearly with springs and dampers and are oscillating in the vertical direction. The second category comprises biomechanically-inspired inverted-pendulum models that were developed originally to simulate walking gait realistically. The final category is made of multi-body models of the human body.

2.4.1 Oscillator-based models

The most simplistic approximation of a human body model is a linear single or multiple degrees-of-freedom (DOF) system (Ji, 2000). Miyamori, et al. (2001) simulated a walking pedestrian with a 3DOF biodynamic model but no comparison was presented with the force-only case to examine the performance of their model. Archbold (2004) used a finite element model to simulate the vertical effects of an SDOF MSD model of a single pedestrian walking across a footbridge structure and compared the results of the force-only models with such interactive walking person model. He used parameters selected from biomechanics literature

developed for standing and running people to simulate a walking pedestrian. He used initial stiffness of 25 kN/m and damping of 800 N.s/m in his simulations. His studies showed that when pacing frequency was close to the modal frequency of structure, force-only model overestimated the 10 second RMS of acceleration response up to 400% whereas the interactive model estimated it with maximum 10% error. He also found out that including higher harmonics in simulation did not improve the accuracy of results.

Kim, et al. (2008) used a 2DOF MSD model to simulate a walking individual in the vertical direction. They adopted the human model parameters mostly from ISO 5982:1981 (1981) which is only valid for standing people (Figure 2.8). The effects of a single walking pedestrian was simulated on a 99m long cable-stayed footbridge located in a Seoul park, South Korea, with empty natural frequency of 1.88Hz and damping ratio of 0.4%. The response of the structure was compared for two scenarios of passive moving force and interactive 2DOF human model. Surprisingly, they found that the response of structure using interactive 2DOF model was 34% higher than that of the force-only model.

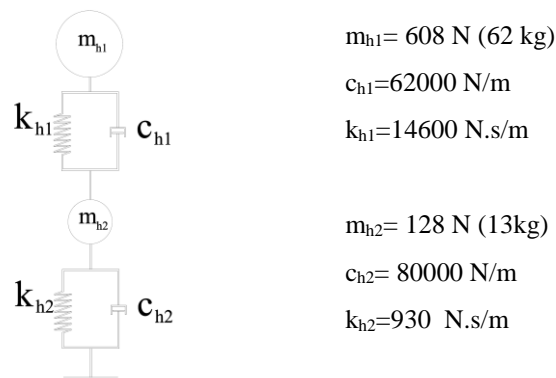


Figure 2.8. Human body model (ISO, 1981)

Caprani et al. (2011) used a moving SDOF MSD model coupled with a walking force to simulate vertical effects of a single walking pedestrian on structure (Figure 2.9). Only the first harmonic of the walking force was used in simulations and human model parameters were selected from the biomechanics literature. A simply-supported beam simulated with an SDOF MSD model was used as a structure. They compared the response of the structure for two cases of force-only and interactive MSD model using response ratio μ :

$$\mu = \frac{\text{Response MSD}}{\text{Response force-only}} \quad (\text{Equation 2.2})$$

They varied the mass and stiffness of MSD model within ranges of 10-130 kg and 10-35 kN/m respectively with constant damping ratio of 0.3, pacing frequency of 1.96 Hz and step length of 0.66m. Figure 2.10 shows the results of their study for three bridge natural frequencies, 1.94, 2.0 and 2.1 Hz. They found that structural responses away from resonance were similar for both models. However, when the SDOF MSD model natural frequency was close to the structural resonance, the responses of the SDOF model were considerably lower compared with the force-only simulations. They suggested that the resulted response ratios μ can be used for finding interactive response of structures using force-only response. However, due to inter- and intra- subject variability and amplitude dependency of the human model parameters (such as modal frequency and damping ratio) the obtained coefficient would lack generality. Their work also lacks experimental validation.

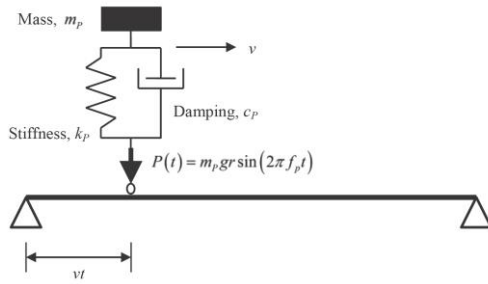


Figure 2.9. Moving MSD model coupled with single harmonic walking force to represent walking human (after Caprani et al., 2011)

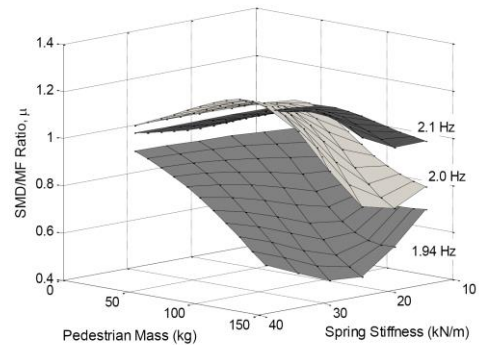


Figure 2.10. Ratio of interactive/force-only models responses for different human model parameters (after Caprani et al., 2011)

Archbold, et al. (2011) used the same model as Caprani, et al. (2011) and investigated in more detail the effects of the pacing frequency and stride length on the response of a structure. They adapted the statistical distributions suggested mostly in biomechanics literature to define the parameter of the MSD walking human model. The pedestrian mass was taken to follow a log normal distribution (Portier et al, 2007) with a mean of 73.9kg and variance of 21.2%. The stride length was taken to be normally distributed with a mean of 0.66m and 10% variance (Barela and Duarte, 2008). The pacing frequency was also considered to be normally distributed with the mean of 1.96Hz and standard deviation of 0.209Hz (Matsumoto et al, 1978; Grundmann and Schneider, 1990; Pachi and Ji, 2005; Ebrahimpour et al, 1996; Karmer and Kebe, 1980). The pedestrian stiffness was again taken to be normally distributed with a mean of 22.5kN/m and a standard deviation of 2.25kN/m (Lee and Farley, 1998). Their study showed that response ratio μ is extremely sensitive to even slight variations in the pacing rate when it is close to the natural frequency of structure. They also found that variations in the step length had little effect on the structural response.

The work of Silva and Pimentel (2011) is very rare to suggest that, in the context of vibration

serviceability of civil structure, it is appropriate to use a range of parameters for an MSD-based walking human model. They identified the parameters of an SDOF MSD walking human model by analyzing correlation of walking force and acceleration of the human body Centre of Mass (CoM) recorded at waist (Figure 2.11).



Figure 2.11. Pedestrian walking with accelerometer attached at waist level representing CoM (after Silva and Pimentel, 2011)

Twenty test subjects took part in their experimental campaign, being eleven men and nine women where they walked with their desired speed on a rigid surface and their CoM acceleration was recorded with an accelerometer attached at waist level. They suggested three equations for mass, damping and stiffness of SDOF human model:

$$m = 97.082 + 0.275 \times M - 37.518 \times f_p \quad (\text{Equation 2.3})$$

$$c = 29.041 \times m^{0.883} \quad (\text{Equation 2.4})$$

$$k = 30351.744 - 50.261 \times c + 0.035 \times c^2 \quad (\text{Equation 2.5})$$

Where, M is the total mass of human body, f_p is the pacing frequency and m , c and k are the SDOF model mass, damping and stiffness respectively.

Their work, however, lacks an appropriate experimental verification. They used synthetic walking force adopted from literature (Kerr, 1998) instead of actual walking force of people which can reduce the reliability of the results. Their choice of range of human model stiffness and damping values for the studies was based on assumed analogy with standing people parameters which is not necessarily correct. For instance, they assumed that damping of a walking person is less than the damping of a standing person.

Silva, et al. (2013) used the moving SDOF oscillator model developed earlier by Silva and Pimentel (2011) to simulate non-synchronized multi-pedestrian walking traffic on structures and compared it with full-scale structural measurements. They used two methods to simulate walking pedestrians. In the first method, both the walking force and the walking people model were moving together along the structure. This method was non-linear and time-varying as location of human DOF on the structure changed with time. In the second method, only the walking force moved along the structure and the location of human model was kept constant. Pedestrians in this method were distributed evenly along the structure.

A simply-supported concrete prototype footbridge with a clear span of 11.30 m and width of 1.8 m is used for study. Modal tests showed that the first vertical mode of the structure has 4.27Hz natural frequency and 1% damping ratio. Three tests with pedestrian densities of 0.3, 0.7 and 0.9 pedestrians/m² involving 12, 31 and 48 test subjects, respectively, were performed. Experimental and analytical frequency spectra of acceleration response of the structure are presented in Figure 2.12, Figure 2.13 and Figure 2.14 for these three tests.

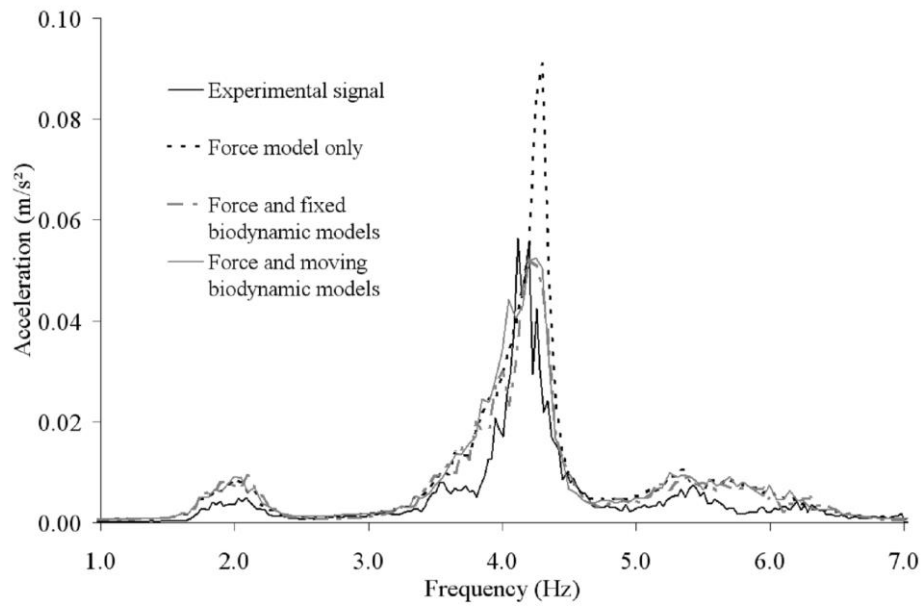


Figure 2.12. Mean power spectra for a density of 0.3 pedestrians/m² (after Silva, et al., 2013)

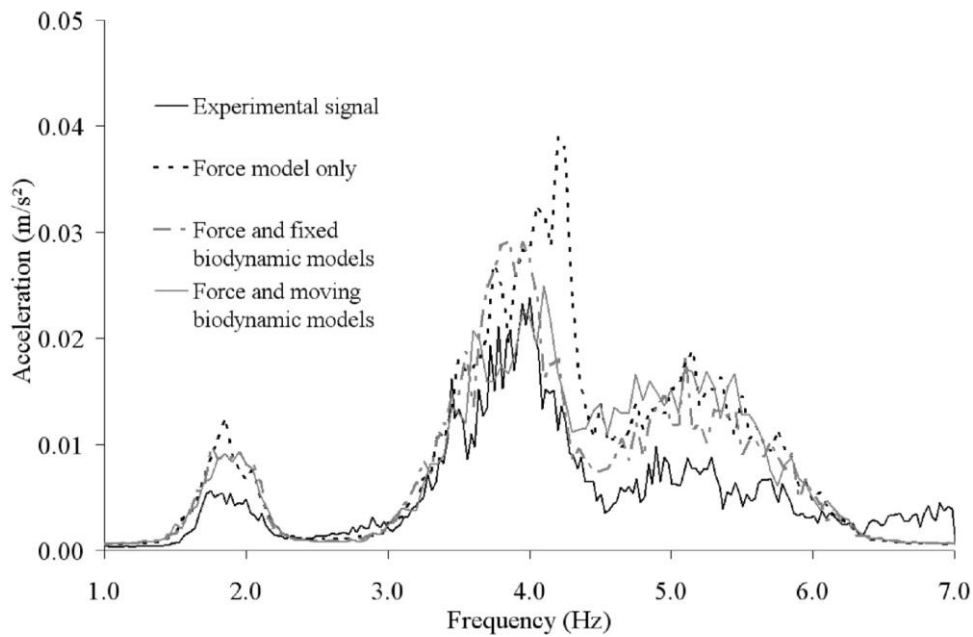


Figure 2.13. Mean power spectra for a density of 0.7 pedestrians/m² (after Silva, et al., 2013)

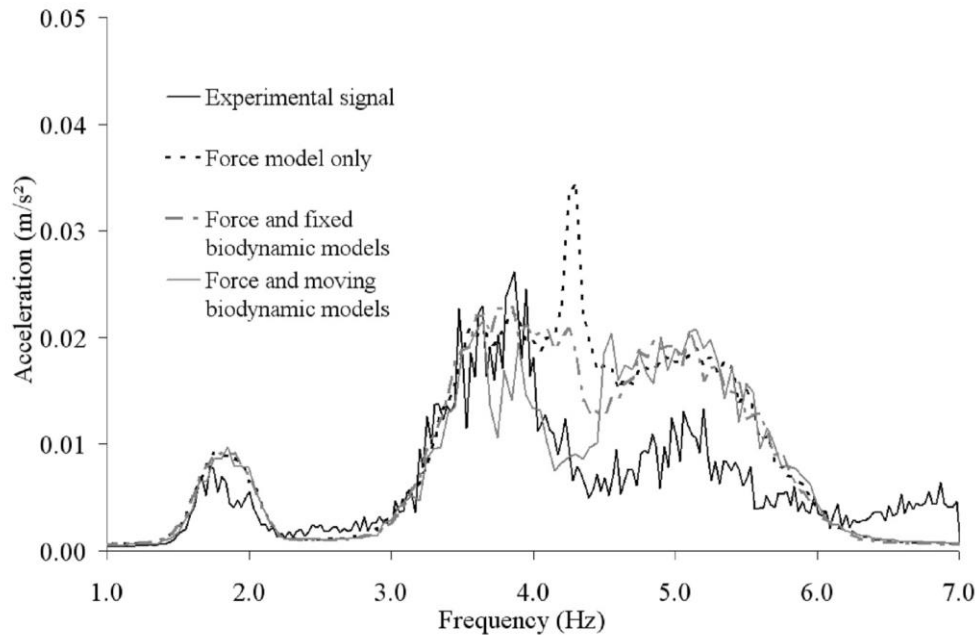


Figure 2.14. Mean power spectra for a density of 0.9 pedestrians/m² (after Silva, et al., 2013)

They observed slight reduction in the natural frequency of the structure and a considerable reduction in the response of structure (increased damping) when using human biodynamic model (both methods). These effects intensified as the number of walking people on structure increased. None of these effects was evident in the response of the structure excited by the walking force-only model.

2.4.2 Inverted-pendulum models

Dynamic behavior of a human body and its response when exposed to various vibration levels have been researched extensively by the biomechanics community since early 1900s. Several researchers have adapted walking human models especially various inverted-pendulum models from the biomechanics literature, to simulate interaction of walking pedestrians with civil structures. This has been the case for the lateral direction in particular, and their application to the vertical direction is rare. Biomechanical models of human body

are usually identified with vibration levels that are higher than the levels that are normally experiences in civil engineering structures. As human body modal properties are amplitude-sensitive, it is very important to use the parameters suitable for civil engineering application (Sachse, 2003; Griffin, 1990).

Bocian, et al. (2011; 2013) used an inverted-pendulum model without spring and damper to simulate the motion of the CoM in walking people in the vertical direction. He studied the behavior of the model subjected to vertical base excitation to find gait adaptation strategies in the presence of structural motion. The equation of motion of the inverted-pendulum model (Figure 2.15) during the single support phase was easily derived by applying D'Alembert's principle:

$$\ddot{\theta} = -\frac{1}{l}(g + \ddot{z})\text{Cos } \theta \quad \text{(Equation 2.6)}$$

Where, θ is support-leg inclination angle; l is equivalent inverted pendulum length; g is gravitational acceleration; z is vertical displacement of the bridge; and dots over the symbols represent derivatives with respect to time. In Figure 2.15, m_p is the mass of pedestrian and F_v is the vertical component of the interaction force.

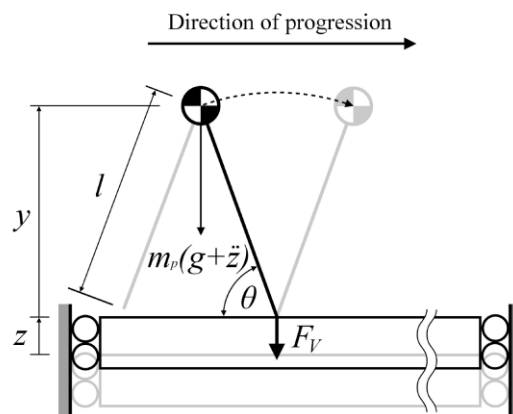


Figure 2.15. Inverted-pendulum walking human model on vertically vibrating structure (after Bocian, et al., 2011)

They found that, depending on the ratio of the pedestrian pacing frequency and base excitation frequency, a walking human can act both as negative or positive damper. For a multi-pedestrian walking traffic the overall effects of pedestrians is more likely to increase damping and mass. This occurs due to the base motion subtly altering the timing of the footfall impulses to bias the net effect but without actually causing synchronization of the pedestrian with the base frequency. Their model, however, was very simplistic as they used a single legged pendulum which is unable to model double-support phase of the walking gait and ignored stiffness and damping of a human body. They also did not take into account the time-varying frequency contents of the structural response and no experimental validation was presented.

Qin, et al. (2013) used a bipedal walking model with damped compliant legs to simulate walking human. Their bipedal model had two degrees of freedom (x and z as shown in Figure 2.16) and the mass was concentrated at CoM. A massless linear spring and time-varying damper in parallel were used to simulate each leg (Figure 2.16). The time-varying damping mechanism was employed to simulate realistically the ground reaction force especially at touch-down of a leading leg. A control force in a feed-back form was applied to the pedestrian in each walking step to compensate for energy dissipated by the damping of the model and to regulate the walking behavior.

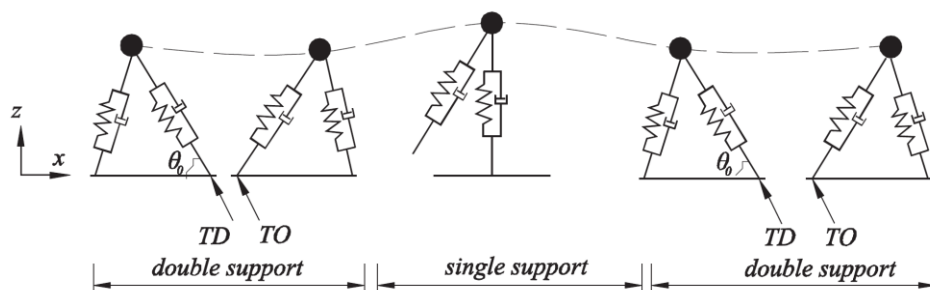


Figure 2.16. The schematics of Qin, et al. (2013) biomechanical walking model (TD: touch down of leading leg; TO: toe off of the trailing leg)

They studied the effects of leg stiffness and damping and the landing angle of attack of leading leg θ_0 on response of structure. Results of their investigation showed that the interaction level increase with increasing vibration magnitude of the structure. Therefore more feedback energy needs to be supplied to the human model to maintain steady walking. Leg stiffness was found to have significant effect on the dynamic response of the structure when the step frequency is close to the natural frequency of the structure.

Their research, however, was limited to analytical study of a single pedestrian on a beam structure and did not include any experimental validation. The parameters used for the model were adapted from biomechanics literature and were not validated for civil structures vibrations. Some of the results of their study, such as considerable increase in the response of a structure when considering HSI and negligible effects of the walking human on modal properties of empty structure were quite contradictory with experimental evidence observed by others on real-world structures.

Dang and Zivanovic (2013) compared the performance of a moving harmonic force model, a moving oscillator-actuator model and an inverted-pendulum model (without spring and damper) in reproducing kinematic and kinetic features of human walking and replicating the vibration patterns observed on a lively footbridge. The structure selected for the study was a light cable-stayed bridge made of fiber reinforced polymer with the length of 113m, the main span of 63 m and the weight of 20,000kg. The structure was very alive with fundamental vibration mode at 1.52Hz, 2,750kg modal mass and 0.42% modal damping ratio.

The inverted-pendulum model DLF, mass, average walking speed and pacing frequency were selected equal to 0.14, 86 kg, 1.43 m/s and 1.52 Hz, respectively, based on the tests done on the footbridge. SDOF MSD model natural frequency, damping ratio and DLF were selected 2.3 Hz, 8% and 0.1, respectively, by analogy of properties of bouncing people found

in literature. However, no appropriate justification or validation was presented for their analogy.

Their study showed that traditional force-only model cannot predict response of the structure accurately in lightweight structures where HSI has prominent contribution. Both inverted-pendulum and SDOF oscillator models predicted interaction level acceptably while inverted-pendulum model can replicate the kinematics of body CoM better. It also can simulate the effects of the structure on the pacing frequency and phase of the walking force.

2.4.3 Whole body models

Maca and Valasek (2011) employed two complex 2D and 3D multi-body models of walking human to simulate its interaction with a vibrating structure. They used a 2D model with 9 degrees of freedom for vertical interaction (Figure 2.17) and a 3D model with 34 degrees of freedom to simulate simultaneous interactions in both vertical and lateral direction (Figure 2.18). To the best of author's knowledge this was the first and only instance that interaction of a walking human and structure was simulated in both directions simultaneously.

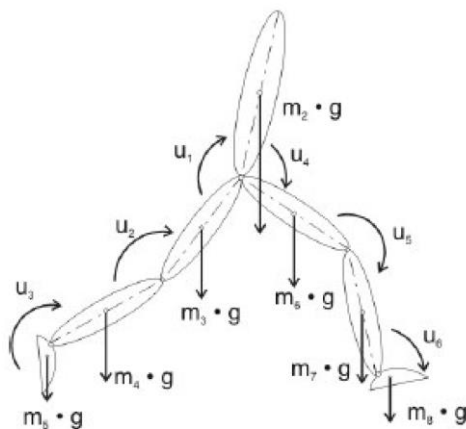


Figure 2.17. The 2D walking human model comprised of 8 bodies / 9 DOFs (after Maca and Valasek, 2011)

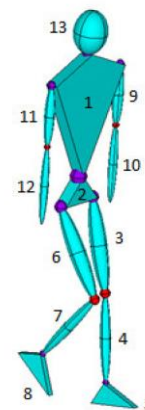


Figure 2.18. The 3D walking human model with 13 rigid bodies and 34 DOFs (after Maca and Valasek, 2011)

A combination of feed-back and feed-forward control algorithms was used in the multi-body models to replicate normal walking motion and gait. A finite element model (FEM) of a structure was coupled with human models and their mutual interactions transferred to one another at each moment of time using interaction force. They concluded that the response of the bridge was affected by the ratio of the pacing frequency and natural frequency of the structure and that the number of pedestrians on structure has no effects on structural response. Although novel and advanced, inherent complexities of the model and high number of input parameters and control assumption make multi-body models highly error-prone and the results hard to interpret. No experimental validation was provided on the capability of the model to simulate the effects of multi-pedestrian walking traffic on vibrating structures.

2.5 Design guidelines/assessment methods

Inherent complexity of human-structure interaction and its yet unclear mechanisms have resulted in the current design guidelines ignoring these effects regardless of their importance. Due to the stochastic nature of multi-pedestrian walking load, most of these guidelines suggest some scaling factors to take into account the probability of different scenarios such as correlation between people in the crowd and their ‘synchronization’. However, these ‘synchronization’ factors take into account the probability of an ‘accidental’ match between the pacing frequency and the natural frequency of the structure rather than lock-in effects.

For instance, the reduction factor ‘k’ used to scale the structural response in Eurocode 5 (Figure 2.19), accepted in the UK in 2004 (EN, 2004), reduces the number of synchronized people in the crowd if the bridge has natural frequency away from the average pacing rate of the pedestrian traffic (Butz, 2008c). The ‘ ψ ’ factor in the guideline developed by the French road authorities (Setra, 2006) and the ‘k’ factor in UK National Annex to Eurocode 1 (BSI,

2008) (Figure 2.19) both reduce the total walking force to account for the probability of walking at a given resonant frequency.

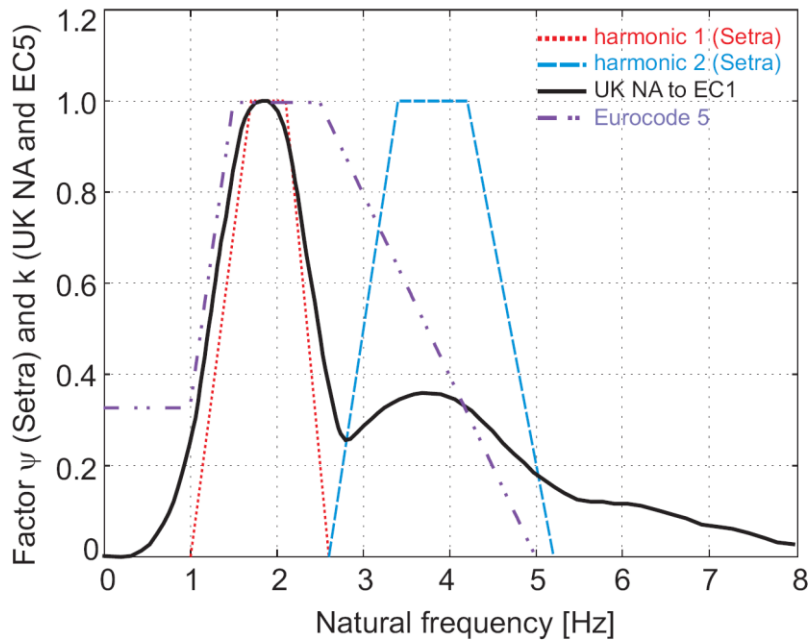


Figure 2.19. Factors ψ (Setra) and 'k' (UK NA to EC1 and EC5) as a function of natural frequency and forcing harmonic (after Zivanovic, et al., 2010)

In the frequency-domain model proposed by Brownjohn, et al., (2004a), the power spectral density (PSD) of acceleration response is scaled with a coherence function $\text{coh}(f, z_1, z_2)$ to take into account the synchronization of pedestrians with each other. In this function, two points z_1 and z_2 denote the positions of each pair of pedestrians. Butz's (2006; 2008b) method further adopted by Research Fund for Coal and Steel for a guideline for footbridge design (HIVOSS, 2008) uses factor k_{red} that reduces the calculated acceleration to account for the mismatch between the mean walking frequency and the natural frequency of the structure.

Zivanovic et al. (2010) did a comprehensive study on the performance of the currently

available design guidelines to estimate response of a structure under spatially unrestricted pedestrian traffic walking load. They used four time-domain methods: Eurocode 5 (EN, 2004), ISO 10137 standard (ISO, 2007), design guidelines presented by the French road authorities (Setra, 2006) and UK National Annex to Eurocode 1 (BSI, 2008), together with three frequency-domain methods: power spectral density method proposed by Brownjohn (2004a), Butz (2006; 2008b) method and response spectrum method formulated by Georgakis & Ingolfsson, (2008) for analysis. The selected methods were used to estimate the response of full-scale measurements done on two real-world footbridges, the Reykjavik City Footbridge (RCF) located in the Icelandic capital and the Podgorica Bridge (PB) in the capital of Montenegro.

Results of their studies showed that these design guidelines tend to overestimate the response of a structure especially in the case of Podgorica footbridge. They concluded that ignoring human-structure interaction was possibly the cause of this overestimation. They later showed that increasing damping of the occupied structure from 0.26% to 0.67% (which is expected due to HSI) resulted in an accurate estimation of experimental response. The key problem clearly remains how to obtain accurate damping of the occupied structure.

The UK recommendations for design of permanent grandstands (2008) is leading the world in promoting a realistic way to take into account explicitly the dynamic interaction of people and grandstands. This work, based on the model proposed by Dougill et al. (2006), uses a combination of two SDOF models to simulate the aggregated effect of passive and active (mostly jumping and dancing) people (Figure 2.20). Although this model aggregates the effects of people and does not take into account the inter- and intra- subjects variability of people, its performance was demonstrably proven to be much more accurate than other methods by Jones, et al. (2011a). Although this model is not applicable to walking people, its

successful approach to explicit modeling of interaction effects could be adapted for walking pedestrians.

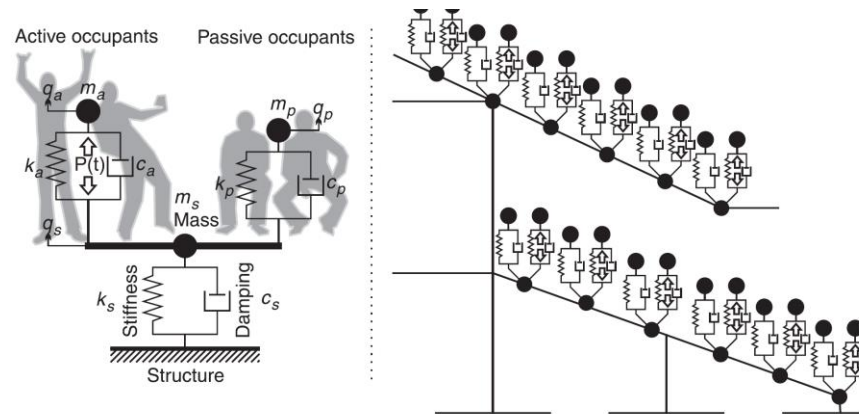


Figure 2.20. The crowd model used by UK recommendations for design of permanent grandstands (2008) (after Jones, et al., 2005)

2.6 Conclusions

The reliable simulation of the walking traffic effects on structures is still an open challenge. No appropriately formulated and experimentally verified model exists to model walking human effects in the vertical direction for a diverse range of loading scenarios and structures. The existing models lack appropriate experimental validation and their time-varying non-linear interaction mechanisms are not straightforward to implement in practice.

Similarly, no verified range of walking human model parameters exists to represent the variability of human parameters. The current walking human/crowd model parameters are mostly adopted from the field of biomechanics and are not validated for application in vibration serviceability assessments. This is mainly due to the scarcity of credible and detailed experimental data of walking-structure interactions. There is an urgent need for an organized experimental and analytical research on underlying mechanisms of human structure interaction during walking.

Chapter 3

Evaluation of Existing Design Guidelines

The contents of this chapter are adapted with minor changes from a conference paper presented at the 30th Conference and Exposition on Structural Dynamics (IMAC XXX). Details of the paper are as follows:

Shahabpoor, E., Pavić, A., 2012. Comparative evaluation of current pedestrian traffic models on structures. Conference Proceedings of the Society for Experimental Mechanics Series 2012. V 26, pp. 41-52.

3.1 Introduction

In this chapter, two of the currently available design guidelines for vibration serviceability assessment of footbridges, French road authorities (Setra, 2006) and UK National Annex to Eurocode 1 (BSI, 2008), are studied. Only spatially unrestricted walking traffic and vertical direction effects are considered. Three monitoring tests were done on the University of Sheffield post-tensioned test footbridge and Podgorica Bridge (PB) located in Montenegro and performance of the selected guidelines in estimating structural response in each test was analysed. In the next step, possibility of increasing damping of the occupied structure (as a measure of human-structure interaction) to improve the accuracy of design guidelines results was investigated. Finally, a brief discussion of the performance of the selected guidelines is presented.

Section 3.2 presents a brief introduction into the selected guidelines. Sections 3.3 and 3.4 describe the test structures and research methodology, respectively. Results of the full-scale measurements are presented in Section 3.5 and are compared with the estimated responses (design guidelines) in Section 3.6. The key findings of the study are highlighted in Section 3.7.

3.2 Design guidelines

3.2.1 Sétra guideline (2006)

The design guideline of the Technical Department for Transport, Roads and Bridges Engineering and Road Safety (2006) (Service d'études techniques des routes et autoroutes - Sétra) on footbridges has presented two primary load cases for vertical pedestrian walking loads; Case 1) sparse and dense crowd with densities between 0.5 - 0.8 pedestrians/m² ; Case 2) very dense crowd; and a complement case for an evenly distributed crowd (2nd harmonic

effect) based on the assumption that the probability distribution of the pacing rate within traffic follows Gaussian distribution. These load cases are developed based on four classes of footbridges (depending on the level of traffic they are expected to experience, Class I: very heavy traffic, Class II: heavy traffic, Class III: moderate traffic and Class IV: low level of traffic) and four classes of frequency ranges (depending on the expected risk of resonance, Range 1: maximum risk of resonance, Range 2: medium risk of resonance, Range 3: low risk of resonance for standard loading situations and Range 4: negligible risk of resonance). Case 1 model which is more relevant to the loading scenarios of this chapter, defines the crowd's vertical walking load as:

$$f_n(t) = 10.8 * 280d\sqrt{\zeta/n}\psi\cos(2\pi f_v t) \quad (\text{Equation 3.1})$$

Where, d is density of 0.5 and 0.8 peds/m² for footbridges class III and II, respectively, n is the number of people in the crowd, 280 N is the dynamic load amplitude of a single pedestrian (0.4×700 N for the first and 0.1×700 N for the second harmonic), f_v is the natural frequency of relevant vibration mode, ζ is the damping ratio of that mode and ψ is a reduction factor that reduces the load for frequencies away from the average pacing rate. Although an extensive set of 500 simulations were used for developing this model and the effects of pedestrians on modal mass of structure was considered, the model does not take into account the effects of pedestrians on damping of structure which considerably reduces the accuracy of the results. The model also, takes into account one harmonic at a time which is problematic in the case of footbridges with more than one excitable mode (Zivanovic, et al., 2010).

3.2.2 UK National Annex to Eurocode 1 (2008)

UK National Annex to Eurocode 1 (BSI, 2008) defines two walking load models corresponding to single pedestrians / pedestrian groups and pedestrian 'crowds' with density

greater than 0.4 pedestrians/m². It also defines four classes of footbridges based on the level of traffic they expect to experience; Class I: very heavy traffic, Class II: heavy traffic, Class III: moderate traffic and Class IV: low level of traffic. The crowd load model used in this chapter is defined as load per unit area, with the load sign matching that of the mode shape:

$$w = 1.8 \left(\frac{F_0}{A} \right) \cdot k(f_v) \cdot \sqrt{\gamma \cdot \frac{\rho \cdot A}{\lambda}} \cdot \text{Sin}(2\pi f_v t) \quad (\text{Equation 3.2})$$

Where, F_0 is the reference dynamic load of one pedestrian (280N), k is a factor that takes into account the excitation potential of the relevant forcing harmonic and probability of walking at the given resonant frequency in the model, ρ is the crowd density with a maximum value of 1.0 pedestrians/m², A is the net area of the span, γ takes into account the lack of correlation between people in the crowd and λ is a factor that reduces the effective number of pedestrians, depending on the location of them on the structure and the target mode shape (Zivanovic, et al., 2010):

$$\lambda = \frac{\int_0^L |\phi(x)| / \phi_{\max} dx}{L} \quad (\text{Equation 3.3})$$

Where, L is the length of the loaded area, and $\phi(x)$ and ϕ_{\max} are the mode shape along the bridge and its maximum ordinate, respectively. For a sinusoidal mode shape, $\lambda=0.634$ and the equation becomes very similar to the S etra equation with the multiplying constant equal to approximately 6.1 instead of 10.8, and k instead of ψ . This shows that the results of UK NA method in this case is 44% less conservative than S etra method which is chosen with logical reasoning that some exceedance of the predicted response should be allowed in real life (Zivanovic, et al., 2010).

Similar to S etra, UK NA method takes into account one harmonic at a time and does not take into account the effects of pedestrians on damping of structure which reduce considerably

the accuracy of the results.

3.3 Description of tested footbridges

3.3.1 The University of Sheffield post-tensioned slab strip

The slab strip used in the following analytical and experimental tests is a simply supported in-situ cast post-tensioned slab strip of net span 10.8 m (Figure 3.1) constructed in the light structure laboratory of The University of Sheffield for research purposes. Its total length is 11.2m, including 200 mm overhangs over the supports. Its width and depth are 2.0 m and 275 mm respectively, and it weighs approximately 15 tonnes (Nyawako and Reynolds, 2000).

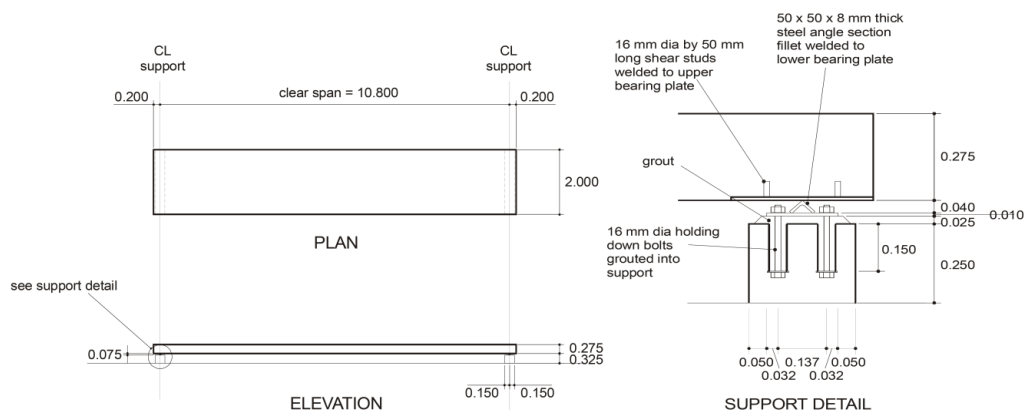


Figure 3.1. Plan of the University of Sheffield footbridge and a typical support detail (after Nyawako and Reynolds, 2000)

3.3.2 Podgorica footbridge

The Podgorica footbridge (PG) spans 104 m over the Morača River and is constructed in Podgorica, capital of Montenegro (Figure 3.2) in early 1970s. The structural system of the footbridge is composed of a steel box girder with 78m main span length between two inclined column supports and two side spans of 13 m each. The top flange of main girder is

3m wide and forms the clear deck of the footbridge. Depth of the girder varies from 1.4m in the mid span to 2.8m over the inclined supports. The structure was stiffened with several stiffeners along the main girder and at the support connection points. Two water supply and drainage pipes pass through the steel box section and are suspended from the top flange of the main girder (Zivanovic, et al., 2006). The PG footbridge was found to be very susceptible to walking induced vibration. The structure later was strengthened by casting a concrete slab over the top steel flange in the mid-span and over the bottom flange in support areas, but it couldn't shift its natural frequency out of excitable region by the human walking.

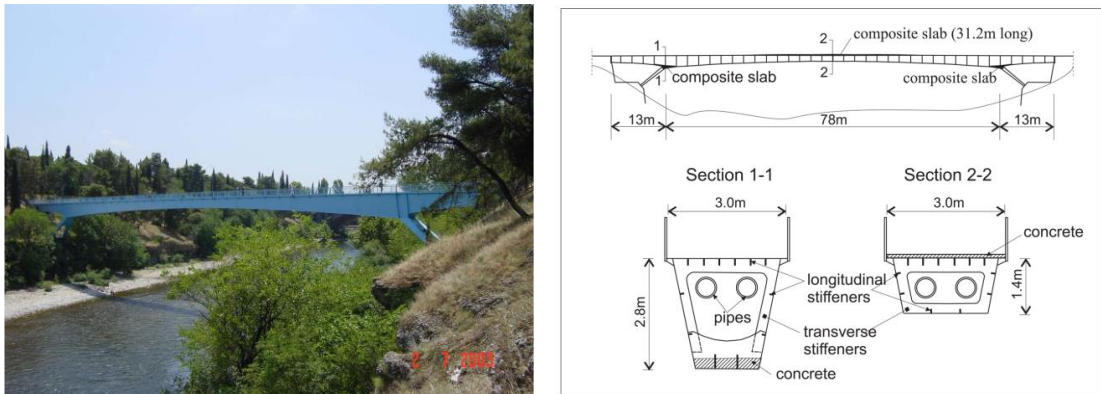


Figure 3.2. Podgorica footbridge view (left) and General arrangement drawing (right)
(after Zivanovic, et al., 2006)

3.4 Methodology

The main goals of this study are first to evaluate the performance of the selected design guidelines, and second to evaluate the effects of human-structure interactions and possibility of using added damping of stationary pedestrians to enhance the accuracy of design models. For Sheffield footbridge, a series of FRF-based modal tests for identification of modal properties of structure and a series of response monitoring tests under various traffic conditions were considered. In each monitoring test, full set of pedestrian traffic statistical

data such as average walking speed, average pacing frequency, weight and their location on structure were recorded. For Podgorica footbridge, results of tests done by Zivanovic, et al. (2006) were used for analysis.

In the next step, the captured modal properties of structure and pedestrian traffic data were used as input for the selected design guidelines to estimate structural response of each monitoring tests. The estimated responses of these guidelines were then compared with the corresponding experimental responses to analyse their accuracy. Finally, the possibility of increasing damping of structure (as a measure of human-structure interaction) to enhance the accuracy of the design guidelines estimation is studied.

The increased structural damping value for Sheffield footbridge was found from an FRF-based modal test conducted on structure when people were standing still on it. In the case of Podgorica footbridge, the increased damping value recommended by Zivanovic, et al. (2010) was used in analysis.

3.5 Full scale measurements

3.5.1 Modal properties estimation

Two FRF-based modal testing was conducted by the author on Sheffield footbridge, one on the empty structure and one on the occupied structure when 6 test participants were standing still and uniformly-distributed along the structure. The tests were done using 18 force balanced QA accelerometers placed parallel to the longer edges of slab, as shown in Figure 3.3, to capture both vertical and torsional modes. An APS electro-dynamic shaker model 400, operated in the inertial mode was used to shake the structure. It was placed at test point (TP) 13 to be able to excite first three vertical mode shapes. The shaker was fed by random excitation with 0-50Hz frequency bandwidth to capture all the modes in this range, and the induced force was measured indirectly using an ENDEVCO accelerometer, attached to the

shaker's moving mass. The shaker, accelerometers and wires were placed in such a way that pedestrians could walk on the slab freely in both directions. The test setup is shown in Figure 3.3.

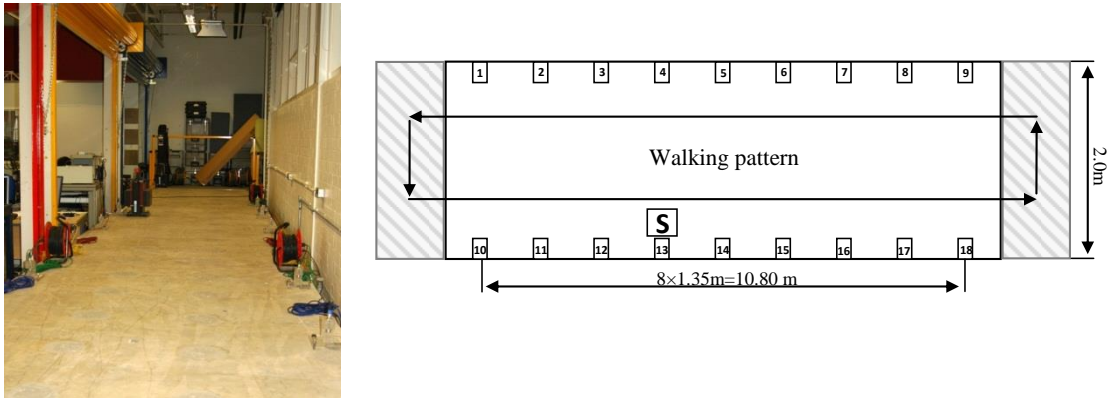


Figure 3.3. Test setup photo (left) and Walking pattern of pedestrians (right)

The modal properties of the structure (Modal frequencies, damping ratios, masses and mode shapes) are obtained by curve fitting the resulted FRFs in ME'Scope software, for both clear and occupied structure. The results are presented in Table 3.1 and Table 3.2 and Figure 3.4. The obtained modal parameters of the empty structure are similar to the values found by Reynolds (2000) for the same structure. It was found that the first mode of structure with 4.5 Hz modal frequency is mainly susceptible to human excitation and therefore was selected to be studied. Cross comparison of the results presented in Table 3.1 and Table 3.2 shows an approximately two times increase in the damping ratio of first two vertical modes due to the presence of standing people on structure (Figure 3.5).

Table 3.1. Estimated modal properties of PT slab (empty structure) using both analytical and experimental methods

Mode #	FE Model	FRF based		M_i	C_i	K_i
	f (Hz)	f (Hz)	ζ (%)			
1	4.55 (V)	4.5 (V)	0.98	6000	3315	4796628
2	17.02 (V)	16.8 (V)	0.61	6000	7739	66854332
3	-	25.9 (T)	0.95	6000	18103	158895104
4	28.92 (T)	28.3 (T)	1.22	23000	99789	727211007
5	37.71 (V)	37.8 (V)	1.20	6000	34201	338450053

Table 3.2. Estimated modal properties of PT slab (occupied structure) using FRF-based methods

Mode #	FRF based		M_i	C_i	K_i
	f (Hz)	ζ (%)			
1	4.37 (V)	1.71	7500	7043	5654365
2	16.8 (V)	1.17	6700	16549	74654004
3	26.1 (T)	1.00	5500	17967	147912011
4	28.6 (T)	1.38	34500	171109	1114065943
5	37.8 (V)	1.34	5500	35008	310245882

Mode shapes of Sheffield footbridge are shown in Figure 3.4.

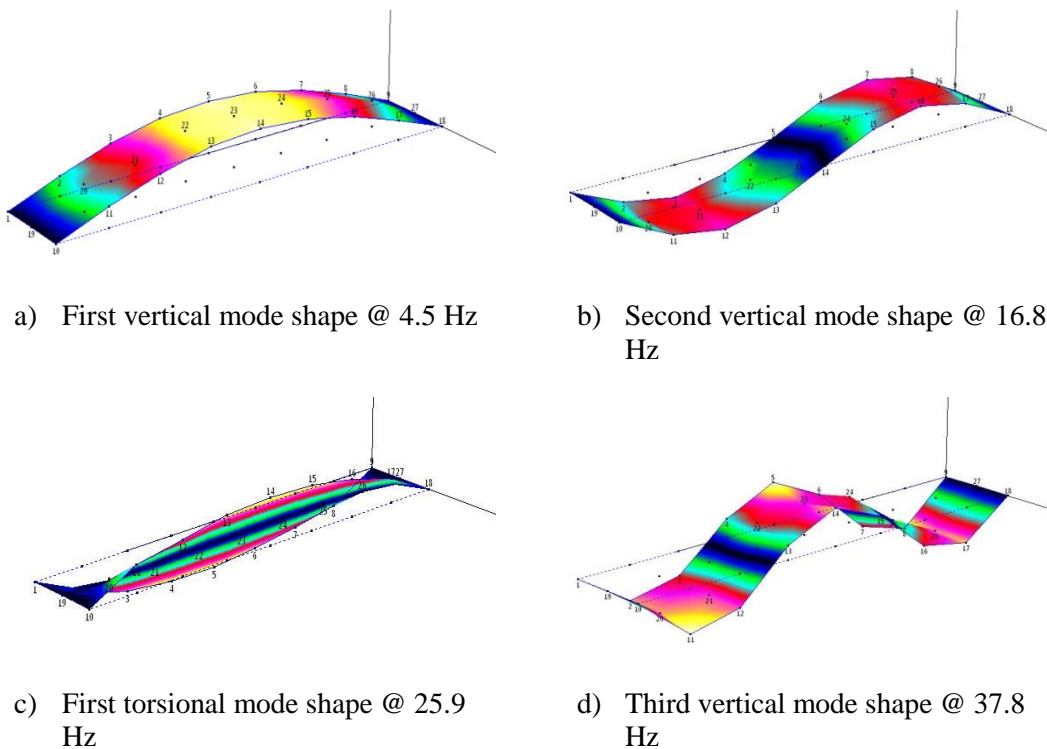


Figure 3.4. Experimentally acquired mode shapes of PT slab

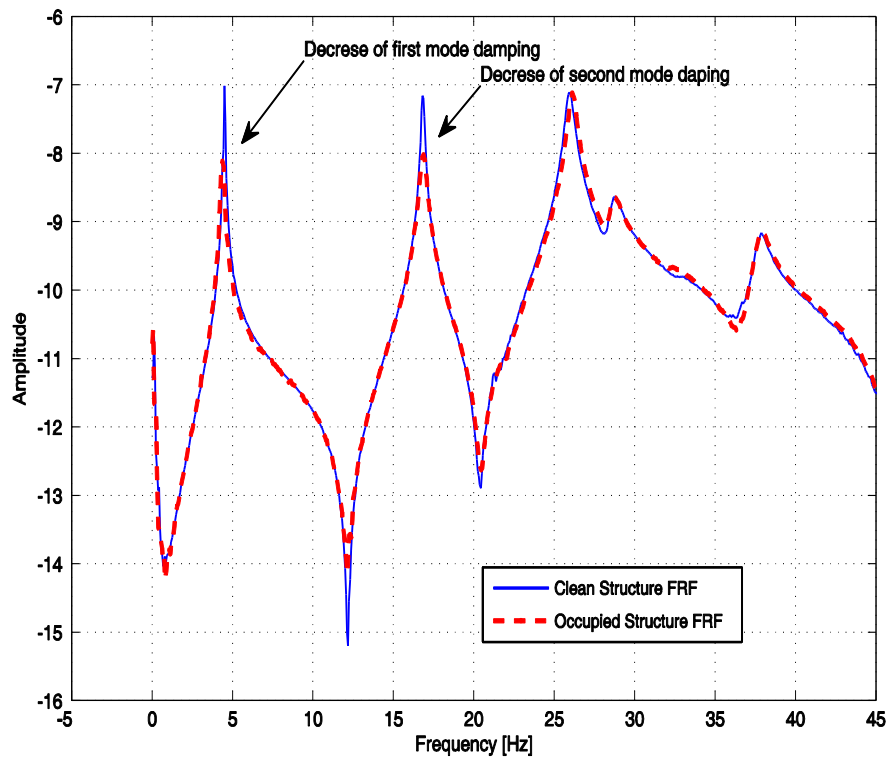


Figure 3.5. Experimentally acquired FRFs of empty and occupied PT slab

For the case of Podgorica footbridge, both FRF-based test and Ambient vibration survey was done by Zivanovic, et al. (2006) for modal properties identification. 14 points along the longer edges of footbridge were chosen for the response to be monitored using Endevco 7754-1000 piezoelectric accelerometers. An APS (model 113) electro-dynamic shaker, placed at the quarter of the mid-span, was used to excite the structure. Detailed description of the tests and modal properties estimation procedure are presented elsewhere (Zivanovic, et al., 2006). The derived modal properties of Podgorico footbridge are presented in Table 3.3.

Table 3.3. Estimated modal properties of Podgorica footbridge using both analytical and experimental methods (after Zivanovic, et al., 2006)

Mode #	FE Model <i>f</i> (Hz)	FRF based		Ambient Vibration Survey (AVS)	
		<i>f</i> (Hz)	ζ (%)	<i>f</i> (Hz)	ζ (%)
1	1.82 (1HS)	1.83 (1HS)	0.26	-	-
2	2.02 (1VS)	2.04 (1VS)	0.26	2.05 (1VS)	0.29
3	3.47 (1VA)	3.36 (1VA)	1.86	3.42 (1VA)	1.04
4	4.36 (1HA)	4.54 (1HA)	0.98	-	-
5	7.15 (2HS)	7.35 (2HS)	2.68	-	-
6	7.34 (2VA)	7.56 (2VA)	0.76	7.55 (2VA)	0.76
7	7.74 (2VS)	7.98 (2VS)	0.60	8.00 (2VS)	0.44

3.5.2 Pedestrian traffic parameters

The Sheffield footbridge was tested under two loading scenarios, 1) normal walking of six people on the slab and 2) synchronized walking of five people to half of first mode natural frequency to excite the slab to resonance. It was found that in monitoring test 1, average pacing frequency, traffic density and average speed of pedestrians were 1.9Hz, 0.278 pedestrians/m² and 1.35 m/s, respectively. These values were 2.25 Hz, 0.235 pedestrians/m² and 1.35 m/s for test 2, respectively.

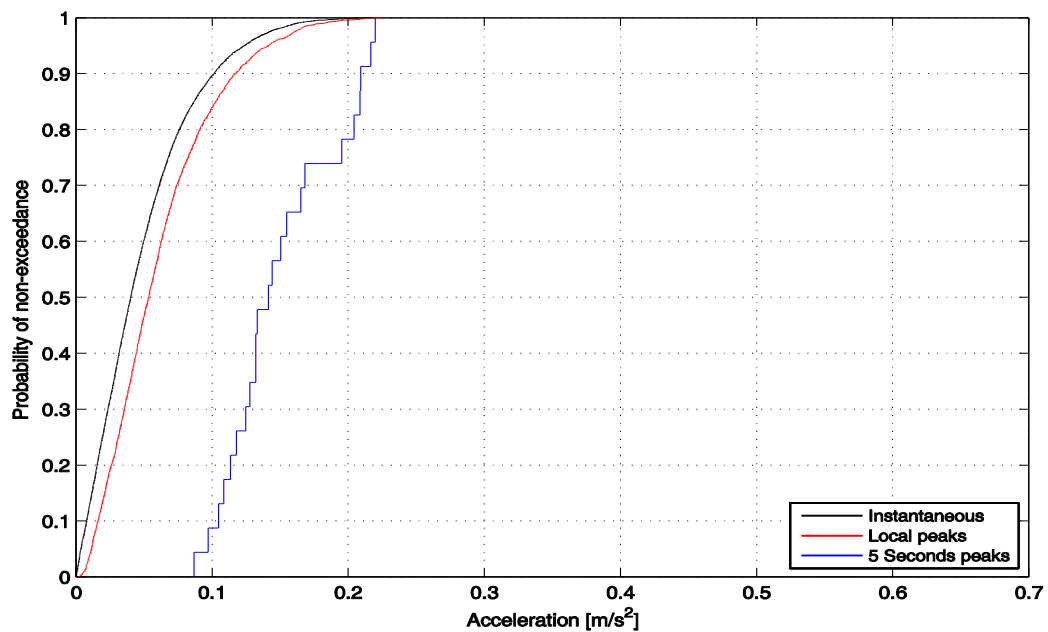
In the case of Podgorica footbridge, Zivanovic, et al. (2010) by analysis of video records of tests has reported that mean pacing frequency was 1.87 Hz, the stream density was 0.05 pedestrians/m² and the average speed of pedestrians was 1.4 m/s.

3.5.3 Structural response

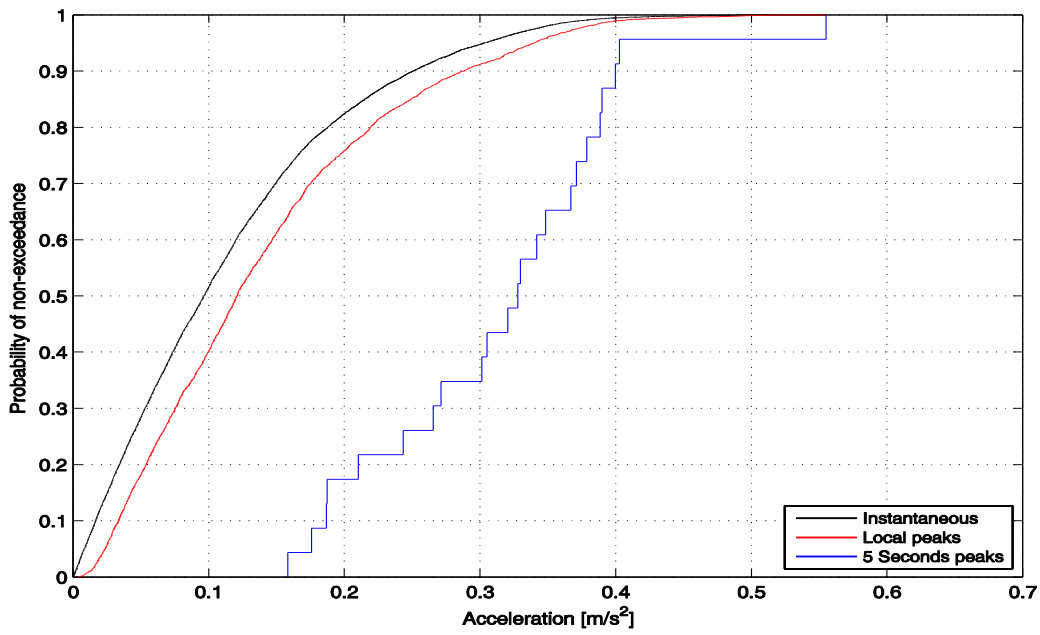
The acceleration response of the Sheffield footbridge were measured at the mid-span, using two force balanced QA accelerometers located at both edges of the slab. Each test lasted 2 minutes. The outputs of these accelerometers are further averaged to remove the effects of torsional modes from the obtained responses. Similarly, the response of the Podgorica footbridge was captured using an accelerometer placed at the mid-span. The monitoring tests lasted 45 minutes. Two of Podgorica footbridge measurements, one with moderate traffic

and the other with slightly heavier traffic, are combined, tail to head, to get a more realistic statistical results.

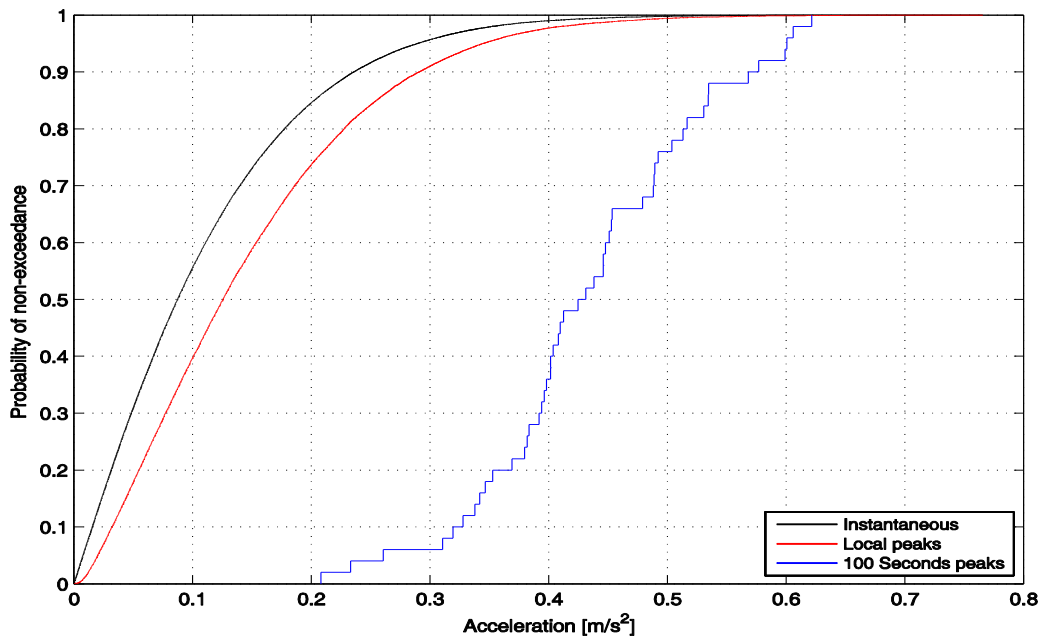
The cumulative distribution functions (CDFs) of instantaneous acceleration response, local peaks (i.e. peak acceleration per cycle) and interval peaks (5 seconds intervals for Sheffield footbridge corresponding to a single crossing time and 100 seconds intervals for Podgorica footbridge corresponding to two average crossing times) are presented in Figure 3.6. In this figure ‘Test 1’ and ‘Test 2’ correspond to normal walking of six people and synchronized walking of five people on the Sheffield footbridge, respectively, and ‘Test 3’ corresponds to Podgorica footbridge monitoring test.



a) Test 1 – CDFs of mid-span acceleration response



b) Test 2 – CDFs of mid-span acceleration response



c) Test 3 – CDFs of mid-span acceleration response

Figure 3.6. CDFs of measured acceleration response at mid-span for Tests 1 (a), Test 2 (b) and Test 3 (c)

3.6 Results of design guidelines

The response of structure is estimated for the following cases for each test using selected design guidelines:

Test 1: Test structure: Sheffield footbridge – Pedestrian traffic: 6 pedestrians walking with their own normal pacing frequency

- Case 1: Results of design models using damping ratio of empty structure ($\zeta=0.0098$)
- Case 2: Results of design models using damping ratio of occupied structure (higher damping values obtained from FRF-based modal test of structure while same pedestrians were standing still on it) ($\zeta=0.0171$)

Test 2: Test structure: Sheffield footbridge – Pedestrian Traffic: 5 synchronized pedestrians, walking with half of first vertical mode natural frequency ($4.5/2=2.25$ Hz)

- Case 1: Results of design models using damping ratio of empty structure ($\zeta=0.0098$)
- Case 2: Results of design models using damping ratio of occupied structure ($\zeta=0.0160$)

Test 3: Test structure: Podgorica footbridge – Pedestrian traffic: real-life situation, moderate to high traffic

- Case 1: Results of design models using damping ratio of empty structure ($\zeta=0.0026$)
- Case 2: Results of design models using damping ratio of occupied structure (higher damping value suggested by Zivanovic, et al. (2010) based on Monte Carlo simulation of pedestrian traffic) ($\zeta=0.0067$)

The list of input parameters used in the guideline methods for these load cases are presented in Table 3.4.

Table 3.4. Input parameters used in selected guidelines methods

Item	Parameter / Description	Sheffield footbridge				Podgorica footbridge		Unit	French Sétra guideline UK NA to ECI (Group) UK NA to ECI (Stream)
		Test 1 Case 1	Test 1 Case 2	Test 2 Case 1	Test 2 Case 2	Test 3 Case 1	Test 3 Case 2		
1	Pacing frequency (f_p)	1.90	1.90	2.25	2.185	1.87	1.87	Hz	
2	Natural frequency (f_n)	4.50	4.37	4.50	4.37	2.00	2.00	Hz	
3	Pedestrian weight (Q)	700	700	700	700	700	700	N	
4	No. of pedestrians	6	6	5	5	15	15	-	
5	Modal damping ratio (ζ)	0.0098	0.0171	0.0098	0.0160	0.0026	0.0067	-	
6	Bridge length(L)	10.8	10.8	10.8	10.8	78	78	m	
7	Bridge width (b)	2	2	2	2	3	3	m	
8	Simulation duration (t)	120	120	120	120	2700	2700	s	
Factors									
1	Load reduction factor (ψ)	0.625	0.8	0.625	0.8	1	1	-	
2	Synch factor (γ) (crowd)	0.0725	0.1265	1.00	1.00	0.0192	0.0496	-	
3	Synch factor (γ) (group)	0.69	0.72	1.00	1.00	0.17	0.23	-	
4	Load reduction factor (k)	0.25	0.29	0.25	0.29	1	1	-	
5	span reduction factor (λ)	0.634	0.634	0.634	0.634	0.634	0.634	-	

* Right hand side columns indicate which parameters are used in each specific code.

The estimated response of the structure for all tests and load cases is presented in Table 3.5 and Figure 3.7. In each case, the contribution of corresponding pedestrians to the modal mass of the structure was taken into account. For stream of pedestrians, pedestrian masses were assumed to be uniformly distributed over the structure and further scaled by the square of the mode shape ordinates. For groups, their mass was exerted on the structure as a dead weight, moving along the walking path.

Table 3.5. Estimated response of structure by design guidelines for Tests 1, 2 and 3

Guideline	Criterion	Experimental value (m/s^2)	Empty structure Difference (%)	Occupied structure Difference (%)		
Test 1: Sheffield footbridge – Normal Walking			$\zeta=0.0098$	$\zeta=0.0171$		
French Sétra	$a_{95\%}$	0.13	1.27	877	0.28	115
	$a_{max,1S RMS}$	0.15	1.00	567	0.20	33
UK NA to Eurocode 1 (Group)	$a_{2.5\sigma}$	0.15	1.31	773	0.47	213
	$a_{max,1S RMS}$	0.15	0.70	367	0.33	120
UK NA to Eurocode 1 (Stream)	$a_{2.5\sigma}$	0.15	1.28	753	0.28	87
	$a_{max,1S RMS}$	0.15	0.90	500	0.16	7
Test 2: Sheffield footbridge – Synchronized Walking			$\zeta=0.0098$	$\zeta=0.0160$		
French Sétra	$a_{95\%}$	0.32	1.16	263	0.22	-31
	$a_{max,1S RMS}$	0.34	0.90	165	0.18	-47
UK NA to Eurocode 1 (Group)	$a_{2.5\sigma}$	0.37	1.39	276	0.49	32
	$a_{max,1S RMS}$	0.34	0.74	118	0.35	3
UK NA to Eurocode 1 (Stream)	$a_{2.5\sigma}$	0.37	4.33	1070	0.54	46
	$a_{max,1S RMS}$	0.34	3.06	800	0.43	26
Test 3: Podgorica footbridge			$\zeta=0.0026$	$\zeta=0.0067$		
French Sétra	$a_{95\%}$	0.55	0.80	45	0.52	-5
	$a_{max,1S RMS}$	0.42	0.80	90	0.40	-5
UK NA to Eurocode 1 (Group)	$a_{2.5\sigma}$	0.34	1.00	194	0.56	65
	$a_{max,1S RMS}$	0.42	0.70	67	0.39	-7
UK NA to Eurocode 1 (Stream)	$a_{2.5\sigma}$	0.34	0.65	91	0.42	24
	$a_{max,1S RMS}$	0.42	0.46	10	0.30	-29

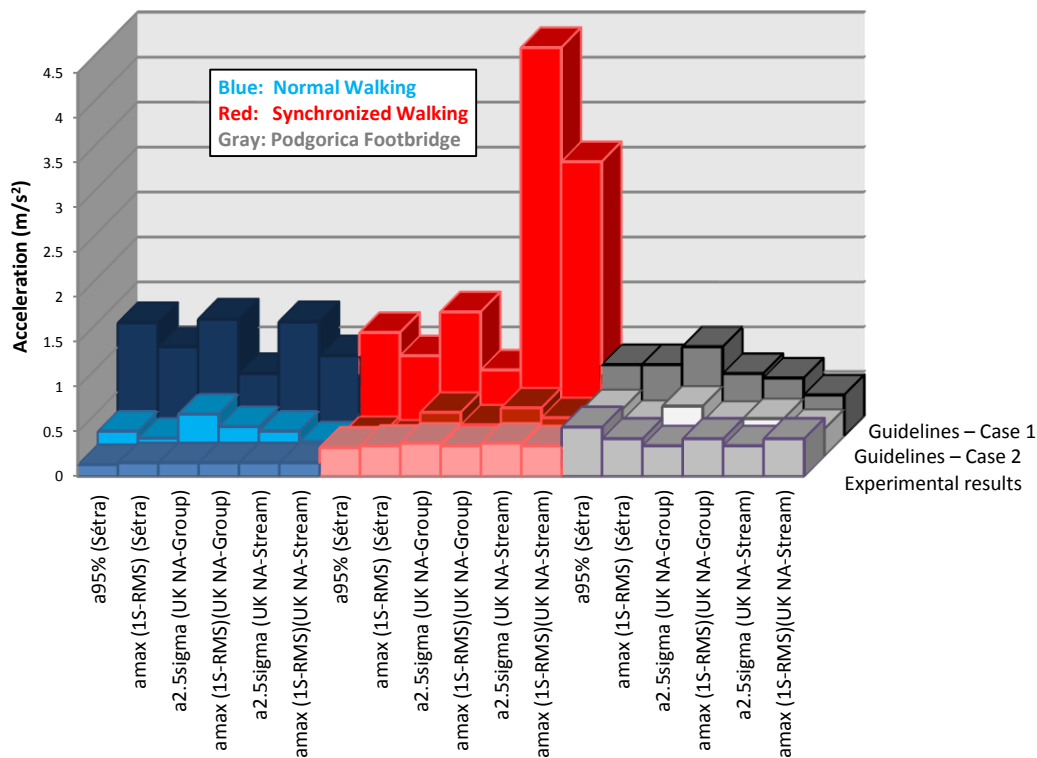


Figure 3.7. Comparison of acceleration response estimated by UK NA to EC1 (BSI, 2008) and French guideline (Setra, 2006) and experimental results

Results show that Sétra guideline overestimates the results in Case 1 of all the tests, but it gives a fairly good estimation of actual response in Podgorica footbridge in comparison with other two cases. Considerable improvement in accuracy of this method’s results is noticeable using standing people added damping (case 2 of tests).

Although UK National Annex to Eurocode 1 overestimates the results in Case 1 of all the tests, it gives a fairly good estimation in Test 3. Use of standing people added damping ratio has greatly enhanced the accuracy of results especially the results of Tests 2 and 3. Even though performance of ‘stream’ and ‘group’ load models of UK NA to EC1 were not consistent in all tests but ‘stream’ load model showed slightly better results.

The observed trend that both Sétra and UK NA to EC1 perform much better in Tests 2 and 3 was due to the fact that pacing frequency of pedestrians were closer to the natural frequency

of structure and therefore closer to the initial assumption of these guidelines. It should also be noted that both codes refer to much denser traffics than were considered in this chapter and therefore they need to be studied in more details in such cases.

Finally, although results of design guidelines are expected to be higher than actual values due to the safety margins considered, but the difference between them and the experimental values (mostly between (150%-800%)) in this research are found higher than the acceptable safety margins (usually less than extra 60%-70%) which results in an uneconomic designs. On the other hand, inconsistency in guideline results reduce considerably their reliability and is an indicator of inadequate accuracy in the design approach.

3.7 Conclusion

This chapter has reviewed two of the most widely used design guidelines for vibration serviceability assessment of footbridges subjected to multi-person traffic. Results of this study shows that these design guidelines mostly overestimate the response due to their conservative assumptions such as deterministic walking load model, neglecting inter- and intra-subject variability (Brownjohn, et al., 2004a), assuming pedestrians pacing frequency equal to frequency of one of excitable modes and overestimating traffic synchronization.

The use of damping of occupied structure (when pedestrians are standing still on it) instead of empty structure in calculations improved the accuracy of design guidelines results. This indicates considerable effects HSI on structural response and emphasizes the urgent need for further investigation of such effects. Quantification of these effects requires more comprehensive real-life measurements and detailed study of possible interaction mechanisms between walking people and vibrating structures.

Chapter 4

Mass-Spring-Damper Model of Walking Pedestrian

A Parametric Study

The contents of this chapter are adapted with minor changes from a conference paper presented at the 31th Conference and Exposition on Structural Dynamics (IMAC XXXI). Details of the paper are as follows:

Shahabpoor, E., Pavić, A. and Racić, V., 2013. Using MSD Model to Simulate Human-Structure Interaction during Walking. Conference Proceedings of the Society for Experimental Mechanics Series 2013. V 4, pp. 357-364.

4.1 Introduction

To address HSI, different types of mechanical or biomechanically-inspired models, such as single/multiple degrees of freedom MSDs (Archbold, 2004; Kim, et al., 2008; Archbold, et al., 2011; Caprani, et al., 2011; Silva and Pimentel, 2011) and single/bipedal inverted pendulum models (Bocian, et al., 2011; 2013; Qin, et al., 2013) are used to simulate kinematics of walking human in vertical direction. Each of these models has its own advantages and disadvantages and to some extent can describe what is happening in reality, but none of them are versatile in the sense that they are not universally applicable to different structures and loading scenarios.

Great level of simplification and approximation is unavoidable when modelling a walking human due to the complexity of its biodynamics. This is a specially the case for serviceability assessment of civil structures, where extensive details and accuracy is unnecessary comparing to the importance of practicality. Based on this, the present research has chosen the SDOF MSD to model walking human as the first and simplest estimation of human body dynamics. Although this model may not be the best option for replicating walking gait, the simplicity of its dynamics allows a very deep investigation of coupled human-structure system dynamics under different loading conditions.

Chapters 4 and 5, form the building blocks of this research by performing parametric study and sensitivity analysis of a SDOF MSD walking human model. The results of these studies can be used to assess the applicability of the model by comparing them with the experimental evidence reported in literature on effects of walking pedestrians on modal properties of structures.

Sections 4.2 and 4.3 describe the proposed coupled SDOF MSD model and its formulation. Section 4.4 discusses the parameters used in the models. Section 4.5 presents the results of the parametric study and discusses in details the effects of human model natural frequency

and damping ratio on modal properties of structures. Finally, section 4.6 closes the discussion by highlighting the important findings and conclusions.

4.2 SDOF MSD model description

For all simulations, a SDOF MSD model is used to simulate human dynamic effects on structures. Dynamic properties of the human model, m_h , k_h and c_h , are selected from a range of properties found in the literature and are presented in Section 0. To simulate the structural dynamics, only the first mode of vibration is considered and is modelled using an SDOF oscillator represented with m_s , k_s and c_s parameters. Considering only one structural mode does not affect the generality of the results as, for linear systems (acceptable assumption for civil structures under walking load), the superposition rule applies and modal contributions to physical response of the structure can be summed up to form the total response.

The SDOF MSD model used in simulations represents ‘Stationary’ walking pedestrian, the imaginary case in which human is walking but its location on the structure does not change. This is similar to the case when a treadmill is placed on a structure and a human is walking on that treadmill as shown in Figure 4.2. Being stationary, coupled system will form a conventional two degrees of freedom system as illustrated in Figure 4.1, the behavior of which can be studied using closed form solutions of 2DOF equations of motion.

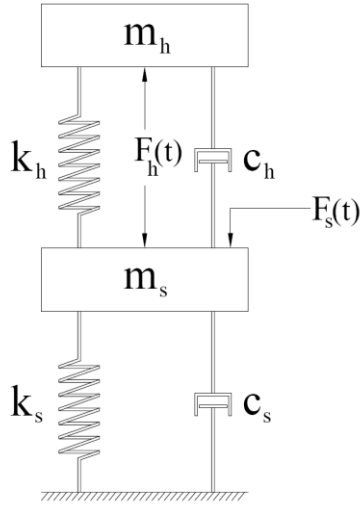


Figure 4.1: Conceptual 2DOF model of coupled system (stationary human)

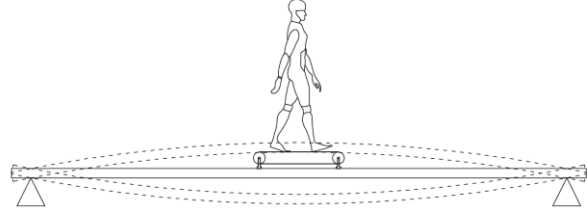


Figure 4.2: Physical representation of S-MSD model - a stationary human walking on the structure

Based on classical mechanics, a system of equations of motion for the presented two degrees of freedom system can be written as:

$$\begin{bmatrix} m_s & 0 \\ 0 & m_h \end{bmatrix} \begin{pmatrix} \ddot{x}_s(t) \\ \ddot{x}_h(t) \end{pmatrix} + \begin{bmatrix} c_s + c_h & -c_h \\ -c_h & c_h \end{bmatrix} \begin{pmatrix} \dot{x}_s(t) \\ \dot{x}_h(t) \end{pmatrix} + \begin{bmatrix} k_s + k_h & -k_h \\ -k_h & k_h \end{bmatrix} \begin{pmatrix} x_s(t) \\ x_h(t) \end{pmatrix} = \begin{pmatrix} F_s(t) - F_h(t) \\ F_h(t) \end{pmatrix}$$

(Equation 4.1)

Where m_s , c_s and k_s are mass, damping and stiffness of the structure and m_h , c_h and k_h are those of the human model. $\ddot{x}_s(t)$, $\dot{x}_s(t)$ and $x_s(t)$ are acceleration, velocity and displacement response of structure in coupled system. Similarly, $\ddot{x}_h(t)$, $\dot{x}_h(t)$ and $x_h(t)$ represent acceleration, velocity and displacement of the human mass. $F_s(t)$ can be any excitation apart from the human walking load and $F_h(t)$ is the human model driving force that excites the human DOF to produce a dynamic force similar to the actual walking force. Details of the selected parameters are described in Section 4.4. For parametric studies of this research, the proposed 2DOF system is solved analytically using modal analysis method and dynamic

properties of the coupled system are analysed accordingly.

4.3 Analysis cases

The natural frequency and the damping of the SDOF human model were selected for parametric studies and their effects on the dynamic behavior of the coupled human-structure system were investigated.

The Case 1 of parametric study comprise a set of simulations in which the stiffness of the human model was changed over a certain range to change the natural frequency of the human model (with constant mass). Effects of changing the human model natural frequency on the behavior of the coupled system was then analysed using Frequency Response Function (FRF) plots of the system for different human model parameters.

In Case 2 of the parametric study, damping of the human model was changed over a certain range. This is done for two different sets. Set 1 represents the case where natural frequency of the structure is higher than that of the human model and Set 2 represent the case where it is lower. Subsequently, the effects of changing the human model damping on behavior of the coupled system were discussed.

4.4 Model parameters

The parameters used in the human and structure combined 2DOF model are described in this section. These parameters are selected to be realistic, to cover the range of possible values (in the case of varying parameters) and to show the interaction effects on dynamic properties of both human and structure models clearly.

4.4.1 Dynamic parameters of the structure model

The dynamic parameters of human and structure models used in simulations are presented in Table 4.1 for different analysis cases. An imaginary light-weight simply supported beam is selected as the structure and its first mode properties, modal mass (m_s), stiffness (k_s) and

damping (c_s), are selected in a way to be both realistic and close to the dynamic properties of the human model to be able to see the interaction effects better.

Table 4.1: Dynamic parameters of human and structure models used in different analysis cases

Analysis case:	Case 1	Case 2		Unit
		Set 1	Set 2	
Empty Structure model parameters		Value/Range		
Modal mass	1000	1000		kg
Modal stiffness	1.0×10^5	2.0×10^5	1.0×10^5	N/m
Modal damping	600	600		Ns/m
Natural frequency	1.59	2.25	1.59	Hz
External force	0	0		N
External force (frequency)	0	0		Hz
Length of structure	12	12		m
Human model parameters		Value/Range		Unit
Mass	70	70		kg
Location	Mid-span	Mid-span		-
Driving force magnitude	210	210		N
Driving force frequency	2.05	2.05		Hz
Stiffness	$1.0 \times 10^3 - 10^5$	0.5×10^4	2.0×10^4	N/m
Damping	700	0 - 1000		Ns/m
Natural frequency	0.6 - 6	1.35	2.69	Hz

4.4.2 Dynamic properties of the human model

Human model stiffness and damping are selected from a range of properties found in the literature, mostly reported by biomechanics scientists based on measurements. According to the literature, stiffness and damping of a human are highly dependent on the type of activity and bio-features (Archbold, et al., 2011). The values reported by different researchers vary and are case sensitive (Lee and Farley, 1998; Geyer, et al., 1998; Zhang, et al., 2000; Rapoport, et al., 2003; Bertos, et al., 2005). Therefore, to cover the whole range of possible values for human stiffness and damping, wider stiffness range of 1×10^3 to 1×10^5 N/m and damping range of 0 to 1000 N.s/m is considered for parametric studies. This damping range is equivalent to 0 – 80% damping ratio for the assumed human mass and stiffness.

4.5 Parametric studies results

The results of parametric studies Cases 1 and 2 are presented in this section. FRF of the coupled system is used as a tool to describe and compare the dynamic properties of system in each case. Both FRF magnitude and phase diagrams are studied to analyze different aspects of the interaction effects.

4.5.1 Effects of human model natural frequency (Case 1)

In Case 1 analysis, the natural frequency of the empty structure is 1.59 Hz (Table 4.1). The stiffness of the human model is changed from 1×10^3 to 1×10^5 N/m to change its natural frequency from 0.6 – 6 Hz while keeping the mass constant. Effects of changing f_h on dynamics of coupled system were studied using its point-mobility FRF (excitation and response at structure DOF). Figure 4.3 and Figure 4.4, display the over-plotted FRF magnitudes and phases of coupled systems for different natural frequencies of the human model, respectively. Empty structure FRF is displayed with the green curve.

As coupled human-structure system form a two degrees of freedom system, it is expected to see two peaks in the FRF magnitude graph. But as the structure dominates the behaviour of the coupled system, often only a single peak with properties close to that of the structure can be seen. In reality, the point-mobility FRF of the coupled human-structure system is almost identical to the FRF of the mode with maximum response at structure DOF. This mode is called '*dominant mode*' and is taken to represent the modal properties of '*occupied*' structure.

Figure 4.3 shows that natural frequency of the occupied structure (dominant mode of 2DOF human-structure system) is slightly different compared with the natural frequency of empty structure as was expected. Comparing Figure 4.3 and Figure 4.5, it can be seen that when the natural frequency of human model f_h is less than the natural frequency of empty structure f_s , occupied structure has slightly higher frequency f_{os} than that of empty structure f_s (Red

curves in Figure 4.3). On the other hand, when the natural frequency of the human model f_h is higher than the natural frequency of the empty structure f_s , occupied structure has slightly lower frequency (Blue traces in Figure 4.3). Figure 4.5 shows that except for a sudden drop when the natural frequencies of the empty structure f_s and human model f_h are equal, the natural frequency of the occupied structure increase by increasing natural frequency of human model.

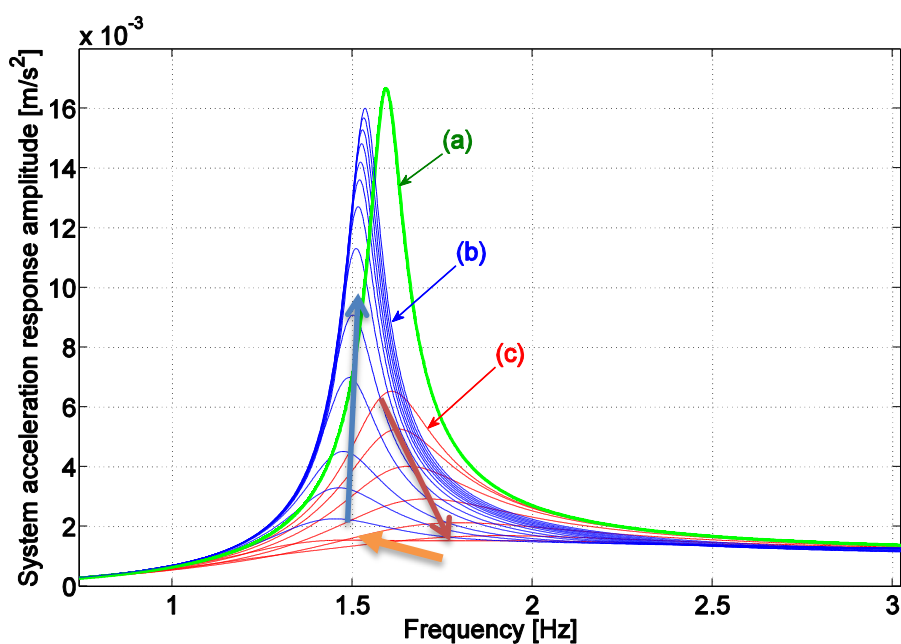


Figure 4.3. FRF magnitude of coupled system for different natural frequencies of human model a) Empty structure, b) Occupied structure with $f_h > f_s$, c) Occupied structure with $f_h < f_s$

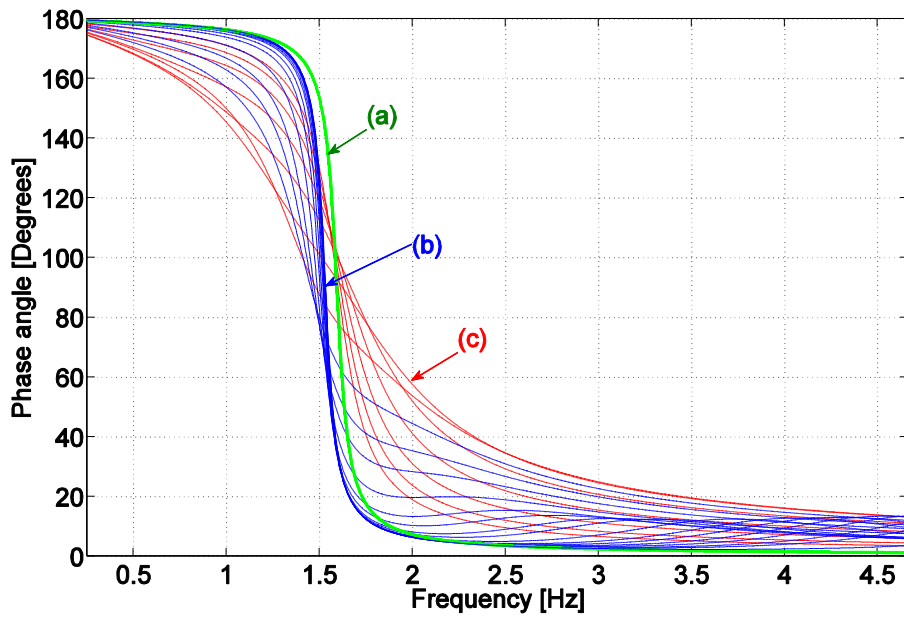


Figure 4.4. FRF phase of coupled system for different natural frequencies of human model a) Empty structure, b) Occupied structure with $f_h > f_s$, c) Occupied structure with $f_h < f_s$

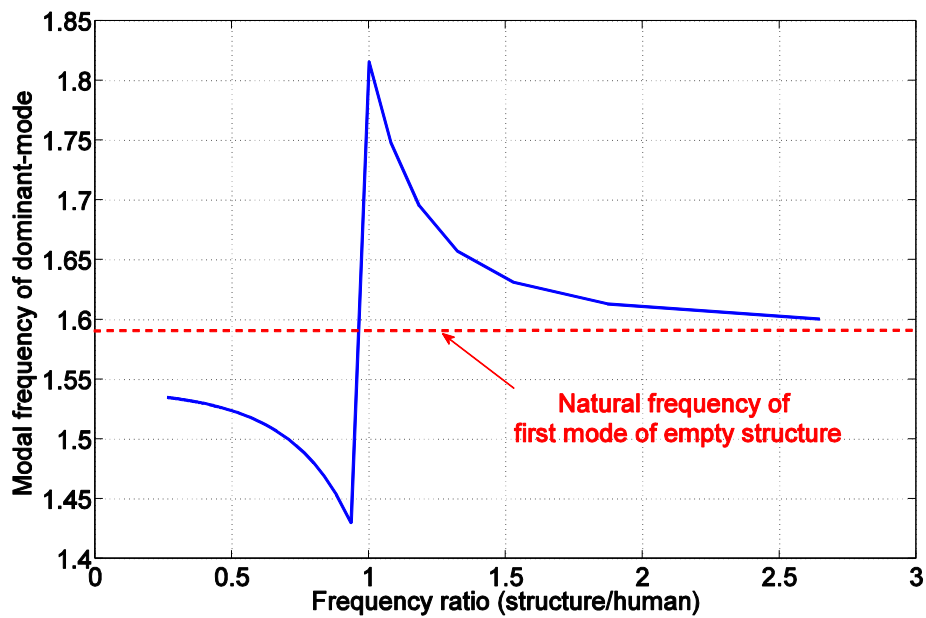


Figure 4.5. Effects of the natural frequency of the human model on the modal frequency of the occupied structure

Figure 4.6 illustrates the effects of changing the human model natural frequency on the damping of the occupied structure. It can be seen that the occupied structure has highest damping and least response, when the natural frequencies of the human model and empty structure are equal $f_h=f_s$ (frequency ratio equal to one).

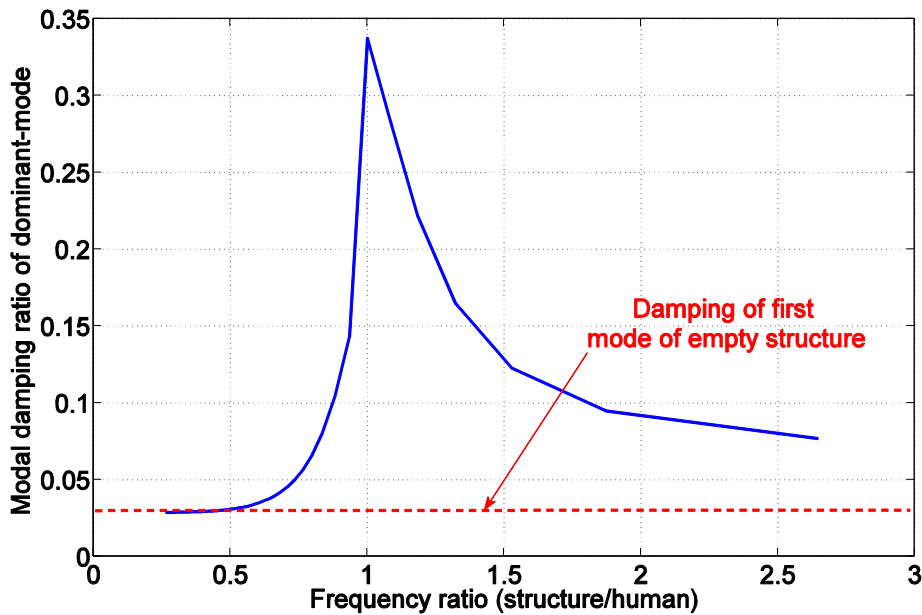


Figure 4.6. Effects of the natural frequency of the human model on the modal damping ratio of the occupied structure

4.5.2 Effects of human model damping (Case 2)

In Case 2, two sets of typical dynamic parameters for human and structure model were selected in such a way that natural frequency of empty structure in the Set 1 was less than natural frequency of empty structure ($f_h = 1.35 \text{ Hz} < f_s = 2.35 \text{ Hz}$) and for the Set 2 was higher ($f_h = 2.69 \text{ Hz} > f_s = 1.59 \text{ Hz}$). For this, the stiffness of the human and structure models are selected as 0.5×10^5 and $2.0 \times 10^5 \text{ N/m}$ in the first set and 2.0×10^4 and $1.0 \times 10^5 \text{ N/m}$ in the second set, respectively. A complete list of parameters used in each case is presented in Table 4.1. Damping of the human model was changed from 0 to 1000 N.s/m and its

effects on modal properties of the occupied structure were studied. Figure 4.8 and Figure 4.10 display the over-plotted FRF magnitude graphs of the occupied structure for different human damping ratio corresponding to Set 1 and 2 simulations.

As it can be seen in Figure 4.7, Figure 4.8, Figure 4.9 and Figure 4.10, damping ratio of occupied structure ζ_{os} increase by increasing damping ratio of the human model ζ_h . However, comparing the Figure 4.7 and Figure 4.9 shows that this increase does not occur with a same rate in Sets 1 and 2. Based on these figures, increasing damping ratio of the human model ζ_h from 0 to about 80%, increases modal damping ratio of occupied structure by 7% in Set 1 while this value is 1% for Set 2. This leads to the conclusion that rather than the damping, the natural frequency of the coupled systems, can determine how effective the presence of walking human can be on attenuation of structural response.

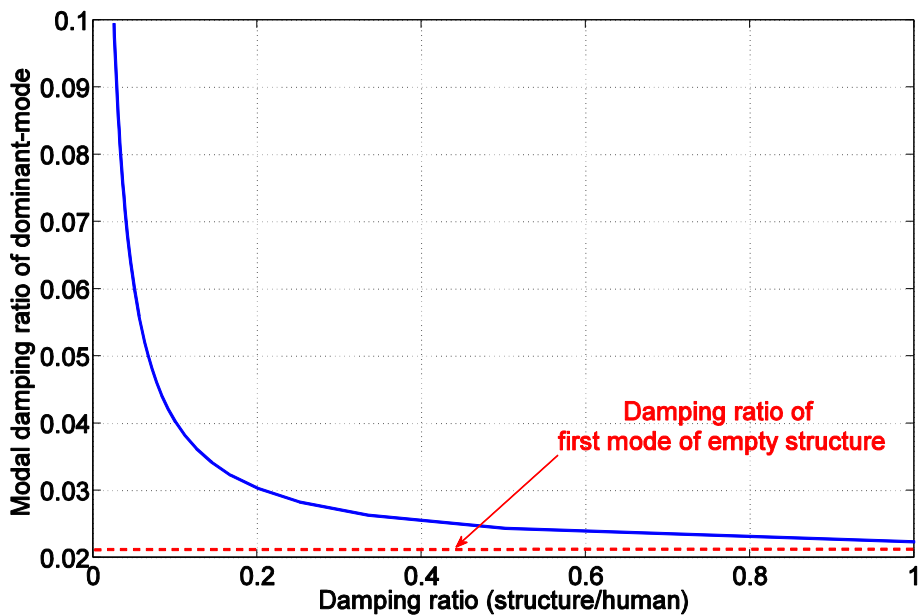


Figure 4.7. Effects of damping of human model on modal damping ratio of occupied structure (Set 1)

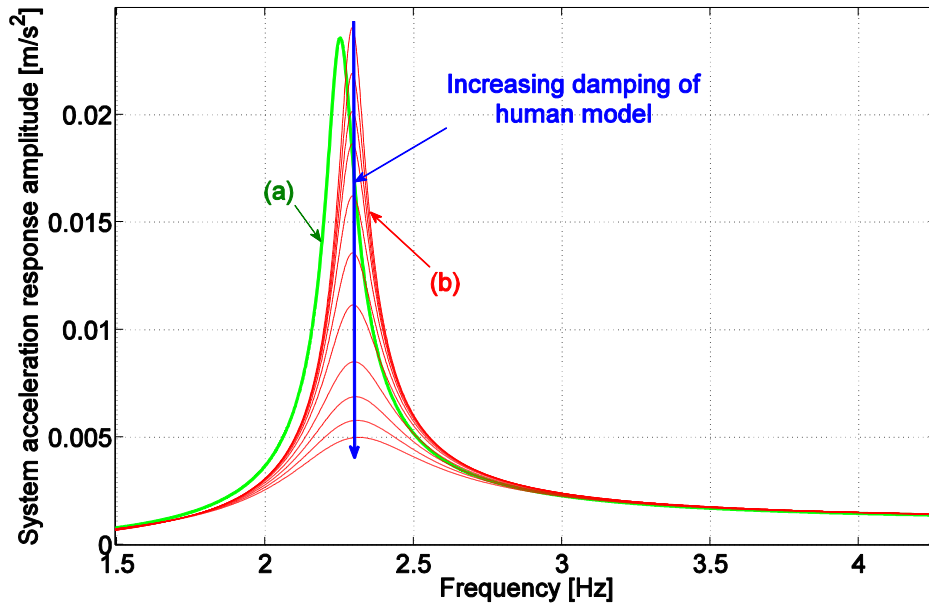


Figure 4.8. FRF magnitude of occupied structure for different damping values of human model (Set 1) a) Empty structure, b) Occupied structure when $f_h < f_s$

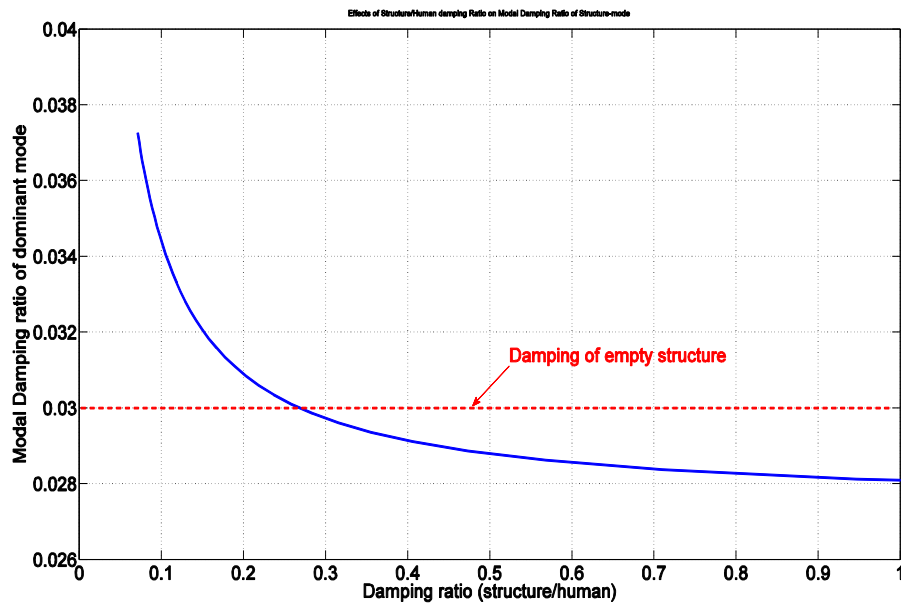


Figure 4.9. Effects of damping of human model on modal damping ratio of occupied structure (Set 2)

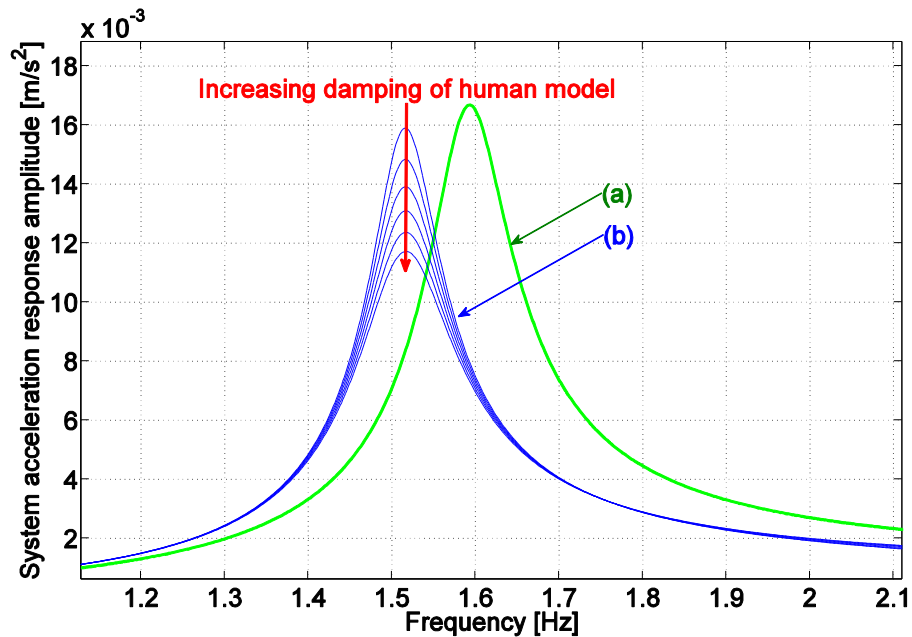


Figure 4.10. FRF magnitude of occupied structure for different damping values of human model (Set 2) a) Empty structure, b) Occupied structure when $f_h > f_s$

4.6 Conclusions

This chapter studied parametrically the performance of a classical SDOF MSD model to simulate effects of walking human on structures. It was found that natural frequency and damping of the human body have significant effects on the dynamic parameters of the structure. The results of this parametric study do not prove on their own that this model can be used to simulate interaction of walking people on structures, but provide valuable understanding of probable underlying mechanisms of HSI. An extensive set of experimental data collected from different types of structures and under different loading scenarios is required to validate and calibrate such models.

Chapter 5

Mass-Spring-Damper Model of Walking Crowd

A Sensitivity Analysis

The contents of this chapter are adapted with minor changes from a conference paper presented at the 5th International Conference on Structural Engineering, Mechanics and Computation (SEMC 2013). Details of the paper are as follows:

Shahabpoor, E., Pavić, A. and Racić, V., 2013. Sensitivity Analysis of Coupled Crowd-structure System dynamics to Walking Crowd Properties. In Proceeding of the 5th International Conference on Structural Engineering, Mechanics and Computation (SEMC 2013). pp. 143-148. ISBN: 978-1-138-00061-2; DOI: 10.1201/b15963-28

5.1 Introduction

This chapter extends the findings of the previous chapter by performing a sensitivity analysis on a crowd-structure system. A classic single-degree-of-freedom (SDOF) mass-spring-damper (MSD) model is used to simulate aggregated effects of a walking crowd on modal properties of supporting structure. The term ‘crowd’ here refers to a group of pedestrians with no correlation. Although this SDOF MSD model may not be the best option for modelling a walking traffic, the simplicity of its dynamics allows easy investigation of highly relevant coupled human-structure system dynamics under different loading conditions. The principal aim of this study is to improve understanding of the sensitivity of the occupied structure dynamic properties to each of the currently uncertain ‘crowd’ parameters. This is done for a range of common structures and crowd occupation scenarios and should help dealing with large uncertainty when modelling crowds on structures during design process.

Section 5.2 describes the proposed coupled MSD model and its formulation. Section 5.3 discusses the analysis specifications and Section 5.4 presents the parameters used in the models. Section 5.5 presents the results of the parametric study and sensitivity analysis and finally Section 5.6 closes this chapter by highlighting the important findings and conclusions.

5.2 SDOF MSD model description

To simplify the simulations, only the first mode of structural vibration is considered and is modelled using an SDOF oscillator represented by m_s , k_s and c_s parameters. Considering only one structural mode does not affect the generality of the results as mode superposition principle applies to linear structures which is an acceptable assumption for this kind of problem.

In all simulations, an SDOF MSD model (m_c , k_c and c_c) is used to simulate the aggregated effects of the crowd on the structure. This model represents ‘stationary’ walking pedestrians -an imaginary case in which people are walking on the ‘anti-node’ of the first mode of vibration but their location on the structure does not change. Being stationary, the coupled crowd-structure system can be formulated as a conventional two degrees of freedom system as illustrated in Figure 5.1.

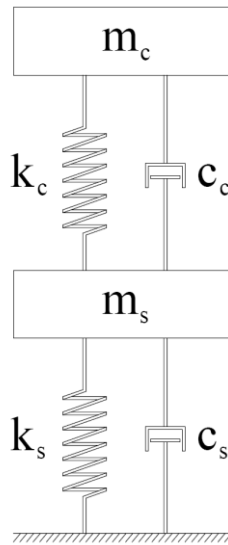


Figure 5.1. Conceptual 2DOF model of coupled crowd-structure system (stationary walking people)

The detailed discussion on the 2DOFs crowd-structure model and its equations of motion is presented in Section 4.2.

5.3 Analysis Specifications

The natural frequency f_{os} and damping ratio ζ_{os} of the occupied structure were chosen to represent dynamics of the occupied structure. In the first step, crowd model parameters m_c , k_c and c_c were changed one at a time and effects of each parameter on natural frequency f_{os}

and damping ratio ζ_{os} of the occupied structure are analysed.

In the next step, the ‘rate of change’ of f_{os} and ζ_{os} with respect to change of crowd’s model properties m_c , k_c and c_c is considered as the sensitivity criteria. The chosen rate of change provides a measure of ‘how fast’ the occupied structure properties f_{os} and ζ_{os} change as uncertain crowd’s parameters m_c , k_c and c_c change.

To allow for comparison, as units of parameters are different, a typical set of initial values for structure and crowd model parameters (m_{ci} , c_{ci} , k_{ci} , f_{si} and ζ_{si}), are selected and unit-less ratios m_c / m_{ci} , c_c / c_{ci} , k_c / k_{ci} , f_{os} / f_{si} and ζ_{os} / ζ_{si} are used for presentation. To ensure the generality of results, the same analysis is repeated for several initial values and results are compared. The effects on f_{os} and ζ_{os} are considered for the changes of m_c (Case 1), k_c (Case 2), and c_c (Case 3). In all three cases, the selected crowd parameter is varying over a certain range and other two parameters of the crowd model are kept constant and equal to the initial set of values.

5.4 Model parameters

The parameters used in the crowd - structure 2DOF model are described in this section. These parameters were selected to be realistic and to cover a range of possible values (in the case of the varying parameter).

5.4.1 Dynamic parameters of structure model

The dynamic parameters of the crowd and structure models used in simulations are presented in Table 5.1 for different analysis cases. An imaginary simply-supported beam is selected as the structure and its first mode properties m_{si} , k_{si} and c_{si} are selected in a way to be both realistic and corresponding to a light weight structure. The latter is needed to show the interaction effects better. Three different natural frequencies (and therefore stiffnesses for the

same mass m_{si} of 6500 kg) were selected for the structure to cover the scenarios in which the natural frequency of the structure f_s is lower, close to and higher than the natural frequency of the crowd model f_c .

Table 5.1. Parameters of human and structure models used in different analysis cases

Analysis case	Initial values	Case 1	Case 2	Case 3	Unit
Structure model parameters					
Mass			6500		kg
Damping ratio			0.005		-
Natural frequency			2 - 4		Hz
Crowd model parameters					
Mass	168	8.4 - 462	168	168	kg
Stiffness	61698	61698	3085 - 169669	61698	N/m
Damping	1803	1803	1803	90 - 4958	N.s/m
Damping ratio	0.28	1.25 - 0.169	0.984 - 0.133	0.014-0.770	-
Natural frequency	3.05	13.64 - 1.84	0.68 - 5.06	3.05	Hz

5.4.2 Dynamic properties of crowd model

The initial parameters of the crowd model m_{ci} , c_{ci} and k_{ci} are adopted from the results of studies done by the authors to simulate crowd's dynamics on a real-life test structure. An extensive set of experiments were carried out on the Sheffield footbridge with groups of 2-15 pedestrians walking on it. An SDOF MSD crowd model was then fitted to each test scenario and the corresponding crowd parameters were found. The parameters corresponding to a group of 6 walking pedestrians were selected as the initial values for the crowd model. A six-people group represents a normal spatially-unrestricted crowd on the studied test structure and is a very good starting point to study the effects of varying crowd parameters.

The ranges of possible crowd parameters m_c , c_c , k_c are adopted from the values reported by researchers for individuals and groups of people (Archbold, et al., 2011; Zhang, et al., 2000; Rapoport, et al., 2003; Bertot, et al., 2005; Lee and Farley, 1998; Geyer, et al., 1998)

and are presented in Table 5.1.

5.5 Results of the analysis

Distinction should be made between the results that are presented in Sections 5.5.1 and 5.5.2. The former provide a measure of ‘*how effective*’ crowd parameters m_c , k_c and c_c are on occupied structure f_{os} and ζ_{os} (parametric study) while the latter gives a measure of the sensitivity of f_{os} and ζ_{os} to crowd’s uncertain parameters.

5.5.1 Parametric analysis

Figure 5.2 and Figure 5.3 present a typical set of results for $f_{si} = 4$ Hz. Results of analysis Cases 1, 2 and 3 corresponding to changing crowd’s m_c , k_c and c_c are plotted on the same graph for comparison. The horizontal axis presents the ratio of the crowd parameters to their initial values, ‘X’, while the vertical axis presents the ratio of the changes in the occupied structure parameters ‘Y’. These parameters are presented in Equation 5.1 and 5.2 respectively.

$$X = x_c / x_{ci} \quad \therefore \quad (x_c = m_c, c_c, k_c) \quad \text{(Equation 5.1)}$$

$$Y = y_{os} / y_{si} \quad \therefore \quad (y_{os} = f_{os}, \zeta_{os}) \quad \text{(Equation 5.2)}$$

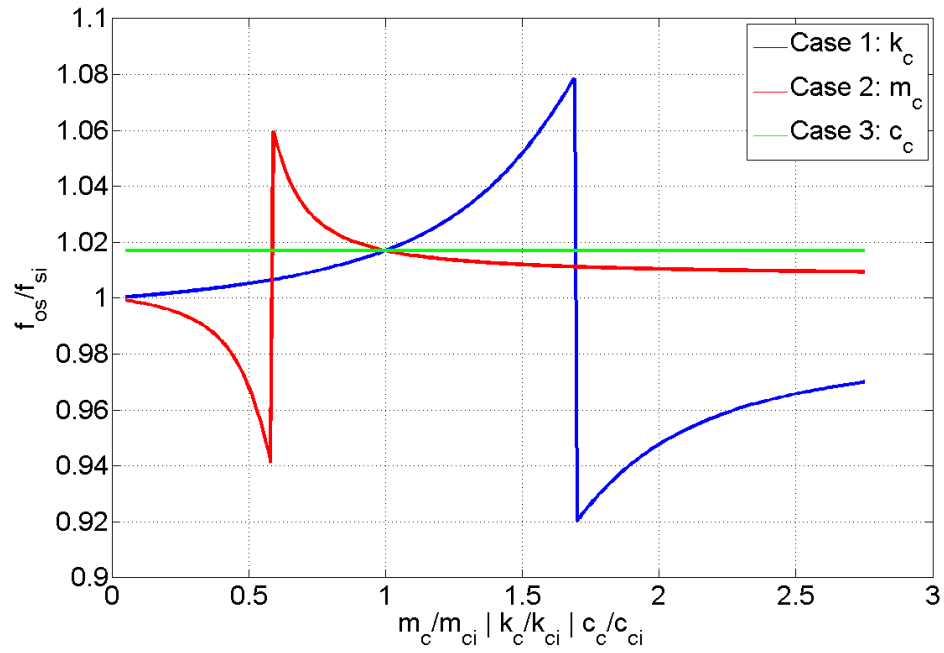


Figure 5.2. Effects of the m_c , k_c and c_c on f_{os} ($f_{si} = 4$ Hz)

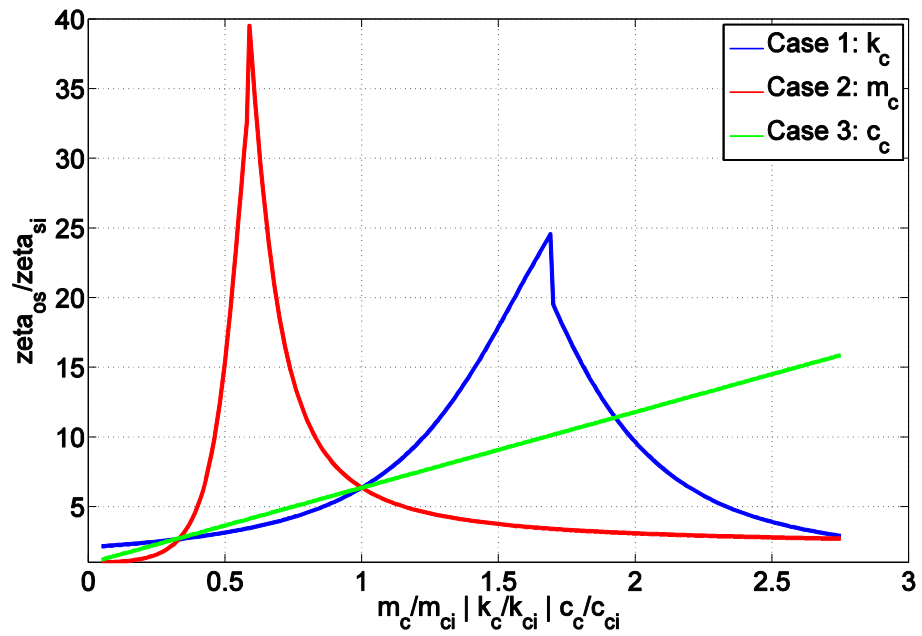


Figure 5.3. Effects of the m_c , k_c and c_c on ζ_{os} ($f_{si} = 4$ Hz)

As the natural frequency of a SDOF is proportional to k/m , increase of stiffness or decrease of mass leads to the increase of the natural frequency. Keeping this in mind and knowing that $f_{ci} = 3.05$ Hz and $f_{si} = 4$ Hz in Figure 5.2 and Figure 5.3, increasing stiffness of the crowd model k_c (blue curves) or decreasing its mass m_c (red curves) leads into increase of the crowd model natural frequency f_c and makes it closer to the structure's initial frequency f_{si} .

A closer look at Figure 5.2 and Figure 5.3 shows that the extreme values of m_c and k_c graphs (red and blue curves) represent the cases where natural frequencies of the crowd and initial structure model are equal ($f_{si}=f_c$). This means that m_c and k_c have maximum effects on f_{os} and ζ_{os} when $f_{si}=f_c$. The abrupt changes in Figure 5.2 is due to change of f_{si} and f_c relation, where $f_{si}<f_c$ scenario turn into $f_{si}>f_c$ for mass curve (red trace) and $f_{si}>f_c$ scenario turn into $f_{si}<f_c$ for stiffness curve (blue trace). It also can be seen that increasing ζ_c has no significant effects on f_{os} but increases ζ_{os} . It needs to be mentioned that the curves presented in Figure 5.2 and Figure 5.3 is corresponding to the system with proportional damping matrix. In systems with non-proportional damping distribution, natural frequency is dependent on damping but its effects is not significant. Further discussion on this issue is beyond the scope of this study.

To compare the effects of the crowd's parameters m_c , c_c , k_c on the occupied structure's dynamics, a family of initial values is considered in which initial natural frequency of crowd model f_{ci} is 3.05 Hz and structure initial natural frequency f_{si} varies from 2 to 4 Hz. For each (f_{ci}, f_{si}) pairs, a set of X vs Y curves similar to the ones presented in Figure 5.2 and Figure 5.3, are plotted. Maximum absolute value of each of X vs Y graphs are then plotted against their corresponding f_{ci}/f_{si} (which is equal to $3.05/f_{si}$) and are presented for f_{os}/f_{si} and ζ_{os}/ζ_{si} in Figure 5.4 and Figure 5.5 accordingly.

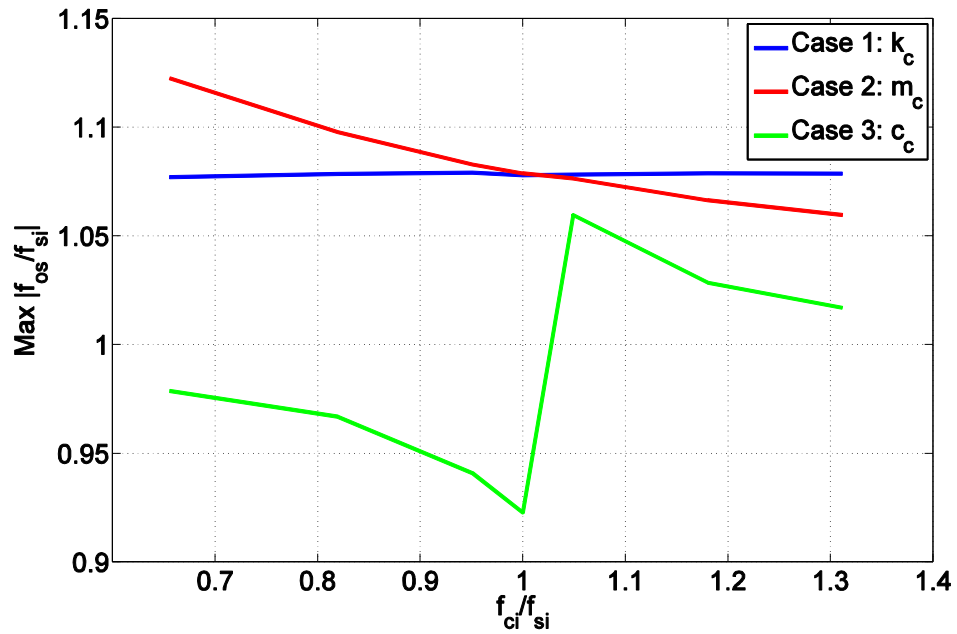


Figure 5.4. Maximum effects of the m_c , k_c and c_c on f_{os} for $f_{ci}= 3.05$ Hz and f_{si} varying from 2-4 Hz

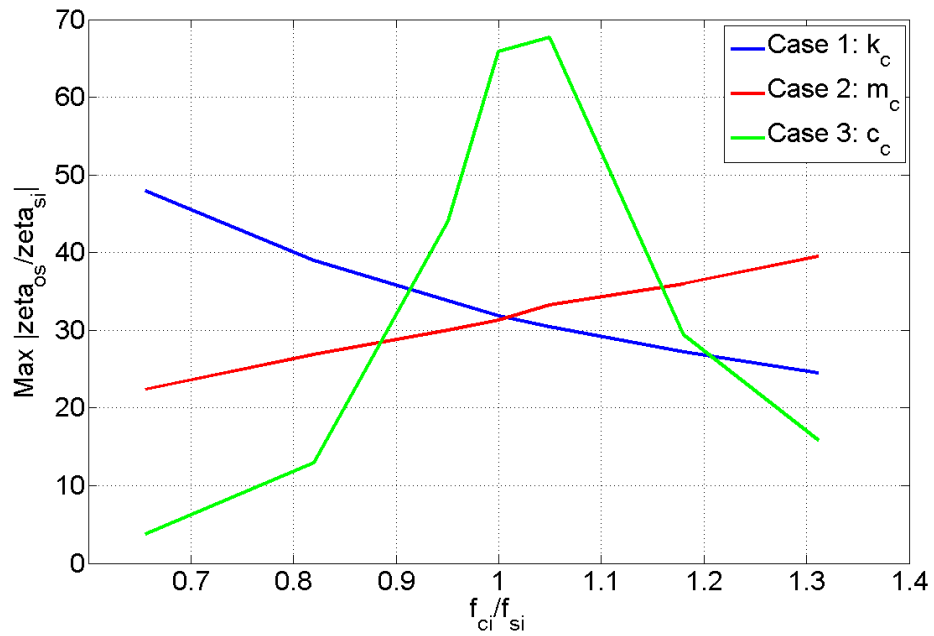


Figure 5.5. Maximum effects of the m_c , k_c and c_c on ζ_{os} for $f_{ci}= 3.05$ Hz and f_{si} varying from 2-4 Hz

As it can be seen in Figure 5.4 and Figure 5.5, as $3.05/f_{si}$ increases, maximum effects of m_c on f_{os} decrease and its effects on ζ_{os} increase. k_c has the opposite effects and as $3.05/f_{si}$ increases, its maximum effects on f_{os} increase and on ζ_{os} decrease. Maximum effects of crowd's damping c_c on both f_{os} and ζ_{os} is highest when $f_{ci}=f_{si}$.

5.5.2 Sensitivity analysis

Sensitivity here is defined as the rate of change of f_{os} and ζ_{os} to the changes in m_c , k_c and c_c . It is an indicator of 'how fast' the effects of the crowd parameters on the occupied structure parameters change. Results of this section are presented in Figure 5.6, Figure 5.7, Figure 5.8 and Figure 5.9. In these figures, the horizontal axis presents the ratio of the crowd parameters X as is given in Equation 5.1 and the vertical axis presents derivative of Y (Equation 5.2) with regards to X.

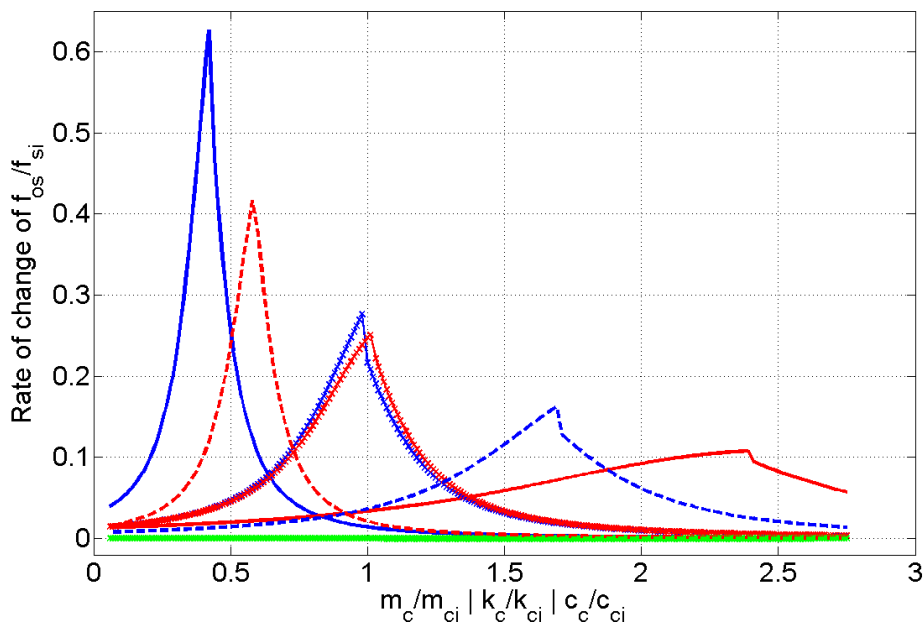


Figure 5.6. Sensitivity of f_{os} to m_c (red curves), k_c (blue curves) and c_c (green curves). Continues curves. $f_{si}=2$ Hz, crossed curves: $f_{si}=3$ Hz and dashed curves: $f_{si}=4$ Hz.

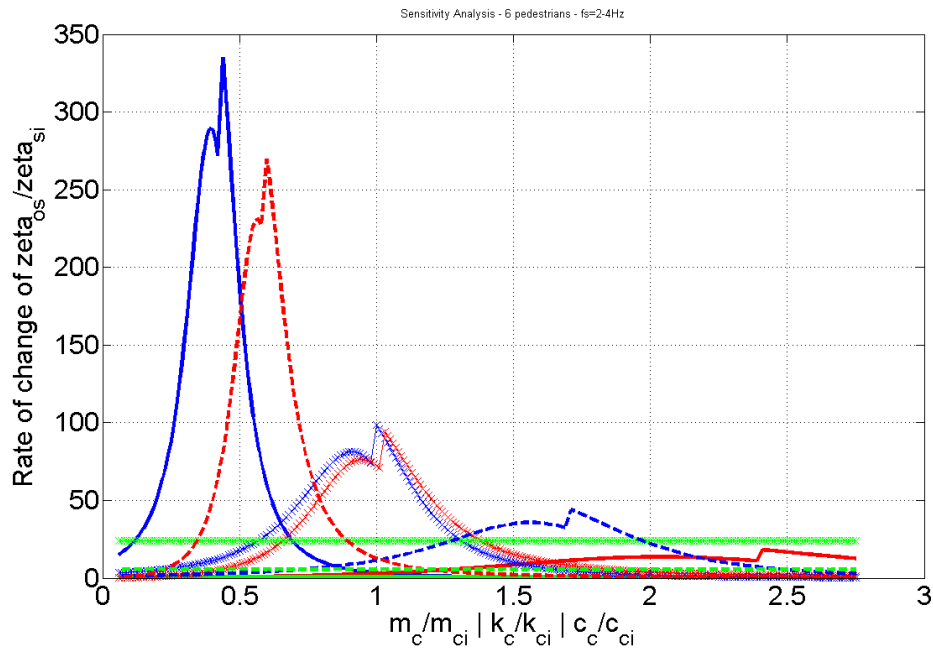


Figure 5.7. Sensitivity of ζ_{os} to m_c (red curves), k_c (blue curves) and c_c (green curves).
 Continues curves: $f_{si} = 2$ Hz, crossed curves: $f_{si} = 3$ Hz and dashed curves: $f_{si} = 4$ Hz.

Figure 5.6 displays the sensitivity of f_{os} and Figure 5.7 displays the sensitivity of ζ_{os} for two typical initial structural frequencies $f_{si} = 2$ and 4 Hz. Similar to the findings in Section 5.5.1, sensitivity of ζ_{os} and f_{os} to m_c and k_c increase significantly when frequency of the crowd and structure models are close in value.

For the case $f_{ci} < f_{si}$ (when $f_{si} = 4$ Hz), as both Figure 5.6 and Figure 5.7 show, when k_c (dashed blue curve) increase from k_{ci} and mass m_c (dashed red curve) decrease from m_{ci} , their corresponding sensitivity curves show a peak. These peaks can be shown to correspond to $f_{si} = f_c$. The same applies when $f_{ci} > f_{si}$ (when $f_{si} = 2$ Hz) and the sensitivity curves show maximum when k_c (blue trace) decrease and m_c (red trace) increase. Also, as Figure 5.6 illustrates, rate of change of f_{os} is not sensitive to c_c while sensitivity of ζ_{os} is maximum when $f_{si} = f_{ci}$ (crossed green line in Figure 5.7).

To compare the sensitivity of f_{os} and ζ_{os} to m_c , k_c , and c_c , the same family of initial values that are described in the previous section is considered in which $f_{ci} = 3.05$ Hz and f_{si} varies from 2 to 4 Hz. For each (f_{ci}, f_{si}) pairs, then, a set of X vs Y' curves similar to the ones presented in Figure 5.6 and Figure 5.7 are plotted. Maximum values of X vs Y' graphs are then plotted against their corresponding f_{ci}/f_{si} and are presented for f_{os} and ζ_{os} in Figure 5.8 and Figure 5.9 accordingly.

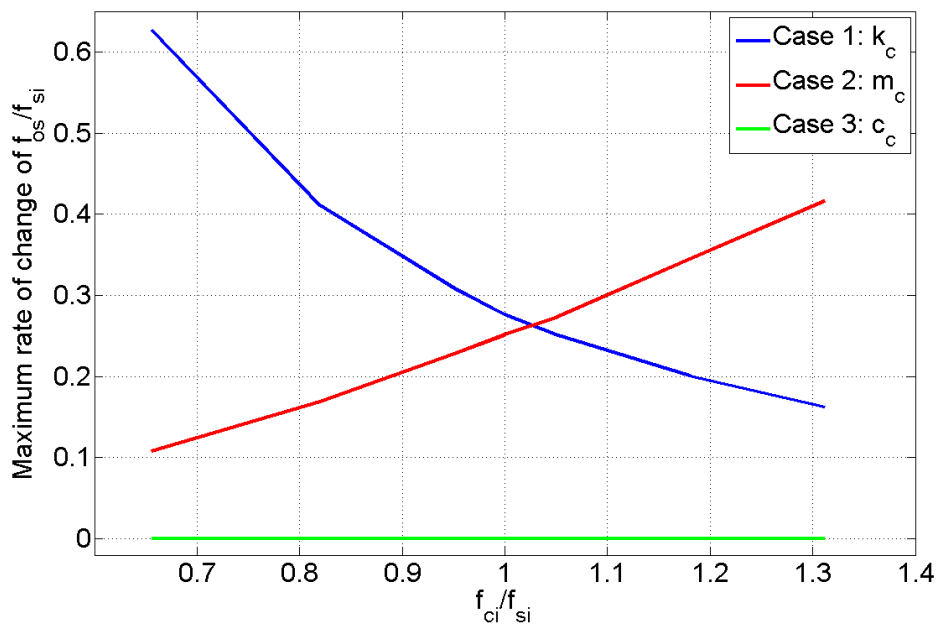


Figure 5.8. Maximum sensitivity of the f_{os} to m_c , k_c and c_c for $f_{ci}= 3.05$ Hz and f_{si} varying from 2-4 Hz

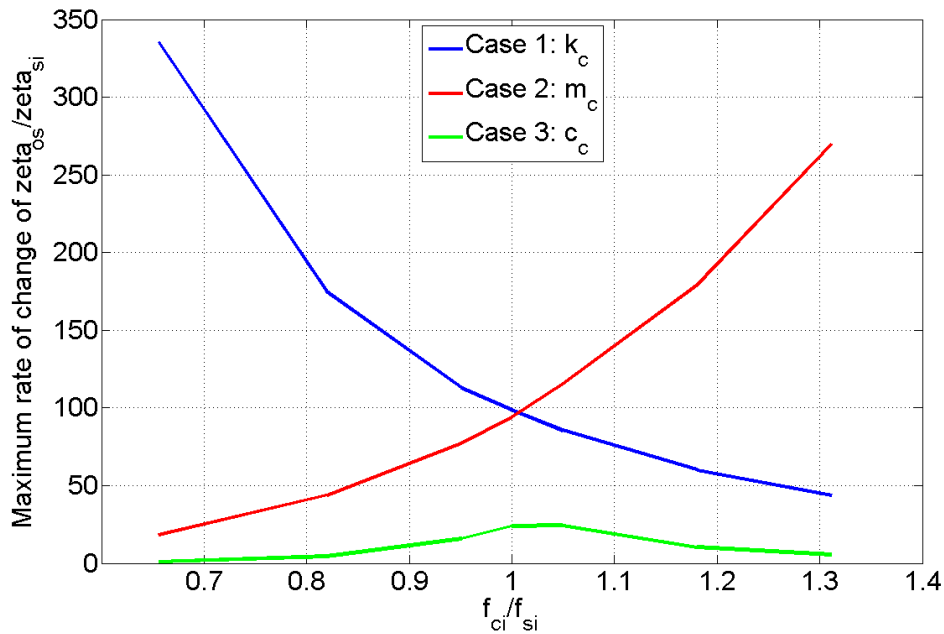


Figure 5.9. Maximum sensitivity of the ζ_{os} to m_c , k_c and c_c for $f_{ci}= 3.05$ Hz and f_{si} varying from 2-4 Hz

It can be seen in Figure 5.8 and Figure 5.9 that by increasing the f_{si} , maximum sensitivity of the f_{os} and ζ_{os} to k_c decrease (blue curves) and its maximum sensitivity to m_c increase (red curves). This means that when $f_{ci} < f_{si}$, both f_{os} and ζ_{os} are more sensitive to k_c , while when $f_{ci} > f_{si}$, both f_{os} and ζ_{os} are more sensitive to m_c . It also can be seen that f_{os} has no sensitivity to c_c while ζ_{os} shows a limited sensitivity to c_c with the maximum at $f_{ci} = f_{si}$.

5.6 Conclusion

Modelling crowd dynamics on structures have always been a challenge due to uncertainty of human parameters. The study presented in this chapter combines results of the parametric study and sensitivity analysis that are done on a 2DOF mass-spring-damper human-structure model to describe effects and sensitivity of the occupied structure to the crowd model parameters m_c , k_c and c_c . Results of this analysis provide valuable insight for engineers to choose more realistic crowd properties during design process and researchers to understand better the human-structure interaction mechanisms.

Chapter 6

Effects of Multiple Pedestrian Traffic on Dynamic Properties of Structures

Experimental Studies

The contents of this chapter are adapted with minor changes from the following journal paper in preparation to be submitted to the Engineering Structures:

Shahabpoor, E., Pavić, A., Racić, V. and Zivanovic, S. Effect of Multiple Pedestrian Traffic on Dynamic Properties of Structures. Engineering Structures.

6.1 Introduction

A number of studies, mostly based on full-scale measurements, have found that a passive human (sitting and standing) has significant effect on dynamic properties of the structure and therefore their effects cannot be ignored. Typical findings include a considerable reduction in vibration response and slight change in the natural frequency of structure occupied by passive pedestrians and excited by some other means (Sachse, 2002; Ellis and Ji, 1994). These effects could be simulated using an SDOF model for stationary people identified by Sachse (2002). Zivanovic, et al. (2009) have observed the similar effect of walking people on modal properties a structure vibrating in the vertical direction. Prompted by their findings, the experimental study presented in this chapter is a logical extension designed to collect much more comprehensive experimental data and to perform a more detailed identification of the modal properties of the *walking*, as opposed to stationary, crowd SDOF model.

In this study, an extensive set of experiments were designed and performed to capture and quantify the effects of standing and walking people on dynamic parameters of vibrating base structure. The key assumptions made in analysis are discussed in Section 6.2 and modal properties of the empty structure are described in Section 6.3. The tests done with standing people and walking people are presented in Sections 6.4 and 6.5, respectively. Results of these two scenarios are compared in Section 6.6 and an analytical verification is presented in Section 6.7 to check and validate the experimental findings. The main findings of the study are finally presented in Section 6.8.

6.2 Key assumptions

In the context of the study presented in this chapter, a group of pedestrians and the occupied structure are each modelled as a stationary SDOF system, thus making a 2DOF system when combined in series together. Curve fitting of measured Frequency Response Functions (FRFs) of the occupied structure is used in Sections 6.4 and 6.5 to obtain the modal

properties of the coupled human-structure system. Unlike the empty structure (Section 6.3) or when occupied by only standing people (Section 6.4), time-varying locations of walking pedestrians (Section 6.5) result in essentially time-varying dynamic properties of the coupled system, which makes the FRF records noisy and difficult to curve-fit using linear models. However, FRFs were measured during tests when people were walking over the test structure using a simultaneous shaker chirp excitation with a narrow frequency bandwidth around the targeted natural frequency of the empty structure. Hence, the pedestrian excitation (walking force) was assumed to be an uncorrelated background noise which could be averaged out.

The modal properties were considered time-invariant under the assumption that the pedestrian flow is in the steady state regime, i.e. individuals in a group do not change significantly their gait during the test. Consequently, it was assumed that the coupled system exhibits a linear behaviour.

Effects of time-varying location of people on the structure, as is ‘random’ in nature, was minimized by averaging the FRFs over test duration so that modal properties of the occupied structure can be estimated as a set of constant values. The data collection lasted for up to 15 minutes for each test to enable sufficient averaging of the FRFs, thus to maximise their stability in time.

6.3 Modal properties of empty test structure

The test structure used in this study was the Sheffield University footbridge. The detailed description of the structure and its modal properties are presented in Sections 3.3.1 and 3.5.1, respectively.

6.3.1 Non-linear behaviour of the empty structure

Knowledge about potential non-linear of the structure plays an important role when judging if changes in the modal properties of the occupied structure are related to the presence of pedestrians or to some form of structural non-linearity. For instance, it is well known that damping often increases with increasing vibration amplitudes due to engagement of additional damping mechanisms, such as hysteresis due to friction at the supports. Therefore, Zivanovic, et al., (2009) analyzed amplitude-dependent behavior of first mode damping ratio and modal frequency of Sheffield footbridge by curve-fitting cycle-by-cycle free vibration decays of structure a mid-span. The results are shown in Figure 6.1.

From visual inspection of the graphs in Figure 6.1 it is apparent that the structure indeed shows some amplitude-dependent non-linear behavior. While acceleration amplitudes increase from 0.2 m/s^2 to 1.8 m/s^2 damping ratio increases from 0.45% to 0.65% and the natural frequency is reduced slightly from 4.45 Hz to 4.385 Hz.

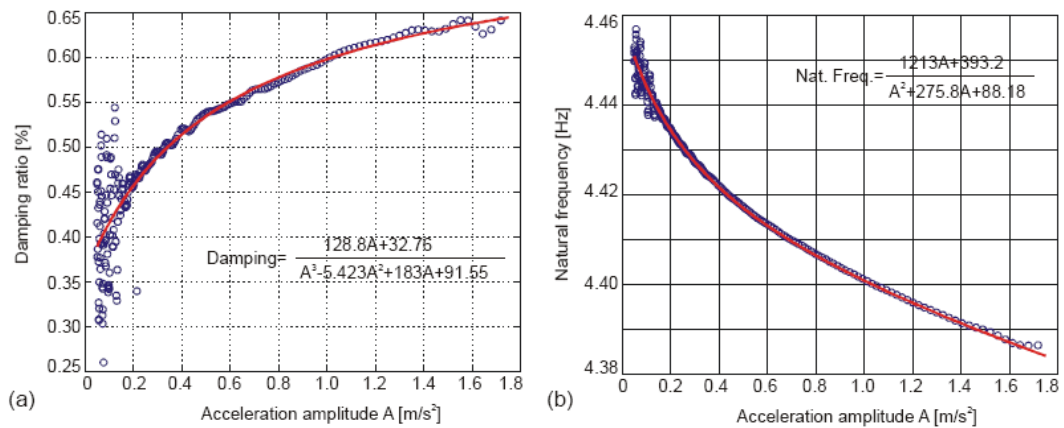


Figure 6.1. Nonlinear amplitude-dependent damping and natural frequency of structure (after Zivanovic, et al., (2009))

The results illustrated in Figure 6.1 suggest that the dynamic properties of the empty

structure need to be identified at the same vibration level as it would be induced by walking people. The next sections show how the relevant information can be obtained for the first two vertical modes of the slab.

6.3.2 Modal testing using narrow band excitation

The pedestrian tests presented in this chapter, referred to as test Series A and B, were done in two test campaigns one year apart with different test subjects, but with nominally identical hardware setup. Two chirp excitations with frequency contents of 3.5-5.5 Hz and 15-18 Hz were applied to the structure targeting the first and the second vertical mode of vibrations, respectively. Operating in the direct-drive mode (the moving part of shaker was connected to the structure directly using a rod), the shaker was placed under the mid-span of the structure to predominantly excite the first mode and in the quarter-span to predominantly excite the second mode of vibration. In each case, the point mobility FRF was used in the subsequent modal identification.

Modal mass of 7128 kg (calculated using mode shapes and distributed mass of structure) was used in the curve-fitting of the measured FRFs for both modes. Unity-scaled sinusoidal mode shapes were assumed for both vertical modes to reduce the number of unknowns and make the curve-fitting easier. The empty structure modal properties are presented in Table 6.1.

Table 6.1. Results of modal analysis of the empty structure

Mode No.	FRF based						
	f_{es} (Hz)	ζ_{es} (%)	m_{es} (kg)	c_{es} (N.s/m)	k_{es} (N/m)	$a_{es,max}$ (m/s ²)	$a_{es,rms}$ (m/s ²)
1 (Series A)	4.44	0.6	7,128	2,386	$5,547 \times 10^3$	1.8782	0.3680
1 (Series B)	4.44	0.7	7,128	2,784	$5,547 \times 10^3$	2.6084	0.4826
2 (Series A)	16.87	0.4	7,128	6,044	$80,086 \times 10^3$	2.5080	0.4769
2 (Series B)	16.77	0.4	7,128	6,009	$79,140 \times 10^3$	3.2123	0.5942

6.4 Tests with standing people

Although the main focus of the present study is on the effects of walking people on modal properties of the structure, a limited number of tests were performed using the same people standing still (i.e. being stationary) as well under nominally identical test conditions to compare their effects with the effects of walking people. The detailed description of these tests is presented in this section and compared with walking tests results in Section 6.6.

6.4.1 Experimental setup

FRF-based modal testing of the human-structure system was carried out using the same accelerometer layout as in the tests with the empty structure described in Section 3.5.1. To make a clear standing space in the mid-span and to ensure safety of the participants, as previously mentioned, the shaker was placed in a recessed pit under the slab and connected to the structure from beneath via a steel rod at the mid-span. The shaker force was measured directly by a uniaxial ENTRAN load cell attached to the rod.

Since the human body is a dynamic system, its location on the slab can considerably influence the FRF measurements. In case of the first vibration mode, a person standing in the mid-span (i.e. the anti-node of the first mode) has the greatest interaction with the structure while a person standing on the supports (i.e. the node of the first mode) interacts little and makes no difference to the FRF measured. Therefore, all participants were standing close together at the mid-span, so their aggregated effects could be modelled using a SDOF attached to the structure in a single point (i.e. mid-span) (Sachse, 2002).

The tests were carried out for groups of three, six and ten people as shown in Figure 6.2. Each circle in the figure represents a single person while the number inside the circles shows the group size in a particular test. For instance, the six circles with number 6 inside correspond to the positions of the participants in the test with six standing people.

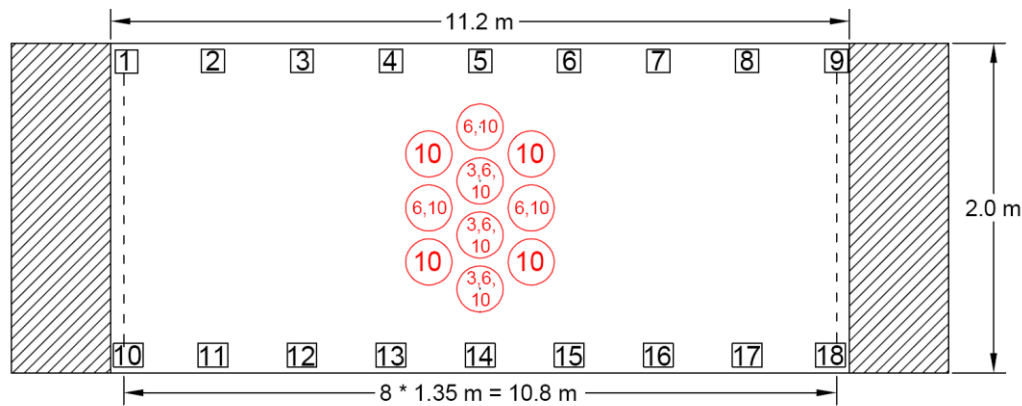


Figure 6.2. FRF-based modal test setup for standing still pedestrians tests (Mode 1)

The same chirp excitation used in Section 6.3.2 was used here to excite the occupied slab around its first vertical mode. In each test, five FRF data blocks each lasting 64s were recorded and averaged. In each data block the excitation lasted the first 51.2s, while the remaining 12.8s allowed the response signal to die out before the acquisition of the next data block started.

A typical force time history during each data block is shown in Figure 6.3 (a) together with its frequency content shown in Figure 6.3 (b). The corresponding time and frequency domain acceleration responses in the mid-span measured during the test with three standing people are shown in Figure 6.3 (c) and (d). The response is the numerical average of accelerations measured in TP 5 and 14 which are nominally identical for the first vertical mode of vibration (Figure 6.2).

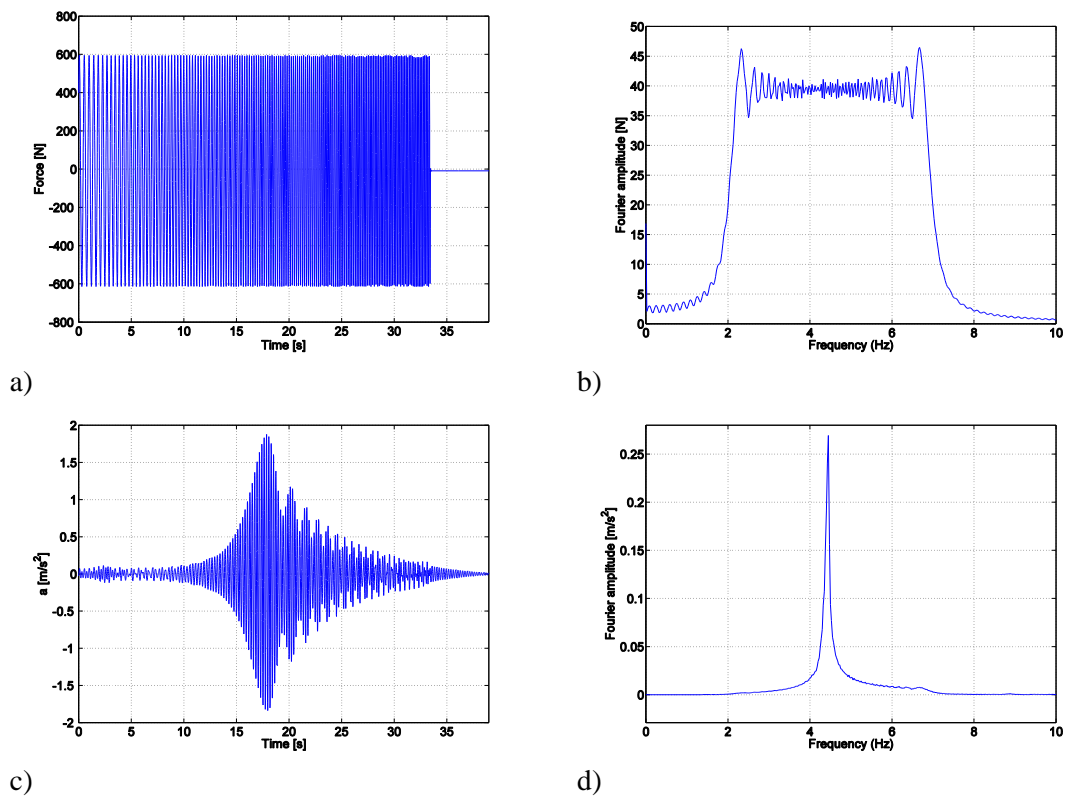


Figure 6.3. Time-domain and frequency-domain representation of excitation (a and b) and structural response (c and d) at mid-span

The captured FRFs of occupied structure are over-plotted in Figure 6.4 (a) and (b). It can be seen that damping of the occupied structure considerably increases and its natural frequency slightly decreases with increasing the number of standing people on the structure. Comparing these results with the findings in Section 6.3.2, it can be concluded that the effect of passive people on the modal properties of the test structure is much more prominent than the effect of structural nonlinearity yielding only small changes in damping and natural frequency. Therefore the observed changes in the damping ratio and natural frequency of the occupied structure result from the presence of people on the structure and not from the structure's non-linearity of the structure.

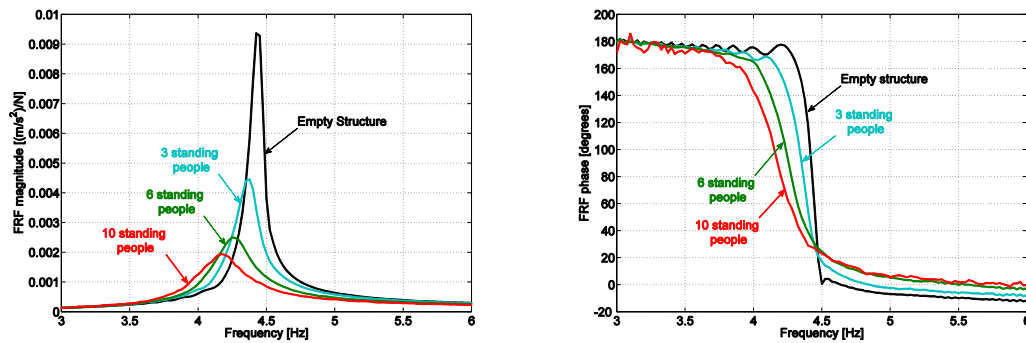


Figure 6.4. Over-plotted experimental FRF magnitude and phase diagrams of occupied structure with different number of standing people

6.4.2 Identification process

As the coupled human-structure dynamic system was modelled as a 2DOF oscillator, two modes of vibration exist. However, the experimentally measured FRFs in Figure 6.4 show only one apparent peak. This is because test setup is designed in a way that maximizes the effects of the desired mode of structure and makes the contribution of the human ‘mode’ negligible in comparison. This is done by using a narrow-band chirp excitation targeted to excite a mode of structure to resonance with maximum energy.

The natural frequency f_{os} and damping ratio ζ_{os} of the occupied structure are initially approximated for each test by applying peak-picking and half-power bandwidth methods to the experimental FRF curves, respectively. A narrow range is defined for each of f_{os} , ζ_{os} and m_{os} using these initially approximated values. These ranges are then used in the identification process where a set of f_{os} , ζ_{os} and m_{os} parameters is identified for each test that creates best analytical fit to the corresponding experimental FRF. Figure 6.5 shows that both amplitude and phase of the analytical FRFs match quite well their experimental counterparts. This gives confidence that the methodology used is robust, and could be used for identification of modal properties.

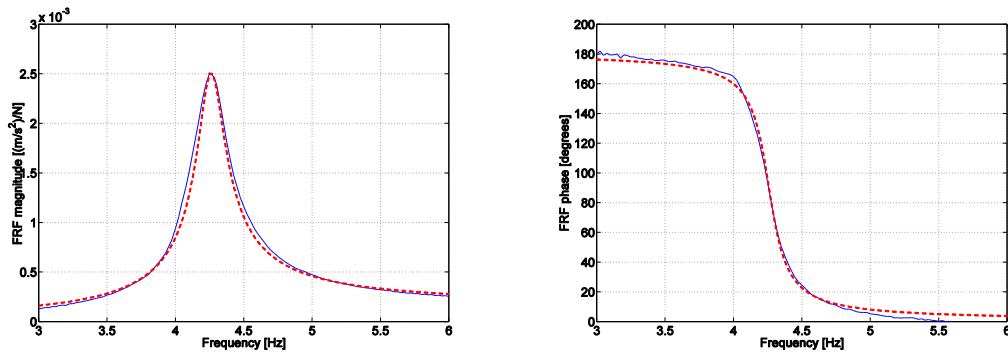


Figure 6.5. Analytical (dashed red) and Experimental (blue) FRF magnitude and phase graphs for the test with 6 standing people

Table 6.2 and Figure 6.6 summarize the results and show trends of changes in the modal properties of the occupied structure. This is very much in line with observations reported by Sachse, (2002) for groups of stationary people. In the next section, the focus of study shifts to the influence of multiple *walking* pedestrians on the dynamic properties of the Sheffield footbridge.

Table 6.2. Occupied structure modal properties with different number of standing people

Number of Standing people	Modal Properties of Occupied Structure					Structural Response	
	f_{os} (Hz)	ζ_{os} (%)	m_{os}	c_{os}	k_{os}	$a_{os,max}$ (m/s ²)	$a_{os,rms}$ (m/s ²)
0	4.440	0.60	7,128	2,386	$5,547 \times 10^3$	1.8782	0.3680
3	4.363	1.35	7,968	5,898	$5,988 \times 10^3$	1.3304	0.2396
6	4.259	2.30	8,808	10,842	$6,307 \times 10^3$	0.8871	0.1722
10	4.175	2.60	9,928	13,543	$6,832 \times 10^3$	0.7125	0.1473

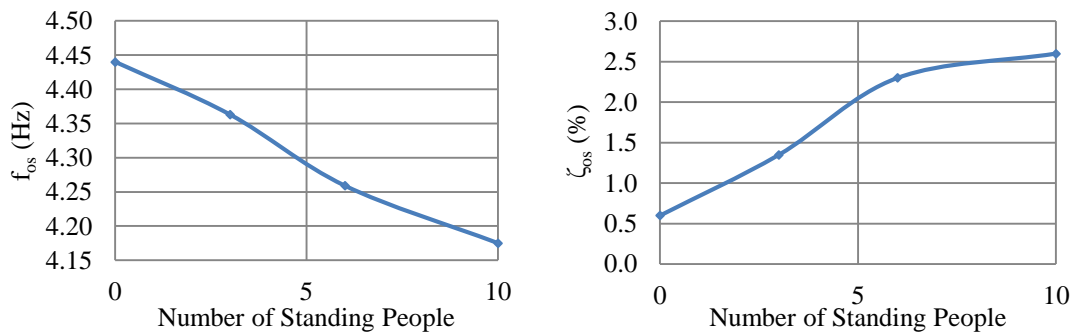


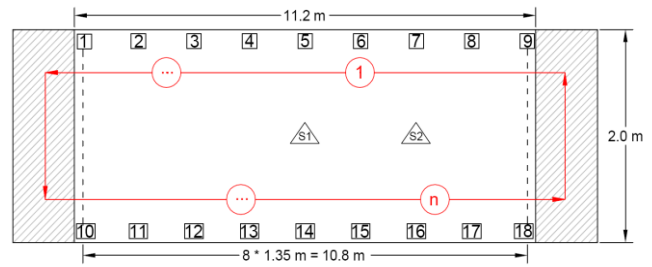
Figure 6.6. Change of occupied structure modal properties with different number of standing people at mid-span

6.5 Tests with walking people

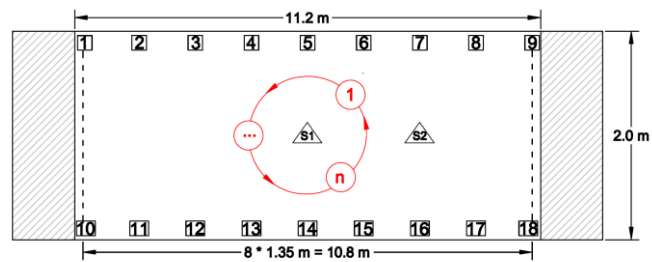
In comparison with stationary occupants, constantly changing positions of moving pedestrians on the structure are expected to generate even ‘noisier’ and less stable FRF data. To average out the noise, the average FRFs were calculated from 15 data blocks each lasting 64 s. This is three times more averages than what was used in the tests with stationary people in Section 6.4. Also, to study the effect of different locations of moving pedestrians on the modal properties of the occupied structure, two *walking* load scenarios were tested here. In Scenario 1 (S1) pedestrians were walking *along the structure*, as illustrated in Figure 6.7 (a). In Scenario 2 (S2) participants were walking in a ‘*tight circle*’ at 1/2, 3/8 and 1/4 of the span (Figure 6.7 (b)). The Scenario 1 loading represents a realistic walking load case while the Scenario 2 allows for minimizing the effects of the varying locations of people during the walking tests. The results from the two scenarios are compared in Section 6.5.2.

6.5.1 Experimental setup

The accelerometer layout (Figure 6.7) in all walking tests was the same and identical to the standing people tests. The cables, reels and the shaker were placed in the pit beneath the slab to minimize tripping hazards. In the tests relevant to the first vibration mode of the structure, the shaker was exciting the structure from underneath at the mid-span (i.e. anti-node of the first mode), to maximise the vibration response in this mode. For the same reason, the shaker was exciting the quarter of the span in the tests relevant to the second vibration mode of the structure.



a) Scenario 1 (S1): Walking along the structure



b) Scenario 2 (S2): Walking in tight circle

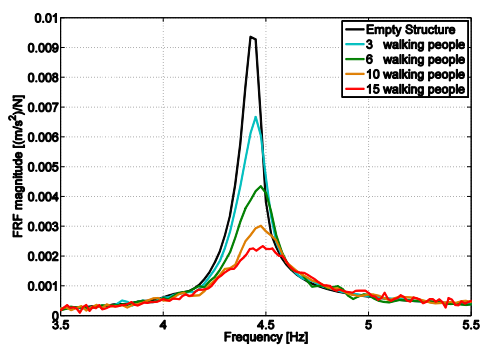
Figure 6.7. A typical walking path and accelerometer (square) and shaker (triangle) placement layout of walking tests

In total, 112 test subjects in groups of 2-15 participated in 23 tests to avoid biased FRF data due to the inter-subject variability. 13 tests were focused on mode one of structure and 10 tests were focused on the second mode. Walking style was free and not controlled by any external stimuli, such as metronome beats. Pedestrians were asked to walk as they would normally do. This means to speed up, slow down and pass others if necessary while maintaining their usual walking pattern.

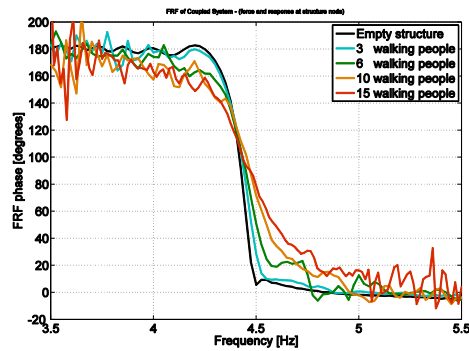
An FRF-based modal testing with pedestrians walking on the structure was carried out in each test using the same chirp shaker excitation used in the tests with standing people, to predominantly excite the first two vertical modes of vibration. In each test, a set of 18 FRFs corresponding to the 18 TPs was collected. As in the case of standing people, the FRFs corresponding to test points on both edges of the structure with same distance from supports

(such as TP5 and TP14) were numerically averaged to eliminate torsional modes contributions.

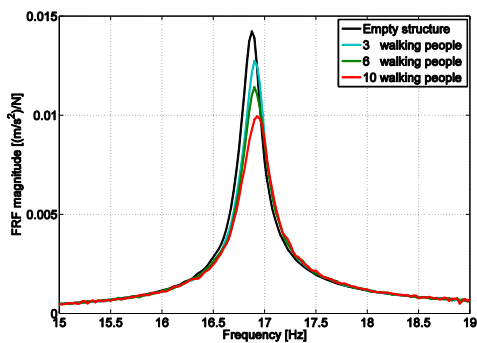
The experimentally measured FRFs of the occupied structure under Scenario 1 loading are presented in Figure 6.8 for modes one and two, respectively.



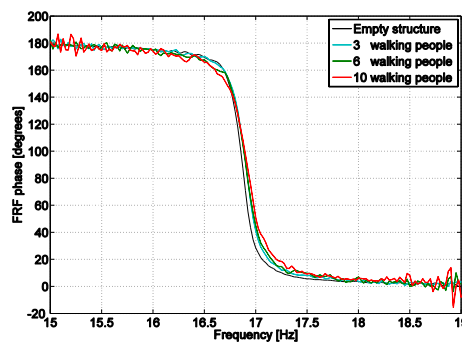
a) Mode 1 (S1) – FRF magnitude curves



b) Mode 1 (S1) – FRF phase curves



c) Mode 2 (S1) – FRF magnitude curves



d) Mode 2 (S1) – FRF phase curves

Figure 6.8. Experimental FRF magnitude and phase curves of the 1st and 2nd vertical modes of the structure with different number of people walking along the structure (Scenario 1)

A common trend can be observed in both figures - as the number of walking people on the structure increases, the maximum structural response considerably decreases which can be interpreted as an increase of the damping ratio. Moreover, the modal frequency of occupied structure increases as number of walking people on structure increase.

6.5.2 Identification process

Similar identification process to standing people was used here. Figure 6.9 presents a satisfactory match between the measured and fitted point-mobility FRFs corresponding to the mode one of structure while 10 people were walking according to Scenario 1.

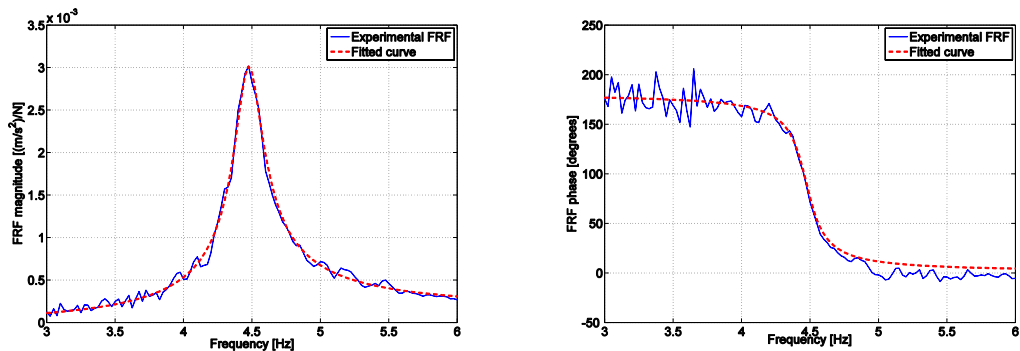


Figure 6.9. The point-mobility experimental FRF amplitude and phase curves (blue) and their analytical fit (red) – Mode 1 - 10 pedestrians walking along the structure (Scenario 1).

Figure 6.10 displays the experimental point-mobility FRF curves for groups of 6 and 10 walking people. Tests were repeated with same group size but different participant. It clearly shows that FRF curves of different tests with the same number of people follow the same trend. The higher the number of pedestrians, the lower and more shifted towards higher natural frequency the FRF peaks are. This demonstrates that difference in human body mechanics for different participants does not affect the general trend of changing the FRF shape for different number of people. The conclusions based on these trends appear to be valid for an arbitrary group of people in the specified test situation.

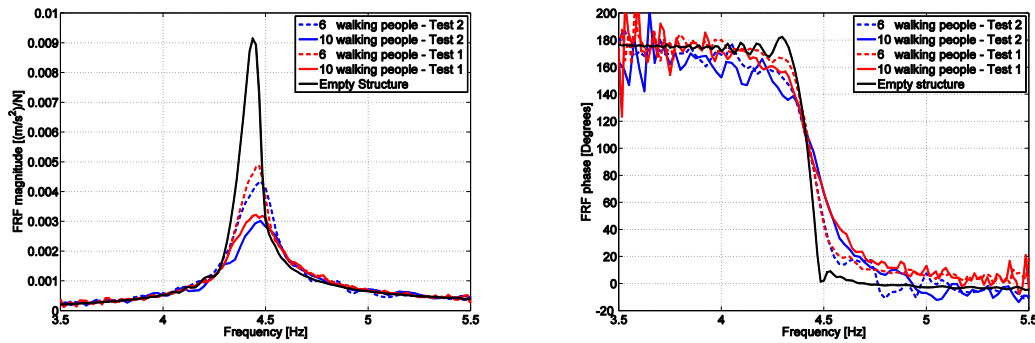


Figure 6.10. The point-mobility FRF magnitude and phase graphs captured for 6 and 10 walking people repeated twice with different participants – Mode 1

6.5.2.1 FIRST STRUCTURAL MODE RESULTS

The identified modal properties for the tests focused on the first mode of structure are summarized in Table 6.3 and their trends are illustrated in Figure 6.11. As can be seen in Figure 6.11 both the natural frequency of the occupied structure f_{os} and its damping ratio ζ_{os} increased for increasing number of walking people. Similarly, modal mass m_{os} , stiffness k_{os} and damping c_{os} of the occupied structure are increased, as would be expected from the previously observed trends. Interestingly, considering the fact that the natural frequency is directly proportional to $\sqrt{k/m}$, it appears that modal stiffness increases faster than its mass counterpart to make the observed increase in natural frequency possible. This is somewhat counter-intuitive, bearing in mind the normal understanding that the walking humans occupying the structure add only mass and hence reduce its natural frequency.

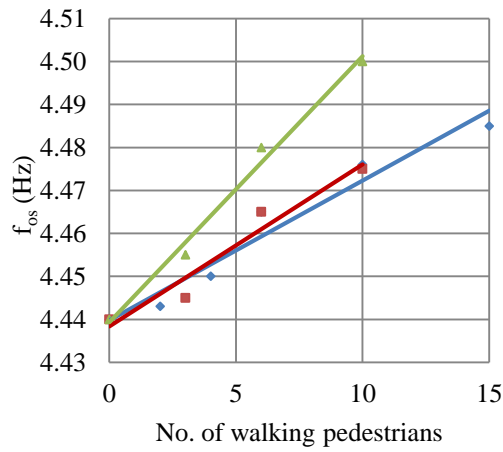
Similarity of changing trends observed in Scenario 2 results with the ones of Scenario 1 confirms again the validity of observed trends in results. On the other hand, higher values of all modal properties in Scenario 2 relative to Scenario 1 with the same participants confirm that human body location relative to a mode shape amplitude plays a significant role in the level of its interaction with the structure. Human-structure interaction is apparently greatest

when walking happens close to the anti-node of the structural mode (mid-span for the first mode).

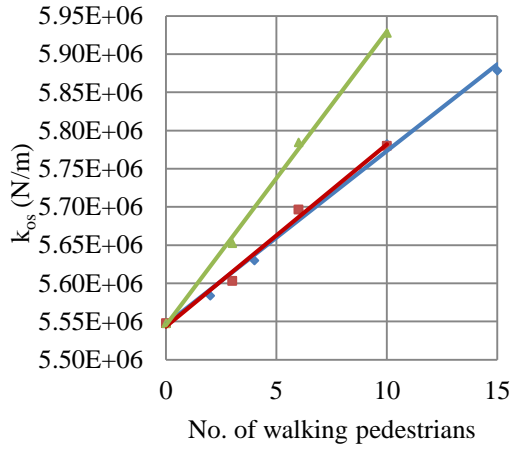
Comparing the results of this set of tests with changes observed in Section 6.3.1 due to the amplitude-dependent behaviour of the structure, it can be concluded that the changes in the modal properties of the structure under walking crowd loading are much more pronounced than the effects of non-linearity of structure. For instance, comparing Tests 1.1 and 1.13, a 0.06HZ increase in f_{os} is noticeable while non-linear frequency change due to change in response magnitude of these tests would be maximum 0.02Hz (according to Figure 6.1). Therefore, the observed changes in Table 6.3 are mostly due to the presence of walking human on the structure.

Table 6.3. Identified modal properties of the first mode of the occupied structure for different number of pedestrians and walking Scenarios

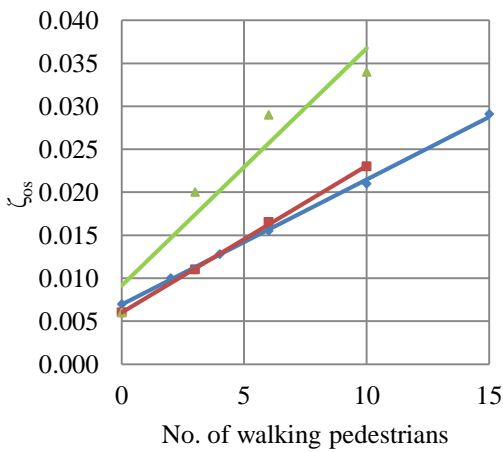
Test no.	Test Series	Location of peds	No. of Peds	Modal properties of the occupied structure – First mode					Structural Response	
				f_{os} (Hz)	ζ_{os}	m_{os} (kg)	c_{os} (N.s/m)	k_{os} (N/m)	$a_{os,max}$ (m/s ²)	$a_{os,rms}$ (m/s ²)
Empty structure properties										
1.1	A	-	0	4.440	0.0060	7,128	2,386	$5,547 \times 10^3$	1.8782	0.3680
1.2	B	-	0	4.440	0.0070	7,128	2,784	$5,547 \times 10^3$	2.6084	0.4826
Scenario 1: Pedestrians are walking along the footbridge										
1.3	B	All-over	2	4.443	0.0100	7,165	4,000	$5,583 \times 10^3$	2.4361	0.4131
1.4	A	All-over	3	4.445	0.0110	7,183	4,413	$5,603 \times 10^3$	1.7489	0.3018
1.5	B	All-over	4	4.450	0.0128	7,201	5,154	$5,630 \times 10^3$	2.1755	0.3637
1.6	B	All-over	6	4.465	0.0155	7,238	6,294	$5,696 \times 10^3$	1.8771	0.3311
1.7	A	All-over	6	4.465	0.0165	7,238	6,701	$5,696 \times 10^3$	1.4882	0.2481
1.8	A	All-over	10	4.475	0.0230	7,311	9,456	$5,780 \times 10^3$	1.1313	0.2050
1.9	B	All-over	10	4.476	0.0210	7,311	8,635	$5,782 \times 10^3$	1.5876	0.2870
1.10	B	All-over	15	4.485	0.0291	7,402	12,140	$5,878 \times 10^3$	1.1251	0.2466
Scenario 2: Pedestrians are walking in a tight circle										
1.11	A	Mid-span	3	4.455	0.0200	7,214	8,077	$5,652 \times 10^3$	1.3226	0.2488
1.12	A	Mid-span	6	4.480	0.0290	7,300	11,918	$5,784 \times 10^3$	1.0903	0.2008
1.13	A	Mid-span	10	4.500	0.0340	7,415	14,256	$5,928 \times 10^3$	0.8656	0.1861
1.14	A	3/8-span	6	4.465	0.0250	7,287	10,222	$5,735 \times 10^3$	0.9920	0.1987
1.15	A	¼ -span	6	4.460	0.0205	7,250	83,29	$5,693 \times 10^3$	1.0996	0.2195



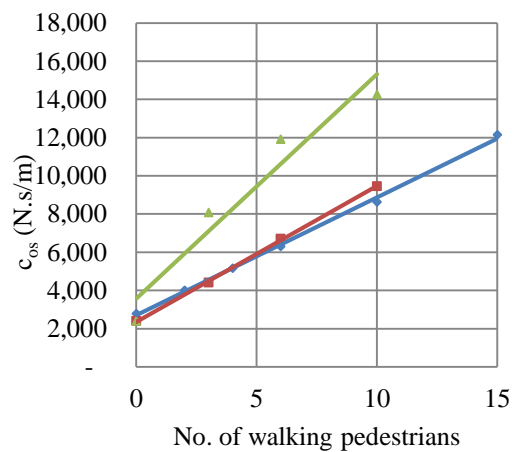
a) f_{0s}



b) k_{0s}



c) ζ_{0s}



d) c_{0s}

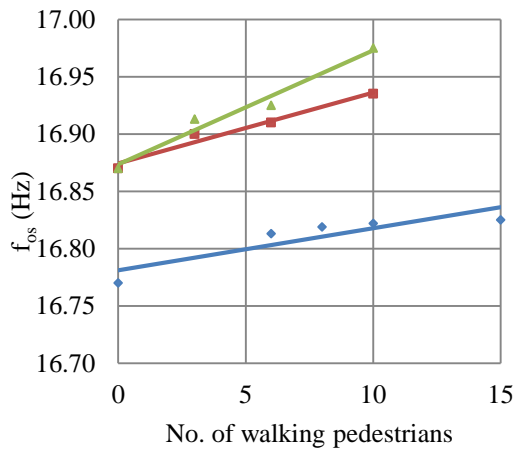
Figure 6.11. Trends of occupied structure modal frequency f_{0s} (a), stiffness k_{0s} (b), damping ratio ζ_{0s} (c) and damping c_{0s} (d) against number of walking pedestrians – Mode 1 – (Red: Series A; Blue: Series B; Green: Circular walking around mid-span)

6.5.2.2 SECOND STRUCTURAL MODE RESULTS

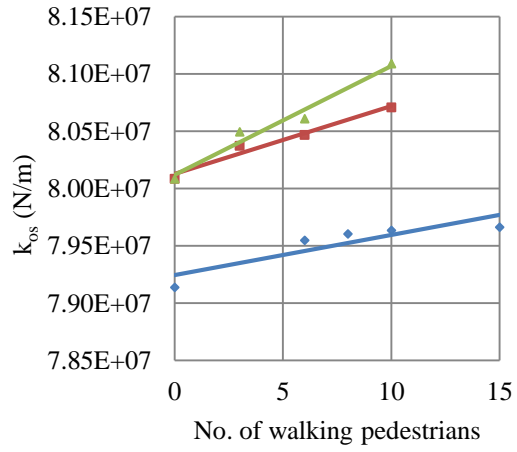
The identified modal properties of the second mode of the occupied structure and their trends are presented in Table 6.4 and Figure 6.12 respectively. The same trend can be observed in all modal properties of the occupied structure. Similar to the results for Mode 1, for Mode 2 f_{os} , ζ_{os} , m_{os} , k_{os} and c_{os} are all increasing by increasing the number of walking people on it.

Table 6.4. Identified modal properties of the second mode of the occupied structure for different number of pedestrians and walking Scenarios

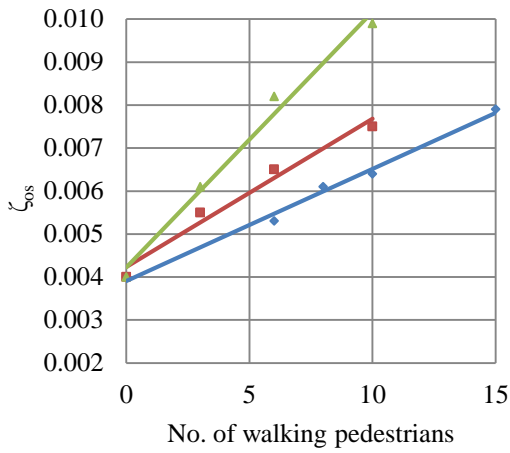
Test No.	Test Series	Location of peds	No. of Peds	Modal properties of the occupied structure - Second mode					Structural Response	
				f_{os} (Hz)	ζ_{os}	m_{os} (kg)	c_{os} (N.s/m)	k_{os} (N/m)	$a_{os,max}$ (m/s ²)	$a_{os,rms}$ (m/s ²)
Empty structure properties										
2.1	A	-	0	16.870	0.0040	7,128	6,044	$80,086 \times 10^3$	2.5080	0.4769
2.2	B	-	0	16.770	0.0040	7,128	6,009	$79,140 \times 10^3$	3.2123	0.5942
Scenario 1: Pedestrians are walking along the structure										
2.3	A	All-over	3	16.900	0.0055	7,128	8,326	$80,372 \times 10^3$	2.4059	0.4482
2.4	B	All-over	6	16.813	0.0053	7,128	7,982	$79,548 \times 10^3$	2.9046	0.5595
2.5	A	All-over	6	16.910	0.0065	7,128	9,846	$80,468 \times 10^3$	2.2905	0.4234
2.6	B	All-over	8	16.819	0.0061	7,128	9,190	$79,605 \times 10^3$	2.5591	0.5133
2.7	B	All-over	10	16.822	0.0064	7,128	9,644	$79,634 \times 10^3$	2.5232	0.5223
2.8	A	All-over	10	16.935	0.0075	7,128	11,377	$80,708 \times 10^3$	2.1387	0.4023
2.9	B	All-over	15	16.825	0.0079	7,128	11,907	$79,665 \times 10^3$	2.2358	0.4725
Scenario 2: Pedestrians are walking around a tight circle										
2.10	A	1/4-span	3	16.913	0.0061	7,128	9,241	$80,496 \times 10^3$	2.2306	0.4188
2.11	A	1/4-span	6	16.925	0.0082	7,128	12,432	$80,611 \times 10^3$	1.9406	0.3544
2.12	A	1/4-span	10	16.975	0.0099	7,128	15,054	$81,091 \times 10^3$	1.6871	0.3660



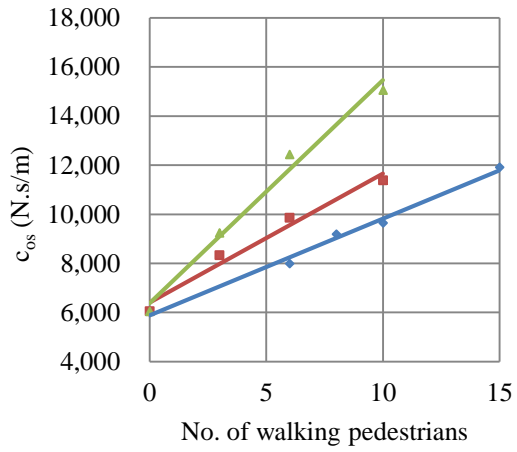
a) f_{os}



b) k_{os}



c) ζ_{os}



d) c_{os}

Figure 6.12. Trends of change of occupied structure modal frequency f_{os} (a), stiffness k_{os} (b), damping ratio ζ_{os} (c) and damping c_{os} (d) against number of walking pedestrians – Mode 2 – (Red: Series A; Blue: Series B; Green: Circular walking around 1/4-span)

6.5.2.3 LOCATION EFFECTS

To see how the location of people on the structure changes the level of HSI, occupied structure f_{os} and ζ_{os} are compared in Figure 6.13 for a group of 6 people walking in a tight circle (Scenario 2) at different locations on the footbridge.

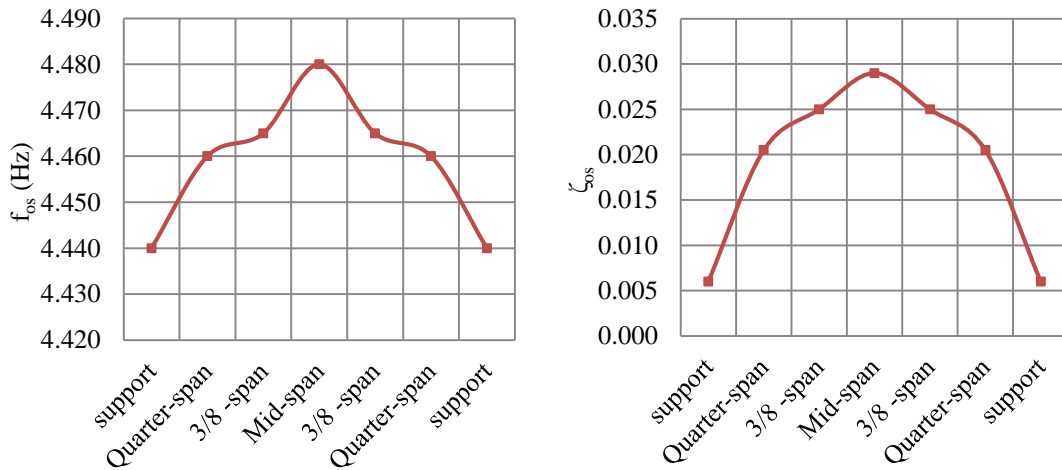


Figure 6.13. Change of natural frequency f_{os} and damping ratio ζ_{os} of occupied structure against the location of 6 walking pedestrians on the structure – Mode 1

As it can be seen in Figure 6.13, the influence of walking humans on the modal properties of the occupied structure f_{os} and ζ_{os} is maximum when they are at mid-span (anti-node of the first mode) and their effects are very small when they are located at supports (nodes of the first mode – compare with the empty structure properties presented in Table 6.1).

6.6 Comparison of Effects of Standing and Walking People

The observed trends in the occupied structure modal properties for nominally identical groups of standing and walking people are compared in this section. The FRF magnitude and phase graphs for groups of 3, 6 and 10 walking and standing people are over-plotted in Figure 6.14. Same test subjects participated in each set of the walking-standing tests. Having in mind the considerable effects of pedestrian’s location on the results, only the results of walking ‘around a tight circle’ (Scenario 2) are compared with the nominally identical tests

featuring the same participants, standing at the same location (as opposed to walking). All the presented results are corresponding to structural mode 1 and groups of walking pedestrians are circle walking at mid-span.

Trend of changes in occupied structure natural frequency f_{os} and damping ratio ζ_{os} with regards to change in number of walking/standing pedestrians are presented in Figure 6.15. As it can be seen in this figure, for standing people, the occupied structure FRF shifts to the left (lower modal frequency) while for the walking people it shifts to the right (higher modal frequency). In both walking and standing Scenarios, the damping ratio of the occupied structure has increased considerably. However and quite interestingly, ζ_{os} in the case of walking is consistently higher compares to its standing counterpart. This is a novel observation never seen before to the best knowledge of authors. This phenomenon could be caused by the more flexible walking human body with mass, stiffness and damping properties which enhance damping compared with their stationary counterpart. It could also be caused by the component of walking force which mimics an ‘active damper’ by getting in-phase with the velocity of the structure. These observations require further research and their discussion is beyond the scope of this chapter.

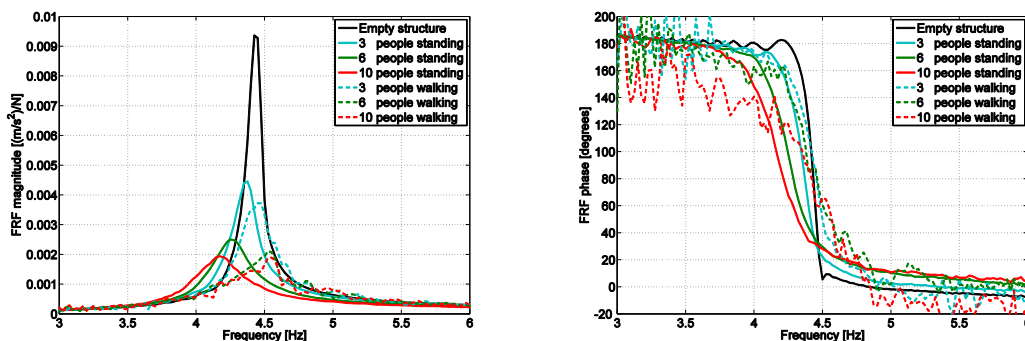


Figure 6.14. Over-plotted FRF magnitude and phase curves for groups of 3, 6 and 10 walking/standing people at mid-span – structural mode 1

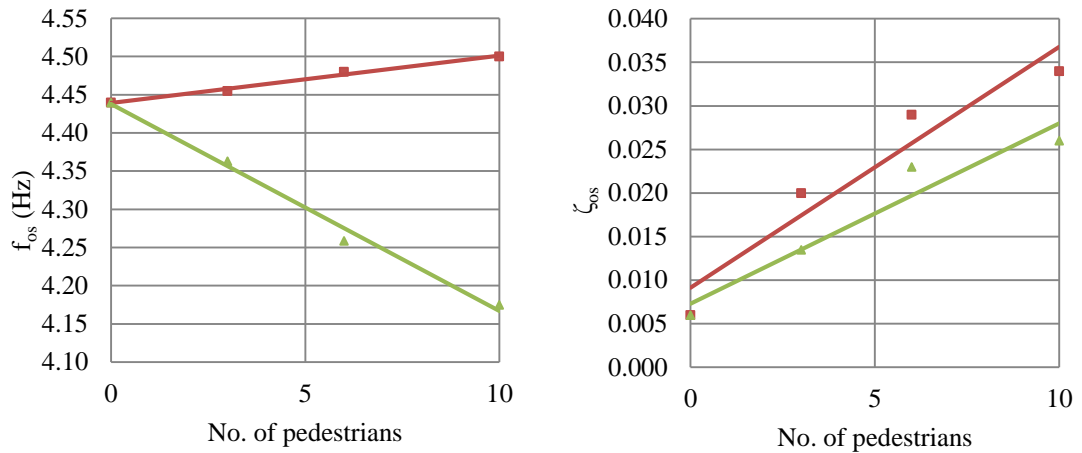


Figure 6.15. Trends of changes in occupied structure modal frequency f_{os} and damping ratio ζ_{os} for varying number of standing and walking people on the structure (Red: Circular walking at mid-span; Green: standing at mid-span)

The results of this research are in line with the observations made by Zivanovic, et al. (2009) during the tests on standing/walking groups of 2, 4, 6 and 10 people using the same test structure. They reported increase in the natural frequency of the occupied structure f_{os} for the walking people and decrease in f_{os} for the standing people. They also report a considerable increase in the damping ratio of occupied structure ζ_{os} for both standing and walking people. The only and rather considerable discrepancy is that they reported the higher ζ_{os} for the standing compared to the walking people. This is opposite to the observations reported in this chapter. The reason is that in Zivanovic, et al. experiments the spatial distributions of people in the walking and standing tests were not the same. They used a dense distribution of people centered at *mid-span* for standing tests while in walking tests the same participants were walking across the *whole length* of structure. This seemed to be logical at the time considering that people normally utilize the whole bridge length. However, due to their constant location at the most effective point on the structure, the effects of the standing crowd were more pronounced in comparison with the walking scenario.

6.7 Analytical verification

The experimental results presented in previous sections show a clear and significant change in the modal properties of the test structure when interacting with a walking or standing people. To validate the findings, aggregated dynamic effects of standing and walking groups of people (will be referred to as *crowd* hereafter) are simulated using a conventional single degree of freedom (SDOF) mass-spring-damper (MSD) model. The aim is to check if such SDOF model can simulate interaction of the crowd with the structure through combing it with an empty structure SDOF model to form 2DOF crowd-structure (CS) dynamic system.

6.7.1 2DOF crowd-structure model

To simulate the crowd-structure system, the first mode of structural vibration is considered and is conceptualized using an SDOF oscillator with the corresponding modal properties (m_s , k_s and c_s). Assuming that the structure behaves linearly, the mode superposition principle applies. Therefore, considering only one structural mode at a time does not affect the generality of the results.

The SDOF MSD model used to simulate the standing-still crowd (m_{sc} , k_{sc} and c_{sc}) represents a group of people standing as close as feasible to the anti-node of the first structural mode. This corresponds to the physical tests with standing crowds at mid-span. Similarly, the SDOF MSD model used to simulate the walking crowd (m_{wc} , k_{wc} and c_{wc}) represents walking on the spot pedestrian the locations which do not change. This is conceptually the same as walking on a series of treadmills located at the mid-span of the structure (Figure 6.16).

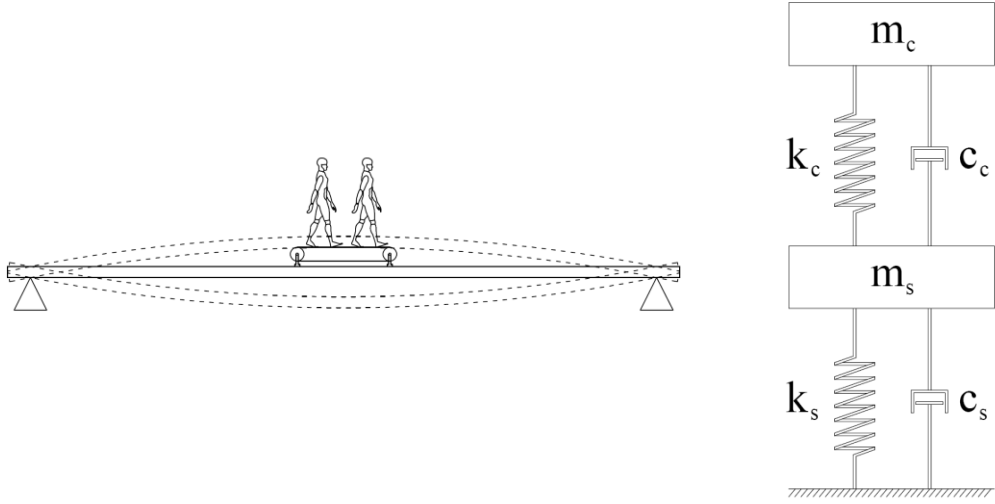


Figure 6.16. Conceptual 2DOF model of coupled crowd-structure system (crowd model parameters are shown generally by m_c , k_c and c_c)

By assuming stationarity, both standing and walking crowd-structure coupled systems (shown generally by m_c , k_c and c_c) can be represented as a simple conventional two degrees of freedom system as illustrated in Figure 6.16 (right), the behaviour of which can be studied using closed form solutions of 2DOF equations of motion. Based on classical mechanics, a system of equations of motion for the presented two degrees of freedom system can be written as:

$$\begin{bmatrix} m_s & 0 \\ 0 & m_c \end{bmatrix} \begin{pmatrix} \ddot{x}_s(t) \\ \ddot{x}_c(t) \end{pmatrix} + \begin{bmatrix} c_s + c_c & -c_c \\ -c_c & c_c \end{bmatrix} \begin{pmatrix} \dot{x}_s(t) \\ \dot{x}_c(t) \end{pmatrix} + \begin{bmatrix} k_s + k_c & -k_c \\ -k_c & k_c \end{bmatrix} \begin{pmatrix} x_s(t) \\ x_c(t) \end{pmatrix} = \begin{pmatrix} f_s(t) \\ f_c(t) \end{pmatrix}$$

(Equation 6.1)

Where m_s , c_s and k_s are mass, damping and stiffness of the empty structure and m_c , c_c and k_c are those of the crowd model. $\ddot{x}_s(t)$, $\dot{x}_s(t)$ and $x_s(t)$ are acceleration, velocity and displacement response of structure in the coupled system. Similarly, $\ddot{x}_c(t)$, $\dot{x}_c(t)$ and $x_c(t)$ represent acceleration, velocity and displacement of the crowd model mass. $f_s(t)$ and $f_c(t)$ are externally applied forces on the structure and crowd degrees of freedom. To extract modal properties from this system a condition of free vibration was assumed:

$$f_s(t) = 0 \quad (\text{Equation 6.2})$$

$$f_c(t) = 0 \quad (\text{Equation 6.3})$$

To be able to check any probable combination of crowd model parameters m_c , c_c and k_c , modal analysis formulation for systems with non-proportional damping matrix is used. A new coordinate vector $\{y\}$ containing displacement and velocity vectors is first defined:

$$\{y(t)\} = \begin{Bmatrix} x(t) \\ \dot{x}(t) \end{Bmatrix} \quad (\text{Equation 6.4})$$

Then Equation 6.1 is re-written into following form for modal analysis (Min, et al., 2011):

$$\begin{bmatrix} [C] & [M] \\ [M] & [0] \end{bmatrix} \{y(t)\} + \begin{bmatrix} [K] & [0] \\ [0] & [-M] \end{bmatrix} \{y(t)\} = \{0\} \quad (\text{Equation 6.5})$$

The Equation 6.5 leads to a standard eigenvalue problem and can be solved for eigenvectors and eigenvalues accordingly. Further discussion of modal analysis of systems with non-proportional damping is beyond the scope of this study.

6.7.2 Analysis specifications

For each test, the described 2DOF crowd-structure (CS) model is used to simulate the observed changes in the dynamic properties of the structure when subjected to its corresponding standing/walking crowd. The modal properties of the first mode of the empty structure obtained from experiments (presented in Table 6.1) are adopted as m_s , k_s and c_s (Equation 6.1).

For each experiment, a set of simulations is carried out with different combinations of crowd parameters (k_c and c_c). The resolution used for these parameters are 1000 N/m and 10 N.s/m, respectively. The ranges of k_c and c_c values used in simulations were selected wide enough

to cover ranges found in the mostly biomechanics literature (Zhang, et al., 2000; Rapoport, et al., 2003; Bertos, et al., 2005; Lee and Farley, 1998; Geyer, et al., 1998). To reduce the level of uncertainty and enhance the accuracy of the modal identification process, the mass of the crowd model m_c is calculated based on weight of test participants in each test and used as a constant in simulations. This was done by assuming sinusoidal mode shape for the first mode of vibration and taking into account the location of each people on the structure. Hence, the mass of the crowd model was approximated using Equation 6.6:

$$m_c = \sum_{i=1}^n m_i \times \sin\left(\frac{\pi x_i}{L}\right) \quad (\text{Equation 6.6})$$

Where m_c is the crowd model mass, x_i is the distance of subject ‘i’ from the left support, m_i is the mass of subject ‘i’, L is the support-to-support clear length of test structure and n is the number of people in the crowd. Distribution of the people for the case of moving walking crowd is considered to be even across the length of test structure L . Consequently, and similar to the relationship of the physical and modal mass of a uniform simply-supported beam, crowd model mass for this Scenario is assumed to be half of the total crowd mass.

For each set of crowd and structure parameters, modal analysis is carried out and corresponding modal properties of the occupied structure are then found. As 2DOF model of the CS system has two modes of vibration, the *dominant* mode of vibration of the CS system is selected as the modal properties of the occupied structure. For consistency and to allow comparison, in all simulations, the ordinate of the structure node of the dominant mode is scaled to unity. Such scaling ensures that modal properties of the crowd-structure system are found with the same scaling as the empty structure and therefore they are comparable. The modal frequency f_{os} , damping ratio ζ_{os} , stiffness k_{os} and damping c_{os} of the occupied structure, FRF peak magnitude and FRF shape (using least square method) are simultaneously used as criteria to compare analytical and experimental results.

6.7.3 Simulation results

The experimentally captured dynamic properties of occupied structure and their corresponding crowd model properties found from simulations are presented for walking and standing tests in Table 6.5 and Table 6.6, respectively. Simulation results in Table 6.5 are presented in different order to make the comparison easier. The trends of walking crowd model properties observed in simulations are plotted in Figure 6.17.

Table 6.5. Walking crowd model properties obtained from simulation of 2DOF crowd-structure model

Test No.	No of peds	Occupied structure – Experimental					Walking crowd model – Analytical				
		f_{os} Hz	ζ_{os} %	m_{os} kg	c_{os} N.s/m	k_{os} N/m	f_{wc} Hz	ζ_{wc} %	m_{wc} kg	c_{wc} N.s/m	k_{wc} N/m
Scenario 1: Walking along the footbridge – Series B											
1.2	0	4.440	0.70	7128	2,784	$5,547 \times 10^3$	-	-	-	-	-
1.3	2	4.443	1.00	7165	4,000	$5,583 \times 10^3$	2.406	0.36	70	762	15,997
1.5	4	4.450	1.30	7201	5,154	$5,629 \times 10^3$	2.552	0.30	140	1,347	35,996
1.6	6	4.465	1.60	7238	6,294	$5,696 \times 10^3$	2.645	0.24	210	1,675	58,000
1.9	10	4.476	2.10	7311	8,635	$5,782 \times 10^3$	2.770	0.22	350	2,680	106,020
1.10	15	4.485	2.90	7402	12,140	$5,878 \times 10^3$	2.800	0.21	525	3,879	162,493
Scenario 1: Walking along the footbridge – Series A											
1.1	0	4.440	0.60	7128	2,386	$5,547 \times 10^3$	-	-	-	-	-
1.4	3	4.445	1.10	7183	4,413	$5,603 \times 10^3$	2.504	0.32	105	1,057	25,991
1.7	6	4.465	1.65	7238	6,701	$5,696 \times 10^3$	2.778	0.28	210	2,053	63,980
1.8	10	4.475	2.30	7311	9,456	$5,780 \times 10^3$	2.900	0.24	350	3,061	116,205
Scenario 2: Walking around a tight circle at mid-span – Series A											
1.11	3	4.450	2.11	9200	10,855	$7,192 \times 10^3$	2.906	0.30	210	2,301	70,012
1.12	6	4.470	2.23	11725	14,687	$9,249 \times 10^3$	2.950	0.26	420	4,048	144,296
1.13	10	4.500	2.86	12675	20,499	$10,133 \times 10^3$	2.962	0.22	560	4,586	193,963

Table 6.6. Standing-still crowd model properties obtained from simulation of 2DOF crowd-structure model – standing at mid-span

No of peds	Occupied structure – Experimental					Standing crowd model – Analytical				
	f_{os} Hz	ζ_{os} %	m_{os} kg	c_{os} N.s/m	k_{os} N/m	f_{sc} Hz	ζ_{sc} %	m_{sc} kg	c_{sc} N.s/m	k_{sc} N/m
0	4.440	0.60	7,128	2,386	$5,547 \times 10^3$	-	-	-	-	-
3	4.363	1.35	7,968	5,898	$5,988 \times 10^3$	5.436	57	210	8,177	244,984
6	4.259	2.30	8,808	10,842	$6,307 \times 10^3$	5.267	45	420	12,509	459,977
10	4.175	2.60	9,928	13,543	$6,832 \times 10^3$	5.171	43	630	17,603	665,042

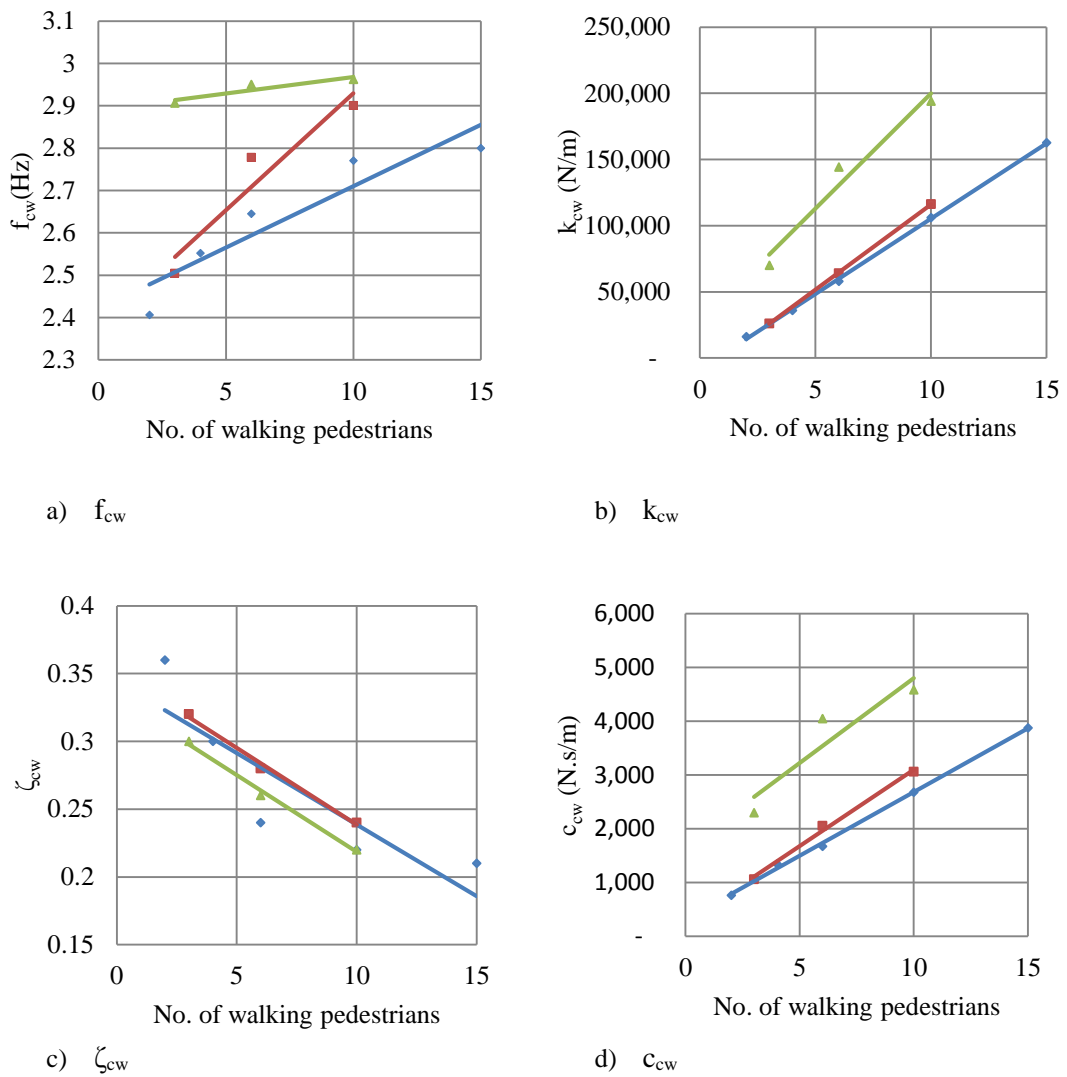


Figure 6.17. Trends of walking crowd SDOF model natural frequency f_{cw} , stiffness k_{cw} , damping ratio ζ_{cw} and damping c_{cw} against number of walking pedestrians (Red: S1-Series A; Blue: S1-Series B; Green: S2)

As it can be seen in Figure 6.17, when the number of people increases, the natural frequency of the walking crowd model f_{wc} increases too. This is also valid for the Scenario 2 ‘walking around a tight circle’ (green trace) in which the effect of people’s location is minimal. The same trend can be seen for the walking crowd model stiffness k_c . Considering the fact that the SDOF natural frequency is proportional to $\sqrt{k/m}$, and knowing that the mass of walking

crowd model m_{wc} increasing by increasing the number of people in the crowd (as calculated and shown in Table 6.5), k_{wc} increases faster than m_{wc} , allowing f_{wc} to increase. One explanation for this phenomenon could be progressively faster stiffening of the body as it reduces the speed of walking in more crowded situations (this theory is not examined experimentally in this study). Although damping of walking crowd model c_{wc} increases by increasing number of people in the crowd, the damping ratio of the walking crowd model ζ_{wc} decreases as it also depends on the modal mass and stiffness (Equation 6.7).

$$\zeta_{wc} = \frac{c_{wc}}{2\sqrt{m_c \times k_c}} \quad (\text{Equation 6.7})$$

In all simulations, changes in parameters of both scenario 1 ‘walking along the structure’ and scenario 2 ‘walking around a tight circle’ crowd models show the same trend which ensures the validity of results.

Figure 6.18 compares the trend of change in natural frequency f_c and damping ratio ζ_c of standing-still and walking crowd models for different number of people on the structure. To increase the accuracy, results of walking ‘around a tight circle’ at mid-span tests are compared with standing-still at mid-span tests as far as the location of people is concerned. As it was expected based on the findings presented in Chapter 5, increasing number of walking people on the structure increases natural frequency of crowd model f_c while increasing number of standing people decreases f_c . In both walking and standing-still scenarios, damping ratio of the crowd model (ζ_{wc} and ζ_{sc}) decrease by increasing the number of people on the structure although their damping (c_{wc} and c_{sc}) increase.

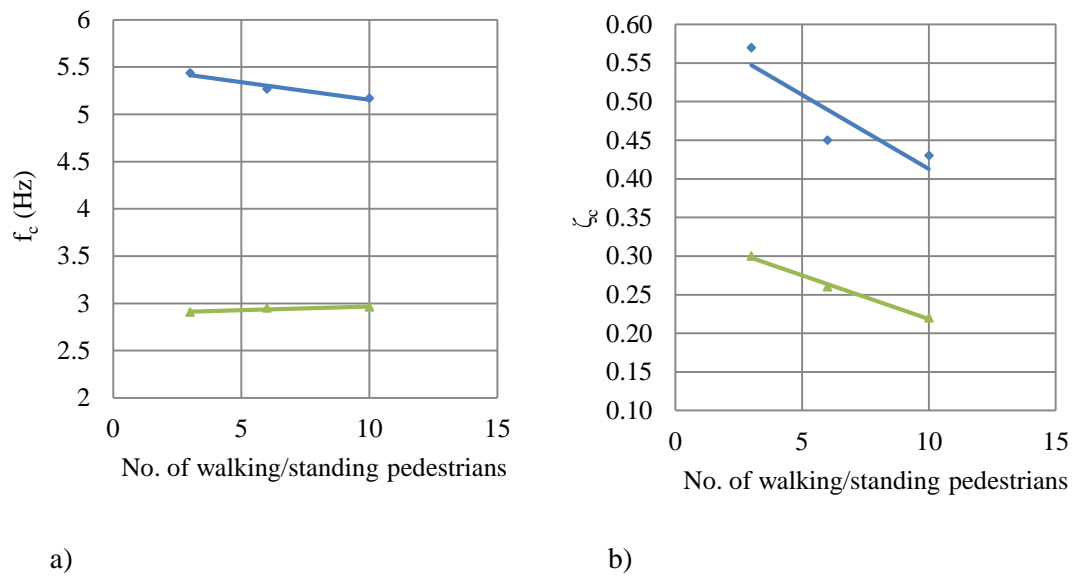


Figure 6.18. Comparison of changes in natural frequency f_c (a) and damping ratio ζ_c (b) of walking (green) and standing (Blue) crowd models against the number of pedestrians

6.8 Conclusion

An extensive set of FRF-based modal identification tests were carried out on Sheffield University footbridge with over 100 participants, walking/standing on it in groups of 2-15. Findings of this study, which is unique in its kind in terms of methodology and large number of participants, show that effects of a crowd on a structure is similar to the effects of a ‘(De)tuned Mass Damper’.

Knowing that structures are usually considerably heavier, stiffer and less damped than a human body and using an SDOF model to simulate crowd-structure interaction, it can be concluded that:

- If the natural frequency of the crowd model f_c is less than the natural frequency of empty structure f_s (similar to the walking people tests in this study), both the natural

frequency f_{os} and damping ratio ζ_{os} of the occupied structure increase.

- If $f_c > f_s$ (similar to the standing-still people tests in this study), the natural frequency of the occupied structure f_{os} decrease and its damping ratio ζ_{os} increase.
- Walking people can increase damping of the occupied structure more than standing people.
- Results of tests focused on mode 2 of the structure show that crowd-structure interactions can affect modes with frequencies far away from the crowd model frequency.
- The effects of crowd on modal properties of structure are most pronounced when natural frequencies of crowd f_c and empty structure f_s are very close.
- And, the effects of crowd on occupied structure parameters always increase as number of people on structure increases.

Concrete evidence presented in this chapter about changes in the occupied structure parameters (m_{os} , c_{os} , k_{os}), highlight the significance of human-structure interaction effects on the response of the structure. Studying the underlying mechanisms of such interactions, more than anything, requires a comprehensive and accurate experimental data from crowds of people walking on real-life structures. Recording the time-history of every individual's interaction force, location and acceleration of different segments of the body in the crowd can shed a new light in this field. Having this data, it will be possible to correlate structural response, human body motion and human-structure interaction forces yielding much improved understanding of the HSI mechanism(s) in the vertical direction.

Chapter 7

Identification of Mass-Spring-Damper Model of Walking Human

Modal-based Methods

The contents of this chapter are adapted with minor changes from the following journal paper in preparation to be submitted to the Journal of Sound and Vibration:

Shahabpoor, E., Pavić, A. and Racić, V. Identification of Mass-Spring-Damper Model of Walking Humans. Journal of Sound and Vibration.

7.1 Introduction

Several models such as the single and multiple degrees of freedom oscillators and inverted pendulum models are suggested in literature to simulate interaction of walking people with structures. However, their parameters are adopted from the biomechanics field and they were adjusted to replicate the walking gate and were not validated for application in vibration serviceability assessment. The recent work of Silva and Pimentel (2011) is probably the only example to date that proposes a range of mass-stiffness-damping values to be used in the SDOF walking human model by analyzing the walking force and acceleration of human centre of mass recorded at waist. They suggested three equations for mass (m), damping (c) and stiffness (k) of the SDOF human model by analyzing the correlation between different model and pedestrian parameters:

$$m = 97.082 + 0.275 \times M - 37.518 \times f_p \quad (\text{Equation 7.1})$$

$$c = 29.041 \times m^{0.883} \quad (\text{Equation 7.2})$$

$$k = 30351.744 - 50.261 \times c + 0.035 \times c^2 \quad (\text{Equation 7.3})$$

Where M [kg] is the total mass of human body, f_p [Hz] is the pacing frequency and m [kg], c [N.s/m] and k [N/m] are the human SDOF model mass, damping and stiffness, respectively. However, Silva, et al. work lacks an appropriate experimental verification. They used synthetic walking force adopted from literature (Kerr, 1998), instead of actual walking force of people which could affect considerably the reliability of the results. Their choice of the range of human SDOF model stiffness and damping values is based on analogy with standing people parameters and this is not necessarily correct. For example, they assumed that damping of a walking person is lower than damping of the same person standing. No verified range of walking human model parameters still exists to reflect the variability of human parameters. This is mainly due to the challenging nature of collecting experimental data on HSI.

To address this issue, the study presented in this chapter utilized the most comprehensive and detailed measurement of pedestrian flow to date over the Sheffield footbridge (Chapter 6). The location and speed of each pedestrian at every moment of time, their weight and the nominally identical walking force on stiff surface (using an instrumented treadmill prior to the test) were recorded in time for all tests. A discrete traffic model was used to simulate walking people in which each individual was modelled as an SDOF MSD model. This model was developed by ‘reverse engineering’ in three different identification procedures. In these procedures, the unknown properties of the walking individuals were estimated by trial and error curve-fitting process to make sure that the regenerated FRF fits its experimental counterpart.

Section 7.2 of this chapter presents a short description of the experimental campaigns and the selection of results used in the study which is presented in this chapter. In Section 7.3 the proposed identification procedures and the discrete walking traffic-structure model are described in detail. Results of the analysis are presented for two ‘stationary’ and ‘moving’ walking scenarios in Section 7.3 and common ranges for each human model parameters are determined. The concluding remarks are finally highlighted in Section 0.

7.2 Experimental campaigns

Two series of tests (referred to as Series ‘A’ and ‘B’) were carried out on the Sheffield University footbridge at different times but with identical test setup. Each series comprise a set of FRF-based modal tests of the empty structure and the structure when a certain number of people are walking on it. In total, 13 tests focused on the first mode of the structure and 10 tests focused on the second mode were carried out. In these tests between 2 and 15 people were walking on structure and modal properties of such loaded structure are found.

7.2.1 Empty structure

The structure used in this study is a simply supported in-situ cast post-tensioned (PT) concrete footbridge purposefully constructed in the structures laboratory of The University of Sheffield. The details of the structure and its modal properties are presented in Sections 3.3.1 and 6.3.2, respectively.

7.2.2 Pedestrian data

A uniquely detailed set of pedestrian data are collected in each test using a digital weighing scale, an instrumented treadmill, a pair of PeCo laser pedestrian counters and a video camera. The weight of each pedestrian was measured using a digital weighing scale and their walking forces on a stiff surface were recorded using an instrumented treadmill. A pair of PeCo laser pedestrian counters, installed one at each end of footbridge above the walkway (Figure 7.1), was used to record in real-time traffic information. Laser counters are located 8 meters apart and can record the time and direction-stamped instances of each pedestrian crossing them. Laser counters are located 8 meters apart and can record the time and direction-stamped instances of each pedestrian crossing them.

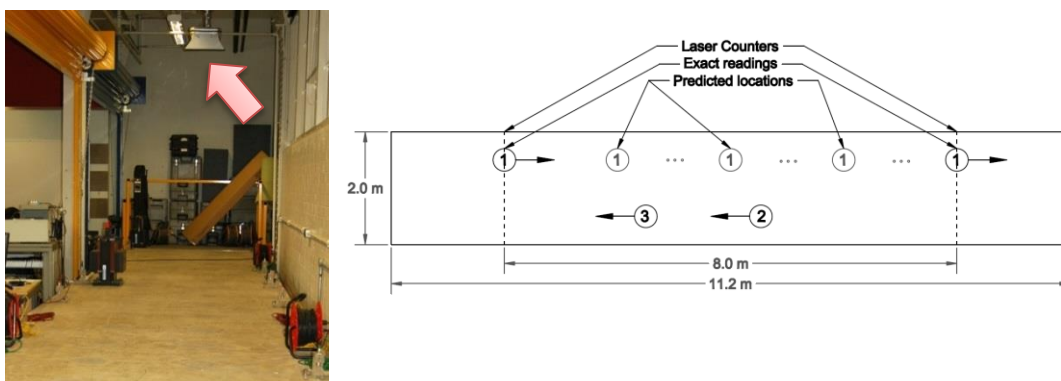


Figure 7.1. Prediction of people location between each two consecutive crossing of laser pedestrian counter

Figure 7.2 presents a typical time-history of pedestrian location on the structure for a test with three pedestrians.

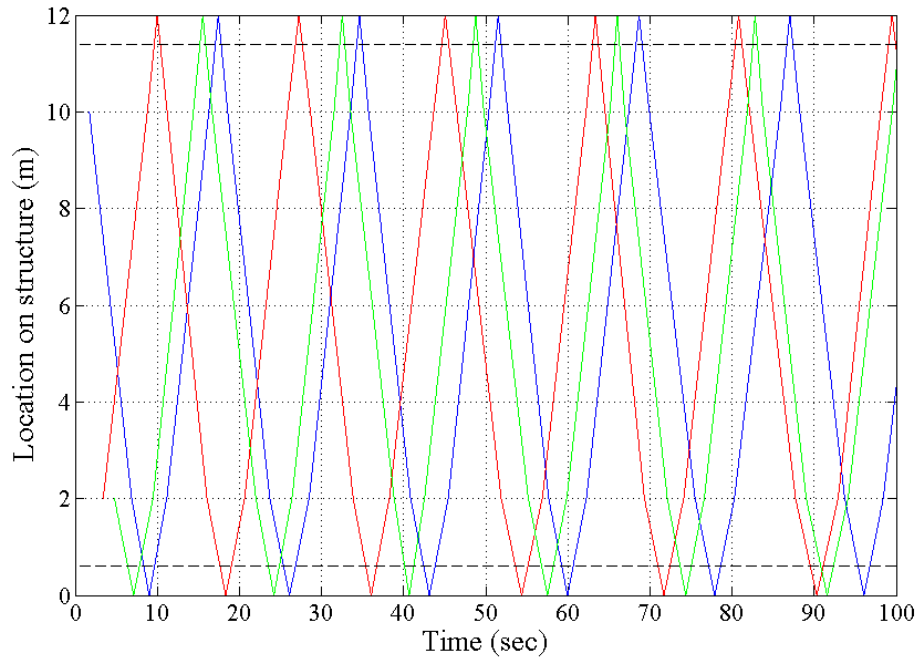
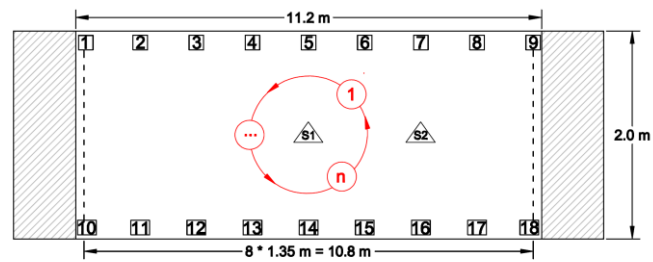


Figure 7.2. A typical time-history of location of three pedestrians on the structure presented with three different colors

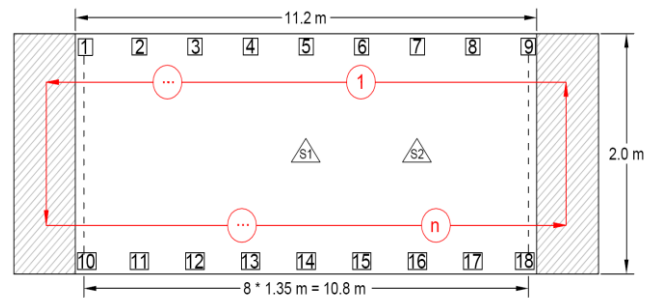
Location of each person is shown with different colour and supports location are shown with dashed lines. Time-history of each pedestrian location and walking speed are calculated by cross-comparing the laser's data with time-stamped video footage of each test. Walking speed is assumed constant between each two consecutive crossings of laser counters.

7.2.3 Occupied structure tests

Two different loading scenarios are designed for the test. In the first loading scenario test participants are asked to walk around a tight circle in specific locations on the structure (mid-span, quarter-span and 3/8 span) (Figure 7.3a).



a) scenario 1: Walking in tight circle



b) Scenario 2: Walking along the structure

Figure 7.3. A typical walking path of designed loading scenarios

In this loading scenario, people are assumed nominally stationary on the structure i.e. their locations on the structure are constant and are equal to the location of center of tight circle. Eight tests, five focused on the first mode of the structure and three focused on the second mode were done using this loading scenario. These tests are labeled with letter ‘C’ at the end of their test number.

In the second loading scenario test participants were asked to walk in a closed-loop path along the structure (Figure 7.3b). 15 tests, eight focused on first mode of structure and seven focused on the second mode designed with this loading scenario. Between 2 and 15 people participated in each test. They were asked to walk with their normal speed and were free to pass each other. 15 data blocks, each lasting 64 seconds, were acquired in each test to average out noise as much as possible and get better quality FRF curves. FRF test setups are identical to the empty structure tests with 18 accelerometers recording response along longer edges of the structure (Figure 7.3).

The occupied structure modal properties f_{os} , m_{os} and ζ_{os} were found for the target mode of the structure by curve-fitting the point-mobility FRF for each test. These parameters are presented in Table 7.1 and Table 7.2 for the tight-circle and along the structure walking patterns, respectively. Reader may refer to Appendix I to see the relation of the tests discussed in this chapter with the ones presented in Chapter 6.

Table 7.1. Modal properties of the occupied structure for different group sizes – walking around the tight circle tests

Test No.	Series	Location	No. of Peds	Modal properties of the occupied structure					Structural Response	
				f_{cs} (Hz)	ζ_{cs}	m_{cs} (kg)	c_{cs} (N.s/m)	k_{cs} (N/m)	a_{max} (m/s ²)	a_{rms} (m/s ²)
Mode 1 (Structure)										
1.1C	B	Mid-span	3	4.455	0.0200	7,214	8,077	$5,652 \times 10^3$	1.3226	0.2488
1.2C	B	Mid-span	6	4.480	0.0290	4,300	11,918	$5,784 \times 10^3$	1.0903	0.2008
1.3C	B	Mid-span	10	4.500	0.0340	7,415	14,256	$5,928 \times 10^3$	0.8656	0.1861
1.4C	B	3/8 -span	6	4.465	0.0250	7,287	10,222	$5,735 \times 10^3$	0.9920	0.1987
1.5C	B	1/4-span	6	4.460	0.0205	7,250	83,29	$5,693 \times 10^3$	1.0996	0.2195
Mode 2 (Structure)										
2.1C	B	1/4-span	3	16.913	0.0061	7,128	9,241	$80,496 \times 10^3$	2.2306	0.4188
2.2C	B	1/4-span	6	16.925	0.0082	7,128	12,432	$80,611 \times 10^3$	1.9406	0.3544
2.3C	B	1/4-span	10	16.975	0.0099	7,128	15,054	$81,091 \times 10^3$	1.6871	0.3660

Table 7.2. Modal properties of the occupied structure for different group sizes – ‘walking along the structure’ tests

Test No.	Series	Location	No. of Peds	Modal properties of the occupied structure					Structural Response	
				f_{cs} (Hz)	ζ_{cs}	m_{cs} (kg)	c_{cs} (N.s/m)	k_{cs} (N/m)	a_{max} (m/s ²)	a_{rms} (m/s ²)
Mode 1 (Structure)										
1.1	A	All-over	2	4.443	0.0100	7,165	4,000	$5,583 \times 10^3$	2.4361	0.4131
1.2	B	All-over	3	4.445	0.0110	7,183	4,413	$5,603 \times 10^3$	1.7489	0.3018
1.3	A	All-over	4	4.450	0.0128	7,201	5,154	$5,630 \times 10^3$	2.1755	0.3637
1.4	A	All-over	6	4.465	0.0155	7,238	6,294	$5,696 \times 10^3$	1.8771	0.3311
1.5	B	All-over	6	4.465	0.0165	7,238	6,701	$5,696 \times 10^3$	1.4882	0.2481
1.6	B	All-over	10	4.475	0.0230	7,311	9,456	$5,780 \times 10^3$	1.1313	0.2050
1.7	A	All-over	10	4.476	0.0210	7,311	8,635	$5,782 \times 10^3$	1.5876	0.2870
1.8	A	All-over	15	4.485	0.0291	7,402	12,140	$5,878 \times 10^3$	1.1251	0.2466
Mode 2 (Structure)										
2.1	B	All-over	3	16.900	0.0055	7,128	8,326	$80,372 \times 10^3$	2.4059	0.4482
2.2	A	All-over	6	16.813	0.0053	7,128	7,982	$79,548 \times 10^3$	2.9046	0.5595
2.3	B	All-over	6	16.910	0.0065	7,128	9,846	$80,468 \times 10^3$	2.2905	0.4234
2.4	A	All-over	8	16.819	0.0061	7,128	9,190	$79,605 \times 10^3$	2.5591	0.5133
2.5	A	All-over	10	16.822	0.0064	7,128	9,644	$79,634 \times 10^3$	2.5232	0.5223
2.6	B	All-over	10	16.935	0.0075	7,128	11,377	$80,708 \times 10^3$	2.1387	0.4023
2.7	A	All-over	15	16.825	0.0079	7,128	11,907	$79,665 \times 10^3$	2.2358	0.4725

Comparing occupied (Table 7.1 and Table 7.2) and empty structure (Table 6.1) modal

properties, considerable difference in the modal frequency and damping ratio are noticeable. These changes are considered as the effects of HSI during walking. The identification method designed for this chapter (described in Section 7.3) tries to use these observed effects to predict the possible properties of human model.

7.2.4 Mode shape changes

One of the key assumptions of the identification procedure used in this chapter is that the presence of walking people on a structure does not affect the mode shape of the structure. This assumption is examined by comparing the mode shapes of the empty and of the occupied structure when 10 people walked on it. The acceleration responses recorded by all 18 accelerometers on structure were used to find the first mode shape of structure in ME'Scope software. First mode shapes of the empty and occupied footbridge are over-plotted in Figure 7.4.

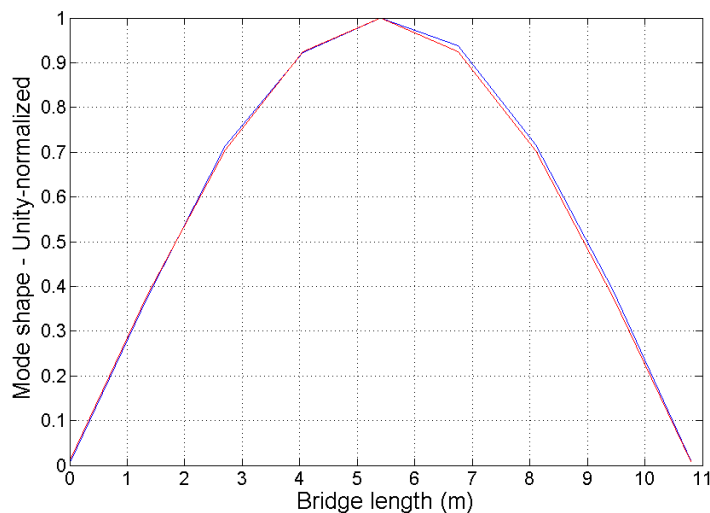


Figure 7.4. First mode shape of empty (blue trace) and occupied (red trace) Sheffield footbridge

These mode shapes are the average of both long sides of structure for each test. No significant difference is noticeable between the two mode shapes indicating that mode shapes do not change for occupied and empty structure. Moreover, based on this finding an assumption was made that for the given constant number of people walking across the structure, modal properties of the structure *averaged* over the test duration, do not vary with time despite the fact that people's location change continuously with time.

7.3 Identification of walking human model

Having acquired the experimental data, all ingredients were in place for the multi-person model identification. The identification process was designed based on reverse engineering concept. This means that the changes observed in modal properties of structure when people were walking on it were used to predict the possible parameters of walking human model. Having such comprehensive experimental data demands a detailed and realistic model to be able to utilise them as best as possible to simulate walking traffic.

7.3.1 Walking traffic – structure model

The heart of all simulations done in this study is the 'stationary' walking traffic-structure model which represents overall average effects of walking pedestrians. This is the model of an imaginary situation in which people are walking but their location on the structure does not change. It can be imagined as people walking on a series of treadmills installed at fixed locations on a structure (Figure 7.5).

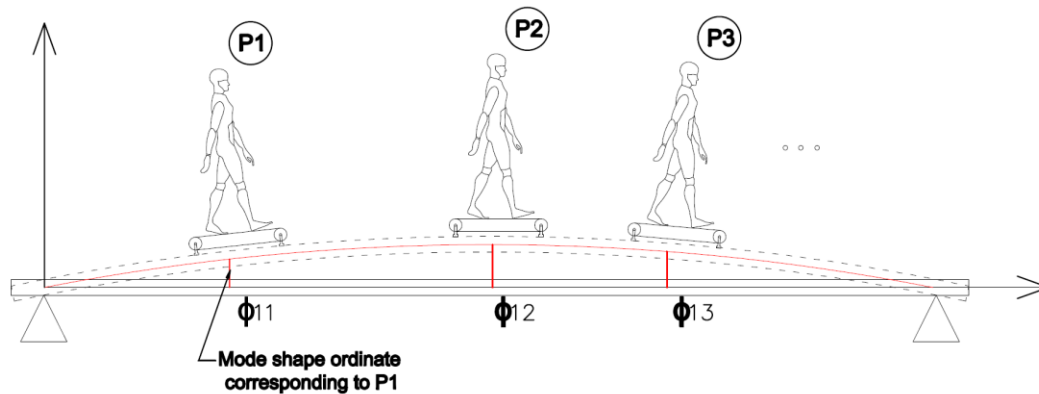


Figure 7.5. A conceptual illustration of stationary walking people

A SDOF mass-spring-damper model was used to simulate dynamics of each walking individual on the structure. Similarly, a SDOF model was used to simulate one mode of the structure at a time. The effects of constant location of each person on the structure were taken into account using structure mode shape ordinate at the location of each person. For simulations done in this study, walking forces of people and shaker force are not considered as only eigenvalue problem is solved to find modal properties of the occupied structure.

Figure 7.6 presents the mass-spring-damper model of a stationary walking traffic-structure system.

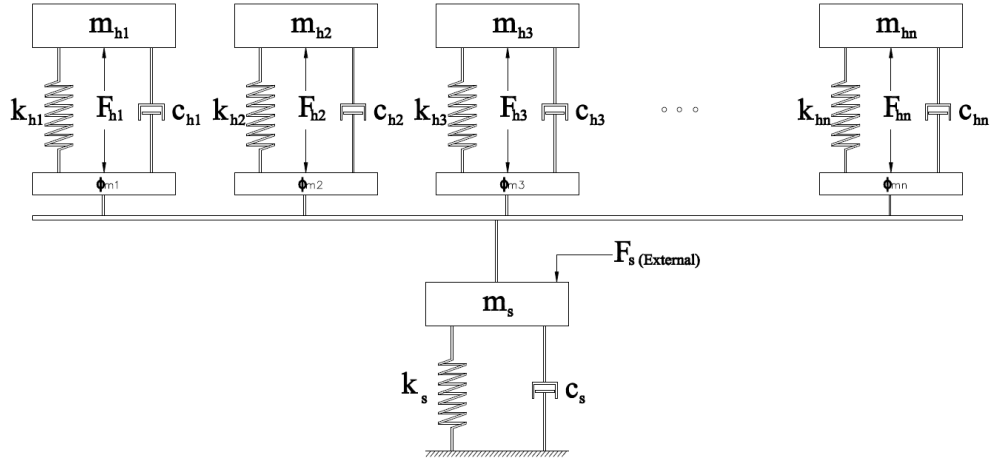


Figure 7.6. MDOF Mass-spring-damper model of stationary walking traffic-structure system

Being stationary, walking traffic-structure system shown in Figure 7.6 can be treated as a conventional multiple degrees of freedom system. A modified system of equations of motion (Equation 7.4) is developed that takes into account the location of people on the structure:

$$\begin{bmatrix} m_{es,j} & 0 & 0 & \cdots & 0 \\ 0 & m_{h1} & 0 & \cdots & 0 \\ 0 & 0 & m_{h2} & \cdots & 0 \\ \vdots & \vdots & \vdots & \ddots & \vdots \\ 0 & 0 & 0 & \cdots & m_{hn} \end{bmatrix} \begin{bmatrix} \ddot{x}_{os,j}(t) \\ \ddot{x}_{h1}(t) \\ \ddot{x}_{h2}(t) \\ \vdots \\ \ddot{x}_{hn}(t) \end{bmatrix} +$$

$$\begin{bmatrix} c_{es,j} + (c_{h1} \times \varphi_{1j}) + (c_{h2} \times \varphi_{2j}) + \cdots + (c_{hn} \times \varphi_{nj}) & -(c_{h1} \times \varphi_{1j}) & -(c_{h2} \times \varphi_{2j}) & \cdots & -(c_{hn} \times \varphi_{nj}) \\ & c_{h1} & 0 & \cdots & 0 \\ & -(c_{h2} \times \varphi_{2j}) & c_{h2} & \cdots & 0 \\ & \vdots & \vdots & \ddots & \vdots \\ & -(c_{hn} \times \varphi_{nj}) & 0 & 0 & \cdots & c_{hn} \end{bmatrix} \begin{bmatrix} \dot{x}_{os,j}(t) \\ \dot{x}_{h1}(t) \\ \dot{x}_{h2}(t) \\ \vdots \\ \dot{x}_{hn}(t) \end{bmatrix} +$$

$$\begin{bmatrix} k_{es,j} + (k_{h1} \times \varphi_{1j}) + (k_{h2} \times \varphi_{2j}) + \cdots + (k_{hn} \times \varphi_{nj}) & -(k_{h1} \times \varphi_{1j}) & -(k_{h2} \times \varphi_{2j}) & \cdots & -(k_{hn} \times \varphi_{nj}) \\ & k_{h1} & 0 & \cdots & 0 \\ & -(k_{h2} \times \varphi_{2j}) & k_{h2} & \cdots & 0 \\ & \vdots & \vdots & \ddots & \vdots \\ & -(k_{hn} \times \varphi_{nj}) & 0 & 0 & \cdots & k_{hn} \end{bmatrix} \begin{bmatrix} x_{os,j}(t) \\ x_{h1}(t) \\ x_{h2}(t) \\ \vdots \\ x_{hn}(t) \end{bmatrix} =$$

$$\begin{bmatrix} f_{ex,j}(t) + (f_{h1}(t) \times \varphi_{1j}) + (f_{h2}(t) \times \varphi_{2j}) + \cdots + (f_{hn}(t) \times \varphi_{nj}) \\ 0 \\ 0 \\ \vdots \\ 0 \end{bmatrix}$$

(Equation 7.4)

Where $m_{es,j}$, $c_{es,j}$ and $k_{es,j}$ are mode 'j' modal mass, damping and stiffness of the empty structure and m_{hi} , c_{hi} and k_{hi} are those of the walking individuals. Viscous damping is assumed for walking human models. $\ddot{x}_{os,j}(t)$, $\dot{x}_{os,j}(t)$ and $x_{os,j}(t)$ are acceleration, velocity and displacement response of occupied structure DOF in the system. As one mode of the structure 'j' is simulated at a time, $\ddot{x}_{os,j}(t)$, $\dot{x}_{os,j}(t)$ and $x_{os,j}(t)$ represent the modal response of occupied structure. Similarly, $\ddot{x}_{hi}(t)$, $\dot{x}_{hi}(t)$ and $x_{hi}(t)$ represent acceleration, velocity and displacement of the i^{th} walking person DOF. $f_{ex,j}(t)$ is the mode 'j' modal force (if any) due to an external force acting on the structural DOF and $f_{hi}(t)$ is a walking forces of person 'i' on a stiff surface. φ_{ij} is the ordinate of 'jth' mode shape of structure at the location of person 'i'.

Equation 7.4 shows that the damping matrix of the system is not necessarily proportional. Therefore, the conventional formulation of the eigenvalue problem will not yield modal vectors (eigenvectors) that uncouple the equations of motion of the system. The technique used here to circumvent this problem was first documented by (Frazer, et al., 1957) and involves the reformulation of the original equations of motion, for an N-degree of freedom system, into an equivalent set of $2N$ first order differential equations known as Hamilton's Canonical Equations.

In the first step, a new coordinate vector $\{y\}$ containing displacement and velocity is defined:

$$\{y(t)\} = \begin{Bmatrix} x(t) \\ \dot{x}(t) \end{Bmatrix} \quad \text{(Equation 7.5)}$$

Then Equation 7.4 is re-written into following form for modal analysis:

$$\begin{bmatrix} [C] & [M] \\ [M] & [0] \end{bmatrix} \{y(t)\} + \begin{bmatrix} [K] & [0] \\ [0] & [-M] \end{bmatrix} \{y(t)\} = \{0\} \quad (\text{Equation 7.6})$$

Equation 7.6 leads to a standard eigenvalue problem and can be solved for eigenvectors and eigenvalues accordingly. Further discussion on modal analysis of systems with non-proportional damping is beyond the scope of this study.

The MDOF system in Figure 7.6 has $n+1$ modes of vibration. The *dominant mode* of vibration is defined as the mode with maximum response at the degree of freedom corresponding to the structure. The modal properties of the dominant mode are selected as the modal properties of the *occupied structure*. For consistency and to allow for mode superposition, mode shapes need to be scaled in a way that the ordinate of the structure DOF is unity. Such scaling ensures that modal properties of the crowd-structure system are found with the same scaling as the empty structure.

7.3.2 Identification process

The identification process used in this study uses an iterative approach. Initial ranges of 1-10 Hz with 0.05 Hz steps for f_h and 5 - 70% with 2.5% steps for ζ_h were selected to model walking human ('h' subscript is used instead of 'h_i' here to refer generally to human model parameters). These ranges were selected based on the values suggested in the biomechanics literature (Sachse, et al., 2004; Miyamori, et al., 2001; Ferris, et al, 1998) and the study done by Silva, et al. (2011) on walking people. For each test, every possible combination of f_h and ζ_h are used one at a time to simulate walking traffic on the structure. Identical f_h and ζ_h was used in each simulation for all pedestrians. Mass of the human model m_h is assumed constant and equal to the average mass of participants in the corresponding test. This is done for two

reasons: first, there was no conclusive agreement in the literature on the percentage of human mass that contribute to the dynamics of walking and its variations over different speeds, etc. The second reason was to keep the number of variables as low as possible to enhance the accuracy of the results of identification process. The empty structure modal properties presented in Table 6.1 were used for m_{es} , k_{es} and c_{es} .

The multi-degree-of-freedom (MDOF) traffic-structure model described in Section 7.3.1 was used to simulate each test and to find occupied structure parameters f_{os} , m_{os} and ζ_{os} . These parameters and peak magnitude of the FRF curve a_{FRF} were compared with their experimental counterparts and the corresponding errors were calculated. This process was repeated for all combinations of f_h and ζ_h for each test.

A series of maximum acceptable errors were defined for the predicted f_{os} , m_{os} , ζ_{os} and a_{FRF} . These are 0.01 Hz for f_{os} , 250 kg for m_{os} , 1% for ζ_{os} and 20% for a_{FRF} . For each test, the ranges of human model parameters f_h and ζ_h were identified that predict f_{os} , m_{os} , ζ_{os} and a_{FRF} with errors less than the maximum values. These ranges will be referred to as ‘test-verified’ ranges. In the next step, the test-verified ranges of f_h and ζ_h were combined for all tests (each mode separately) and a common range of f_h and ζ_h across all tests is found. This ensures that if any combination of f_h and ζ_h , selected from these common ranges, was used to simulate people in any of test, predicted f_{os} , m_{os} , ζ_{os} and a_{FRF} would be within acceptable error ranges.

7.3.2.1 SCENARIO 1: NOMINALLY STATIONARY WALKING TRAFFIC

Eight tests, five focused on first mode of structure and three focused on second mode is done using this loading scenario. The tight-circle walking pattern (Figure 7.3a) of this scenario is designed in a way that walking people can be assumed stationary on the structure. This eliminates physically the time-variance of the modal properties of the structure due to change of location of walking people on it and makes possible to use Equation 7.4 without any

assumptions. As previously mentioned, the centre of circular walking path is used as the constant location of all walking people for each test.

Table 7.3 presents the test-verified ranges of human model f_h and ζ_h resulted from simulations. A typical over-plot of occupied structure FRF graphs for test-verified f_h and ζ_h corresponding to test 1.1C (Table 7.3) is presented in Figure 7.7. As it can be seen in this figure, any combination of f_h and ζ_h selected from the corresponding test-verified ranges estimate the occupied structure FRF accurately.

Table 7.3. Test-verified ranges of SDOF human model parameters – Scenario 1

Test No.	No. of Peds	Location	Average human mass (kg)	Acceptable ranges of SDOF human model parameters				
				f_h (Hz)		m_h (kg)	ζ_h	
				Min	Max		Min	Max
Mode 1 (Structure)								
1.1C	3	Mid-span	70	2.75	3.25	70	0.250	0.350
1.2C	6	Mid-span	70	2.75	3.25	70	0.250	0.325
1.3C	10	Mid-span	70	2.25	3.00	70	0.250	0.300
1.4C	6	3/8 -span	70	2.50	3.20	70	0.275	0.350
1.5C	6	1/4-span	70	2.50	3.40	70	0.275	0.400
Mode 2 (Structure)								
2.1C	3	1/4-span	70	5.75	7.75	70	0.100	0.200
2.2C	6	1/4-span	70	5.50	6.75	70	0.125	0.200
2.3C	10	1/4-span	70	5.75	6.75	70	0.125	0.175

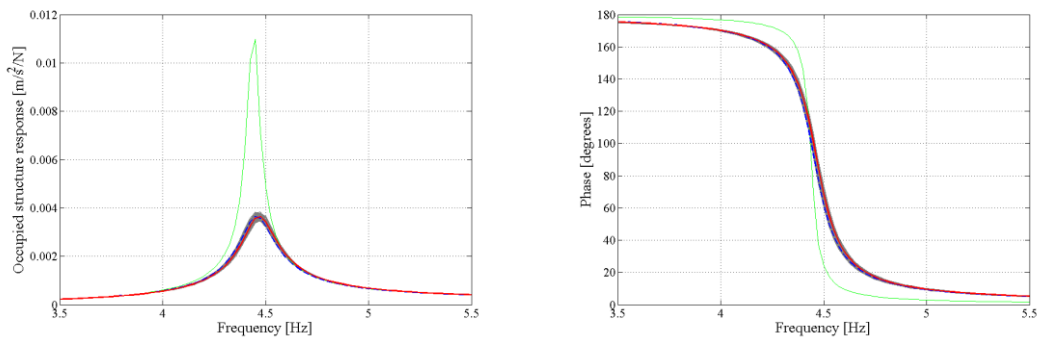


Figure 7.7. A typical over plot of occupied structure FRF graphs resulted from accepted human model parameters (Grey curves) – Test No 1.1C – (3 pedestrians walking at mid-span – Empty structure: green; Experimental: Blue; Best analytical match: Red)

7.3.2.2 SCENARIO 2: MOVING ALONG THE STRUCTURE

The Scenario 2 comprises 15 tests in which pedestrians are walking along structure freely and therefore their locations on structure change with time. As location of people in this scenario cannot be assumed stationary, the stationary traffic-structure model described in Section 7.3.1 cannot be used directly. To tackle this problem, two methods are designed to approximate moving people with a series of stationary cases. Using these methods makes it possible to use the stationary traffic-structure model to find occupied structure modal properties under the moving pedestrians load.

7.3.2.2.1 Method 1

Method 1 is based on the assumption that a uniform moving traffic can be simulated using a series of pre-defined location patterns and their corresponding probability of occurrence. This means that instead of simulating moving people, they can be ‘frozen’ in their location in few consecutive snapshots and claim that people repeat this pattern. Using this assumption, occupied structure modal properties can be found by averaging occupied structure properties of each pre-defined pattern based on their probability of occurrence.

For each test, a series of pre-defined location patterns similar to one presented in Figure 7.8 is defined.

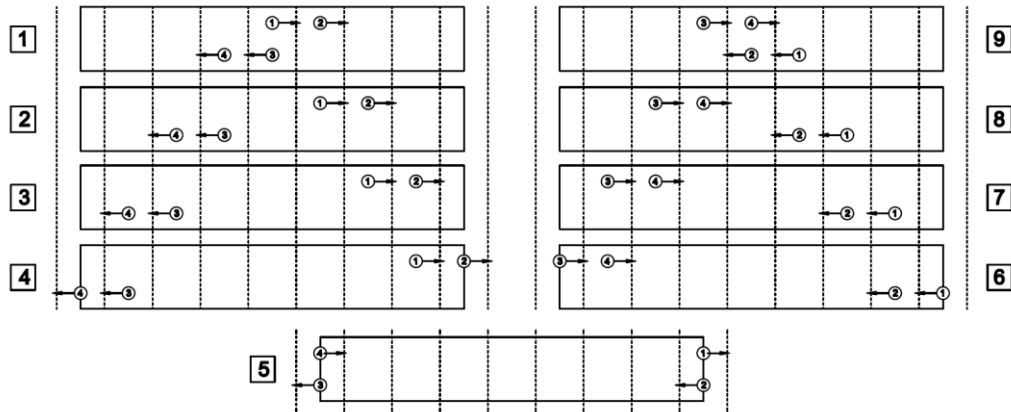


Figure 7.8. The illustration of pre-defined location patterns for the group of 4 pedestrians

The structure and its two side platforms (Figure 3.3) are divided into 9 equal size segments and equal constant walking speed is assumed for all pedestrians. Based on these assumptions, probability of presence of people in each of these nine segments is the same. For instance for the group of 4 walking people (presented in Figure 7.8), 9 patterns with equal probability of happening were defined. As both mode 1 and 2 shapes are (anti-)symmetric with respect to mid-span point, pairs of 1 and 9, 2 and 8, 3 and 7, and 4 and 6 patterns create the same effect on the structure. Therefore 5 unique location patterns with the following probabilities are considered for this test:

- Pattern 1 (or 9) - Probability: $2/9$
- Pattern 2 (or 8) - Probability: $2/9$
- Pattern 3 (or 7) - Probability: $2/9$
- Pattern 4 (or 6) - Probability: $2/9$
- Pattern 5 - Probability: $1/9$

Each of location patterns is simulated with the stationary traffic-structure model in which locations of people are assumed stationary within their corresponding segments. The resulted occupied structure modal properties are then averaged for all location patterns based on their

probability of occurrence. For example, Figure 7.9 shows a typical over plot of occupied structure FRF graphs for 5 pre-defined location patterns (grey curves) and the average FRF (red) corresponding to test 1.2 (Table 7.4). The good match between the average analytical and experimental FRF curves can be seen in this figure. The same identification process was followed here assuming that the average FRF found for each simulation is representing occupied structure FRF.

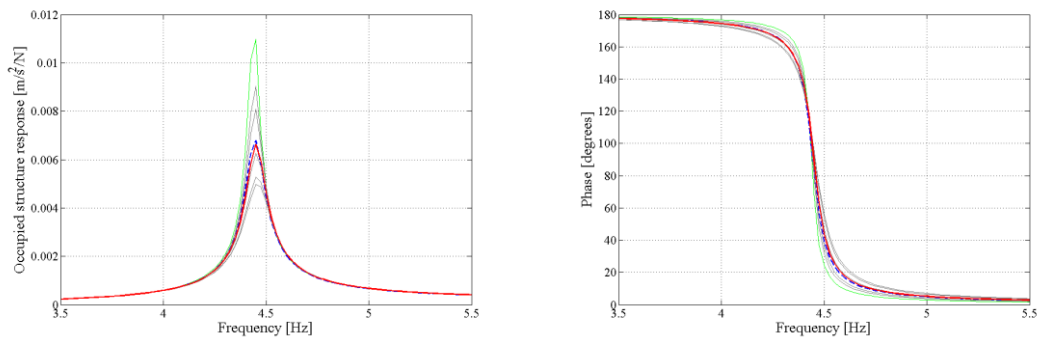


Figure 7.9. A typical over plot of occupied structure FRF graphs for different location patterns and the average FRF– Test No. 1.2 – (Empty structure: Green; Curves corresponding to different patterns: Grey; Average analytical: Red; Experimental: Blue)

The test-verified ranges of human model f_h and ζ_h resulted from simulations are presented in Table 7.4. A typical over-plot of average occupied structure FRF graphs for test-verified f_h and ζ_h corresponding to test 1.2 (Table 7.4) is presented in Figure 7.10. As it can be seen in this figure, similar to Scenario 1, any combination of f_h and ζ_h selected from corresponding test-verified ranges approximate occupied structure dynamics accurately enough.

Table 7.4. Test-verified ranges of SDOF human model parameters
Scenario 2- Method 1

Test No.	No. of Peds	Location	Average human mass (kg)	Acceptable ranges of SDOF human model parameters				
				f_h (Hz)		m_h (kg)	ζ_h	
				Min	Max		Min	Max
Mode 1 (Structure)								
1.1	2	All-over	55	2.50	3.50	55	0.225	0.400
1.2	3	All-over	70	1.50	3.00	70	0.250	0.400
1.3	4	All-over	55	2.25	3.50	55	0.225	0.375
1.4	6	All-over	55	2.50	3.25	55	0.200	0.300
1.5	6	All-over	70	2.50	3.25	70	0.225	0.325
1.6	10	All-over	70	2.50	3.25	70	0.275	0.325
1.7	10	All-over	60	2.75	3.25	60	0.225	0.325
1.8	15	All-over	70	2.50	3.00	70	0.275	0.325
Mode 2 (Structure)								
2.1	3	All-over	80	6.50	8.00	80	0.100	0.200
2.2	6	All-over	55	6.50	7.25	55	0.100	0.175
2.3	6	All-over	70	5.75	7.00	70	0.100	0.200
2.4	8	All-over	75	5.50	6.75	75	0.100	0.175
2.5	10	All-over	55	6.00	7.00	55	0.100	0.175
2.6	10	All-over	70	5.75	6.75	70	0.100	0.200
2.7	15	All-over	70	5.00	6.75	70	0.100	0.175

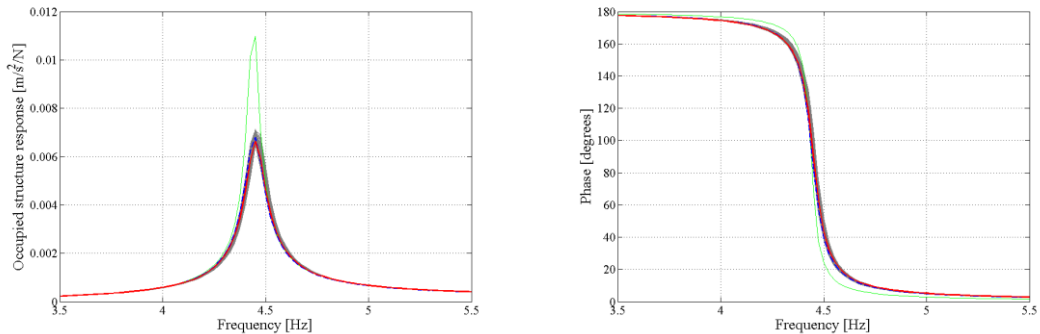


Figure 7.10. A typical over plot of average occupied structure FRF graphs resulted from accepted human model parameters (Grey curves) – Test No 1.2– (Empty structure: Green; Average analytical: Red; Experimental: Blue)

7.3.2.2.2 Method 2

The second method takes the procedure of location simulation one step forward and uses the instantaneous location of each person recorded during each test. For each time-step, location

of each pedestrian on the structure is read from the corresponding recorded location time-histories. Walking people are assumed stationary at their locations for that time-step and stationary traffic-structure model is used to find occupied structure modal properties for that particular time-step. Simulation is repeated for all time-steps of each test and time-history of change of occupied structure modal properties f_{os} , ζ_{os} and m_{os} are found. These parameters are then averaged for each test over-time and the averaged parameters are used as modal properties of occupied structure. The test-verified ranges of SDOF human model parameters f_h and ζ_h found in these simulations are presented in Table 7.5.

Table 7.5. Test-verified ranges of SDOF human model parameters
Scenario 2 - Method 2

Test No.	No. of Peds	Location	Average human mass (kg)	Acceptable ranges of SDOF human model parameters				
				f_h (Hz)		m_h (kg)	ζ_h	
				Min	Max		Min	Max
Mode 1 (Structure)								
1.1	2	All-over	55	2.50	3.50	55	0.200	0.400
1.2	3	All-over	70	2.25	3.25	70	0.200	0.400
1.3	4	All-over	55	2.25	3.25	55	0.250	0.375
1.4	6	All-over	55	2.50	3.25	55	0.200	0.300
1.5	6	All-over	70	2.25	3.00	70	0.225	0.325
1.6	10	All-over	70	2.50	3.00	70	0.250	0.325
1.7	10	All-over	60	2.75	3.00	60	0.225	0.300
1.8	15	All-over	70	2.25	3.00	70	0.275	0.325
Mode 2 (Structure)								
2.1	3	All-over	80	6.50	7.75	80	0.100	0.175
2.2	6	All-over	55	6.50	7.50	55	0.100	0.175
2.3	6	All-over	70	6.00	6.75	70	0.100	0.200
2.5*	10	All-over	55	6.00	7.00	55	0.100	0.175
2.6	10	All-over	70	6.00	6.75	70	0.100	0.175

* 2.4 and 2.7 are not analyzed as location time history was not available.

A typical time-history of f_{os} and ζ_{os} resulted from a set of test-verified f_h and ζ_h corresponding to test 1.2 is presented in Figure 7.11. The over plotted occupied structure FRF graphs corresponding to this test-verified f_h and ζ_h are also presented in Figure 7.12. As it can be seen in this figure, similar to the results of Method 1, any combination of f_h and ζ_h selected from corresponding test-verified ranges approximate occupied structure dynamics accurately.

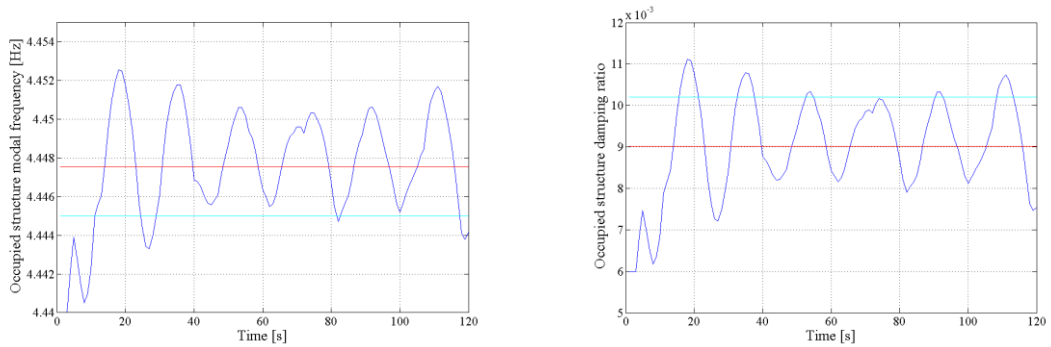


Figure 7.11. A typical time-history of f_{os} and ζ_{os} (blue), average value (red) and experimental value (cyan) resulted from a typical accepted human model parameter set – Test No 1.2 – (3 pedestrians)

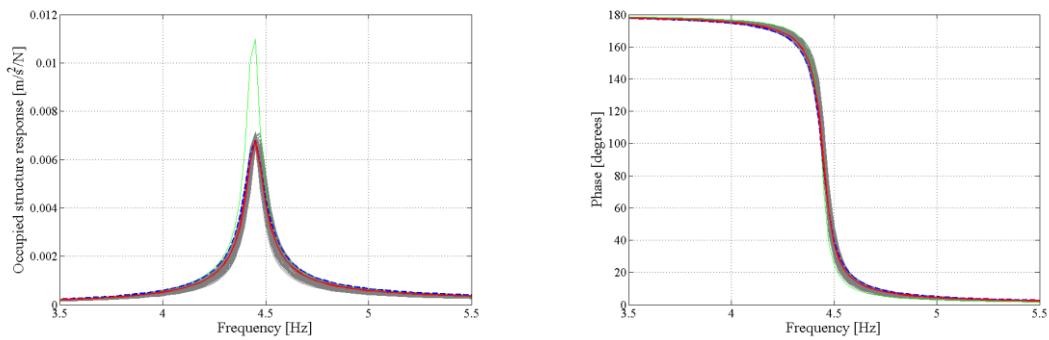


Figure 7.12. A typical over plot of empty (green), test-verified occupied structure FRF graphs (grey), analytical average FRF (red) and experimental FRF (blue) resulted from test-verified human model parameters – Test No 1.2 – (3 pedestrians)

7.3.3 Common ranges of human model parameters

The test-verified ranges found in all simulations of both scenarios are compared and a common range is found for f_h and ζ_h for each mode. These common ranges are shown in Figure 7.13. As it can be seen in this figure, the common ranges found for f_h and ζ_h for first mode tests are 2.75 – 3.00 Hz and 27.5 % – 30% respectively. These ranges are found 6.5 – 6.75 Hz and 12.5 % – 17.5% respectively for the tests targeting second mode of structure. The difference between the ranges of human model parameters found from mode 1 and mode 2 tests might be an indicator of the ‘multi-mode’ dynamics of human body, the study

of which is beyond the scope of this research.

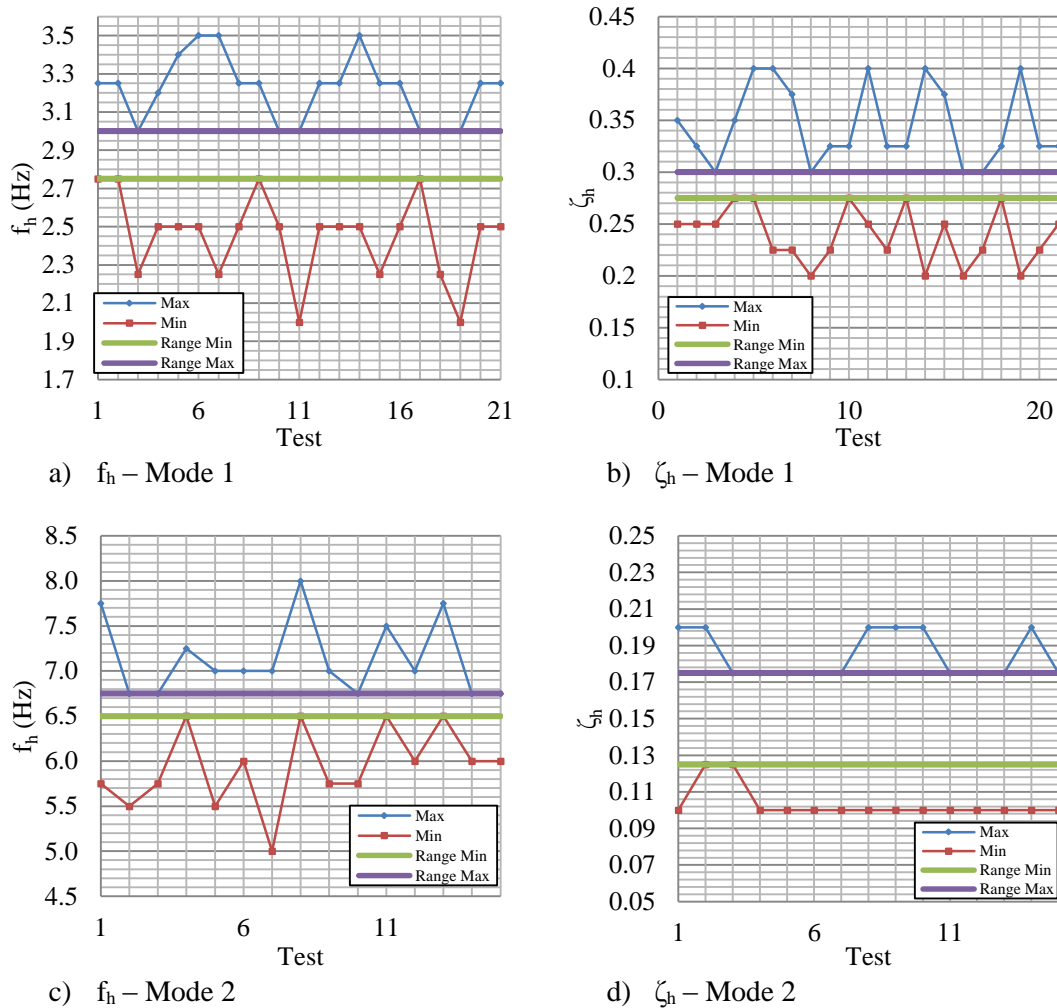


Figure 7.13. Test-verified ranges of f_h and ζ_h found in different tests and their common ranges

7.3.4 Expected errors

To understand how good each arbitrary combination of f_h and ζ_h selected from their common ranges (selected across all tests) can predict occupied structure dynamics, the analysis is taken one step forward. Simulations are repeated again for all mode 1 tests but this time with common ranges of f_h and ζ_h as input. The occupied structure parameters f_{os} , ζ_{os} and a_{FRF} are estimated for each combination of f_h and ζ_h and compared with their corresponding experimental values to find their associated errors. The errors associated with estimated f_{os} ,

ζ_{os} and a_{FRF} for each combination of f_h and ζ_h are averaged over all tests and presented in Figure 7.14. As it can be seen in these graphs, the minimum errors of estimating f_{os} , ζ_{os} and a_{FRF} are not associated with a unique set of f_h and ζ_h i.e. no particular set of f_h and ζ_h can predict all f_{os} , ζ_{os} and a_{FRF} with minimum error at the same time.

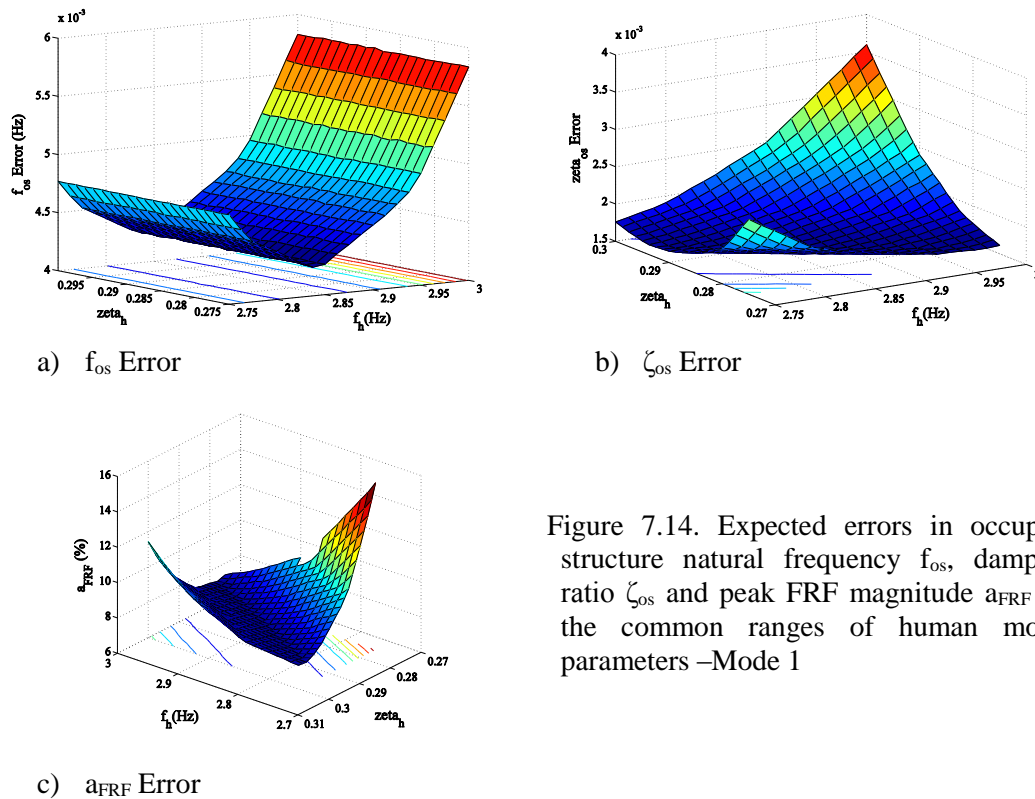


Figure 7.14. Expected errors in occupied structure natural frequency f_{os} , damping ratio ζ_{os} and peak FRF magnitude a_{FRF} for the common ranges of human model parameters –Mode 1

7.4 Conclusions

The work presented used probably the most comprehensive traffic-structure experimental data collected to date, to identify the parameters of SDOF walking human model. Three different identification processes with increasing level of details were used. The analysis results suggest the ranges of 2.75 – 3.00 Hz and 27.5 % – 30% for natural frequency and damping ratio of the SDOF walking human model, respectively. Average mass of people of 70 kg was assumed for the walking human model. These results compare reasonably well

with values suggested by other researchers and specifically for walking people. The comprehensive experimental data, variety of loading scenarios, detailed simulation process and coherent results from different methods provide high level of confidence about the validity of the findings.

The experimental data set used in this research can serve as a benchmark for data collection for multi-pedestrian HSI studies. Moreover, the proposed methodologies for simulating time-varying location of walking people on the structure proved accurate and practical and can be used by design engineers to simulate the walking traffic.

The different human model parameters found for mode 1 and 2 of structure is a novel finding, but was observed for stationary people (Sachse, 2002) with different SDOF parameters identified. Further research on different real-life structures need to be done to extend and validate the findings of this research for different structures and loading scenarios.

Chapter 8

Identification of Mass-Spring-Damper Model of Walking Human

Agent-based Modelling

The contents of this chapter are adapted with minor changes from the following journal paper in preparation to be submitted to the Journal of Sound and Vibration:

Shahabpoor, E., Pavić, A. and Racić, V. Identification of Walking Human Model using Agent-based Modelling. Journal of Sound and Vibration.

8.1 Introduction

This chapter, similar to Chapter 7, is focused on identifying the parameters of the SDOF MSD model of the walking human but using an *agent-based* discrete traffic-structure model. Each walking pedestrian and structure was modelled using an SDOF MSD model. The natural frequency and damping ratio of the walking human model is identified for each test using ‘reverse engineering’. This is done by adjusting the unknown properties of the walking individuals in a way that the regenerated structure FRF fits its experimental counterpart.

Section 8.2 of this chapter presents a short introduction into agent-based modelling (ABM) and its application to vibration serviceability assessment. A detailed description of the experimental campaigns and the selection of results used in this study are presented in Section 8.3. In Section 7.3 the proposed identification procedures and the ABM discrete walking traffic-structure model are described in detail. Results of the analysis were combined with findings presented in Chapter 7 and are presented in Section 8.5 in the form of mathematical models describing statistical distributions of the natural frequency and damping ratio of the walking human SDOF MSD model. The concluding remarks are presented in Section 8.6.

8.2 Agent-based Modelling

An agent-based model (ABM) or sometimes called individual-based model (IBM) is a class of computational micro-scale models (Gustafsson and Sternad, 2010) for simulating the actions and interactions of autonomous ‘agents’ to assess the overall system behavior. Agents are the smallest elements of the system that interact with other parts of the system. Conceptually, ABM defines the behavior of agents at the micro level and the macro behavior of the system emerges from all the interactions between entities (Macy and Willer, 2002). This architecture allows agents to perceive environment and provides them with initiative, independence and the ability to interact with other agents (Jennings et al., 1998).

Most agent-based architectures are generally composed of: (1) numerous agents specified at various types; (2) decision-making heuristics; (3) learning rules or adaptive processes; (4) an interaction topology; and (5) a non-agent environment (Barker, 2006). In general, for each time-step of simulation and for each agent, all the boundary conditions, forces and previous state of each agent is used to find the next state of that agent. This is done by using the pre-defined behavioral rules, decision-making processes and interaction mechanisms in the model. Repeating this process in time generates the overall behavior of the system.

ABMs are widely used in simulation of pedestrian movement, particularly in simulation of traffic routing and evacuations, but their application in vibration serviceability assessment is almost not existent. This method of simultaneous modelling of multiple interaction mechanisms while taking into account the inter- and intra- subject variability of pedestrians has the potential to improve significantly the analytical studies of human-structure interaction. To the best of the authors' knowledge, Carroll's work (2013) is the first attempt in vibration serviceability that uses ABM to simulate human-structure interaction. He used inverted pendulum model of an individual walking person to model *lateral* interaction of a multi-pedestrian traffic with structure. The hybrid interactions of pedestrians (i.e. with both structure and other people in the vicinity) are considered in his simulations. This pioneering work sheds light on the potential of ABM in simulation of human-environment interaction. However, the potential of ABM in the *vertical* direction has not been explored, yet. This is important as the human-structure interaction mechanism in the vertical direction is considerably different from that in the lateral direction.

The ABM protocol used in this chapter is adopted from work of Grimm et al. (2006). Each individual pedestrian and the targeted mode of structure are modelled as an agent with dynamics formulated with a SMSD model. Although ABM is capable of simulating complex behaviours such as decision making; heuristic behaviour, learning rules and adaptiveness,

but due to the uncertainty associated with the predicted results, its decided to use actual experimental values in the model, instead.

The interactions of people with each other were introduced into the model by using the measured instantaneous location and speed of each agent during experiments and interactions of the people with obstacles in the pathway and with the surrounding environment were assumed to be negligible due to the controlled situation of the tests. The ABM is only focused on simulating interaction of walking people with the structure in the vertical direction ad no specific additional modelling of the human-human and human-environment interaction was performed. This increased significantly the accuracy of the simulations since the associated errors of estimating these interactions were eliminated.

8.3 Experimental work

Two series of tests (referred to as Series ‘A’ and ‘B’) were carried out on the Sheffield footbridge at different times but with identical test setup. Each series comprise a set of FRF-based modal tests on empty structure and structure when certain numbers of people are walking on it. In total, 8 tests focused on first mode of structure and 3 tests focused on the second mode were selected or this study. In these tests 2 to15 people were asked to walk on structure and modal properties of the occupied structure are found.

8.3.1 Empty structure

The structure used in this study is a simply supported in-situ cast post-tensioned (PT) concrete footbridge purposefully constructed in the structures laboratory of The University of Sheffield. The details of the structure and its modal properties are presented in Sections 3.3.1 and 6.3.2, respectively.

8.3.2 Occupied structure tests

Eleven tests, eight focused on first mode of structure and three focused on the second mode were designed with range of 2-15 people walking in a closed-loop path along the structure (Figure 8.1).

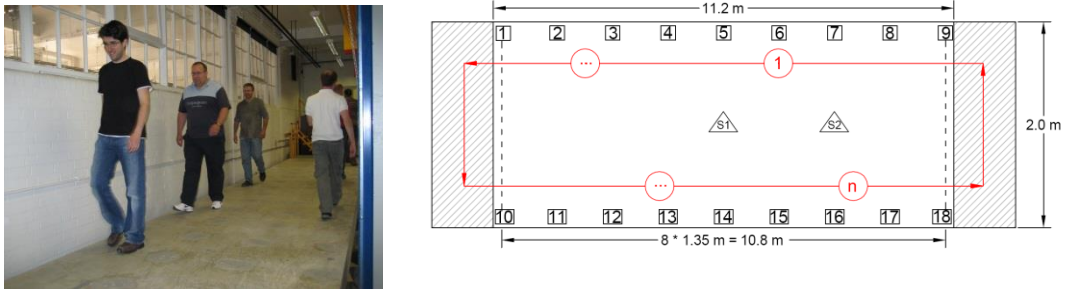


Figure 8.1. A typical walking path

Tests participants were asked to walk with their desired speed and they were free to pass each other. 15 data blocks, each lasting 64 seconds, were acquired in each test to average out noise as much as possible and get better quality FRF curves. FRF test setups were identical to the empty structure tests with 18 accelerometers recording response along longer edges of the structure as shown in Figure 8.1.

The occupied structure modal properties f_{os} , m_{os} and ζ_{os} were found for the target mode of the structure by curve-fitting the point-mobility FRF for each test. These parameters are presented in Table 8.1. Reader may refer to Appendix I to see the relation of the tests discussed in this chapter with the ones presented in Chapters 6 and 7.

Table 8.1. Modal properties of the occupied structure for different group sizes

Test No.	Series	No. of Peds	Modal properties of the occupied structure				Structural Response		
			f_{os} (Hz)	ζ_{os}	m_{os} (kg)	c_{os} (N.s/m)	k_{os} (N/m)	a_{max} (m/s ²)	a_{rms} (m/s ²)
Mode 1 (Structure)									
1.1	A	2	4.443	0.0100	7,165	4,000	$5,583 \times 10^3$	2.4361	0.4131
1.2	B	3	4.445	0.0110	7,183	4,413	$5,603 \times 10^3$	1.7489	0.3018
1.3	A	4	4.450	0.0128	7,201	5,154	$5,630 \times 10^3$	2.1755	0.3637
1.4	A	6	4.465	0.0155	7,238	6,294	$5,696 \times 10^3$	1.8771	0.3311
1.5	B	6	4.465	0.0165	7,238	6,701	$5,696 \times 10^3$	1.4882	0.2481
1.6	B	10	4.475	0.0230	7,311	9,456	$5,780 \times 10^3$	1.1313	0.2050
1.7	A	10	4.476	0.0210	4311	8,635	$5,782 \times 10^3$	1.5876	0.2870
1.8	A	15	4.485	0.0290	7402	12,140	$5,878 \times 10^3$	1.1251	0.2466
Mode 2 (Structure)									
2.1	B	3	16.900	0.0055	7,128	8,326	$80,372 \times 10^3$	2.4059	0.4482
2.2	B	6	16.910	0.0065	7,128	9,846	$80,468 \times 10^3$	2.2905	0.4234
2.3	B	10	16.935	0.0075	7,128	11,377	$80,708 \times 10^3$	2.1387	0.4023

Comparing the occupied and empty structure modal properties presented in Table 8.1 and Table 6.1, respectively, considerable difference in the modal frequency and damping ratio is noticeable. These changes are considered as the effects of HSI during walking. The identification method designed for this chapter (described in Section 8.4) tries to use these observed effects to predict the possible properties of human model.

8.4 Identification of walking human model

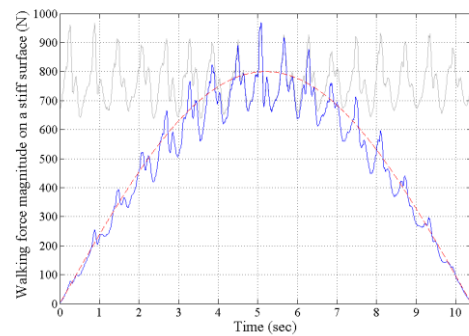
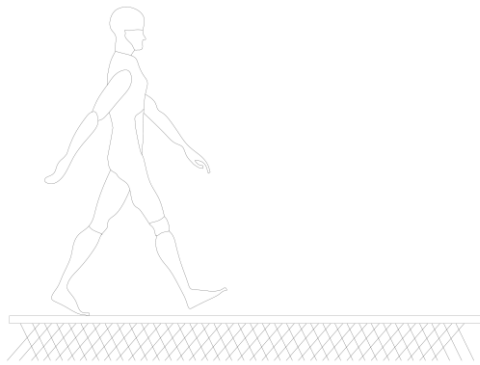
Having acquired the experimental data, all ingredients were in place for multi-person model identification. The identification process was designed based on the reverse engineering concept. This means that the changes observed in the modal properties of structure when people were walking on it were used to predict the possible parameters of walking human model.

8.4.1 Agent-based model of discrete traffic – structure system

When people are walking on a structure, their bodies act similar to a mechanical mass-spring-damper system. Mass of the human body is excited by the structure’s vibration and, similar to earthquakes, generates a ground reaction force that in turn excites the structure and

affects the structure’s response in a ‘feedback loop’ process. This force is different from the walking force and is the result of subjecting human body to a base excitation. Conceptually, in its simplest form, by assuming each individual as an SDOF system, the walking traffic-structure will form a multi-degree of freedom MSD system interacting in real-time with each other. The ABM used in this study uses this philosophy to simulate interaction of the walking people and structure.

Each walking person is simulated using a SDOF mass-spring-damper model. Based on this, the interaction force between each walking individual and the structure can be described as summation of two forces: 1) The walking force of that person on a stiff surface and 2) the ground reaction force generated by his SDOF human model excited by the structural response (Figure 8.2). This decomposition is made possible by assuming that the human body behaves linearly.



a) Walking force on stiff surface (grey) scaled by the first mode shape of a the test structure (blue)

+

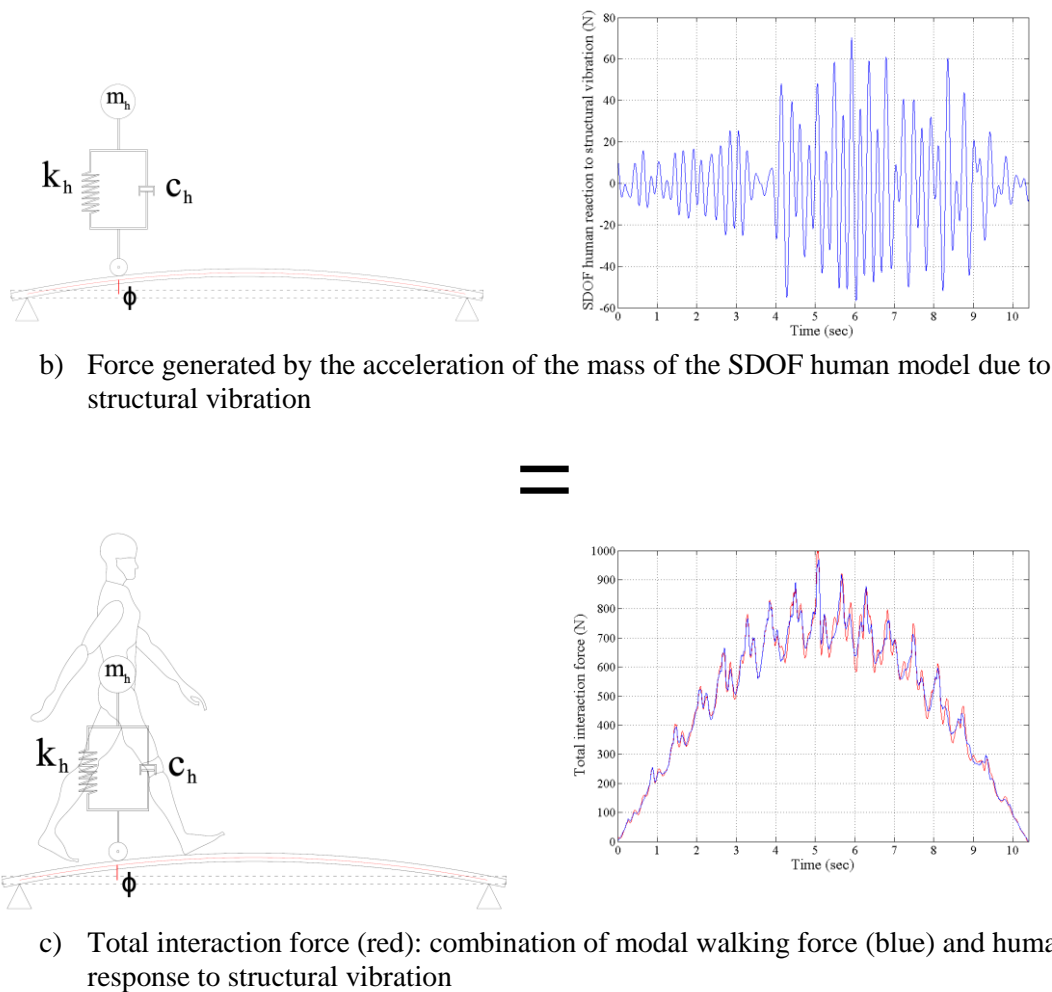


Figure 8.2. The interaction force composed of modal walking force on stiff surface and human model response to structural vibrations

Dynamic behaviour of the structure is modelled by a SDOF model representing a single mode of the structure at a time. It is assumed again that behaviour of the structure is linear and therefore its behaviour can be decomposed into modes. This way, the effects of the walking people on each mode of the empty structure can be calculated on a mode by mode basis and then superimposed to get the total response of the occupied structure.

Figure 8.3 presents the mechanical architecture of the ABM used to simulate each walking test. Each of the walking people, the target mode of the structure and the shaker excitation

were simulated as an agent. These agents were interacting with each other in real time. The ABM was responsible to regulate the interactions between different agents. A MATLAB code was developed by the author to simulate the dynamic behaviour of the structure and walking individuals and their interactions using ABM.

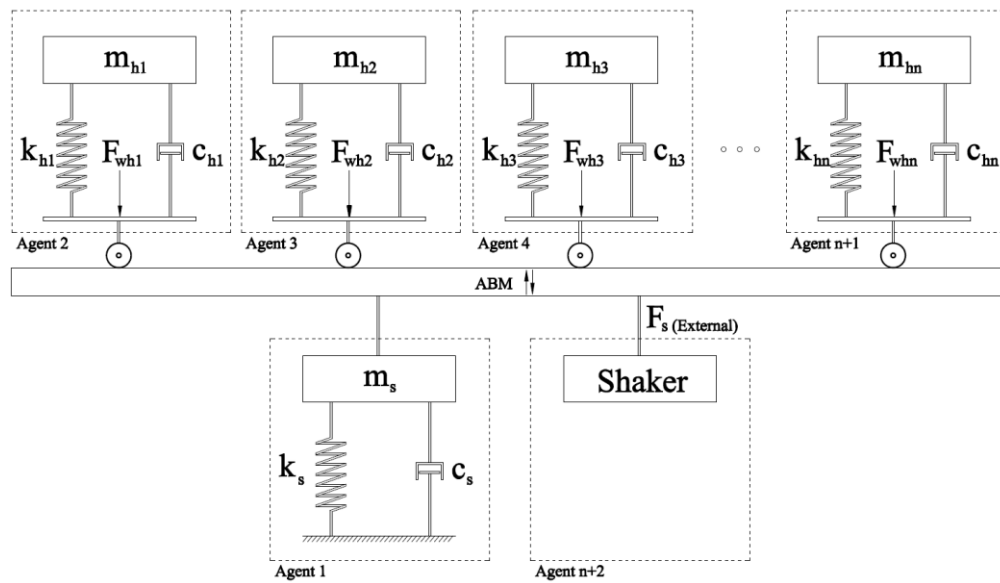


Figure 8.3. Mechanical model of walking people-structure system simulated by ABM

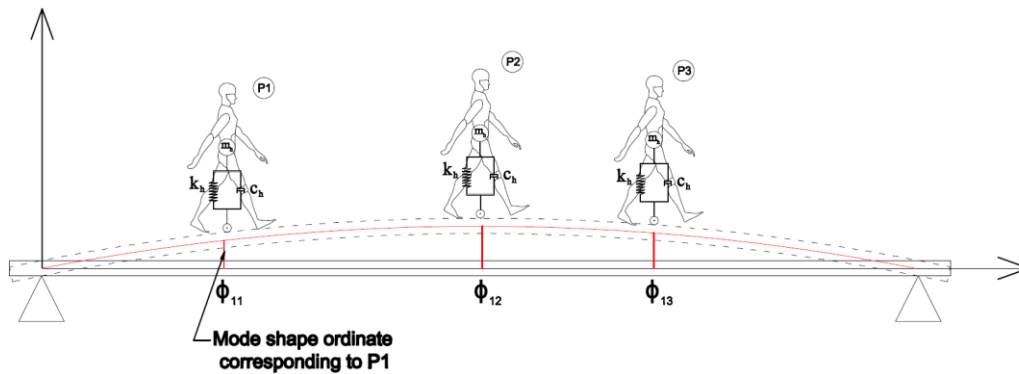


Figure 8.4. Taking into account the modal effects of each pedestrian based on their location on structure

During the ABM simulations, in each time step, the following steps took place sequentially:

Initialization: walking people SDOF models were placed at their initial positions on the structure at the start of the test that was going to be simulated. The structure was assumed to be at rest so the structural response was set to zero for the first time step. The same assumption was made for the human SDOF models.

- I. Set the next time step.
- II. The walking people were moved to their new locations based on their location time history recorded during corresponding tests.
- III. The structural response (from the previous time-step) is transmitted to each SDOF human model as base excitation. As shown in Figure 8.4, the structural response that each person feels is scaled with the mode shape amplitude of the person's location.
- IV. The response of each SDOF human model to the received base excitation was calculated by taking into account their displacement, velocity and acceleration in the previous time step as initial condition for the current step (Figure 8.2).

- V. The interaction force was calculated for each person by summing their normal walking force (recorded on a stiff surface using an instrumented treadmill) at current time step and the SDOF ground reaction force (Figure 8.2).
- VI. The interaction force of all the agents and shaker force was applied at their corresponding current locations on the structure (scaled by the mode shape based on their location at this time step) (Figure 8.4).
- VII. The response of the structure was calculated for the applied forces by taking into account its displacement, velocity and acceleration in the previous time step as initial condition for the current step.
- VIII. The walking people were moved to their new locations based on their location time history recorded during corresponding tests.
- IX. Repeat the process starting from I.

For the model used in this study it was assumed that presence of people on the structure does not change the mode shape of the empty structure. This assumption was validated experimentally in Section 7.2.4.

8.4.2 Identification process

The identification process used in this study uses an iterative approach. Initial ranges of 1-12 Hz with 0.05 Hz steps for f_h and 5 - 50% with 2.5% steps for ζ_h were selected to model the walking human ('h' subscript is used instead of 'h_i' here to refer generally to the human model parameters). These ranges were selected based on the values suggested in the biomechanics literature (Sachse, et al., 2004; Miyamori, et al., 2001; Ferris, et al, 1998) and the study done by Silva, et al. (2011) on walking people. For each test, every possible combination of f_h and ζ_h was used one at a time to simulate the walking traffic on the structure. The same f_h and ζ_h were used in each simulation for all pedestrians. Mass of the

human model m_h was assumed equal to the average mass of all participants in corresponding test. The empty structure modal properties presented in Table 6.1 were used for m_{es} , k_{es} and c_{es} .

The analytical acceleration response (resulted from the simulation) at anti-node of the target mode and the corresponding shaker force were used to calculate the analytical FRF of the occupied structure. These FRFs were then curve-fitted to find the properties of the occupied structure f_{os} , m_{os} and ζ_{os} . These parameters and peak magnitude of the FRF curve a_{FRF} were compared with their experimental counterparts and the corresponding errors were calculated. This process was repeated for all combinations of f_h and ζ_h for each test.

Maximum acceptable errors were defined for the estimated f_{os} , m_{os} , ζ_{os} and a_{FRF} . These were 0.01 Hz for f_{os} , 250 kg for m_{os} , 1% for ζ_{os} and 20% for a_{FRF} . For each test, the ranges of human model parameters f_h and ζ_h that predict f_{os} , m_{os} , ζ_{os} and a_{FRF} with errors less than the maximum values were identified. These ranges are referred to as *test-verified* ranges. Figure 8.5 shows a typical over-plot of the occupied structure FRF curves corresponding to these test-verified f_h and ζ_h ranges for test 1.5.

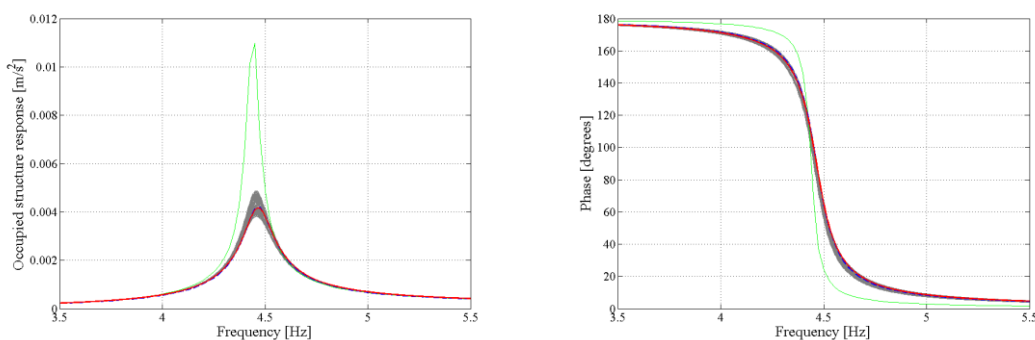


Figure 8.5. A typical over plot of empty (green), experimental (red) and acceptable analytical occupied structure FRFs (grey) magnitude and phase – Test No. 1.5 – (6 pedestrians)

In the next step, the test-verified ranges of f_h and ζ_h were combined for all tests (each mode separately) and a common range of f_h and ζ_h across all tests was found. This ensures that if any combination of f_h and ζ_h , selected from these common ranges is used to simulate people in any of the tests, the predicted f_{os} , m_{os} , ζ_{os} and a_{FRF} will be within the acceptable error ranges. Finally, the test-verified ranges of f_h and ζ_h of all tests (obtained in this study and studies presented in Chapter 7) related to mode one of the structure were analyzed statically and a statistical distribution was suggested for each of f_h and ζ_h .

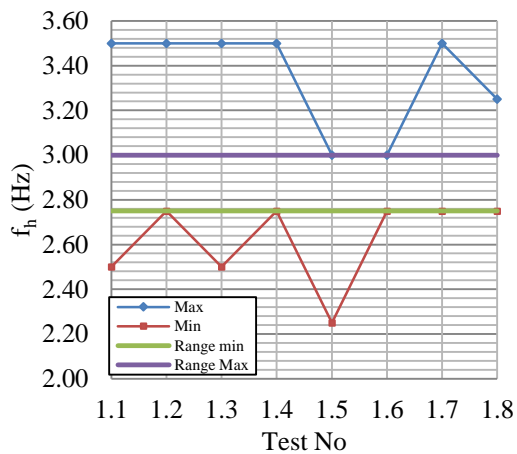
8.5 Results

The test-verified ranges of the human model parameters f_h and ζ_h are presented in Table 8.2 and Figure 8.6. As it can be seen, the test-verified ranges of f_h and ζ_h are different for mode 1 (Tests 1.1 – 1.8) and 2 (Tests 2.1 – 2.3) of the structure. This might be because two different modes of the walking human body were dominant when testing different structure modes. Detailed study of this interesting observation needs specially designed experiments on different structures and is beyond the scope of this study. However, a similar observation had been made for stationary pedestrians but with different modal properties f_h and ζ_h (Sachse, 2002).

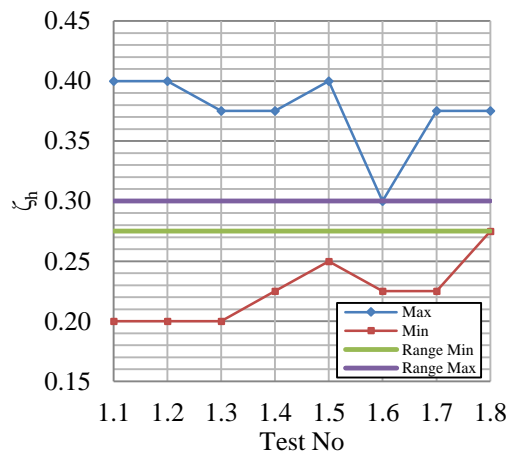
Table 8.2. Test-verified ranges of SDOF human model parameters

Test No.	No. of Pedestrians	Average m_h (kg)	Acceptable ranges of SDOF human model parameters				
			f_h (Hz)		m_h (kg)	ζ_h	
			Min	Max		Min	Max
Mode 1							
1.1	2	55	2.50	3.50	55	0.200	0.400
1.2	3	70	2.75	3.50	70	0.200	0.400
1.3	4	55	2.50	3.50	55	0.200	0.375
1.4	6	55	2.75	3.50	55	0.225	0.375
1.5	6	70	2.25	3.00	70	0.250	0.400
1.6	10	70	2.75	3.00	70	0.225	0.300
1.7	10	60	2.75	3.50	60	0.225	0.375
1.8	15	70	2.75	3.25	70	0.275	0.375
Mode 2							
2.1	3	80	6.5	9.0	80	0.100	0.175
2.2	6	70	6.0	8.0	70	0.100	0.225
2.3	10	70	6.0	7.5	70	0.100	0.225

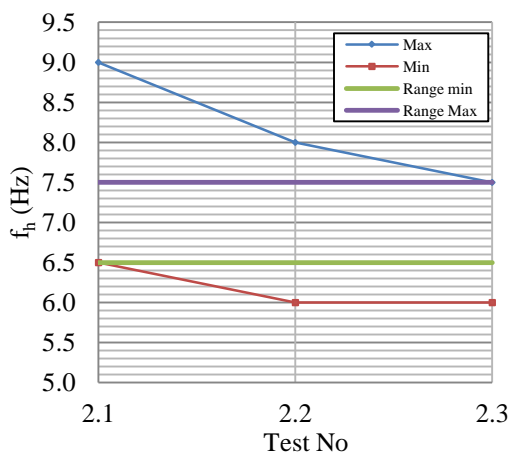
The common ranges of f_h and ζ_h for the first mode tests are 2.75 – 3.00 Hz and 27.5 % – 30%, respectively, as shown in Figure 8.6. These ranges are 6.5 – 7.5 Hz and 10 % – 17.5%, respectively, for the tests targeting the second mode of structure.



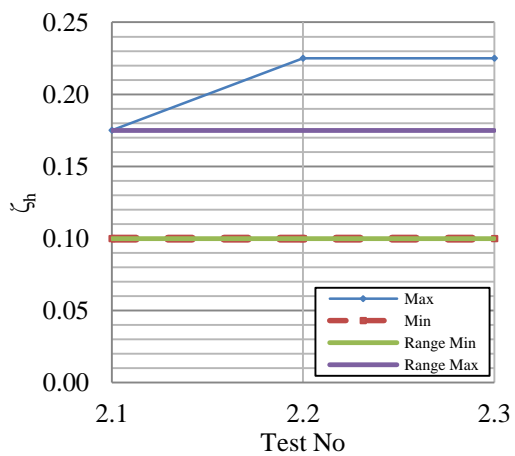
a) f_h – Mode 1



b) ζ_h – Mode 1



c) f_h – Mode 2



d) ζ_h – Mode 2

Figure 8.6. Test-verified ranges of f_h and ζ_h found in different tests and their common ranges

To understand how good each arbitrary combination of f_h and ζ_h selected from their common ranges (Figure 8.6) can predict occupied structure dynamics, simulations were repeated again for all mode 1 tests but this time only with common ranges of f_h and ζ_h as input. The

corresponding errors in predicting occupied structure parameters f_{os} , ζ_{os} and a_{FRF} were found for each combination of f_h and ζ_h and then averaged across all tests.

Figure 7.14 presents the average errors expected in f_{os} , ζ_{os} and a_{FRF} by using any combination of f_h and ζ_h .

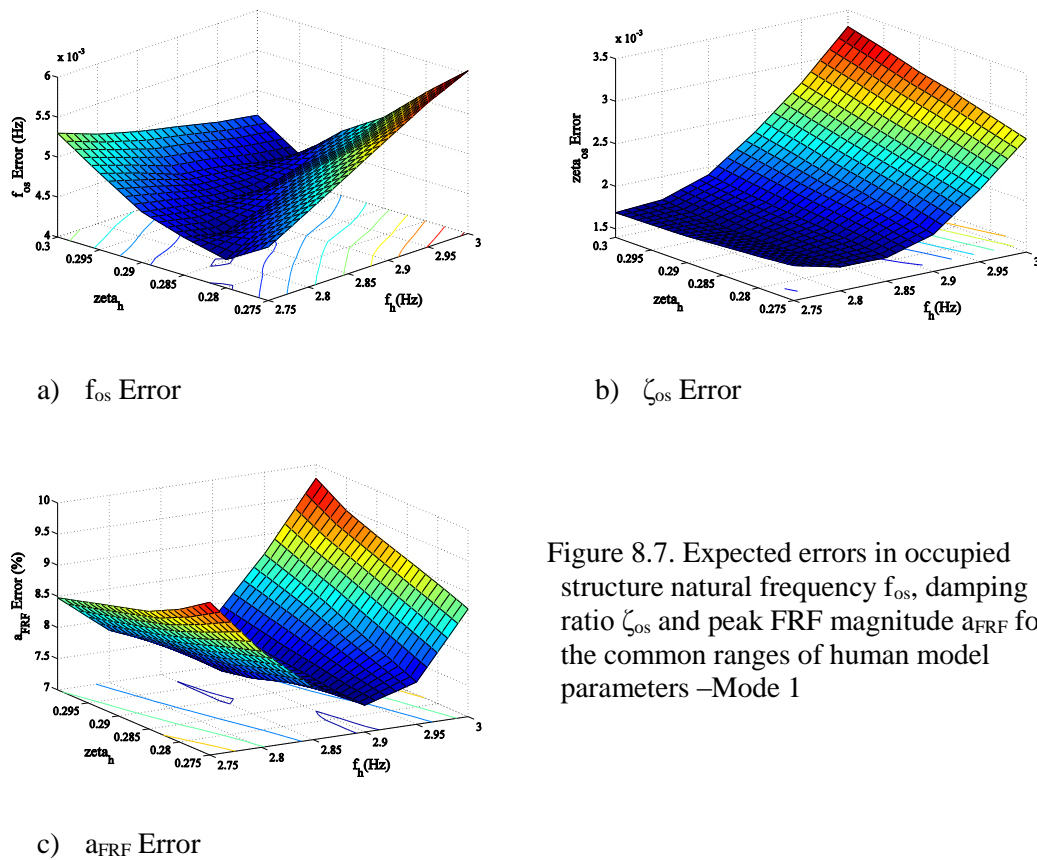
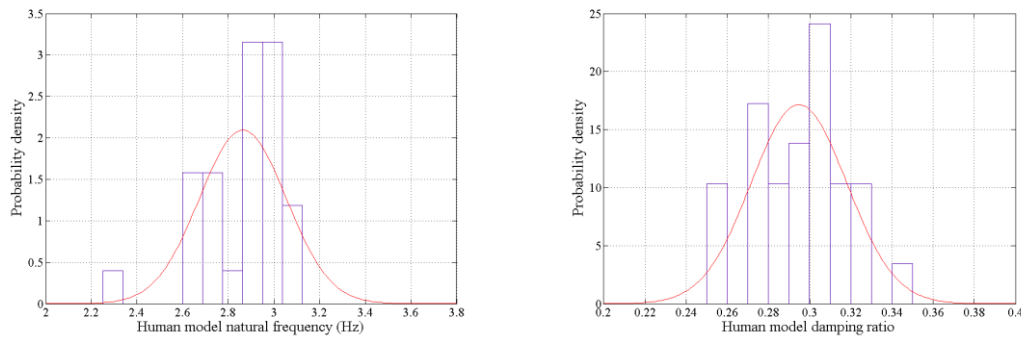


Figure 8.7. Expected errors in occupied structure natural frequency f_{os} , damping ratio ζ_{os} and peak FRF magnitude a_{FRF} for the common ranges of human model parameters –Mode 1

Statistical distributions can be used to describe narrow-band stochastic parameters such as human model f_h and ζ_h . For each test/simulation, a combination of f_h and ζ_h that can predict occupied structure parameters with least error is found. Distribution of the found f_h and ζ_h values (obtained both in this study and studies presented in Chapter 7) are presented in Figure 8.8.



a) Normal distribution of natural frequency of human SDOF model f_h - $\mu=2.864$ Hz and $\sigma= 0.191$ Hz

b) Normal distribution of damping ratio of human SDOF model ζ_h - $\mu=0.295$ and $\sigma= 0.023$

Figure 8.8. Probability density function of human SDOF model natural frequency (a) and damping ratio (b)

Normal distribution presented in Figure 8.8 found to be the best model to describe f_h and ζ_h ranges found in this study. The mean and variance of suggested normal distributions are $\mu=2.864$ Hz and $\sigma= 0.191$ Hz for f_h and $\mu=0.295$ and $\sigma= 0.023$ for ζ_h . As the accuracy of the statistical model is dependent on the size of the data, a very extensive experimental and analytical study need to be done to increase the accuracy of the statistical fit. An appropriate mass m_h distribution must be selected for simulation based on the weight of expected users of the structure in any particular locations. These results are comparable with the SDOF walking human model parameters suggested by Silva and Pimentel (2011) determined independently by an entirely different procedure. Assuming human mass equal to 70 kg and 1.8 Hz mean pacing frequency, their model suggests $f_h=2.64$ Hz and $\zeta_h = 0.55$ for SDOF walking human model.

8.6 Conclusions

The present work utilized probably the most comprehensive traffic-structure experimental data collected to date, to identify the parameters of SDOF walking human model. A discrete agent-based model of the traffic-structure system is used to simulate tests. The analysis results suggest that normal distributions with $\mu=2.864$ Hz and $\sigma= 0.191$ Hz and $\mu=0.295$ and

$\sigma = 0.023$ are good models to describe human model natural frequency and damping ratio, respectively. The comprehensive experimental data, detailed simulation process and outputs consistent with the previous findings of the authors (Chapter 7) and other researchers give high level of confidence about good reliability of the findings.

The experimental data set used in this research can serve as a benchmark for data collection for other multi-pedestrian HSI studies in the future. Also, the agent-based model used in this study acts as a showcase of valuable potentials of this model for realistic simulation of human interactions.

The agent-based model used in this study, has been demonstrated to be a potentially powerful tool to simulate simultaneously different interaction types in multiple directions and with a desired level of details.

The results of this research are coherent with the findings of other authors for both stationary and walking people. The difference between human model parameters found for mode 1 and 2 of structure opens up an interesting discussion on the underlying mechanisms. Further research on different real-life structures need to be done to extend and validate the findings of this research for different structures and loading scenarios.

Chapter 9

Assessment of Vibration Serviceability Due to Walking-Induced Vibrations Including Human-Structure Interaction

Interaction-based VSA Method

The contents of this chapter are adapted with minor changes from the following journal paper in preparation to be submitted to the ASCE Journal of Structural Engineering:

Shahabpoor, E., Pavić, A., Racić, V. and Zivanović, S. Assessment of Vibration Serviceability Due to Walking-Induced Vibrations Including Human-Structure Interaction. The ASCE Journal of Structural Engineering.

9.1 Introduction

Although the interaction of walking people with structures is proven to have critical effects on the structural response, no design guideline and assessment method exist to date that takes into account such effects. This is mainly due to the lack of credible and validated knowledge on the underlying interaction mechanisms.

UK recommendations for design of permanent grandstands (2008) is leading the world in promoting a more realistic way to take into account explicitly the interaction of people in grandstands. This work, based on the model proposed by Dougill et al. (2006), uses a combination of two SDOF models to simulate the effect of passive and active (jumping or bouncing in place) people. Although this model aggregates the effects of people and does not take into account the inter- and intra- subjects variability of people, its performance was demonstrated by Pavic and Reynolds (2008) to be much more accurate than that of other methods neglecting the HSI. Despite its apparent high importance, no guideline or standard has yet adopted such advanced modelling approach for simulating the effects of the walking people on structural vibrations by taking into account human-structure interactions.

This research extends this concept to walking people and proposes a novel interaction-based serviceability assessment method that takes into account the interaction of every walking individual with the structure. An SDOF MSD model was proposed to simulate dynamics of the walking individual. Inter- and intra- subject variability of people was taken into account by using statistical input parameters and discrete modelling approach. The proposed assessment method also features a new statistical assessment tool that increases the accuracy of the assessment. This is by taking into account the individualized experience of vibration at the location of every user of the structure, rather than the maximum response of the structure which may not be experienced by anybody.

Section 9.2 of this chapter discusses in detail the four steps of the proposed assessment method. Section 9.3 highlights the important features of this method and describes the challenges that it addresses. An extensive sensitivity analysis was performed to examine the sensitivity the outputs of the proposed method to its inputs. Results of this analysis are presented in Section 9.4 and should enable designers to use the method with confidence. Few more recommendations are presented in Section 9.5 for simulating more complicated loading scenarios. Concluding remarks are presented in Section 9.6.

9.2 Assessment method description

The vibration serviceability assessment method presented in this chapter (will be referred to as *interaction-based VSA method* hereafter) is developed to address three main challenges of realistic assessment of walking-induced vibration:

- Human-structure interaction
- Stochastic parameters of the human body and the walking force (Inter- and intra-subject variability), and
- Unknown loading scenario and people's location on structure

The backbone of the method is based on the modal superposition whereby responses of SDOF models representing modes of an empty structure are replaced by SDOF responses of the occupied structure modes. Human model parameters, walking force and structural response are treated statistically and the results are presented in terms of their probability of occurrence. The *interaction-based VSA method* also features a new assessment criteria based on percentage of satisfied users instead of percentage of time that bridge response is within the acceptable range.

The *interaction-based VSA method* is described in four steps. Firstly, the occupied structure modal properties f_{os} , ζ_{os} and m_{os} are found. This is done by taking into account the effects of

every individual walking on the modal properties of the empty structure f_{es} , ζ_{es} and m_{es} . These occupied structure modal properties are used to calculate response of structure instead of the ones of empty structure. The philosophy is that when people are walking on a structure, the empty structure modal properties change to what we call ‘*occupied structure*’ properties. In the second step, all individuals’ walking forces are combined together as a modal force obtained via the structure’s mode shape. People’s arrival rate and walking speed were also used to generate modal walking force of the traffic. Modal response of the structure is found in the third step using traffic modal walking force and occupied structure modal properties. Finally, the response of the structure is presented in a statistical/probabilistic form to assess structure serviceability. These steps are described in detail in the following sections.

9.2.1 Input parameters

Versatility is one of the key requirements of an assessment method and its directly related to its usability in practice. In principle, assumptions, approximations and simplifications reduce versatility of a method by limiting its application to specific cases. This is particularly a challenge for cases such as vibration assessment of a multi-pedestrian walking traffic, where a large number of stochastic parameters are involved. To maximize the versatility of the interaction-based VSA method, the number of assumptions is reduced to minimum and everything else needed was calculated explicitly rather than assumed.

Figure 9.1 presents the four categories of input parameters used in the interaction-based VSA method.

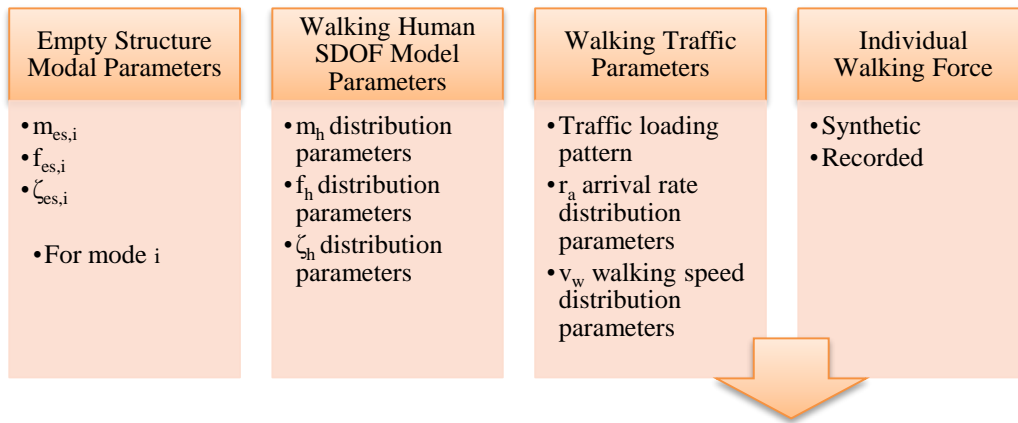


Figure 9.1. Input parameters of proposed assessment method

The first category comprises empty structure modal properties (modal mass $m_{es,i}$, frequency $f_{es,i}$ and damping ratio $\zeta_{es,i}$). These can be obtained either analytically or preferably experimentally when possible. Empty structure modal properties are assumed accurate and associated errors are not considered in the assessment method.

The second category comprises the parameters of the SDOF MSD model of individual walking human: m_h , f_h and ζ_h . The human model used in the interaction-based VSA method is based on the findings presented in Chapter 8. It was shown that dynamics of a single walking human can be modelled using an SDOF MSD model with parameters described by normal distribution. The mean and variance of suggested normal distributions were $\mu=2.864$ Hz and $\sigma= 0.191$ Hz for natural frequency f_h and $\mu=0.295$ and $\sigma= 0.023$ for damping ratio ζ_h (Figure 8.8). Depending on the weight of expected users of the structure in a particular location, appropriate mass m_h must be selected for SDOF human models. The selected m_h values can either be based on a distribution pertinent to the local demographic data or equal to the average mass of the users.

The third category of input parameters contains the walking traffic parameters. These parameters define the loading scenario in statistical terms. An appropriate load pattern first needs to be defined. This can be simply a stream of pedestrians with arrival rate r_a

[pedestrians/time unit] at the bridge and walking speed v_w [m/s] defined by their corresponding distributions or rather a more complicated scenario with different levels of traffic volume and durations.

The last category of inputs is individuals' walking force. These are either real walking forces measured using an instrumented treadmill or synthetic walking forces generated using statistical features of walking force (Zivanovic, et al., 2007; Racic and Brownjohn, 2011).

9.2.2 Step 1: Human-structure interaction

The first step of the interaction-based VSA method addresses one of the most important and least dealt with challenges of human-induced vibration assessment; the human-structure interaction. In this method, the walking traffic-structure interaction is considered in the form of effects of walking people on modal properties of the empty structure. Modal properties of the structure under walking traffic are called '*occupied structure*' modal properties f_{os} , ζ_{os} and m_{os} and are used instead of empty structure f_{es} , ζ_{es} and m_{es} in the response calculation.

When people are walking on a structure, their bodies act similar to a MSD mechanical system. The mass of the human body is excited by the structure's vibration and generates a force that excites the structure and hence affects structure's response. This force is different from the walking force and is the result of subjecting human body to a base excitation (Section 8.4.1). In simplest form, by assuming each individual acting as an SDOF system, the walking traffic and empty structure system will form a multi-degree of freedom system which elements are interacting in real-time with each other.

In reality as people are walking, their locations on the structure are changing with time. To be able to use modal analysis, people's locations need to be stationary i.e. the system needs to be linear. To overcome this challenge, walking traffic is 'frozen' in time (a snapshot of

walking traffic) and their location is assumed ‘stationary’ for that particular moment. This is similar to the case that people are walking on a series of treadmills installed at fixed locations on the structure and therefore their location on the structure do not change while walking (Figure 9.2).

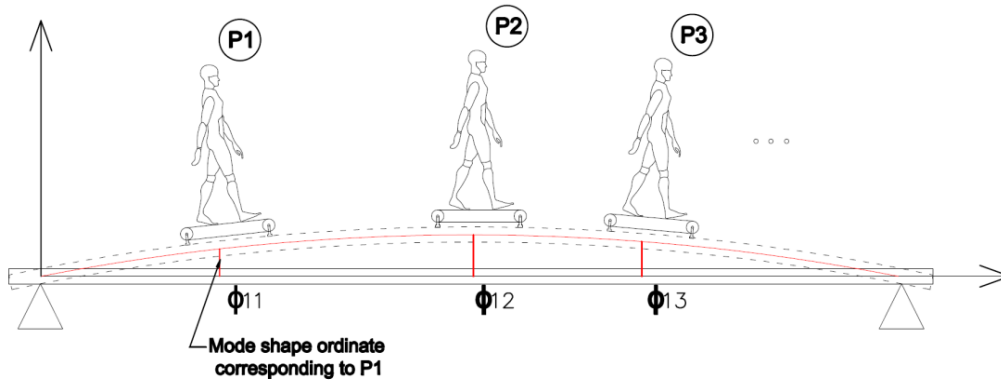


Figure 9.2. A conceptual illustration of ‘stationary’ walking people. Φ_{ab} represents ordinate of mode ‘a’ at the location of human ‘b’

The methodology used in the first step of the interaction-based VSA method is basically an iterative process. In each iteration, a random distribution of peoples’ location on the structure is considered. Walking people are assumed stationary at their location at that particular moment of time. The occupied structure modal properties f_{os} , ζ_{os} and m_{os} are found for this configuration. The unity-normalized mode shapes must always be used throughout the method. By repeating this process for different location configurations and averaging the found occupied structure modal properties, each parameter gradually converges to its average value which is called *stabilized value*. These stabilized modal properties of the occupied structure are used in next steps for response calculation instead of the empty structure ones. Figure 9.3 presents the step-by-step procedure to find *occupied structure* modal properties for a stream of walking people.

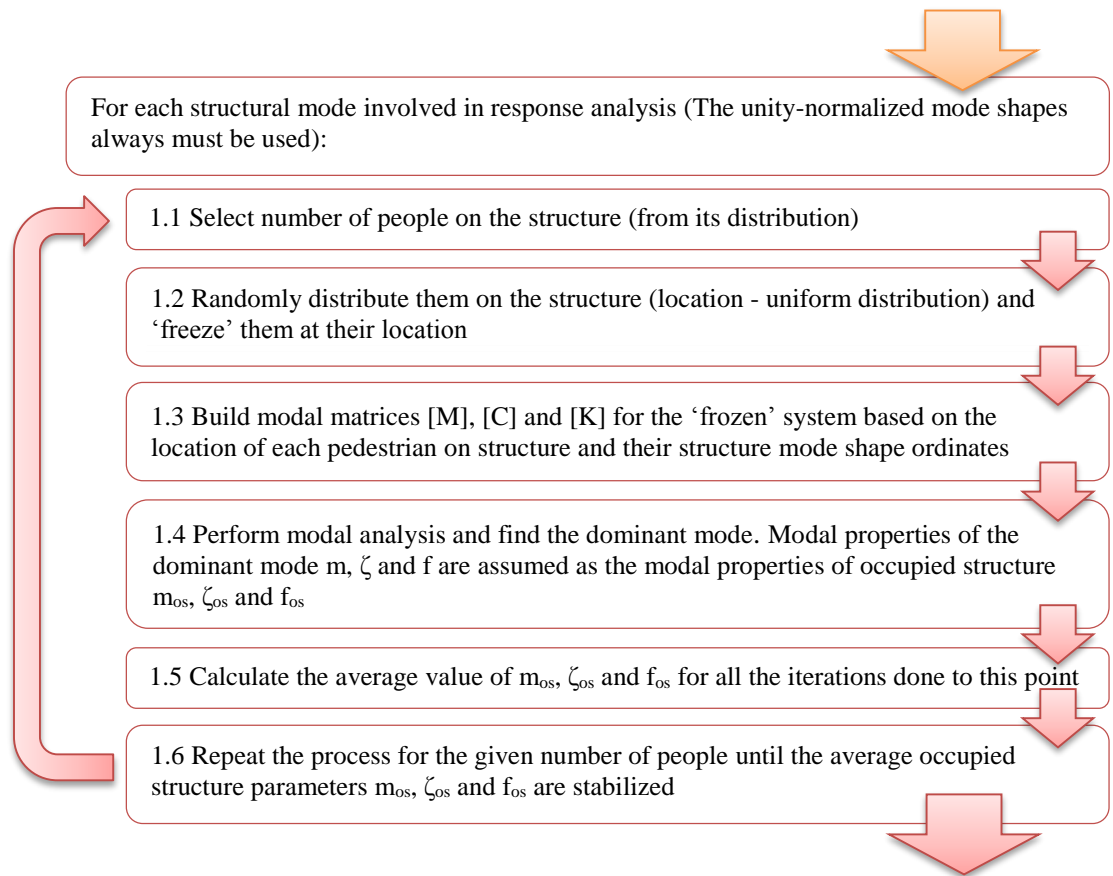


Figure 9.3. Interaction-based VSA method step 1 procedure

In each iteration, the number of people on the structure must be selected initially. This can be done using arrival rate statistical distribution and average crossing time (i.e. the average time needed for a walking person to walk along the structure). For instance, for arrival rate of 10 pedestrians per minute and average crossing time of 2 minutes, it is expected to have 20 people walking on the structure at a time assuming that walking speeds of people are equal and constant.

In Step 1.2, a location must be assigned to each person either randomly (uniform distribution) or based on a particular pattern that the loading scenario may require. The

assigned location to each person is assumed constant (stationary) for that particular moment of time.

The mass-spring-damper model of stationary walking traffic-structure system is then built in step 1.3. An SDOF MSD model is used to simulate each walking individual on the structure. Similarly an SDOF model is used to simulate one mode of the structure at a time. The effects of the constant location of each person on the modal properties of the occupied structure are taken into account using structure mode shape ordinate at the location of each person. Walking force of each person on a stiff surface is applied directly on the structure at the same location of that person. Figure 9.4 presents the mass-spring-damper model of stationary walking traffic-structure system.

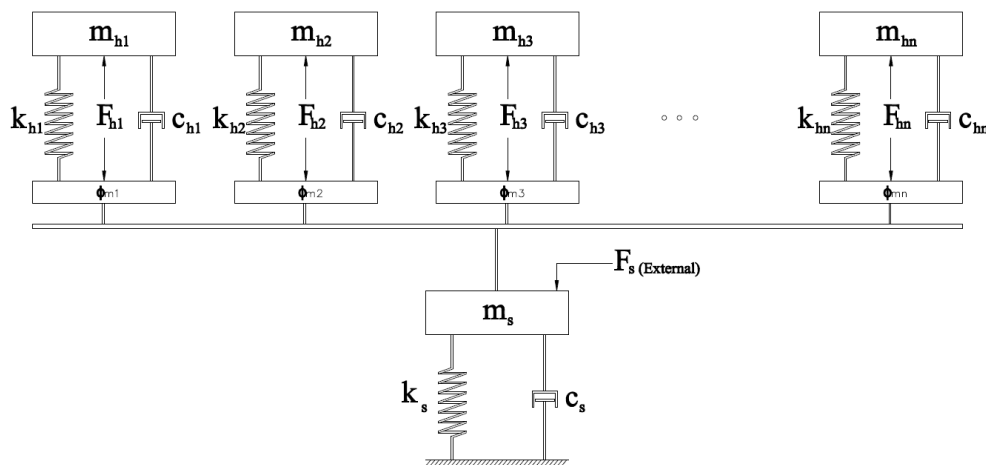


Figure 9.4. Mass-spring-damper model of stationary walking traffic-structure system

Being stationary, walking traffic-structure system shown in Figure 9.4 can be treated as a conventional multiple degree of freedom system the solution of which is described in Section 7.3.1. The modal properties of the *dominant mode* are selected as the modal properties of the *occupied structure*. The ‘dominant mode’ of vibration is the mode with maximum response at the degree of freedom corresponding to the structure. For consistency and to allow for

mode superposition, mode shapes need to be scaled in a way that the ordinate of the structure DOF is unity. Such scaling ensures that modal properties of the crowd-structure system are found with the same scaling as the empty structure.

By repeating this process for different location configurations and averaging the found occupied structure modal properties, each parameter gradually converges to its stabilized value. These stabilized modal properties of occupied structure f_{os} , ζ_{os} and m_{os} are used in next steps for response calculation instead of empty structure ones. Figure 9.5 shows a typical fluctuation of f_{os} and ζ_{os} during step 1 analysis. As it can be seen in this figure, f_{os} and ζ_{os} are stabilized after around 600 iterations.

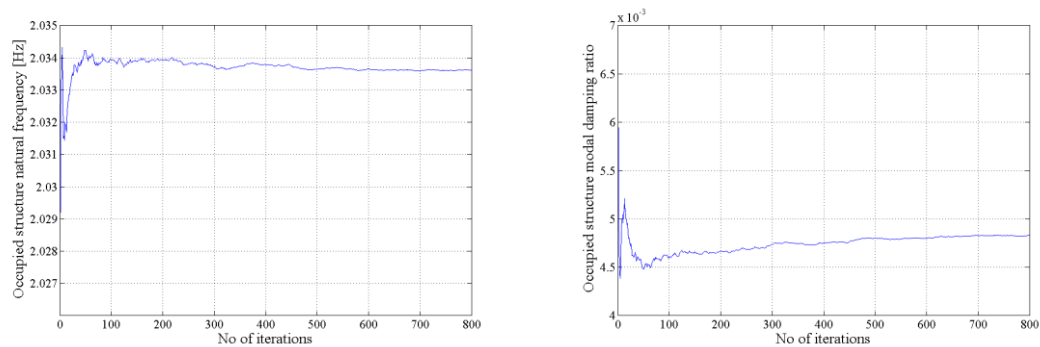


Figure 9.5. A typical fluctuation of average occupied structure natural frequency f_{os} and damping ratio ζ_{os}

9.2.3 Step 2: Generating modal traffic walking force

The second step of the interaction-based VSA method is to generate the modal force due to multi-pedestrian walking traffic. This force will be applied on the occupied structure in Step 3 and response will be calculated. Most of the traffic walking force parameters such as people's arrival rate r_a , arrival time t_a , location $x(t)$, walking speed $v_w(t)$ and walking force $F_w(t)$ are time-varying and stochastic (narrow-band) in nature. This makes it impossible to predict exactly the traffic force. The way forward is to treat it statistically.

Figure 9.6 presents the step-by-step procedure to generate modal force due to walking traffic.

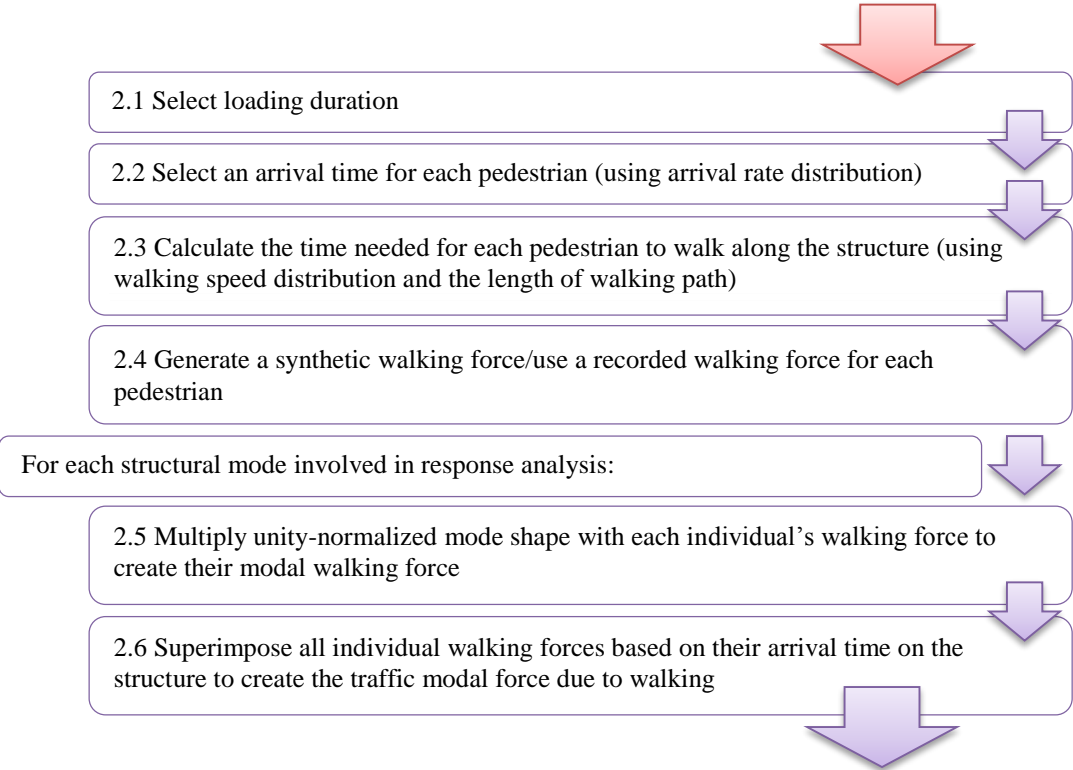


Figure 9.6. Interaction-based VSA method Step 2 procedure

In the first instance, a ‘sufficiently long’ duration for simulation needs to be selected. Assessment of the structural serviceability in the interaction-based VSA method is based on the probability of occurrence of different levels of structural response. In every probability-based analysis, it is crucial to have sufficiently large sample data to get accurate results. Implication of this fact in the interaction-based VSA method is that ‘sufficiently long’ time needs to be allowed for the structure to experience all possible variations of the traffic walking load. The ‘sufficiently long’ simulation duration can be different for different design cases depending on the level of variation of traffic load.

An iterative method is suggested here to find the ‘sufficiently long’ simulation duration. An initial value must be selected for the duration of simulation. A criterion is introduced in Step 4 which can be used to check if the selected duration was long enough or not. In the case that

duration proved to be insufficient, it needs to be increased and simulations (Steps 2-4) need to be repeated for the new duration.

In Step 2.2, the number of people entering the structure in each minute of simulation selected using arrival rate statistical distribution. Then an arrival time must be assigned randomly to each of pedestrians. For instance, for arrival rate of 4 pedestrians per minute entering the structure between minute 12 and 13 of simulation, a typical set of random arrival time might be 12:03, 12:12, 12:38 and 12:51.

In the step 2.3 a walking speed need to be selected for each pedestrian using walking speed statistical distribution. Using this walking speed and the length of structure, the time duration that person will walk on the structure can be found (crossing time). For instance, for a pedestrian with $v_w=1.8$ m/s and structure length of 36 meters, it takes 20 seconds for that person to walk along the structure.

A walking force needs to be assigned to each pedestrian in the step 2.4. The duration of the walking force for each person should be equal to the crossing time of that person. Either an experimentally recorded or a synthetically generated walking force can be used in the simulation. If walking force is to be generated synthetically, it is crucial to use the methods which take into account the inter- and intra- subject variability of walking force and realistically simulates its frequency contents. The methods suggested by Zivanovic, et al. (2007) and Racic and Brownjohn (2011) are proved to be accurate enough for this application. Further discussion on generating walking force is beyond the scope of this study.

As people are walking along the structure, their location on the structure and consequently their level of interaction with structure change. To account for this, walking force of each individual is scaled with the mode shape of target mode of structure. Figure 9.7 presents a typical walking force of an individual scaled with the first mode shape of a simply-supported

beam structure. This person crosses the structure in 10.4 seconds. It is assumed that empty structure mode shape is equal to occupied structure mode shape.

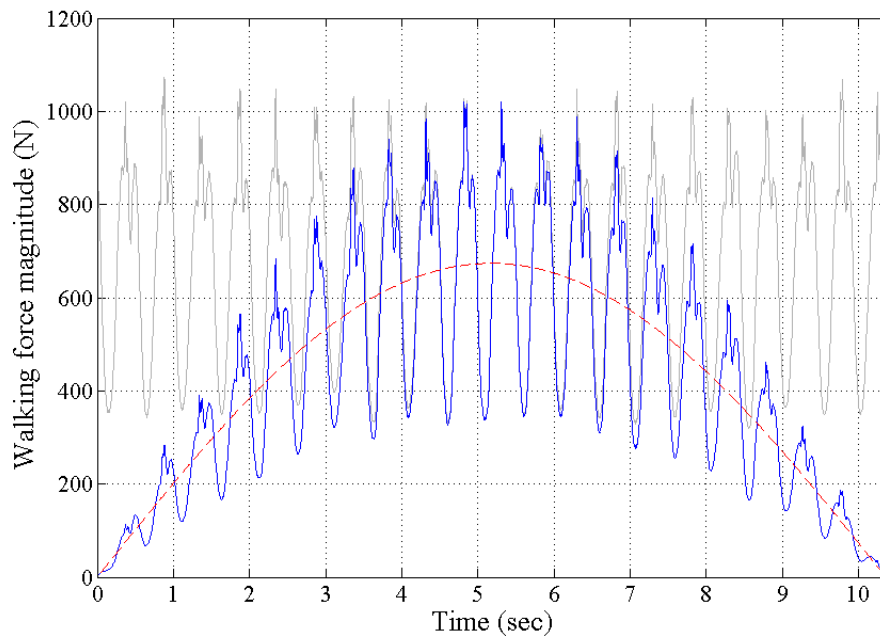


Figure 9.7. A typical mode 1 modal walking force of an individual – Walking force (grey), modal walking force (blue) and mode shape (red)

Finally, in Step 2.6, the modal walking forces of pedestrians must be superimposed based on their arrival time on the structure to generate the modal force of the walking traffic. Figure 9.8 presents a typical superposition process where modal walking forces of three pedestrians (a, b and c) are superimposed to generate the modal force of the walking traffic (d). The pedestrians 1, 2 and 3 arrive on structure at $t_a = 2, 6$ and 8 seconds respectively and each take 10.4 seconds to cross the structure. The total modal force of walking traffic is shown in Figure 9.8 (d). $X_{w,i}$, $V_{w,i}$ and $F_{w,i}$ are distance from right support, speed and walking force of walking pedestrian ‘i’, respectively.

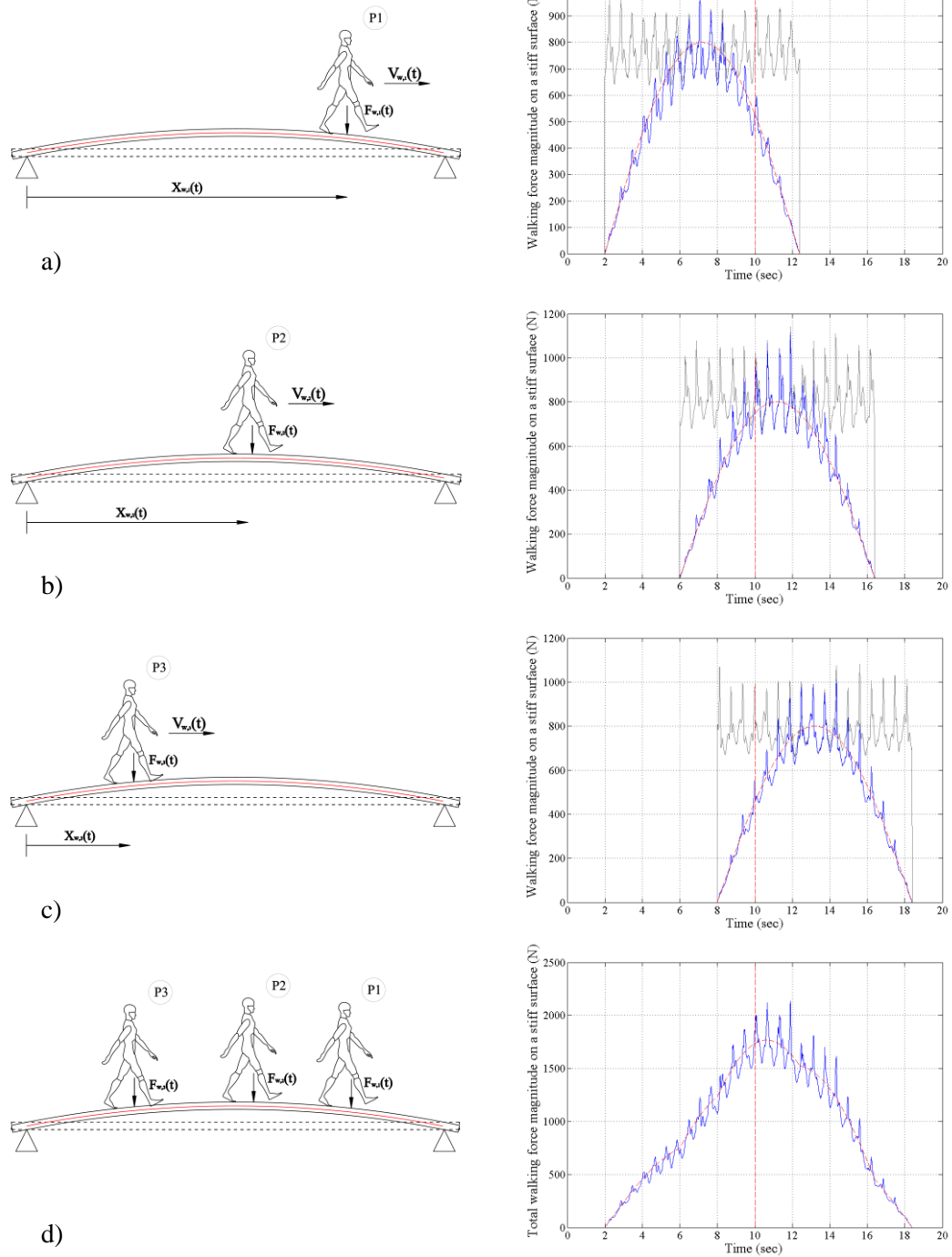


Figure 9.8. Superposition of modal walking of three pedestrians (a, b and c) to generate modal force of walking traffic (d) – walking force (grey), modal walking force (blue) and mode shape (red)

9.2.4 Step 3: Calculating structural response

In the Step 3 of the assessment method, the modal force of the walking traffic (calculated in Step 2) is applied on relevant occupied structure modes (calculated in Step 1) and modal responses are calculated. This is done using conventional modal analysis method. The resulted modal responses are then superimposed to generate the nodal response of structure.

9.2.5 Step 4: Results interpretation

The final step of the interaction-based VSA method, Step 4, is responsible for assessing the serviceability level of the structure based on its acceleration response. A new statistical tool called '*traffic-domain Cumulative Distribution Function (CDF)*' of '*stabilized*' structural response is used here to assess the vibration serviceability of structure under walking traffic load. The '*traffic-domain CDF*' and response '*stability*' concepts are defined below.

9.2.5.1 TRAFFIC-DOMAIN CDF

The CDF of modal acceleration response of structure at the anti-node of that mode (will be referred to as *time-domain* CDF in this study) is typically maximum response which is frequently used by the researchers such as Zivanovic, et al. (2010) to assess structural serviceability. This CDF links magnitude of the structural response with its corresponding probability of non-exceedance in time. However, time-domain response CDF is misleading in scenarios when traffic volume is not constant on the structure. It also does not take into account the location of people on the structure. Following examples highlights the shortcomings of the time-domain CDF.

Assume an extreme scenario where a beam-like structure is exposed to traffic for only 9 minutes in 1 hour time frame (15% of time) and rest of the time its empty (85% of time). Also, assume that structure always fail to meet the vibration serviceability requirements

when exposed to walking traffic. If the time-domain CDF of response of this structure for 1 hour test is used for serviceability assessment, results will suggest that structure meets the serviceability requirement for 85% of the time while in reality the structure never meets this requirement.

The time-domain CDF also includes no information about the actual location of the people on the structure. For instance, using time-domain CDF, response of the first mode of a simple beam-like structure at the mid-span might be found unacceptable for 60% of time. But people on the structure are not always walking at the mid-span and consequently they experience much less response than the maximum value at mid-span. Therefore high responses of the structure for 60% of the time do not necessarily mean that 60% of users of the structure are unsatisfied!

These shortcomings are results of neglecting the fact that vibration serviceability of a structure must be assessed based on the satisfaction of its users (as ‘receivers’ of vibration) and not on just the structural response. To address this issue, a new serviceability assessment tool called ‘*Traffic-domain*’ CDF is defined and used in the interaction-based VSA method. Traffic-domain CDF links magnitude of the structural response with the percentage of users that experience no more than that response magnitude. The maximum response experienced by a target percentage of users can be immediately found from this graph.

Traffic-domain CDF uses the time-history of experience of each pedestrian as they walk along the structure. Figure 9.9 shows the process of calculating time-history of experience of a typical pedestrian crossing a beam-like simply-supported structure.

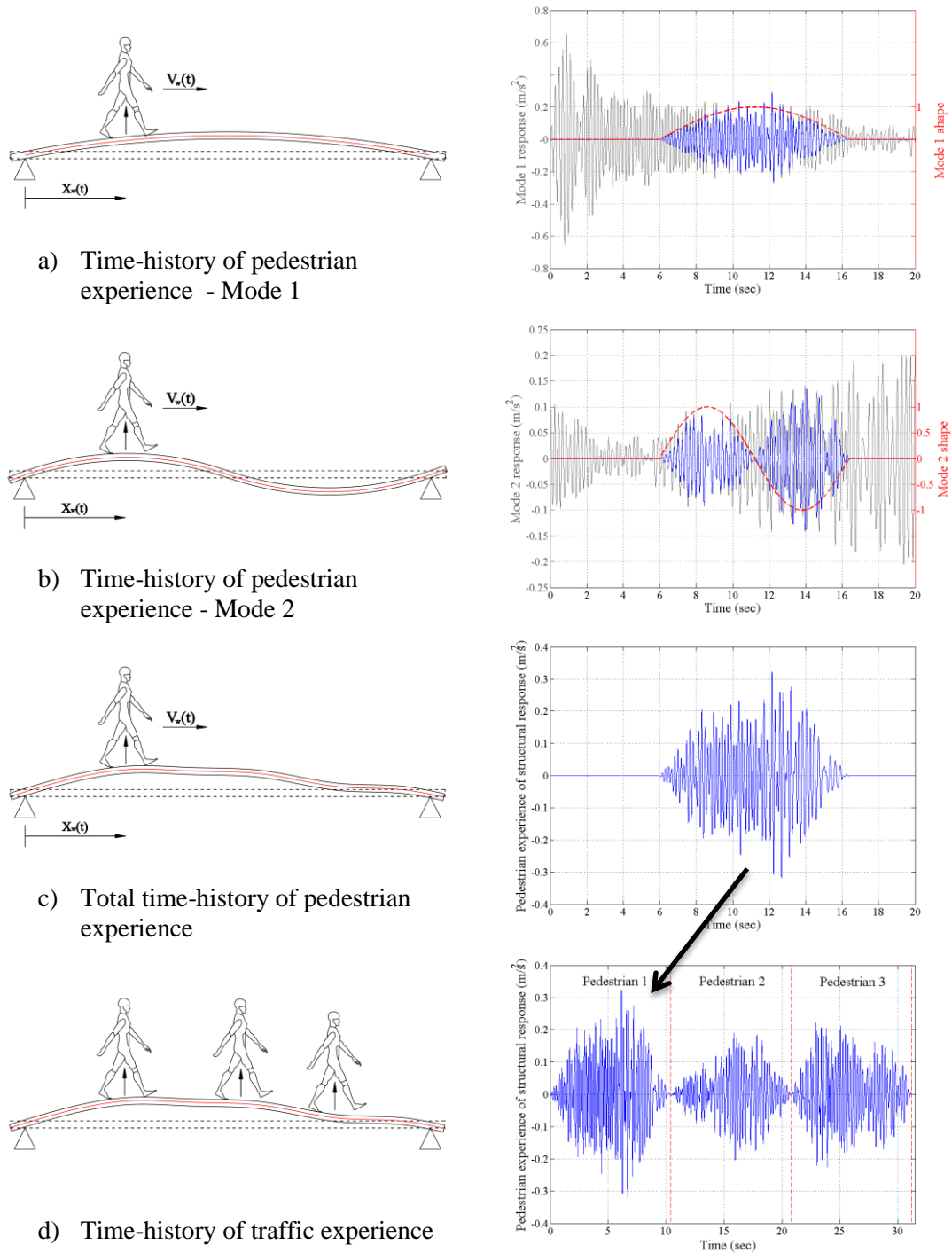


Figure 9.9. Time-history of each pedestrian's experience as they walk along the structure

Pedestrian experience here is referred to the magnitude of the structural response that a pedestrian receives as it walks along the structure. The pedestrian experience for each mode of the structure can be calculated by multiplying modal response with the corresponding unity-normalized mode shape curve. This mode shape curve starts at arrival time of pedestrian and its duration is equal to the crossing time of that pedestrian. For instance for the case of the pedestrian shown in Figure 9.9, it enters structure at $t_a=6$ seconds and takes 10.4 seconds to cross the structure. It is assumed that first two vertical modes of structure are relevant in this case. Figure 9.9 (a) and (b) show time-history of experience of this pedestrian from mode 1 and 2 response respectively (blue trace). Response of each mode (grey trace) is multiplied by corresponding mode shapes (red trace) starting at $t_a=6$ seconds and with duration of 10.4 seconds to calculate the experience of the pedestrian from each modal response (blue trace). The two modal experience time-histories are simply summed together in time to generate the time-history of total experience of the pedestrian (Figure 9.9 (c)).

If this process is repeated for all the pedestrians crossing the structure and time-histories of their experiences are connected together back-to-back, the total time-history of traffic would be created. This time-history is shown for 3 pedestrians in (Figure 9.9 (d)). *Traffic-domain CDF* of structural response is defined as the CDF of this time-history of traffic experience.

Figure 9.10 compares the performance of the time-domain and traffic-domain CDFs in the assessment of vibration serviceability of a typical structure.

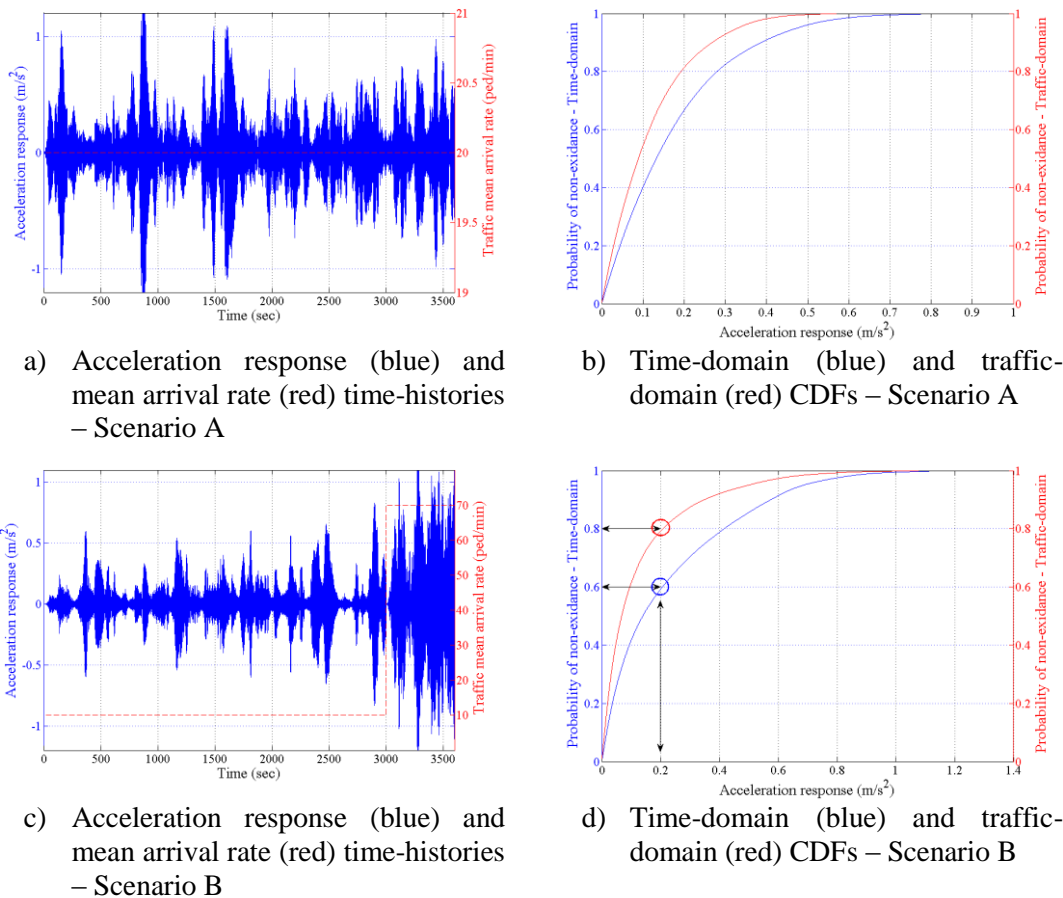


Figure 9.10. Comparison of Time and Traffic domain CDFs

The acceleration response of the structure is captured for 60 minutes for two loading scenarios A and B. As it can be seen in Figure 9.10 (a) and (c), the mean arrival rate in scenario A is constant (20 pedestrians / minute) whereas in scenario B it shows 6 fold increase from 10 peds/min to 70 peds/min for 10 minutes. A considerable difference between time-domain and traffic-domain CDFs is noticeable in both scenarios (Figure 9.10 (b) and (d)). In Scenario A, neglecting the location of people on the structure results in an over estimation of the response in the time-domain CDF ((Figure 9.10 (b) - blue trace) whereas in Scenario B, change of traffic volume is the main reason of over-estimation of response in time-domain CDF ((Figure 9.10 (d) - blue trace). Based on Figure 9.10 (d), if 0.2 m/s² is considered as the maximum acceptable response, only for 60% of the time structural

response is acceptable according to the time-domain CDF while 80% of the users would be satisfied according to traffic-domain CDF!

9.2.5.2 STABILITY OF STRUCTURAL RESPONSE CDF

As described in Section 9.2.3, a ‘sufficiently long’ simulation duration needs to be selected to ensure that CDF of structural response shows accurate probabilities for different magnitudes of response. The criteria that is used here to check this sufficiency, is ‘*stability*’ of response CDF. It is based on the fact that every simulation after some time reaches a state where the CDF of the structural response does not change any more by increasing the duration of simulation. This constant CDF is called ‘stabilized’ CDF and the fact that it does not change any more means that structure has experiences all possible combinations of the walking traffic.

To check the stability of the response CDF, its variations during simulation need to be monitored. This can be done for instance by plotting variation of response magnitudes corresponding to 95%, 85%, 75% and 50% probability of non-exceedance ($a_{95\%}$, $a_{85\%}$, $a_{75\%}$ and $a_{50\%}$) for a gradually growing window of response. Figure 9.11 presents a typical fluctuation of these values for over 14 hours of a simulation.

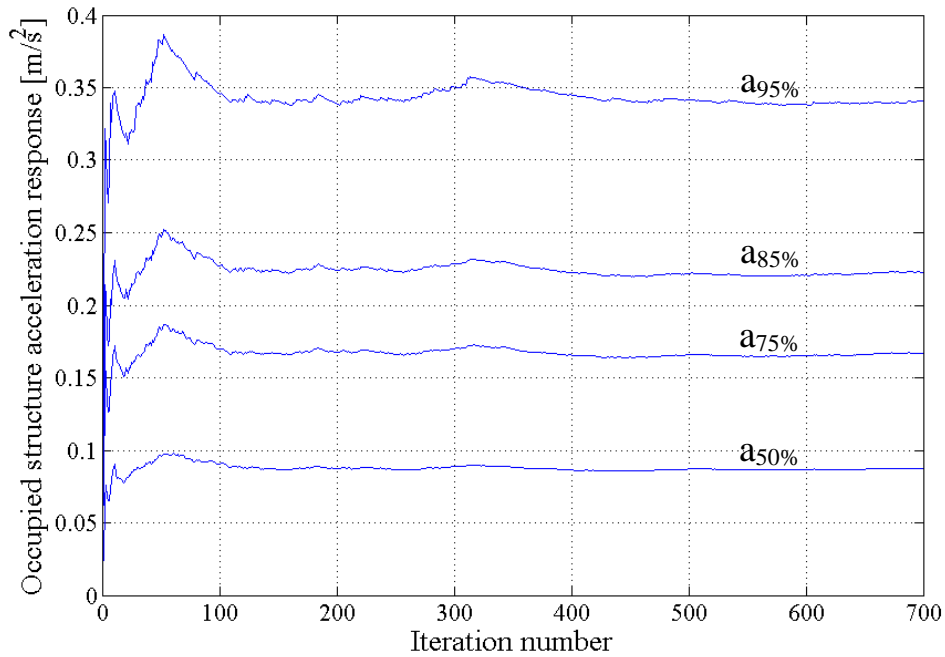


Figure 9.11. Typical fluctuation of acceleration response with 95%, 85%, 75% and 50% probability of non-exceedance (from top to bottom)

In each subsequent iteration, the length of the time window ‘ t_w ’ used for calculating $a_{95\%}$, $a_{75\%}$, $a_{75\%}$ and $a_{50\%}$ is increased by 75 seconds ($t_{w1}=75s$, $t_{w2}=150s$, $t_{w3}=225s$, etc.). As it can be seen in Figure 9.11, response CDF is acceptably stabilized after 500 iterations (equivalent to 10 hours and 25 minutes of simulation). If response CDF is not stabilized at the end of the simulation, loading duration in step 2 need to be increased and steps 2-4 need to be repeated until the stabilized CDF is achieved.

9.2.5.3 SERVICEABILITY ASSESSMENT

The vibration serviceability of a structure can be checked using an acceptable magnitude of response. Using this response magnitude, percentage of satisfied users can be found directly from the stabilized traffic-domain CDF of response.

9.3 Challenges addressed

The main shortcomings of the current serviceability assessment methods such as neglecting HSI and inter- and intra- subject variability of human parameters and limited versatility and practicality are highlighted in Section 9.1. The interaction-based VSA method proposed in this research tries to tackle these challenges of simulating walking traffic on structures by introducing the novel features described in this section.

9.3.1 Human-structure interaction

Shahabpoor et al. (2013a and b) and Zivanovic et al. (2010) have shown previously that the interaction of the walking people with structure in the vertical direction have significant effect on the structural response (sometime up to 75% reduction in structural response (Table 3.5)) and yet ways to take it into account are very rudimentary compared with the importance. Current design methods tend to ignore these effects due to the limited data available about the HSI in the vertical direction and its relative complexity. To the best knowledge of authors, the interaction-based VSA method proposed in this research is the first method of its kind to feature interaction of the walking people with the structure in the vertical direction. Similar to the highly successful concept employed by UK recommendations for design of permanent grandstands (2008), a MSD SDOF model is used to simulate the interactions. The interaction-based VSA method simulates every individual's interaction separately to include inter- and intra- subject variability and get more accurate results.

9.3.2 Versatility

As mentioned before, versatility is one of the key requirements of a practical assessment method. To maximize the versatility of the interaction-based VSA method, minimum

number of assumptions is used and, rather than assumed, the traffic parameters are calculated in the assessment process. Moreover, the structure of the method is based on conventional modal analysis so that it can be used for all linear structures.

The interaction-based VSA method is designed in a way that can be used for any loading scenarios and structure type. Single pedestrian walking along a footbridge, a dense group of walking people on a shopping mall floor and a stream of walking traffic with time-varying volume all can be modelled using this method. Combination of human activities, such as walking and standing is also possible to be simulated if reliable human models for other activities (similar to SDOF walking human model used in this study) are available. As long as the user can apply the desired loading scenario *consistently* throughout the procedure, the interaction-based VSA method will provide accurate results. Some technical tips are presented in Section 9.5 for simulating more complicated loading scenarios.

9.3.3 Practicality

Designing a practical and simple-to-use assessment method for a walking traffic is challenging if approximations are to be avoided. Within the acceptable range of errors, for each step of analysis, the simplest possible analytical method is used. This ensures the efficient use of the interaction-based VSA method by practice engineers with only basic knowledge of modal analysis and statistics.

9.3.4 Realistic simulation

Ignoring the time-variance and stochastic nature of the human parameters and loading scenarios greatly reduces the accuracy of the current assessment method. To address this issue, the structure of the interaction-based VSA method is based on a statistical analysis and probability theory. Input parameters are used in the form of statistical distributions. Monte

Carlo method is used to find the occupied structure modal properties and ultimately structural response is analyzed in terms of the probability of occurrence of different magnitudes of response.

In parallel, a realistic discrete model is used to simulate the walking traffic – structure interaction which features individualized behavior and parameters of the walking people. A combination of detailed load definition, realistic model and statistical approach results in a significantly improved prediction of structural response.

9.3.5 Refined assessment tool

It has been shown in Section 9.2.5 that conventional time-domain CDF can be a misleading tool to assess vibration serviceability of structures. The novel traffic-domain CDF used in the interaction-based method is consistent with the philosophy of vibration serviceability and assesses satisfaction of users directly. It takes into account the location of people on the structure as they walk and the actual level of vibration they experience. It also enables designers to simulate loading scenarios with time-varying traffic volume.

9.4 Sensitivity analysis

This section explores the sensitivity of the interaction-based VSA method outputs to the key input parameters. The results of this analysis provide designers with a sound understanding of the effects of each input parameter on the results of the method. For all the simulations performed in this analysis, empty structure modal properties and individual walking forces are assumed to be accurate.

A series of input and output parameters of the interaction-based VSA method are selected and sensitivity of outputs to each of inputs is analyzed. This is done by varying input parameters one at a time and monitoring its effects on different output parameters. As it can

be seen in Table 9.1, human model parameters, f_h , ζ_h and m_h , mean arrival rate r_a and walking speed v_a are selected as input parameters for the sensitivity analysis. On the other hand, occupied structure parameters f_{os} and ζ_{os} , response magnitude with 95% chance of non-exceedance $a_{95\%}$ and response RMS a_{rms} are selected as outputs to study. Selected input parameters are varied within ± 25 -30% range.

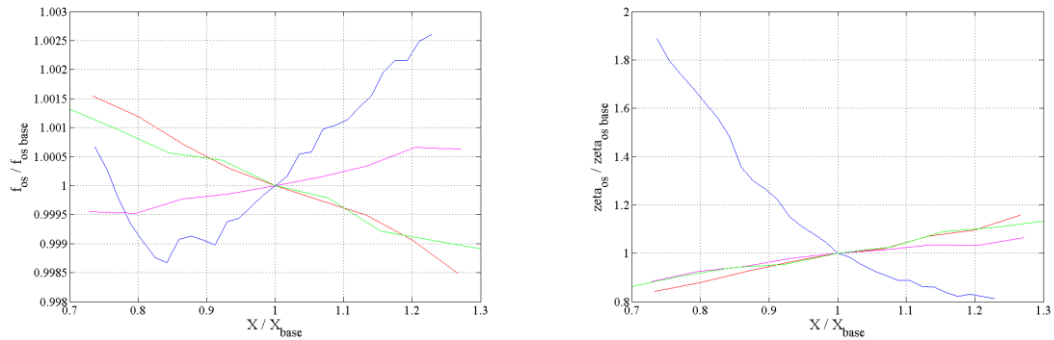
Table 9.1. Base value of sensitivity analysis parameters

Input Parameter			Output parameter (stabilized)	
Parameter	Base value	range	Parameter	Base value
f_h mean (Hz)	2.85	$\pm 25\%$	f_{os} (Hz)	2.029
ζ_h mean	0.295	$\pm 25\%$	ζ_{os}	0.0065
m_h mean (Kg)	75	$\pm 25\%$	$a_{95\%}$ (m/s^2)	0.341
r_a mean (peds/75s)*	26.3	$\pm 30\%$	a_{rms} (m/s^2)	0.155
v_w mean (m/s)	1.38	$\pm 30\%$		

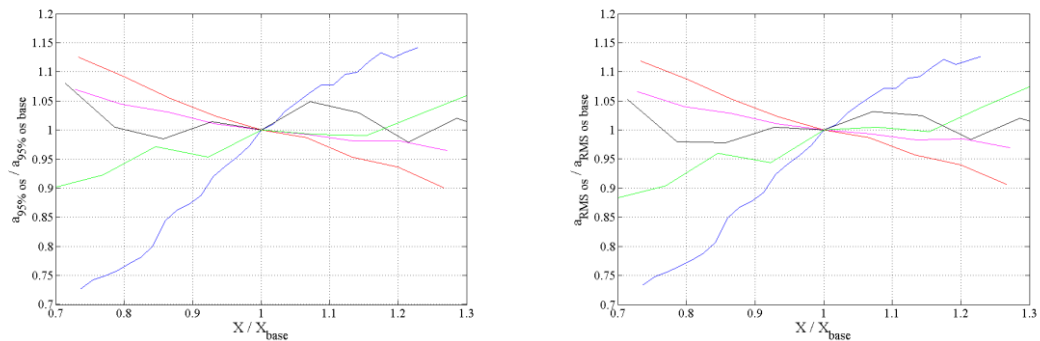
* 75 seconds is the average time needed for a person to walk along this structure

To be able to compare sensitivity of each output parameter to different inputs, a constant base value (Table 9.1) for each parameter is selected. All varying parameters are then divided by their corresponding base values to turn them into unitless ratios. The base values used in this analysis are adopted from a real-world structure and traffic on it but choice of these values does not affect the generality of the conclusions.

Figure 9.12 presents sensitivity curves for each output parameters ratio $f_{os}/f_{os\ base}$, $\zeta_{os}/\zeta_{os\ base}$, $a_{95\%}/a_{95\% \ base}$ and $a_{rms}/a_{rms\ base}$. In these graphs, the horizontal axis shows input parameters ratios $f_h/f_{h\ base}$, $\zeta_h/\zeta_{h\ base}$, $m_h/m_{h\ base}$, $r_a/r_{a\ base}$, and $v_w/v_{w\ base}$, presented with blue, pink, red, green and black colored curves, respectively.



a) Sensitivity of the occupied structure modal frequency f_{os} to input parameters
 b) Sensitivity of the occupied structure modal damping ratio ζ_{os} to input parameters



c) Sensitivity of acceleration response with 95% probability of non-exceedance $a_{95\%}$ to input parameters
 d) Sensitivity of acceleration response RMS a_{rms} to input parameters

Figure 9.12. Sensitivity of the interaction-based VSA method outputs f_{os} , ζ_{os} , $a_{95\%}$ and a_{rms} to input parameters (x/x_{base}): mean f_h (blue), m_h (red), ζ_h (pink), arrival rate r_a (green) and walking speed v_w (black)

As it can be seen in Figure 9.12 (a), the occupied structure natural frequency f_{os} shows low sensitivity to the variation of input parameters. On the other hand, Figure 9.12 (b) shows that the occupied structure damping ratio ζ_{os} is highly sensitive to human model natural frequency f_h when f_h and the empty structure modal frequency f_{es} are very close. For instance based on Figure 9.12 (b), when $f_h/f_{h\ base} = 0.8$ ($f_h=2.28$ Hz and close to $f_{es} =2.04$ Hz), ζ_{os} increase by 65% comparing to its base value $\zeta_{os\ base}$ ($\zeta_{os} / \zeta_{os\ base} =1.65$). When f_h and f_s are not

very close, ζ_{os} is not very sensitive to f_h . This great sensitivity shows its effects subsequently in high sensitivity of $a_{95\%}$ and a_{rms} to f_h as well (blue curve in Figure 9.12 (c) and (d)) when f_h and f_{es} are very close. Apart from f_h , up to 30% variation of the rest of the input parameters changes the response up to 10%. In this sense, system shows an acceptably low sensitivity to the variation of relatively uncertain inputs.

9.5 Technical recommendations for designers

Modelling a multi-pedestrian walking traffic to obtain vibration responses in the vertical direction can be a rather complex task. The following recommendations on ‘modelling unsteady traffic volume’ and ‘non-stabilized response assessment’ should help designers to maximize the capabilities of the interaction-based VSA method to simulate these complex scenarios.

9.5.1 Modelling unsteady traffic volume

One of the advantages of the interaction-based VSA method is that it allows for modelling of loading scenarios with highly time-varying traffic volume. In scenarios similar to the one presented in Figure 9.10 (c), where traffic volume significantly changes in time, it is recommended to simulate different traffic volumes separately instead of using average level. This considerably increases the accuracy of results.

Consider a case where flow rate (or arrival rate) of traffic is 70 pedestrians/min for 1/6 of the total duration of time considered and 10 pedestrians/min for 5/6 of the duration (Figure 9.13). On average there are 20 pedestrians/min for the whole duration. This is similar to the loading scenario analyzed in Figure 9.10. Comparison of Time and Traffic domain CDFs.

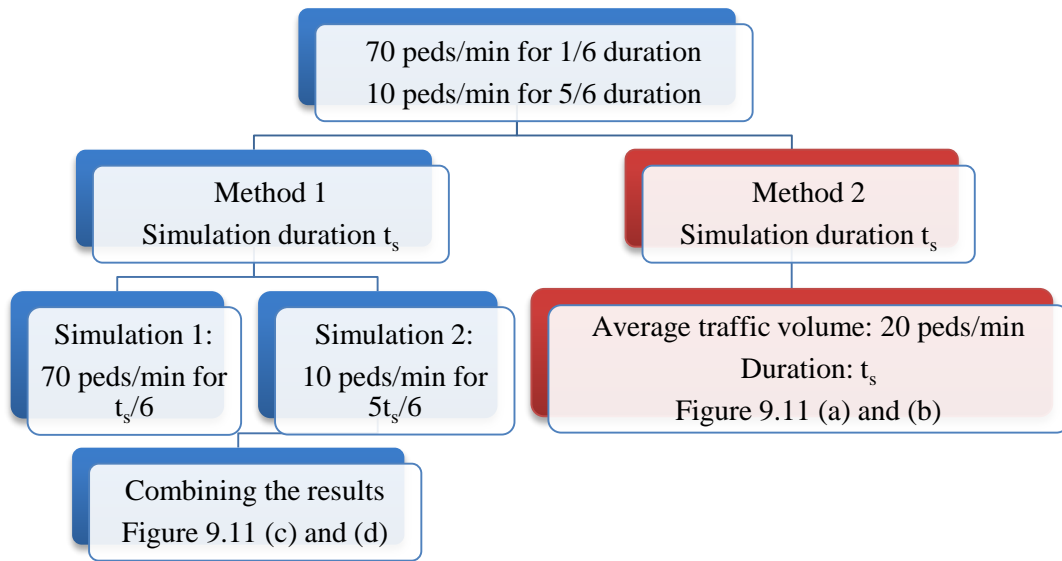


Figure 9.13. Possible methods to simulate time-varying traffic volumes

In such cases, it is strongly recommended not to use the average traffic volume (20 peds/min) for simulation and instead simulate traffic with arrival rates of 10 pedestrians/min (5/6 duration) and 70 pedestrians/min (1/6 duration) separately and then combine the results to assess the overall behavior of structure. Steps 1-3 of the interaction-based VSA method (Sections 9.2.2, 9.2.3 and 9.2.4) should be performed for each traffic volume separately. The simulation duration for each traffic volume should be selected with the same duration ratio as original traffic. For instance, for 60 minutes simulation, 10 peds/min scenario must be simulated for 50 minutes (5/6 duration) and 70 peds/min scenario must be simulated for 10 minutes (1/6 duration). The responses of the structure in both simulations then need to be connected together back-to-back in Step 4 (Section 9.2.5) to form the 60 minute total response. In the case that the CDF of the total response is not stabilized, simulation duration needs to be increased with the same ratio of the duration of the two.

Figure 9.10 (a) and (b) present the results of simulating this traffic using the average arrival

rate of 20 peds/min while Figure 9.10 (c) and (d) correspond to the case with separate simulations for 10 and 70 peds/min volumes. The considerable difference between the CDF graphs presented in Figure 9.10 (b) and (d) emphasize the importance of simulating the traffic as detailed as possible.

9.5.2 Non-stabilized response assessment

In cases where performance of a structure needs to be assessed for a duration ' t_s ' which is shorter than the time required for its response to stabilize, the 'stabilized' CDF is no longer an appropriate assessment tool. The reason is that the CDF of a stabilized response of a structure can be rather different from the same structure non-stabilized response CDF.

Consider an imaginary example where 10 hours of response is needed to achieve the stabilized CDF of the structural response, but only 1 hour measured response of structure is available for serviceability assessment. As is shown in Figure 9.14 (b), the CDF of this 1 hour response (any of gray curves) is not stabilized and is different from stabilized CDF of response (blue curve). Non-stabilized CDF here means it can be different for any arbitrary 1 hour block of response. Therefore, serviceability assessment of structure based on a specific 1 hour response CDF lack generality and may not be valid for another 1 hour response of the same structure.

For such scenarios where the CDF of the structural response is not stabilized, the '*envelope*' CDF is recommended to be used as the assessment tool instead of 'stabilized' CDF. The procedure to calculate the '*envelope*' CDF is as follows:

- I. Calculate the stabilized CDF of the structural response following the general procedure presented in Section 9.2.

- II. Select a series of response blocks each lasting t_s seconds with 90% overlap and calculate CDF of response for each block. t_s is the assessment duration which is 1 hour for our example. The selected response blocks should cover the whole duration of stabilized response (10 hours in our example) (Figure 9.14 (a)).
- III. Find the envelope curve of all the t_s seconds CDFs (1-hour CDFs in our example - Figure 9.14 (b) - dashed red curve). This envelope curve is suggested to be used for serviceability assessment of the structure. Using envelope CDF, designer ensures that response of structure in any arbitrary t_s period will not exceed the design target.

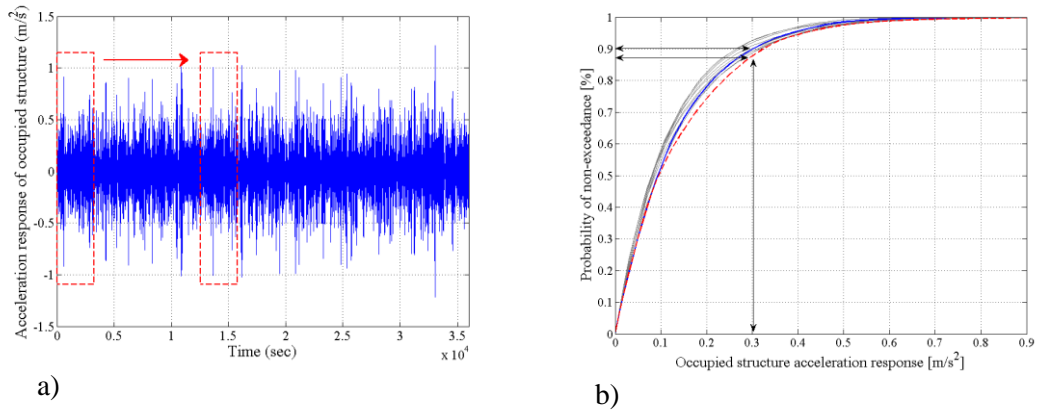


Figure 9.14. A typical over-plot of CDFs with t_s duration and their stabilized (blue) and envelope (dashed red) CDF curves

Based on Figure 9.14 (b), for 0.3 m/s^2 response magnitude, envelope CDF suggests that 88% of the users are satisfied while stabilized CDF shows that about 90% of users will be satisfied. This shows that, as it was expected, stabilized CDF is slightly more conservative than stabilized CDF criteria.

9.6 Conclusions

The interaction-based VSA method proposed in this research is developed to address some of the most important shortcomings of current vibration serviceability assessment methods such as neglecting HSI and inter- and intra- subject variability of human parameters and

limited versatility and practicality. The novel features of the method are:

- HSI: To the best knowledge of authors, the interaction-based VSA method is the first method of its kind to feature individualized interaction of the walking people with the structure in the vertical direction. Similar to the highly successful concept employed by UK recommendations for design of permanent grandstands (2008), a MSD SDOF model is used to simulate the interaction of each walking pedestrian.
- Versatility: Minimum number of assumptions is used in the method and, rather than assumed, the traffic parameters are calculated in the assessment process. Moreover, the structure of the method is based on conventional modal analysis so that it can be used for all linear structures.
- Practicality: The interaction-based VSA method was developed in a way that it can be used easily by practice engineers with only basic knowledge of modal analysis and statistics.
- Refined assessment tool: A novel assessment tool is used in the method that takes into account the actual experience of the users of the structure rather than the structural response. This assessment tool gives considerably more relevant results in comparison with currently available methods.

Results of the sensitivity analysis showed maximum 10% error in estimated structural response within possible range of inputs as long as human model frequency is not very close modal frequency of structure. In this sense, system shows an acceptably low sensitivity to the variation of relatively uncertain inputs. Further research on finding walking human model parameters can further increase the accuracy of the model.

Chapter 10

Validation of Interaction-based Vibration Serviceability Assessment Method Using Full-scale Structures

The contents of this chapter are adapted with minor changes from the following journal paper in preparation to be submitted to the ASCE Journal of Performance of Constructed Facilities:

Shahabpoor, E., Pavić, A., Racić, V. and Zivanović, S. Validation of Interaction-based Vibration Serviceability Assessment Method Using Full-scale Structures. The ASCE Journal of Structural Engineering.

10.1 Introduction

This chapter applies the interaction-based VSA method described in Chapter 9 to six different tests on two real-world structures: the University of Sheffield footbridge and Podgorica footbridge, Montenegro. In each test, analytical results are compared with corresponding experimental ones and performance of the interaction-based VSA method in estimating structural response is discussed. The performance of this method is then compared with a selection of design guidelines currently used widely around the world: the ISO 10137 standard (2007), French road authorities standard (Setra, 2006), UK National Annex to Eurocode 1 (BSI, 2008) and method proposed by Butz (2006).

Section 10.2 of this chapter presents an overview of the interaction-based VSA method. Sections 10.2 and 10.3 describe the structures and details of the six vibration monitoring tests done on them. A step-by-step description of the application of the interaction-based VSA method is presented in Section 10.4. The method was used to estimate measured responses in all six tests and the results are presented in corresponding sub-sections of Section 10.4. The same section then compares the performance of the interaction-based VSA method with the selected guidelines for all six tests. The concluding remarks are presented in Section 10.5.

10.2 Empty structures

To examine the performance of the interaction-based VSA method in serviceability assessment, a complete set of tests are designed and performed on two real-world footbridges. The selected structures are built from different materials and are different structural systems. They both are very lightly damped and have natural frequencies in the

range excitable by walking force and are reasonably close to the natural frequency of the human walking model which engages human-structure interaction mechanisms.

10.2.1 Sheffield footbridge

The first structure used in this study is a simply supported in-situ cast post-tensioned (PT) concrete footbridge purposefully constructed in the structures laboratory of The University of Sheffield. The details of the structure and its modal properties are presented in Sections 3.3.1 and 6.3.2, respectively. Modal frequency, damping ratio and modal mass of the first vertical mode of the structure were found to be 4.44 Hz, 0.6% and 7128 kg respectively (Table 10.1). These parameters are used as the ‘empty’ Sheffield footbridge modal properties (f_{es} , ζ_{es} and m_{es}) in rest of the chapter.

Table 10.1. Results of modal analysis of the empty structure

Mode	FRF based modal testing				
#	f (Hz)	ζ (%)	M_i (kg)	C_i (N.s/m)	K_i (N/m)
1	4.44	0.6	7,128	2,386	$5,547 \times 10^3$

10.2.2 Podgorica footbridge

The second structure used in this study is a steel box girder footbridge spans 104 m over the Morača River in Podgorica, capital of Montenegro. The details of the structure and its modal properties are presented in Sections 3.3.1 and 3.5.1, respectively. Only the first vertical mode of the structure with 2.04 Hz modal frequency and 0.26% damping ratio is considered susceptible to excessive vertical vibration by a vertical component of a walking force. Figure 10.1 presents the unity-normalized mode shape of the first vertical mode of the Podgorica footbridge.

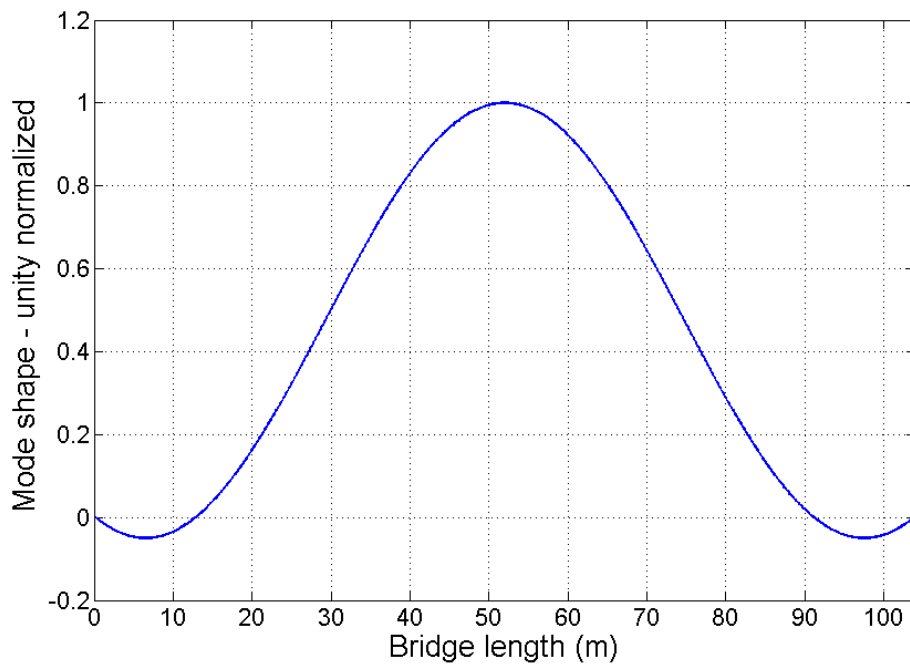


Figure 10.1. Mode shape of the first vertical mode of the Podgorica footbridge

10.3 Monitoring tests

The loading scenarios were designed for each experiment in a way that performance of the interaction-based VSA method was examined under distinct traffic configurations.

10.3.1 Sheffield footbridge tests

Three tests were designed on the Sheffield footbridge with 3, 6 and 10 pedestrians walking in a closed-loop path along the footbridge (Figure 10.2). Test participants were asked to walk with their desired speed and they were free to pass each other. Each test was run for about 2 minutes. Similar to modal tests configuration, the response of structure was recorded using 18 accelerometers placed along the longer edges of the structure as shown in Figure 10.2. Only the response at mid-span (average of test points (TPs) 5 and 14) was used for the response comparison purposes.

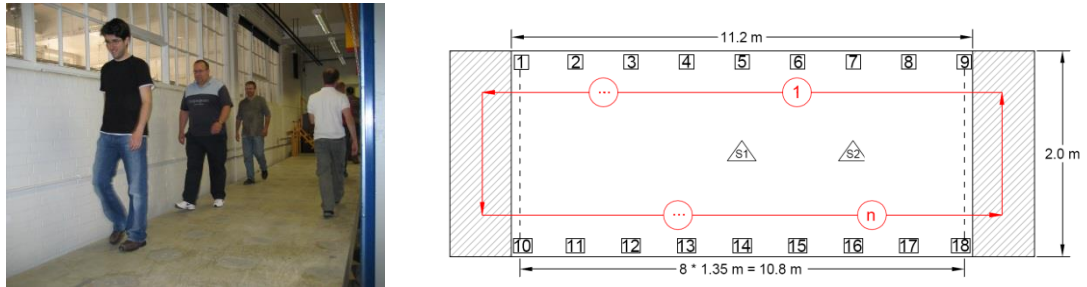


Figure 10.2. A typical walking path

Pedestrian data were collected using a digital weighing scale, an instrumented treadmill, a pair of PeCo laser pedestrian counters and video camera. Weight of each pedestrian was measured using a digital weighing scale and their walking forces on a stiff surface were recorded using an instrumented treadmill. A pair of PeCo laser pedestrian counters, installed at both ends of the footbridge over the walkway (Figure 10.3 – arrow pointing to one of the two PeCo devices), was used to record in real-time each individual’s location, walking direction and walking speed on the structure (Figure 10.3).

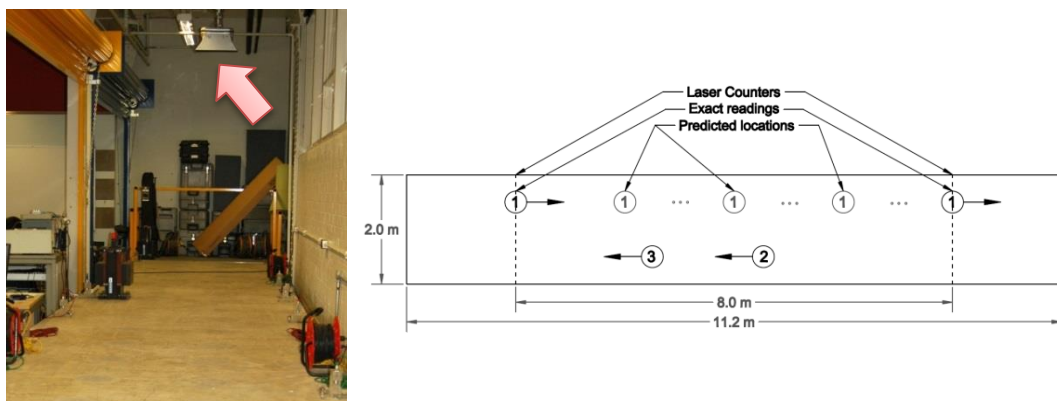


Figure 10.3. Prediction of people location between each two of the consecutive crossings of the PeCo laser pedestrian counter (arrow pointing to it)

10.3.1.1 STATISTICS RELATED TO TRAFFIC

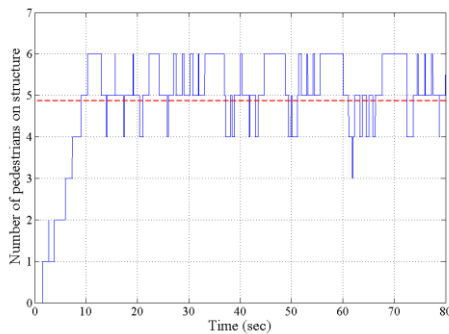
Statistical parameters of Tests 1-3 are presented in Table 10.2 where three, six and 10 people

were participating, respectively. Due to the walking pattern of people in these tests, arrival rate and the number of people on the structure showed limited variations. Therefore no statistical distribution was used to describe these parameters and only their mean values were instead used for analysis. Normal distribution was found suitable to describe walking speed of different pedestrians. Using average walking speed of 1.28 m/s, an average pedestrian needs 8.4 seconds to cross the 10.8 m support-to-support length of footbridge.

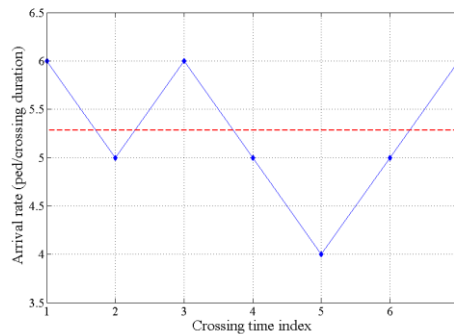
Table 10.2. Traffic statistics of Sheffield University footbridge tests

Parameter	Unit	Distribution	Test 1	Test 2	Test 3	Average
Number of participants	peds	-	3	6	10	-
Mean arrival rate (r_a)	peds/ crossing time	-	2.64	5.29	8.27	-
Mean number of pedestrians on footbridge	peds	-	2.5	4.9	7.86	-
Mean walking speed (v_w)	m/s	Normal	1.41	1.06	1.36	1.28
Variance walking speed (v_w)	m/s	Normal	0.06	0.04	0.29	0.13
Average crossing time (t_c)	s	-	7.7	10.2	7.9	8.6
Average body mass (m_h)	kg	-	70	70	70	70

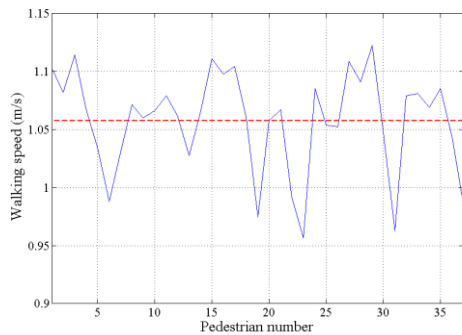
A typical representation of traffic statistical data for the Test 2 is shown in in in Figure 10.4. The crossing time index in Figure 10.4 (b) indicates the index of the time blocks with duration equal to average crossing time (10.2 s): 1st 10.2s of test, 2nd 10.2s of test, etc.



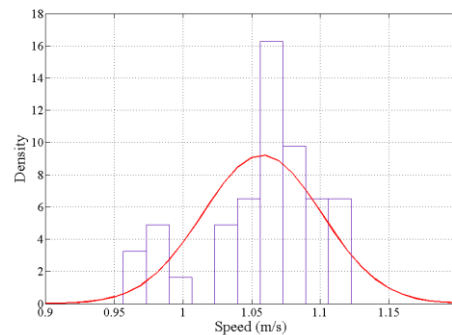
a) Time-varying number of pedestrians on the structure (mean equal to 4.9 pedestrians)



b) Traffic arrival rate per average crossing time (10.2 s)



c) Pedestrian average walking speed (1.06 m/s overall average)



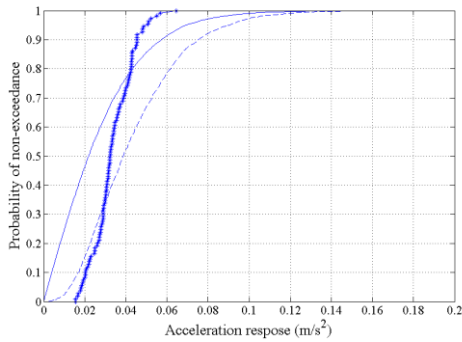
d) Normal distribution fitted on individual walking speed data (mean equal to 1.06 m/s and variance 0.04 m/s)

Figure 10.4. A typical statistical presentation of the traffic data - Sheffield footbridge Test 2

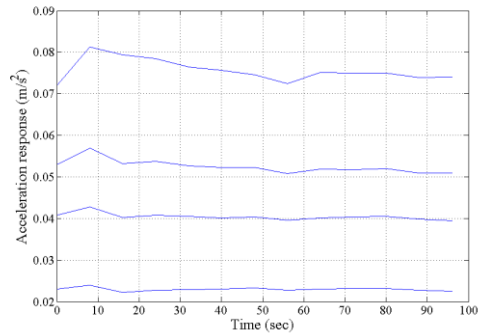
As it can be seen in in Figure 10.4 (a), variations of the number of pedestrians on the structure was limited to 4-6 people due to the controlled loading scenario. Similarly, variations of the arrival rate in (Figure 10.4 (b)) were limited to 5-6 pedestrians per average crossing time (of 10.2s) and sample size was also limited. Therefore, statistical distribution was not an appropriate tool to describe variations of both parameters and their mean value is used in simulations.

10.3.1.2 STRUCTURAL RESPONSE

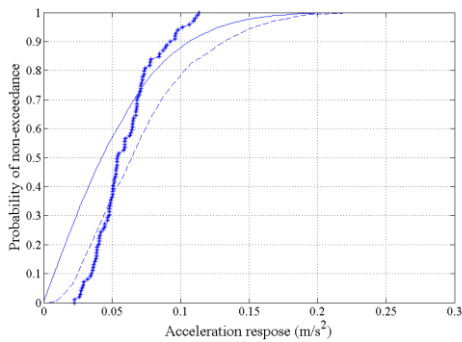
The response experimentally recorded at mid-span (anti-node of mode 1) is used for analysis. The time-domain cumulative distribution functions (CDFs) of instantaneous, peaks per cycle (local peaks) and 1 second running RMS of acceleration response of structure for tests 1-3 are presented in Figure 10.5 (a) (3 people), (c) (6 people) and (e) (10 people). As expected, magnitude of the structural response increases as the number of walking people increases.



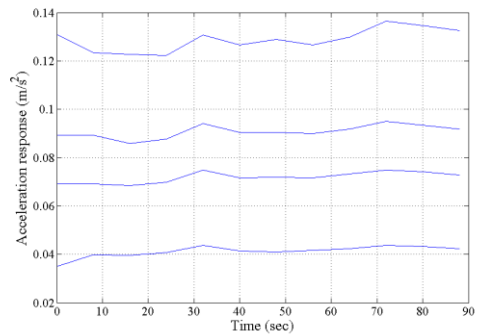
a) Test 1 - CDFs of instantaneous (-), peak per cycle (--) and 1s – RMS (-*-) acceleration response



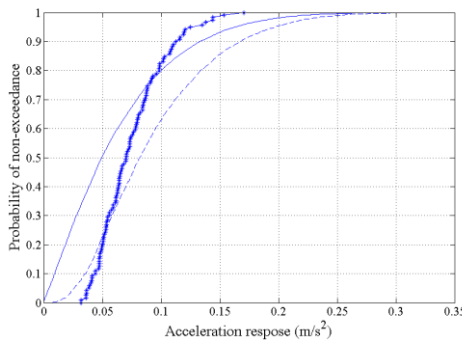
b) Test 1 - Time-history of acceleration response with 95%, 85%, 75% and 50% probability of non-exceedance (from top to bottom)



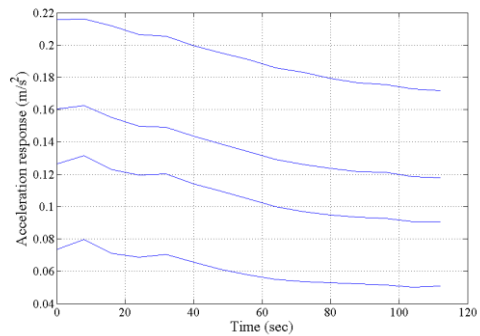
c) Test 2 - CDFs of instantaneous (-), peak per cycle (--) and 1s – RMS (-*-) acceleration response



d) Test 2 - Time-history of acceleration response with 95%, 85%, 75% and 50% probability of non-exceedance (from top to bottom)



e) Test 3 - CDFs of instantaneous (-), peak per cycle (--) and 1s-RMS (-*-) acceleration response



f) Test 3 - Time-history of acceleration response with 95%, 85%, 75% and 50% probability of non-exceedance (from top to bottom)

Figure 10.5. Statistical representation of Sheffield footbridge response - Tests 1 – 3

To check the stability of these CDFs, variation of their corresponding acceleration responses with 95%, 85%, 75% and 50% probability of non-exceedance ($a_{95\%}$, $a_{85\%}$, $a_{75\%}$ and $a_{50\%}$) during tests are plotted in Figure 10.5 (b), (d) and (f). As it can be seen in these graphs, $a_{95\%}$, $a_{85\%}$, $a_{75\%}$ and $a_{50\%}$ are not stabilized (especially $a_{95\%}$) which indicates that response CDFs of Tests 1-3 are not stabilized. The statistical parameters of structural response in tests 1-3 responses are presented in Table 10.3. These values will be used later in Section 10.4.5 to compare the performance of the interaction-based VSA method with a selection of currently available assessment methods.

Table 10.3. Statistics of Sheffield University footbridge acceleration response

Test No.	a_{peak} (m/s ²)	$a_{95\%}$ (m/s ²)	$a_{2.5\sigma}$ * (m/s ²)	a_{rms} (m/s ²)
Test 1	0.220	0.074	0.083	0.035
Test 2	0.292	0.133	0.150	0.065
Test 3	0.352	0.172	0.188	0.080

* The response magnitude corresponding to 2.5 standard deviation away from mean value of structural response

One of the key assumptions of the interaction-based VSA method in Steps 1 (Section 9.2.2) and 3 (Section 9.2.4) is that presence of walking people on structure does not affect the mode shape of structure. This assumption is validated in Section 7.2.4.

10.3.2 Podgorica footbridge tests

Three monitoring tests were performed on the Podgorica footbridge under normal pedestrian traffic each lasting about 44 minutes. A piezoelectric accelerometer Endevco 7754-1000 was used at mid-span to record acceleration response of structure. Pedestrian traffic was monitored at the same time using two video cameras located at both ends of the footbridge and synchronized with recorded acceleration response. Pedestrians' crossing time, average speed and pacing frequency and number of people on the structure at any particular moment

were measured using these time-stamped video footage (Zivanovic, 2012).

10.3.2.1 STATISTICS RELATED TO TRAFFIC

Pedestrian traffic in all three tests was free flowing and spatially unrestricted, that is, pedestrians were able to walk at their preferred walking speed, overtake each other, etc. The pedestrian traffic in the first two tests can be considered as usual traffic on the bridge, while traffic during third test was rush-hour traffic, and it includes very busy periods with lots of people on the bridge. Statistical parameters of the pedestrian traffic during these three tests are presented in Table 10.4. These tests will be referred to as Tests 4, 5 and 6 in this study.

Table 10.4. Traffic statistics of Podgorica footbridge tests

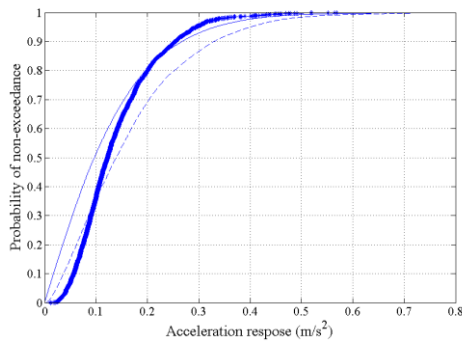
Parameter	Unit	Distribution	Test 4	Test 5	Test 6	Average
Mean arrival rate (r_a)	Peds/75s	Poisson	15.5	15.3	26.3	-
Mean number of pedestrians on footbridge	-	Normal	14.9	15.7	26.1	-
Variance - number of pedestrians on footbridge	-	Normal	4.3	5.9	13.6	-
Mean walking speed (v_w)	m/s	Normal	1.42	1.38	1.38	1.39
Variance walking speed (v_w)	m/s	Normal	0.20	0.21	0.19	0.20
Average crossing time (t_c)	s	-	73.2	75.4	75.4	75
Average body mass (m_h)	kg	-	75	75	75	75

Normal distribution proves to be a good model to describe walking speed and number of people on footbridge while Poisson distribution is used to describe arrival rate. The mean speed of 1.39 m/s means that, on average, one person needs about 75 s to cross this 104m long bridge. Detailed description of the tests and statistical analysis of traffic parameters are presented in (Zivanovic, 2012).

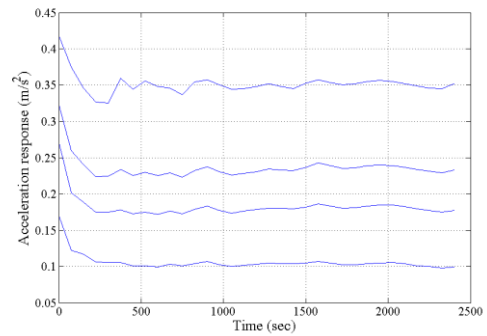
10.3.2.2 STRUCTURAL RESPONSE

The time-domain CDFs of instantaneous, peaks per cycle and 1-second running RMS of the acceleration response of Podgorica footbridge for Tests 4-6 are presented in Figure 10.6 (a),

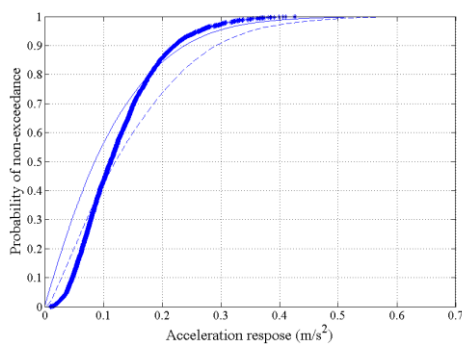
(c) and (e). To check the stability of these CDFs, variation of their acceleration responses with 95%, 85%, 75% and 50% probability of non-exceedance ($a_{95\%}$, $a_{85\%}$, $a_{75\%}$ and $a_{50\%}$) are plotted in Figure 10.6 (b), (d) and (f). Although the $a_{95\%}$, $a_{85\%}$, $a_{75\%}$ and $a_{50\%}$ of Podgorica footbridge tests are more stabilized than the ones of Sheffield footbridge tests due to the longer duration of tests, they are not stabilized enough (The stability criterion here was taken as maximum 0.01 m/s^2 fluctuation in $a_{95\%}$ for continues 1000 seconds of response). This conclusion is later proved to be correct in Section 10.4.



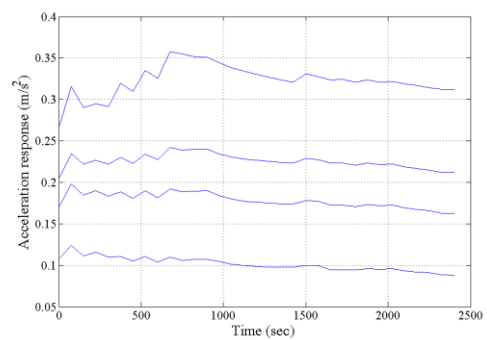
a) Test 4 - CDFs of instantaneous (-), peak per cycle (--) and 1s-rms (-*-) acceleration response



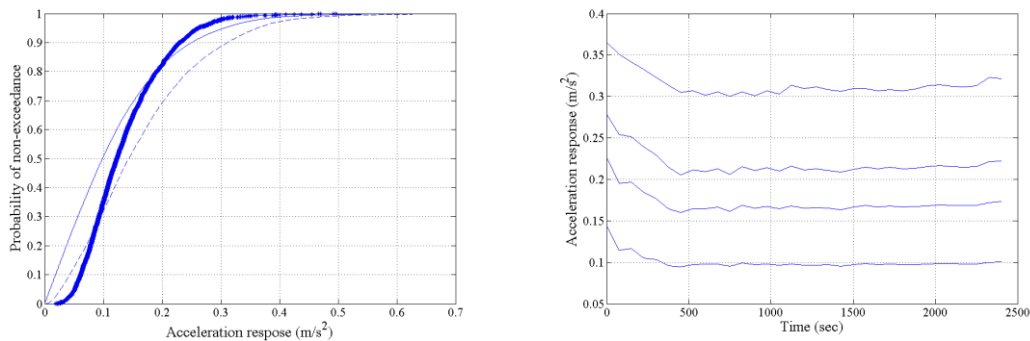
b) Test 4 - Time-history of $a_{95\%}$, $a_{85\%}$, $a_{75\%}$ and $a_{50\%}$ (from top to bottom)



c) Test 5 - CDFs of instantaneous (-), peak per cycle (--) and 1s-rms (-*-) acceleration response



d) Test 5 - Time-history of $a_{95\%}$, $a_{85\%}$, $a_{75\%}$ and $a_{50\%}$ (from top to bottom)



- e) Test 6 - CDFs of instantaneous (-), peak per cycle (--) and 1s-rms (-*-) acceleration response
- f) Test 6 - Time-history of $a_{95\%}$, $a_{85\%}$, $a_{75\%}$ and $a_{50\%}$ (from top to bottom)

Figure 10.6. Statistical representation of Podgorica footbridge response - Tests 4 – 6

A selection of statistical parameters of tests 4-6 responses are presented in Table 10.5. These values again will be used later in Section 10.4.5 to compare the performance of the interaction-based VSA method with few other currently available assessment methods.

Table 10.5. Statistics of Podgorica footbridge acceleration responses

Test No.	a_{peak} (m/s^2)	$a_{95\%}$ (m/s^2)	$a_{2.5\sigma}$ (m/s^2)	a_{rms} (m/s^2)
Test 4	0.801	0.352	0.387	0.163
Test 5	0.649	0.312	0.343	0.144
Test 6	0.780	0.321	0.357	0.153

10.4 Vibration serviceability assessment

This section describes step-by-step the application of the interaction-based VSA method to simulate walking traffic in tests 1-6 with the relevant statistics described in Table 10.2 and Table 10.4. In each step, results of the interaction-based VSA method, but without considering interaction are also presented and compared with the interactive results to examine the effects of taking into account the interaction between walking traffic and the structure. Finally, in Section 10.4.5, the performance of the interaction-based VSA method is compared with a selection of frequently used current assessment guidelines.

10.4.1 Input parameters

Table 10.6 presents the input parameters used in the interaction-based VSA method to simulate traffic in Tests 1-6. For the Sheffield footbridge tests (Tests 1-3), each individual’s walking force was recorded on stiff surface using an instrumented treadmill and used in simulations. For the Podgorica footbridge tests (Tests 4-6) the walking forces are randomly selected from a pool of 1200 recorded walking forces. The walking forces were selected in a way that their average static mass matches the average weight of test participants in that test.

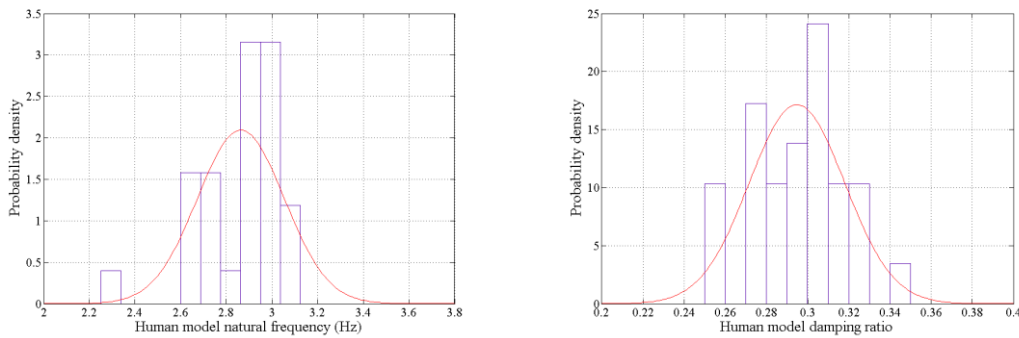
Table 10.6. Input parameters of 6 tests used in the interaction-based VSA method

Category	Parameters	Units	Distribution	Sheffield footbridge			Podgorica footbridge		
				Test 1	Test 2	Test 3	Test 4	Test 5	Test 6
Empty Structure modal properties	m_{es}	Kg	-		7128		58000		
	f_{es}	Hz	-		4.44		2.04		
	ζ_{es}	%	-		0.6		0.26		
Walking human model parameters	m_h mean	Kg	-		70		75		
	f_h mean	Hz	Normal		2.864		2.864		
	f_h variance	Hz	Normal		0.191		0.191		
	ζ_h mean	%	Normal		29.5		29.5		
Traffic parameters	ζ_h variance	%	Normal		2.3		2.3		
	r_a mean	Peds/crossing time	Poisson	-	-	-	15.5	15.3	26.3
	v_w mean	m/s	Normal	2.64	5.29	8.27	-	-	-
Walking force	v_w variance	m/s	Normal	1.41	1.06	1.36	1.42	1.38	1.38
	F_w total	N		0.06	0.04	0.29	0.20	0.21	0.19

In Steps 1 and 2 of Interaction-based VSA method (Sections 9.2.2 and 9.2.3), number of people on structure is predicted using the corresponding arrival rate distribution. In general for a long duration of response and constant walking speed, mean arrival rate for average crossing time is equal to the mean number of people on the structure in that period. For instance, for constant walking speed of 1.5 m/s and structure length of 15 meters, crossing time is 10 seconds. The arrival rate of ‘ r_a ’ pedestrians / 10 seconds for this structure means ‘ r_a ’ person are on structure at each moment of time.

Parameters of SDOF MSD walking human model m_h , f_h and ζ_h , are adapted from results

presented in Chapter 8. Figure 10.7 presents the probability density function (PDF) of SDOF human model natural frequency f_h and damping ratio ζ_h suggested in Chapter 8. The human mass m_h is selected equal to the average mass of people on the structure in each test.



- a) PDF of the SDOF human model natural frequency. $\mu=2.864$ Hz , $\sigma=0.191$ Hz
- b) PDF of the SDOF human model damping ratio. $\mu=0.295$, $\sigma=0.023$

Figure 10.7. PDF of human SDOF model natural frequency f_h (a) and damping ratio ζ_h (b)

10.4.2 Step 1 implementation

The first step of the interaction-based VSA method is to find occupied structure modal properties (Section 9.2.2). The methodology used in this step is basically an iterative process. In each iteration, a random distribution of peoples' location on the structure is considered. Walking people are assumed stationary at their location at that particular moment of time (Figure 10.8). Each human and the target mode of the structure are modelled with an SDOF model. These SDOF models are assembled based on the location of each person on the structure to form a traffic-structure mass-spring-damper model (Figure 10.9). The occupied structure modal properties f_{os} , ζ_{os} and m_{os} are then found for this MDOF configuration. The unity-normalized mode shapes must always be used throughout the interaction-based VSA method.

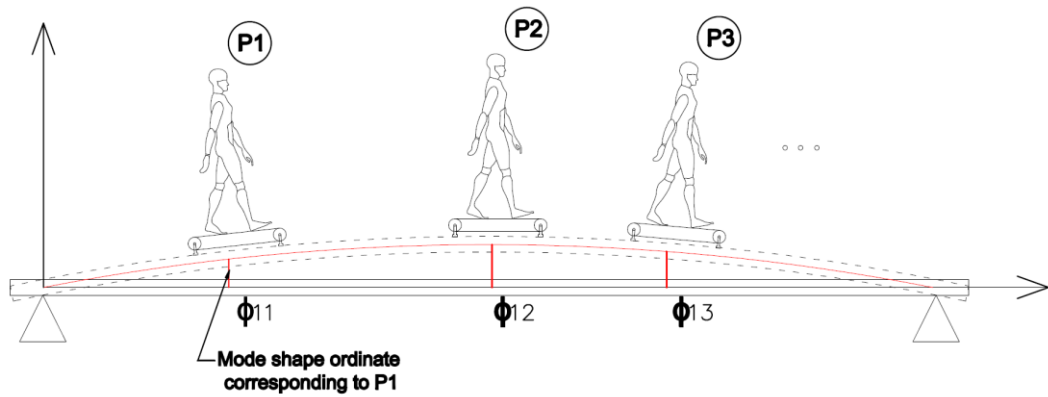


Figure 10.8. A conceptual illustration of stationary walking people. Φ_{ab} represents ordinate of mode ‘a’ at the location of human ‘b’

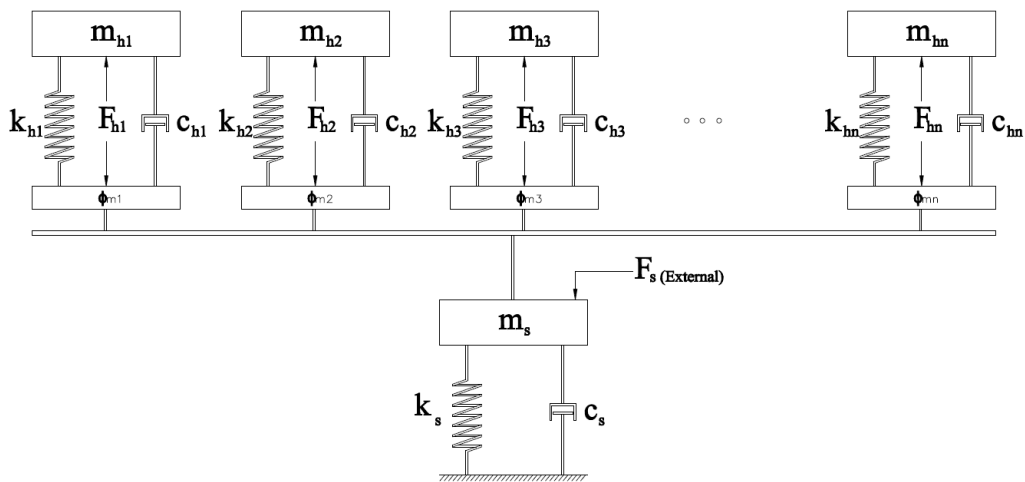


Figure 10.9. Mass-spring-damper model of stationary walking traffic-structure system

For each test in this study, modal analysis of the traffic-structure system was repeated 800 times with varying number of people and location configurations. The number of people on the structure for each simulation was selected using the corresponding arrival rate distribution and their locations were selected randomly assuming uniform distribution. Figure 10.10 presents a typical fluctuation of the average occupied structure f_{os} and ζ_{os} against the number of simulations for Test 5. It can be seen that average f_{os} and ζ_{os} are

acceptably stabilized after 600 simulations.

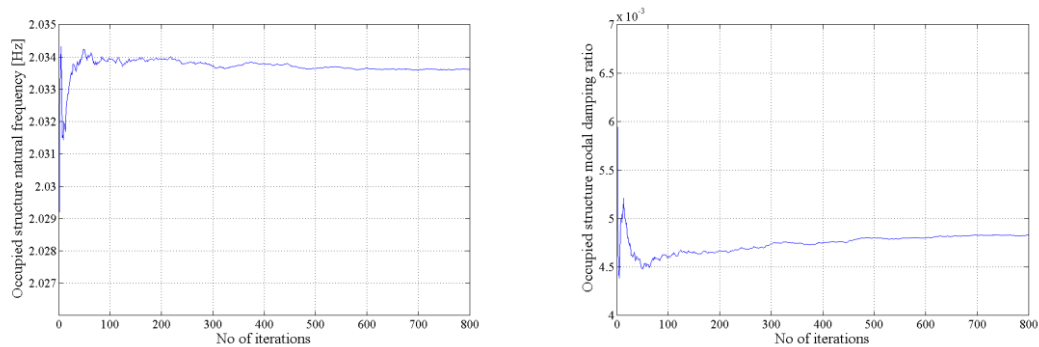


Figure 10.10. Fluctuation and stabilization of average occupied structure natural frequency f_{os} and damping ratio ζ_{os} – Test 5

Experimental and analytically calculated modal properties of the two occupied structures in various tests are presented in Table 10.7 for all six tests. To examine the accuracy of these parameters, results of Tests 1-3 are compared with their corresponding experimentally found modal properties from identical tests. The experimental occupied structure parameters used here are results of the FRF-based modal tests (Tests 1.4, 1.7 and 1.8 in Table 6.3) performed in identical situations with Tests 1-3 i.e. same people and same structure at the same time. Reader may refer to Appendix I to see the relation of the tests discussed in this chapter with the ones presented in Chapters 6, 7 and 8.

Table 10.7. Modal properties of occupied structure

Test Number	Experimental			Analytical		
	f_{os} (Hz)	ζ_{os} (%)	m_{os} (kg)	f_{os} (Hz)	ζ_{os} (%)	m_{os} (kg)
Sheffield footbridge						
Empty	4.440	0.60	7128	-	-	-
Test 1	4.445	1.10	7183	4.445	1.10	7183
Test 2	4.465	1.65	7238	4.465	1.65	7238
Test 3	4.475	2.30	7311	4.475	2.30	7311
Podgorica footbridge						
Empty	2.04	0.26	58000	-	-	-
Test 4	-	-	-	2.034	0.49	58750
Test 5	-	-	-	2.034	0.49	58750
Test 6	-	-	-	2.029	0.65	59300

Figure 10.11 presents the empty and occupied structure FRF plots corresponding to Tests 1-3. Close match between the analytical and experimental FRFs demonstrates the excellent performance of the interaction-based VSA method in predicting the occupied structure parameters. Similar graphs for Tests 1-6 are presented in Figure 10.12 but no experimentally measured occupied structure FRF was available to compare the data against.

Trend wise, the FRF curves of Figure 10.11 and Figure 10.12 match the trends found in Chapter 4. It was found that when modal frequency of an empty structure f_{es} is higher than the natural frequency of walking human model f_h (similar to Tests 1-3 where $f_{es}= 4.44 \text{ Hz} > f_h=2.864 \text{ Hz}$), occupied structure modal frequency f_{os} is expected to be higher than that of the empty structure f_{es} (shift of the FRF peak to the right). Moreover, when $f_{es}<f_h$ (similar to Tests 4-6 where $f_{es}= 2.04 \text{ Hz} < f_h=2.864 \text{ Hz}$), f_{os} is expected to be lower than f_{es} (Shift of the FRF peak to the left). In both cases higher damping ratio for the occupied structure ζ_{os} is expected.

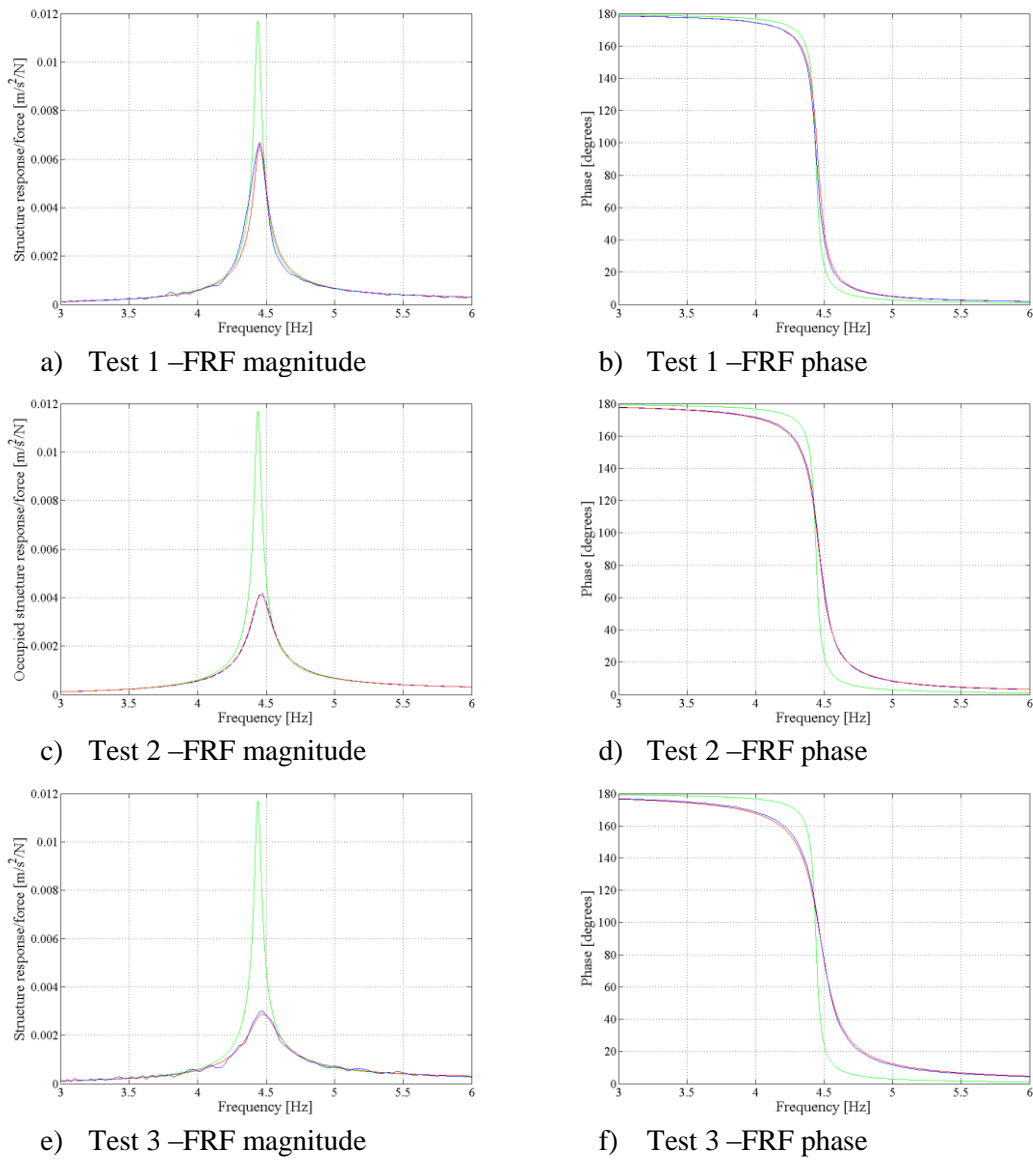


Figure 10.11. FRF plots of Sheffield footbridge tests - Empty structure (green), occupied structure experimental (blue) and occupied structure analytical (red)

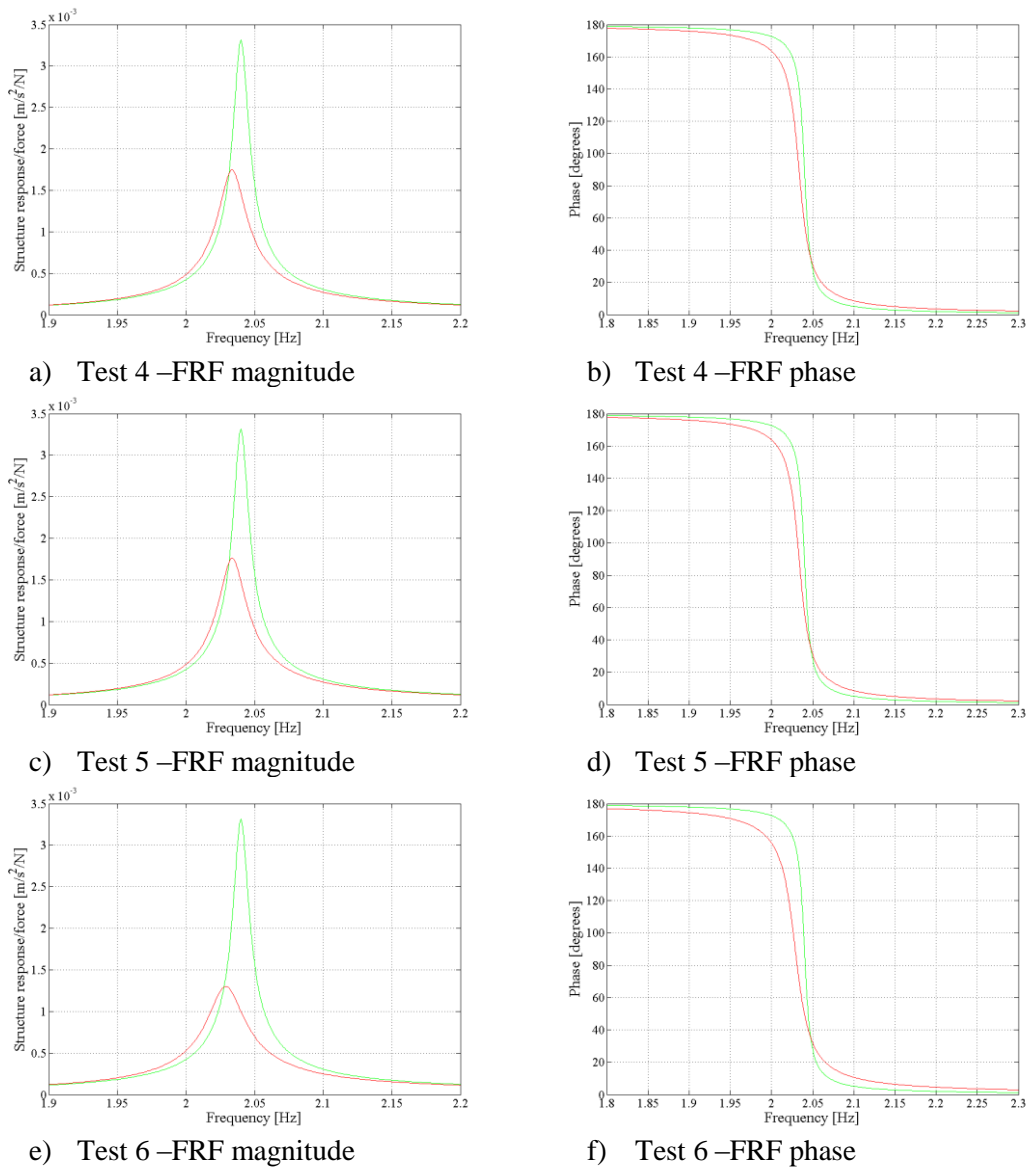


Figure 10.12. FRF graphs of Podgorica footbridge tests - Empty structure (green) and occupied structure analytical (red)

10.4.3 Step 2 implementation

Modal walking load of the multi-pedestrian traffic is calculated in Step 2 for each of the six tests. 15 hours simulation duration was performed and considered for each test to get a stabilized response. This assumption is later examined in Step 4. Experimentally recorded walking forces on stiff surface were used in all simulations. In Tests 1-3, exact time-history

of people location and their recorded walking forces on stiff surface are used in the simulations to increase accuracy. For each person, a random window of their recorded walking force with duration equal to their crossing time is used in the simulation.

The individual walking forces of Tests 4-6 are selected randomly from a pool of 1200 recorded walking forces (Racic and Brownjohn, 2011) using an instrumented treadmill. This pool was considered to represent a sufficiently diverse group of people although none of the hundreds of people who participated in Tests 4-6 actually had their walking force measured. The selection of the walking forces used in simulations was performed so that average weight of people corresponding to these walking forces would be equal to average weight of test participants in each test. These individual walking forces were scaled in the next step using the structure’s mode shape to find modal walking force of each individual. Figure 10.13 shows a typical modal walking force of an individual scaled with the assumed unity-scaled fundamental mode shape of the structure.

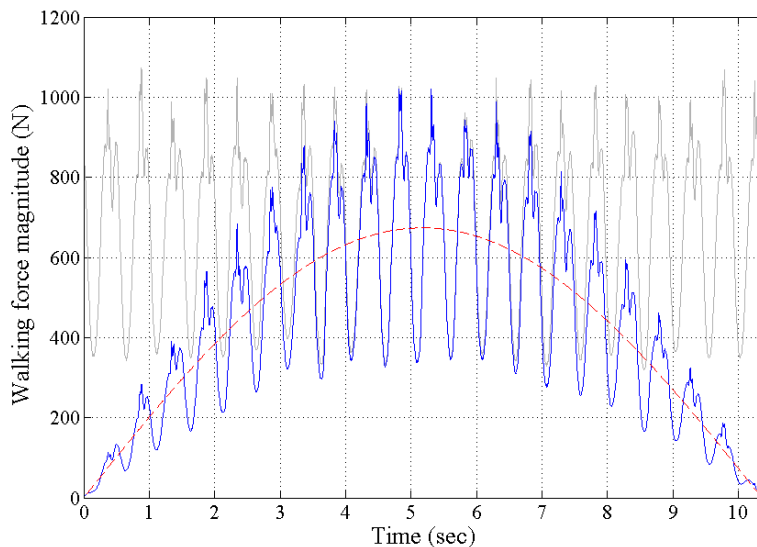
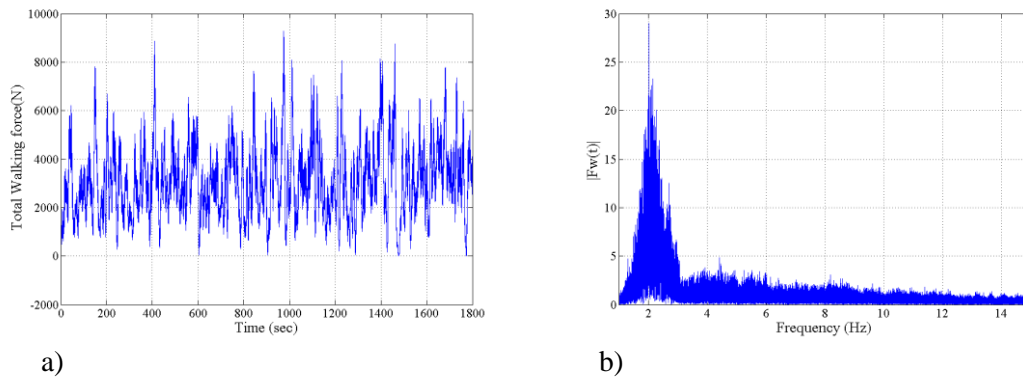


Figure 10.13. A typical mode 1 modal walking force

Resulting modal walking forces of individuals are then summed up based on their corresponding arrival time. Arrival time of pedestrians for Tests 1-3 are read directly from

their location time-history while for Tests 4-6, are predicted based on arrival rate distribution. Figure 10.14 presents a typical total walking force and its frequency domain contents for 30 minutes of Test 2 simulation. High magnitude of force is noticeable around first harmonic frequency.



a) b)
Figure 10.14. A typical total modal walking force (a) and its frequency domain content (Fourier transform)(b)

10.4.4 Steps 3 and 4 analysis

The response of the occupied structures to the corresponding modal traffic loads generated in Step 2 were calculated in Step 3 and presented in the form of ‘*time-domain*’ CDF in Step 4 (Sections 9.2.4 and 9.2.5). The time-domain CDF links magnitude of structural response with its corresponding probability of non-exceedance in time. The ‘*traffic-domain*’ CDF, which links magnitude of structural response with percentage of users that experience no more than that response magnitude, was not used in this study as required traffic data was not available for comparison. As only one mode of both structures is used for the response calculation, no mode superposition is done. Simulation of each test lasted for 15 hours to get stabilized response.

Analysis of the experimental CDFs in Section 10.3 indicated that they are not stabilized for both structures. Therefore the ‘envelope’ CDF was used for serviceability assessment (Section 9.5.2). For each test simulation was run for 15 hours so that stabilized response is achieved. A series of response windows with the length equal to the corresponding test duration (2 minutes for Tests 1-3 and 44 minutes for Tests 4-6) with 90% overlap was selected. CDF of the response for each of these response windows was then calculated. The envelope of these CDFs was used for vibration serviceability assessment of structure.

Results of the simulations are presented in Table 10.8 and Figure 10.15 for Tests 1-6. To examine the effects of taking into account the HSI, identical simulations were repeated for each test without taking into account the interaction effects (i.e. empty structure modal parameters were used in simulations instead of occupied structure modal properties). Results of these simulations are presented as ‘Non-interactive method’ in Table 10.8 and the corresponding stabilized CDFs are shown as green curves in Figure 10.15. Comparing the results in Table 10.8 and Figure 10.15, a significant difference can be seen between the interactive and non-interactive results.

Table 10.8. Statistical features of the ‘interactive’ and ‘non-interactive’ responses

	Interaction-based VSA method						Non-interactive method			
	a_{peak}	$a_{95\%}$	$a_{95\% \text{ min}}$	$a_{95\% \text{ max}}$	$a_{2.5\sigma}$	a_{rms}	a_{peak}	$a_{95\%}$	$a_{2.5\sigma}$	a_{rms}
Sheffield footbridge										
Test 1	0.280	0.091	0.060	0.125	0.098	0.041	0.607	0.167	0.181	0.072
Test 2	0.505	0.173	0.130	0.180	0.186	0.075	0.944	0.308	0.325	0.131
Test 3	0.673	0.186	0.150	0.190	0.207	0.087	0.907	0.377	0.415	0.174
Podgorica footbridge										
Test 4	1.218	0.397	0.300	0.440	0.426	0.172	1.703	0.548	0.589	0.239
Test 5	1.117	0.345	0.290	0.350	0.370	0.150	1.697	0.480	0.523	0.170
Test 6	0.963	0.341	0.270	0.370	0.376	0.155	1.638	0.560	0.622	0.256

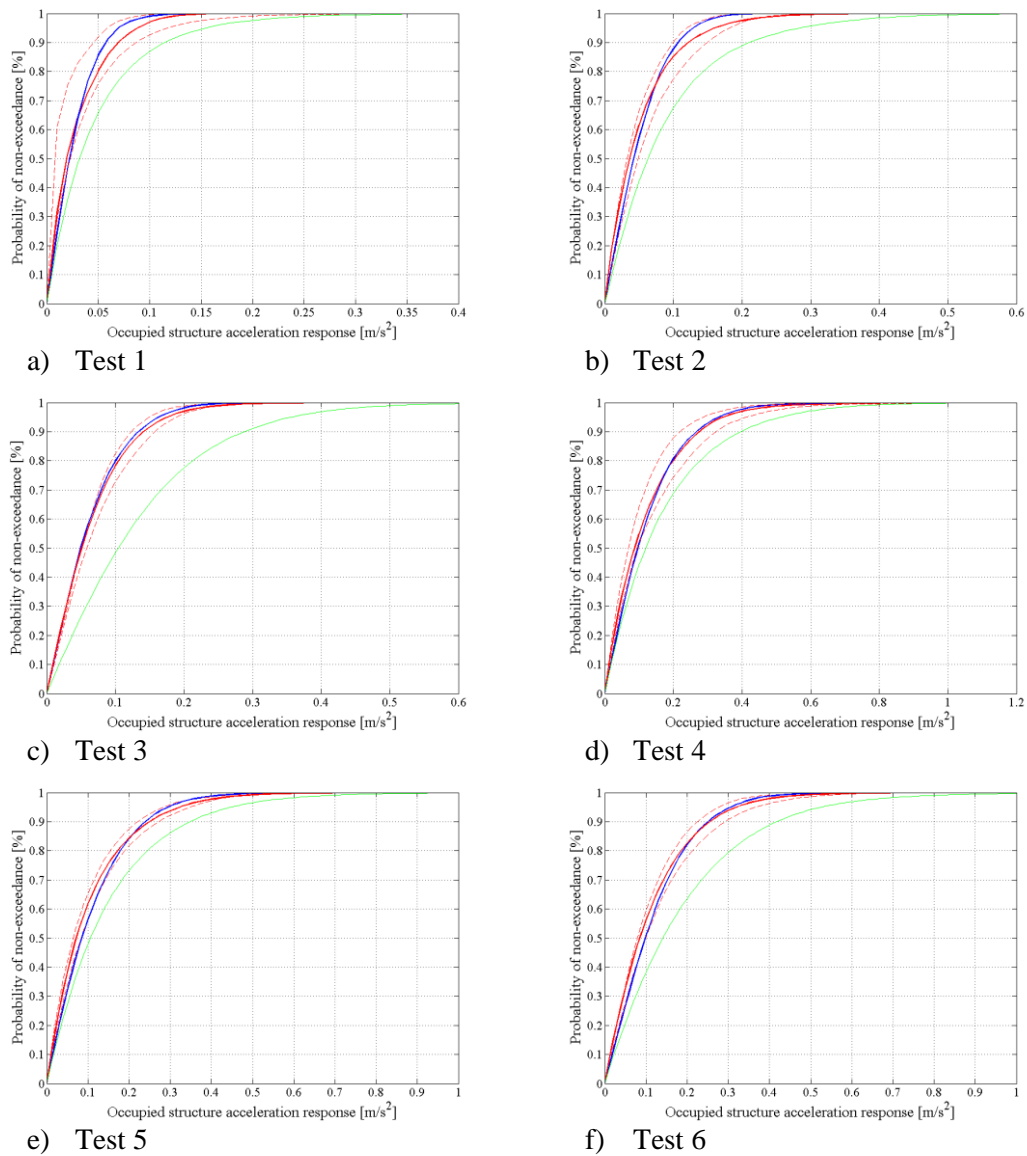


Figure 10.15. Comparison of experimental and analytical CDFs. Experimental (blue), envelope of analytical CDFs (dashed red), stabilized analytical CDF (red) and stabilized CDF of non-interactive model (green)

For each test, the stabilized CDF and the minimum and maximum envelope CDFs are plotted in Figure 10.15. As it can be seen in this figure, experimental CDF in all tests (blue curve) is within the predicted envelope CDF range (two dashed red curves). The estimated stabilized CDFs for Tests 4-6 are very close to their experimental counterparts as experimental CDFs of these tests were nearly stabilized (Section 10.3.2.2). Wide range of envelope CDFs in Tests 1 and 2 is the result of the limited number of people on structure and short duration of

tests which have increased the variety of traffic forces that can be generated. Close correlation between experimental and analytical results indicates good performance of the interaction-based VSA method in predicting response level on structure.

Although the non-interactive CDF takes into account all inter- and intra- subject variability and simulates loading scenarios realistically, it significantly over-estimates the response of both structures in all tests. This highlights the fact that even the most advanced statistical VSA methods cannot estimate the structural response accurately enough without taking into account the interaction of the walking people with the structure.

Stability of the response CDFs is checked in all tests by monitoring the variation of $a_{95\%}$, $a_{85\%}$, $a_{75\%}$ and $a_{50\%}$ during simulations. Values of $a_{95\%}$, $a_{85\%}$, $a_{75\%}$ and $a_{50\%}$ were recorded iteratively for a window of structural response where the duration of this window is increased by corresponding average crossing time in each iteration. For instance, for Tests 1-3, first 10.2 seconds of stabilized response (average crossing time) was initially selected. CDFs of the selected segment of response and the corresponding values of $a_{95\%}$, $a_{85\%}$, $a_{75\%}$ and $a_{50\%}$ were then calculated. In the next iteration, the length of the selected window of structural response was increased by 10.2 seconds to 20.4 seconds and the corresponding values of $a_{95\%}$, $a_{85\%}$, $a_{75\%}$ and $a_{50\%}$ were then found. This process was repeated until the whole 15 hours of the response was covered. Same analysis was done for Tests 4-6 unless the duration of window that was 75 seconds instead of 10.2 seconds.

A typical fluctuation of $a_{95\%}$, $a_{85\%}$, $a_{75\%}$ and $a_{50\%}$ is presented in Figure 10.16 for Tests 3 and 6. As it can be seen, statistical features of Test 3 CDF are satisfactorily stabilized after 25 iterations (equal to 255 seconds of simulation) whereas about 500 iterations (equal to 10.5 hours of simulation) was needed for response CDF of Tests 6 to stabilize. This observation supports our assertion in Section 10.3.2.2 that CDF of 44 minutes experimental response was not stabilized.

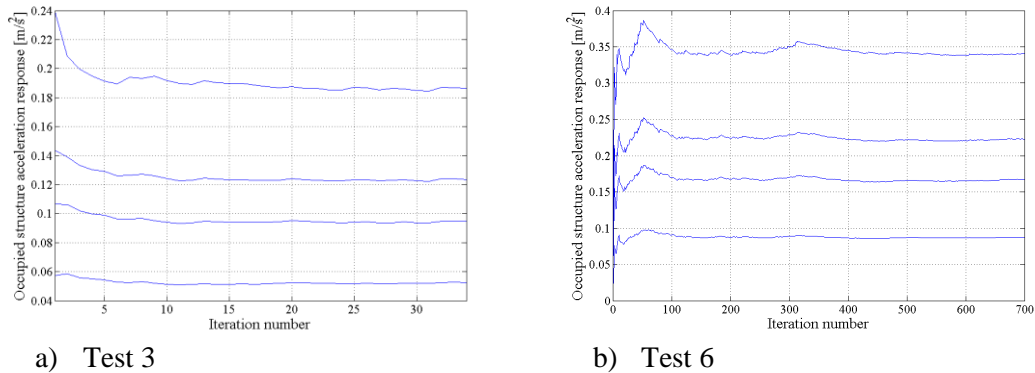
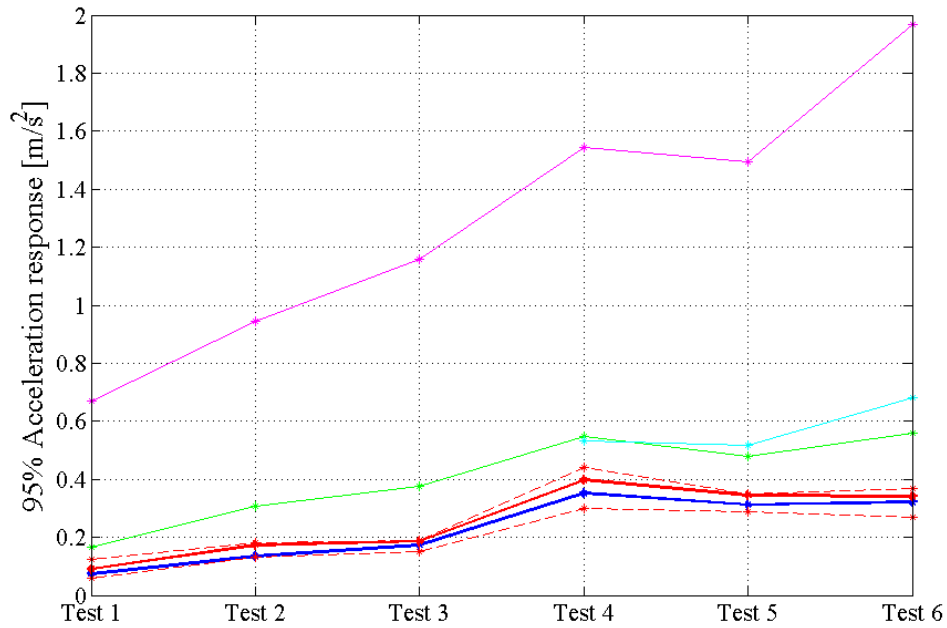


Figure 10.16. Typical fluctuation of acceleration response with 95%, 85%, 75% and 50% probability of non-exceedance (in order from top to bottom)

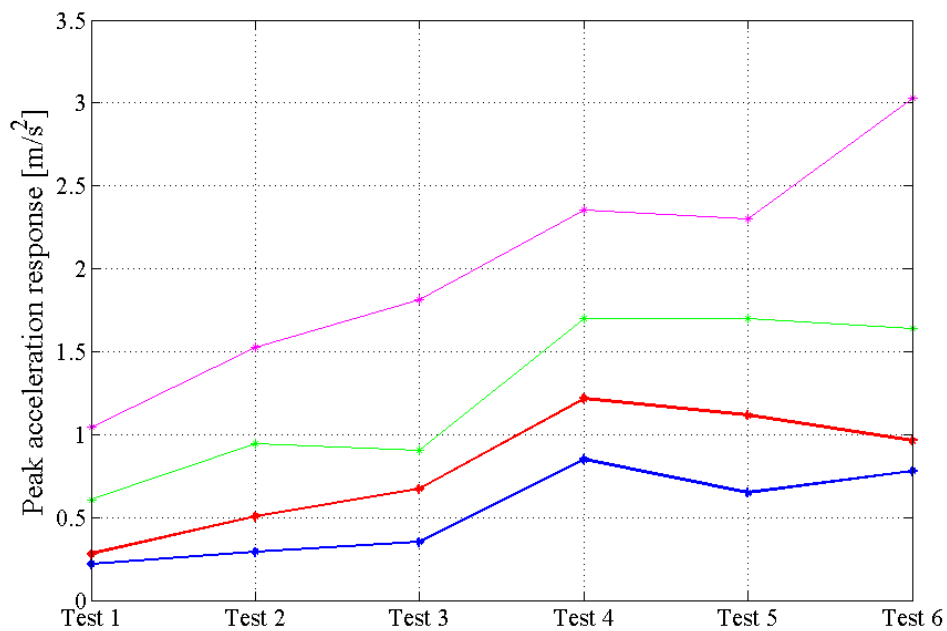
10.4.5 Comparison with design guidelines

This section compares the performance of the interaction-based VSA method with a number of currently available design guidelines. The ISO 10137 standard (2007), French road authorities standard (Setra, 2006), UK National Annex to Eurocode 1 (BSI, 2008) and method proposed by Butz (2006) have been selected for this analysis. For each test, input parameters of the design guidelines were selected in a way to simulate as best as possible (within the provision of the guideline) the corresponding walking traffic. Extensive discussion of selected guidelines and their shortcomings are presented by Shahabpoor and Pavic (2012) and Zivanovic, et al. (2010) and are not repeated here.

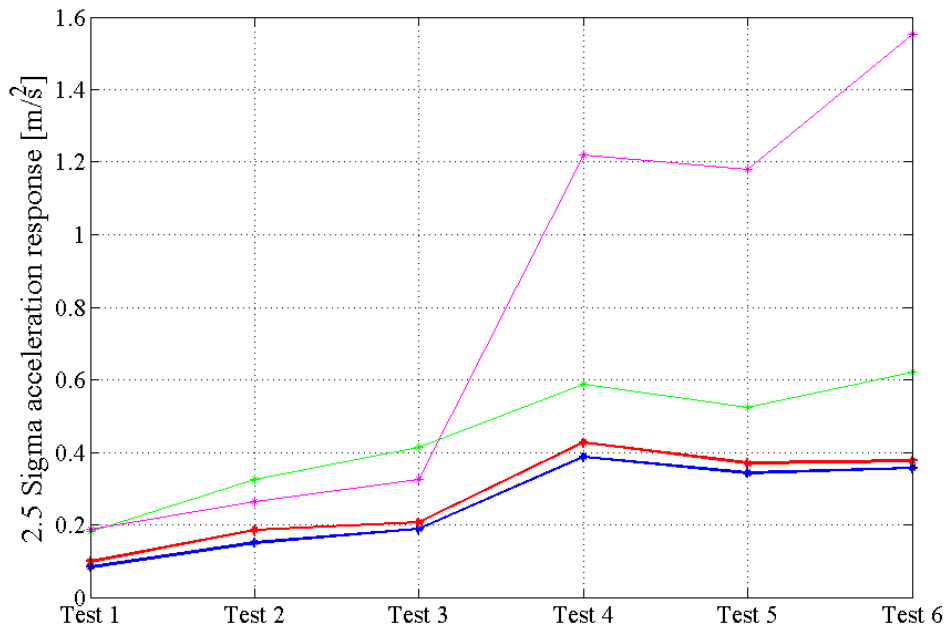
Figure 10.17 compares the performance of the interaction-based VSA method with the selected design guidelines. Setra and Butz methods use response magnitude with 95% probability of non-exceedance $a_{95\%}$ for assessment. ISO uses peak response and UK NA suggests mean response plus 2.5 times standard deviation ($a_{2.5\sigma}$) for serviceability assessment. The interaction-based VSA method results are also compared with non-interactive results for all tests.



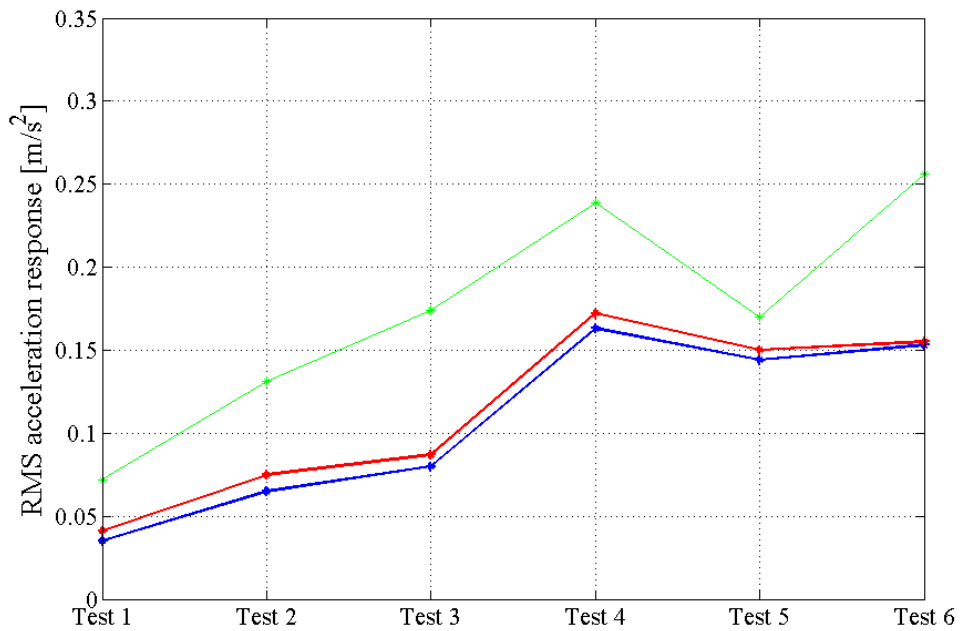
a) Comparison of acceleration response with 95% probability of non-exceedance - experimental (blue), interactive (red), non-interactive (green), Setra (magenta) and Butz (cyan)



b) Comparison of peak acceleration response - experimental (blue), interactive (red), non-interactive (green) and ISO (magenta)



c) Comparison of acceleration response with $\mu+2.5\sigma$ probability of non-exceedance - experimental (blue), interactive (red), non-interactive (green) and UK NA (magenta)



d) Comparison of acceleration response RMS - experimental (blue), interactive (red), and non-interactive (green)

Figure 10.17. Comparison of performance of the interaction-based VSA method with non-interactive, ISO, UK National Annex, Setra and Butz assessment methods

As it can be seen in Figure 10.17, accuracy of the interaction-based VSA method in predicting structural response is considerably higher than all other methods in all six tests. Comparing like with like, Setra, ISO, UK NA and Butz methods show 300-700%, 200-500%, 100-400% and 50-100% error in estimating structural response, respectively. This error range is 100-200% for non-interactive method. In comparison, the interaction-based VSA method results show maximum 10% error in estimating $a_{95\%}$, $a_{2.5\sigma}$ and a_{rms} and maximum 30% error in estimating peak acceleration a_{peak} .

10.5 Conclusions

This study used the interaction-based VSA method to simulate six vibration monitoring tests done on two real-world footbridge structure under different walking traffic. It was found that the interaction-based VSA method predicted the occupied structure modal frequency and damping ratio with less than 0.1% and 1% error, respectively. The comparison of the interaction-based VSA method results with those of a selection of current design guidelines showed that it has considerably reduced the error in predicting vibration response compared with the key internationally used design guidelines. Taking extensive experimental results as a benchmark, the error of the interaction-based VSA method was maximum 5-10%, comparing with 200-500% error made using the key design guidelines. The main improvements of the interaction-based VSA method have been the explicit consideration of the human-structure interaction and its ability to model realistic multi-pedestrian traffic. The findings of this research show the great performance of the interaction-based VSA method in accurate and realistic estimation of structural response under vertical walking load of a multi-pedestrian traffic.

Chapter 11

Conclusions and Recommendations for Future Work

11.1 Conclusions

The key findings of the research can be summarized as follows:

- The current design guidelines for predicting vibration of structures under multi-pedestrian walking traffic tend to overestimate the response due to their conservative assumptions, such as (Chapter 3):
 - neglecting human-structure interaction(s)
 - neglecting inter- and intra-subject variability of people,
 - using deterministic walking load,
 - assuming pedestrian's pacing frequency to be equal to the resonance frequency and
 - overestimating the level of traffic synchronization.
- In a coupled 2DOF human-structure system, when the natural frequency of the walking human SDOF model is less than the natural frequency of the empty structure, the occupied structure has slightly higher natural frequency than that of the empty structure. On the other hand, when the natural frequency of the human model is higher than the natural frequency of the empty structure, the natural frequency of the occupied structure is slightly lower than that of empty structure (Chapters 4 and 6).
- The damping ratio of the occupied structure increases by increasing the damping ratio of the human SDOF model. It is also dependent on the natural frequency of the occupied structure and its relationship with the natural frequency of the human SDOF model (Chapters 4 and 6).
- In a coupled 2DOF crowd-structure system (aggregated effects of crowd is simulated using a SDOF MSD model attached to the SDOF model of structure), when the natural frequency of the crowd model is lower than the natural frequency of the

empty structure, both natural frequency and damping ratio of the occupied structure are most sensitive to crowd's model stiffness. On the other hand, when the natural frequency of the crowd model is greater than the natural frequency of the empty structure, both the natural frequency and damping ratio of the occupied structure are most sensitive to crowd's model mass. It also can be seen that natural frequency of the occupied structure is not sensitive to damping of the crowd model while its damping ratio shows a limited sensitivity to the crowd's model damping being at maximum when both natural frequencies of the crowd and the occupied structure are equal (Chapter 5).

- Experimental studies showed that (Chapter 6):
 - Walking people can increase damping of occupied structure more than the standing people.
 - Results of tests focused on the second mode of a beam-like structure at 16.8Hz showed that crowd-structure interactions can affect the modes with frequencies far away from the crowd model fundamental frequency, indicating that MDOF model is possibly more appropriate modelling crowd.
 - The effects of crowd on the modal properties of the structure are at maximum when the natural frequencies of the crowd model and the empty structure are very close.
 - The effects of crowd on the occupied structure dynamic properties always increase as the number of people on the structure increases.
- The experimental data set used in this research can serve as a benchmark for data collection for multi-pedestrian HSI studies (Chapter 6).
- Normal distributions with $\mu=2.864$ Hz and $\sigma= 0.191$ Hz and $\mu=0.295$ and $\sigma= 0.023$ are good statistical models to describe the natural frequency and damping ratio of

SDOF MSD human model, respectively (Chapters 7 and 8).

- The agent-based model used in this study has been proven to be a powerful tool to take into account simultaneously different HSI types in multiple directions and with a desired level of detail. This makes ABM an ideal tool to simulate complex human models and multi-direction interaction mechanisms (Chapter 8).
- The interactive assessment method proposed in this study (termed the *interaction-based VSA method*) is the first of its kind that takes into account both variability of the walking people as well as their individualized interaction with the structure. This includes the level of vibration individually felt by each pedestrian at the location where they are, rather than the maximum level of structural vibration which may not be felt by any pedestrian not present at the location of maximum response at the time when it happens. The method can be used for different loading scenarios with any complexity and for different structures. The method shows acceptable low sensitivity to uncertain inputs as long as the human model frequency is not very close to the modal frequency of the structure (Chapter 9).
- The application of the interaction-based VSA method to estimating the response of two full-scale structures under multi-pedestrian walking traffic load has shown that it can predict the occupied structure modal frequency and damping ratio with less than 0.1% and 1% error, respectively. The comparison of the interaction-based VSA method performance with that of a selection of the current design guidelines showed that it can estimate the structural response considerably more accurately with maximum 10% error (30% error for peak acceleration) compared with the error of 200-500% when using design guidelines. These findings, together with the method's versatility and ease of use, demonstrate a considerable potential of the interaction-based VSA method to be adopted as the next generation of methods used in

vibration serviceability assessment of structures vibrating vertically under multi-pedestrian traffic (Chapter 10).

11.2 Recommendations for future work

One of the main shortcomings in this area of research is the lack of credible and comprehensive experimental data on the interaction of walking people with structures. Studying the underlying mechanisms of such interactions, more than anything, requires a comprehensive and accurate experimental data from crowds of people walking on real-life structures. Recording the time-history of every individual's interaction force, location and acceleration of different segments of the body in the crowd can open a new research avenue in this field. Having this data, the measured structural response, human body motion and interaction forces can all be correlated and their interaction can be studied in much more details.

The range of parameters identified in this research for the SDOF MSD walking human model need to be validated for different structures and different loading scenarios. The possibility of using more complex MDOF models (including biomechanical models) and their advantages and disadvantages need to be further explored in detail. If proved useful, parameters of these models need to be identified accurately for the vibration serviceability of pedestrian structures application.

Finally, the proposed interaction-based VSA method needs to be validated and refined for different structures and loading scenarios.

References

Agu, E. and Kasperski, M., 2011. Influence of the random dynamic parameters of the human body on the dynamic characteristics of the coupled system of structure–crowd. *Journal of Sound and Vibration*, 330(3), pp.431-444. ISSN 0022-460X.

Alexander, N. A., 2006. Theoretical treatment of crowd-structure interaction dynamics. *Proceeding of the ICE - Structures and Buildings*, 159(6), pp.329–338.

Allen, D.E. and Rainer, J.H., 1975. Floor vibration, NRCC, Canadian Building Digest (CBD) 173.

Archbold, P. J., 2004. Interactive Load Models for Pedestrian Footbridges. PhD thesis. National University of Ireland, University College Dublin.

Archbold, P., 2008. Evaluation of novel interactive load models of crowd loading on footbridges. *Proceedings of 4th Symposium on Bridge and Infrastructure Research in Ireland*, National University of Ireland, Galway, pp. 35-44.

Archbold, P. J., Keogh, J., Caprani, C., and Fanning, P., 2011. A Parametric Study of Pedestrian Vertical Force Models for Dynamic Analysis of Footbridges. *Proceeding of Experimental Vibration Analysis for Civil Engineering Structures Conference (EVACES 2011)*.

Bachmann, H., and Ammann, W., 1987. Vibrations in structures induced by man and machines. *International Association for Bridge and Structural Engineering (IABSE)*.

Barela, A.M.F. and Duarte, M., 2008. Biomechanical characteristics of elderly individuals Walking on land and on water. *Journal of Electromyography and Kinesiology*, 18(3), pp.446-454.

- Barker, M., 2006. A Survey on Agent-Based Modeling of Pedestrian Movement. ESI6532, Spring 2006.
- Barker, C., and Mackenzie, D., 2008. Calibration of the UK National Annex. The Proceedings of the Third Footbridge International Conference, Porto, Portugal.
- Baumann, K. and Bachmann, H., 1988. Durch Menschen verursachte dynamische Lasten und deren Auswirkungen auf Balkentragwerke (Man-induced dynamic loads and their influence on beam structures). Zürich, Switzerland: Institute of Structural Engineering (IBK), Swiss Federal Institute of Technology (ETH). Report 7501-3.
- Bertos, G., Childress, D. & Gard, S., 2005. The vertical mechanical impedance of the locomotor system during human walking with applications in rehabilitation, Proceeding of the 2005 IEEE Ninth International Conference on Rehabilitation Robotics.
- Bishop, N.W.M., Willford, M. and Pumphrey, R., 1993. Multi-person excitation of modern slender staircases. Engineering for crowd safety, London, UK, pp. 399-408.
- Bocian, M., Macdonald, J., and Burn, J., 2011. Modelling of self-excited vertical forces on structures due to walking pedestrians. Proceedings of the 8th International Conference on Structural Dynamics (EURODYN 2011) ISBN 978-90-760-1931-4.
- Bocian, M., Macdonald, J., and Burn, J., 2013. Biomechanically Inspired Modeling of Pedestrian-Induced Vertical Self-Excited Forces. Journal of Bridge Engineering 18, pp.1336–1346.
- British Standards Institution (BSI), 2008. UK national annex to Eurocode 1: Actions on structures. Part 2: Traffic loads on bridges, NA to BS EN 1991-2:2003 London.
- Brownjohn, J.M.W., Pavic, A. and Omenzetter, P. A., 2004a. Spectral density approach for

modeling continuous vertical forces on pedestrian structures due to walking. *Canadian Journal of Civil Engineering*, 31 (1), pp.65–77.

Brownjohn, J.M.W., Fok, P., Roche, M. and Omenzetter, P., 2004b. Long span steel pedestrian bridge at Singapore Changi Airport—part 2: crowd loading tests and vibration mitigation measures, *Structural Engineer*, 82 (16), pp.28–34.

Brownjohn, J.M.W., 2004. Vibration serviceability of footbridges. *The Second International Conference on Structural Engineering, Mechanics and Computation*, pp. 419-423.

Brownjohn, J.M.W., and Fu, T., 2005. Vibration Excitation and control of a pedestrian walkway by individuals and crowds. *Engineering and Technology, Civil and Structural Engineering and Electromagnetics and Mechanics*, 12(5).

Brownjohn, J.M.W., Zivanovic, S. and Pavic, A., 2008. Crowd dynamic loading on footbridges. In *proceedings of Footbridge conference*, 2008.

Butz, C., Feldmann, M. and Heinemeyer, C., 2008. Advanced load models for synchronous pedestrian excitation and optimized design guidelines for steel footbridges. RFSRCT- 2003-00019, European Commission, Brussels, Belgium.

Butz, C., 2006. Beitrag zur Berechnung fußgängerinduzierte Bruckenschwingungen. PhD Thesis (in German), ISBN-10 3-8322-5699-7, Shaker Verlag Aachen.

Butz, C., 2008a. A Probabilistic Engineering Load Model for Pedestrian Streams. In *Proceedings of the Third International Conference Footbridge 2008*, Porto, 2-4 July.

Butz, C., 2008b. Codes of Practice for Lively Footbridges: State-of-the-Art and Required Measures. In *Proceedings of the Third International Conference Footbridge 2008*, Porto, 2-4 July.

- Caprani, C. C., Keogh, J., Archbold, P., and Fanning, P., 2011. Characteristic vertical response of a footbridge due to crowd loading. *Proceeding of the 8th International Conference on Structural Dynamics (Eurodyn 2011)*, pp.978–985.
- Caprani, C.C., Keogh, J., Archbold, P. and Fanning, P., 2012. Enhancement factors for the vertical response of footbridges subjected to stochastic crowd loading. *Computer and Structures* 102–103, pp.87–96.
- Caprani, C.C., 2014. Application of the pseudo-excitation method to assessment of walking variability on footbridge vibration. *Computers and Structures* 132, pp. 43–54.
- Carroll, S.P., 2013. Crowd-induced lateral bridge vibration. PhD thesis, University of Nottingham.
- Curtis, J., 2001. Letter: Pedestrians can contribute to lock-in. *New Civil Engineer (ICE)* 8 March 2001: 18.
- Dang, H. V. and Zivanovic, S., 2013. Modelling Pedestrian Interaction with Perceptibly Vibrating Footbridges. *FME Transactions*, 41 (4), pp. 271-278.
- Dong, W., Kasperski, M. and Shiqiao, G., 2011. Change of dynamic characteristics of a pedestrian bridge during a mass event. *Proceedings of the 8th International Conference on Structural Dynamics (EURODYN 2011)*. ISBN 978-90-760-1931-4.
- Dougill, J. W., Wright, J. R., Parkhouse, J. G. & Harrison, R. E., 2006. Human structure interaction during rhythmic bobbing, *The Structural Engineer*, 84(22).
- Ebrahimpour, R.L., Sack, P.D., Van Cleek, 1989. Computing Crowd Loads using a Nonlinear Equation of Motion. *Proceedings of the Fourth International Conference on Civil and Structural Engineering Computing*, Civil-Comp Press, Edinburgh, UK, pp. 47-52.

doi:10.4203/ccp.9.11.3

Ebrahimpour, A. and Sack, R.L., 1992. Design live loads for coherent crowd harmonic movements. *Journal of Structural Engineering (ASCE)*, 118(4), pp. 1121-36.

Ebrahimpour, A. and Sack, R.L., 1996. Design Live Loads for Crowds in Motion. Conference proceeding of Building an International Community of Structural Engineers, ASCE, 1, pp. 420-427.

Ebrahimpour, A., Hamam, A., Sack, R.L. and Patten, W.N., 1996. Measuring and modeling dynamic loads imposed by moving crowds. *ASCE Journal of Structural Engineering*, 122(12), pp. 1468 – 1474.

Ellis, B.R. and Ji, T., 1994. Floor vibration induced by dance-type loads: verification. *The Structural Engineer*, 72 (3), pp. 45–50.

Ellis, B.R. and Ji, T., 1997. Human-structure interaction in vertical vibrations. *Structures of buildings, the proceeding of Civil engineers* 122(1), pp.1-9.

Ellis, B.R. and Ji, T., 2003. Understanding the interaction between people and structures. *The structural engineers*, 81(14), pp.12-13.

EN, 2004. Eurocode 5: Design of timber structures – Part 2: Bridges, EN 1995-2:2004, European Committee of Standardization.

Fanning, P., Archbold, P. and Pavic, A., 2005. A Novel interactive Pedestrian load model for Flexible Footbridges. *Proceeding of the 2005 Society for Experimental Mechanics Annual Conference on Experimental and Applied Mechanics*, Portland, Oregon, June 7-9.

Fanning, P., Healy, P. and Pavic, A., 2010. Pedestrian Bridge Vibration Serviceability: A Case Study in Testing and Simulation. *Advances in Structural Engineering*, (13)5.

Ferris, D. P., Louie, M. and Farley, C. T., 1998. Running in the real world: adjusting leg stiffness for different surfaces. *Proc. R. Soc. London B* 265, pp. 989-994.

The International Federation for Structural Concrete (FIB), 2005. Guidelines for the design of footbridges.

Figueiredo, F.P., da Silva, J.G.S., de Lima, L.R.O., da S. Vellasco, P.C.G. and de Andrade, S.A.L., 2008. A parametric study of composite footbridges under pedestrian walking loads. *Engineering Structures*, 30, pp. 605–615.

Fitzpatrick, A., Dallard, P., le Bourva, S., Low, A., Ridsill Smith, R. and Willford, M., 2001. *Linking London: The Millennium Bridge*, The Royal Academy of Engineering, London.

Frazer, R.A., Duncan, W.J. and Collar, A.R., 1957. *Elementary Matrices*. Cambridge University Press.

Fujino, Y., Pacheo, B.M., Nakamura, S.I. and Warnitchai, P., 1993. Synchronisation of human walking observed during lateral vibration of a congested pedestrian bridge. *Earthquake Engineering and Structural Dynamics*, 22(9), pp. 741-58.

Georgakis, C.T. and Jorgensen, N.G., 2013. Change in mass and damping on vertically vibrating footbridges due to pedestrians. *Proceedings of the 31st Conference on Structural Dynamics (IMAC 2013)* 3(4), pp.37-45.

Geyer, H., Seyfarth, A., Blickhan, R., 1998. Compliant leg behavior explains basic dynamics of walking and running, *Proc. of the Royal Society B: Biological Sciences*, 273(1603), pp. 2861–2867.

Griffin, M. J., 1990. *Handbook of human vibration*, Academic Press, London.

Grimm, V., Berger, U., Bastiansen, F., Eliassen, S., Ginot, V., Giske, J., Goss-Custard, J., Grand, T., Heinz, S.K., Huse, G., Huth, A., Jepsen, J.U., Jørgensen, C., Mooij, W.M., Muller, B., Pe'er, G., Piou, C., Railsback, S.F., Robbins, A.M., Robbins, M.M., Rossmanith, E., Ruger, N., Strand, E., Souissi, S., Stillman, R.A., Vabo, R., Visser, U., DeAngelis, D.L., 2006. A standard protocol for describing individual-based and agent-based models. *Ecological Modelling*, 198(1–2), pp.115–126.

Grundmann, H. and Schneider, M., 1990. Stochastic representation of Footbridge Vibrations Taking into Account Feedback Effects. In proceeding of European Conference on Structural Engineering, Eurodyn '90, Bochum, Balkema, Rotterdam.

Grundmann, H., Kreuzinger, H. and Schneider, M., 1993. Dynamic calculations of footbridges. *Bauingenieur*, 68 (1993), pp. 215–225 (in German).

Gustafsson, L., Sternad, M., 2010. Consistent micro, macro, and state-based population modelling. *Mathematical Biosciences*, 225, pp. 94–107.

Hamam, A.S., 1994. Measuring and modelling dynamic loads imposed by moving crowds. Thesis (PhD). University of Oklahoma, Norman, USA.

Harrison, R., Yao, S., Wright, J., Pavic, A., and Reynolds, P., 2008. Human Jumping and Bobbing Forces on Flexible Structures: Effect of Structural Properties. *Journal of Engineering Mechanics*, 134(8), 663–675.

Hinz, B. and Seidel, H., 1987. The non-linearity of the human body's dynamic response during sinusoidal whole body vibration. *Industrial Health*, 25(4), pp.169-81.

Ingólfsson, E. T., Georgakis, C. T., and Svendsen, M. N., 2008. Vertical footbridge vibrations: Details regarding and experimental validation of the response spectrum methodology. Proceeding of Footbridge conference.

Ingólfsson, E. T., Georgakis, C. T., Ricciardelli, F., and Jönsson, J., 2011. Experimental identification of pedestrian-induced lateral forces on footbridges. *Journal of Sound and Vibration*. 330(6), pp.1265–1284.

Institution of Structural Engineers (ISE), 2001. Dynamic performance requirements for permanent grandstands subject to crowd action: Recommendations for management, design and assessment, London.

International Organization for Standardization (ISO), 1981. Mechanical driving point impedance of the human body. ISO 5982:1981.

International Organization for Standardization (ISO), 2007. Bases for design of structures: Serviceability of buildings and walkways against vibrations. ISO 10137:2007, Geneva.

IStructE/DCLG/DCMS Joint Working Group, Dynamic Performance Requirements for Permanent Grandstands: Recommendations for Management Design and Assessment, Institution of Structural Engineers, London, 2008.

Jennings, N.R., Sycra, K., Wooldridge, M., 1998. A Roadmap of Agent Research and Development. *International Journal of Autonomous Agents and Multi-Agent Systems*, 1(1), pp.7-38.

Ji, T., 2000. On the combination of structural dynamics and biodynamics methods in the study of human-structure interaction. The 35th UK Group Meeting on Human Response to Vibration, Institute of Sound and Vibration Research, University of Southampton, England, September 13–15, 2000, 1, pp. 183–194.

Jones, C. A., Pavic, A., Reynolds, P. and Harrison, R.E., 2011a. Verification of equivalent mass-spring-damper models for crowd-structure vibration response prediction. *Canadian*

Journal of Civil Engineering Structures, NRC Research Press. 38(10), pp. 1122-1135, ISSN 0141-0296.

Jones, C.A., Reynolds, P. and Pavic, A., 2011b. Vibration serviceability of stadia structures subjected to dynamic crowd loads: A literature review. *Journal of Sound and Vibration*, 330(8), pp.1531-1566.

Kasperski, M. and Niemann, H.J., 1993. Man induced vibrations of a stand structure. In proceeding of EUROLYN'93 conference, Trondheim, Norway, pp. 977-983.

Kasperski M, Sahnaci C., 2007. Serviceability of pedestrian structures. Proceedings of the 25th international modal analysis conference, Orlando, Florida. pp.774–98.

Kerr, S.C., 1998. Human Induced Loading on Staircases, PhD Thesis, Mechanical Engineering Department, University College London, UK.

Kramer, H. and Kebe, H., 1980. Man-induced structural vibrations. *Der auingenieur*, 54(5), 195–199.

Krenk S., 2012. Dynamic response to pedestrian loads with statistical frequency distribution. *ASCE Journal of Engineering Mechanics*, 138(10), pp.1275–81.

Kim, S. H., Cho, K. I., Choi, M. S., and Lim, J. Y., 2008. Development of human body model for the dynamic analysis of footbridges under pedestrian induced excitation. *International Journal of Steel Structures*, 8(4), pp.333–345.

Lee, C. and Farley, C., 1998. Determinants of the center of mass trajectory in human walking and running. *The Journal of Experimental Biology*, 201, pp. 2935-2944.

Máca, J. and Valášek, M., 2011. Interaction of Human Gait and Footbridges. Proceedings of the 8th International Conference on Structural Dynamics, EUROLYN 2011.

- Macy, M.W. and Willer, R., 2002. From Factors to Actors :Computational Sociology and Agent-Based Modeling. *Annual Sociology Review*, 28, pp.143-66.
- Mansfield, N.J. and Griffin, M.J., 2000. Non-linearities in apparent mass and transmissibility during exposure to whole-body vertical vibration. *Journal of Biomechanics*, 33(8), pp. 933-41.
- Matsumoto, Y., Nishioka, T., Shiojiri, H. and Matsuzaki, K., 1978. Dynamic design of footbridges. *IABSE Proceedings*, 2, Paper P-17/78, Zurich.
- Matsumoto, Y. and Griffin, M.J., 1998. Dynamic response of the standing human body exposed to vertical vibration: Influence of posture and vibration magnitude. *Journal of Sound and Vibration* 212(1), pp. 85-107.
- McRobie, A., Morgenthal, G., Lasenby, J. and Ringer, M., 2003. Section model tests on human – structure lock-in. *Proceedings of the ICE - Bridge Engineering*, Volume 156(2), pp. 71 –79.
- Miyamori, Y., Obata, T., Hayashikawa, T., Sato, K., 2001. Study on identification of human walking model based on dynamic response characteristics of pedestrian bridges, in: *Proceedings of the Eighth East Asia-Pacific Conference on Structural Engineering & Construction (EASEC-8)*, Singapore.
- Mohanty, P. and Reynolds, P., 2006. Modelling of Dynamic Crowd-Structure Interactions in a Grandstand During a Football Match. *Proceeding of 24th International Modal Analysis Conference (IMAC XXIV)*.
- Mottershead, J.E., 1996. *Identification in Engineering Systems*. Swansea, UK, pp. 648-57.
- Nyawako, D., Reynolds, P., 2000. Active Control of Human Induced Floor Vibrations. In the

proceeding of International IMAC Conference, Society for Experimental Mechanics (SEM), Jacksonville, Florida.

Ohlsson, S., 1982. Floor vibrations and human discomfort. Thesis (PhD). Chalmers University of Technology, Gothenburg, Sweden.

Pachi, A. and Ji, T., 2005. Frequency and velocity of people walking. *The Structural Engineer*, 83(3), pp. 36–40.

Pavic, A. and Reynolds, P., 2008. Experimental verification of novel 3DOF model for grandstand crowd-structure dynamic interaction. The proceeding of 26th International Modal Analysis Conference (IMAC XXVI).

Pavic, A., 2011. Vertical crowd dynamic action on footbridges: review of design guidelines and their application, *Proceedings of Footbridge 2011*.

Paulissen, J.H. and Metrikine. A.V., 2011. Non-linear dynamic modelling of adaptive pedestrian behavior on lively footbridges. *Proceedings of the 8th International Conference on Structural Dynamics (EURODYN 2011)*.

Pecol, P., Dal Pont, S., Silvano, E., Joanna, B. and Argoul, P., 2011. A 2D discrete model for crowd-structure interaction. *Proceeding of the 4th Footbridges international conference*.

Piccardo, G. and Tubino, F., 2012. Equivalent spectral model and maximum dynamic response for the serviceability analysis of footbridges. *Engineering Structures*, 40(7), pp.445–56.

Pimentel, R. L. and Waldron, P., 1996. Validation of the numerical analysis of a pedestrian bridge for vibration serviceability applications. *International Conference on Identification in Engineering Systems*, pp. 648-657, Swansea, UK, March.

- Pimentel, R.L., 1997. Vibration performance of pedestrian bridges due to human-induced loads. Thesis (PhD). University of Sheffield, Sheffield, UK.
- Pimentel, R.L., Pavic, A., and Waldron, P. 2001. Evaluation of design requirements for footbridges excited by vertical forces from walking. *Canadian Journal of Civil Engineering*, 28(5), pp. 769–777. doi:10.1139/101-036.
- Portier, K., Tolson, J.K., and Roberts, S.M., 2007. Body weight distributions for risk assessment. *Risk Analysis*, 27(1), pp. 11-26.
- Qin, J.W., Law, S.S., Yang, Q.S. and Yang, N., 2013. Pedestrian–bridge dynamic interaction, including human participation. *Journal of Sound and Vibration*, 332(4), pp.1107-1124, ISSN 0022-460X, <http://dx.doi.org/10.1016/j.jsv.2012.09.021>.
- Racic, V., Pavic, A., and Brownjohn, J. M. W., 2009. Experimental identification and analytical modelling of human walking forces: Literature review. *Journal of Sound and Vibration*, 326(1–2), pp.1–49.
- Racic, V. and Brownjohn, J.M.W., 2011. Stochastic model of near-periodic vertical loads due to humans walking. *Advanced Engineering Informatics*, 25, pp.259–75.
- Rapoport, S., Mizrahi, J., Kimmel, E., Verbitsky, O. & Isakov, E., 2003. Constant and variable stiffness and damping of the leg joints in human hopping, *Journal of Biomechanical Engineering*, ASME, 125, pp. 507-514.
- Reynolds, P., 2000. The effects of raised access flooring on the vibrational performance of long-span concrete floors. PhD Thesis, University of Sheffield, UK, February 2000.
- Reynolds, P., Pavic, A. and Ibrahim, Z., 2004. Changes of Modal properties of a stadium structure occupied by a crowd. *Proceeding of the 22nd International Modal Analysis*

Conference (IMAC XXII).

Sachse, R., 2002. The Influence of Human Occupants on the Dynamic Properties of Slender Structures, PhD Thesis, University of Sheffield, Sheffield, UK.

Sachse, R., Pavic, A. and Reynolds, P., 2002. The Influence of a Group of Human Occupants on Modal Properties of a Prototype Assembly Structure. Proceeding of the 5th European Conference on Dynamics EURODDYN, pp.1241-1246.

Sachse, R., Pavic, A. and Reynolds, P., 2003. Human-structure dynamic interaction in civil engineering dynamics: A literature review. The Shock and Vibration Digest, 35 (1), pp. 3-18. ISSN 0583-1024.

Sachse, R., Pavic, A. and Reynolds, P., 2004. Parametric study of modal properties of damped two-degree-of-freedom crowd-structure dynamic systems. Journal of Sound and Vibration, 274, pp. 461-480.

Salyards, K. and Firman, R., 2011. Human-structure interaction effects of crowd characteristics. Conference Proceedings of the Society for Experimental Mechanics Series, Civil Engineering Topics, 4, pp 247-254.

Setra, 2006. Assessment of vibrational behavior of footbridges under pedestrian loading. Technical guide. Service d'Etudes Techniques des Routes et Autoroutes, Paris.

Silva, F.T., and Pimentel, R. L., 2011. Biodynamic walking model for vibration serviceability of footbridges in vertical direction. Proceeding of the 8th International Conference on Structural Dynamics (Eurodyn 2011), pp.1090-1096.

Silva, F.T. Brito, H.M. and Pimentel. R.L., 2013. Modeling of crowd load in vertical direction using biodynamic model for pedestrians crossing footbridges. *Canadian Journal of Civil Engineering*, 40, pp.1196–1204. <http://dx.doi.org/10.1139/cjce-2011-0587>

Shahabpoor, E., Pavić, A., 2012. Comparative evaluation of current pedestrian traffic models on structures. *Conference Proceedings of the Society for Experimental Mechanics Series. V 26*, pp 41-52.

Shahabpoor, E., Pavić, A. & Racic, V., 2013a. Using MSD Model to Simulate Human-Structure Interaction during Walking. *Conference Proceedings of the Society for Experimental Mechanics Series.*

Shahabpoor, E., Pavić, A. & Racic, V., 2013b. Sensitivity Analysis of Coupled Crowd-structure System dynamics to Walking Crowd Properties. *Conference Proceedings of The Fifth International Conference on Structural Engineering, Mechanics and Computation (SEMC 2013).*

van Staalduinen, P. and Courage, W., 1994. Dynamic loading of Feyenoord stadium during pop concerts. in *Symposium: Places of Assembly and Long-Span Building Structures*, Birmingham, UK, 7-9 September, 1994. Zürich, Switzerland: IABSE. Report 71, pp. 283-8.

Technical Department for Transport, Roads and Bridges Engineering and Road Safety/French Association of Civil Engineering (SETRA/AFGC), 2006. *Footbridges: Assessment of vibrational behavior of footbridges under pedestrian loading. Technical Guide 0611*, Paris.

Tredgold, T., 1828. *Elementary principles of carpentry*. 2nd edition.

Walley, F., 1959. St James's Park Bridge. In *proceedings of the ICE 12(6297)*, pp. 217-22.

Willford, M., 2002. Dynamic actions and reactions of pedestrians. In proceedings of the International Conference on the Design and Dynamic Behaviour of Footbridges, Paris, France, November 20–22, 2002, pp. 66–73.

Williams, C., Rafiq, M.Y. and Carter, A., 1999. Human structure interaction: the development of an analytical model of the human body. In proceeding of the International Conference of Vibration, Noise and Structural Dynamics '99, Venice, Italy, April, pp. 32–39.

Yao, S., Wright, J.R., Pavic, A. and Reynolds, P., 2006. Experimental Study of Human-Structure Interaction for Jumping on a Perceptibly Moving Structure. *Journal of Sound and Vibration*, 296, pp.150-165. ISSN 0022-460X.

Zhang, L., Xu, D., Makhsous, M. & Lin, F., 2000. Stiffness and viscous damping of the human leg, *Proceedings of the 24th Annual Meeting of the American Society of Biomechanics*.

Zheng, X., and Brownjohn, J.M.W., 2001. Modelling and simulation of human-floor system under vertical vibration. In proceedings of SPIE conference, *Smart Structures and Materials*, Newport Beach, CA, USA, 4327, pp. 513–520.

Zivanovic, S., Pavic, A. and Reynolds, P., 2005a. Human-Structure Dynamic Interaction in Footbridges. *Institution of Civil Engineers*. In proceedings of *Bridge Engineering conference*, 158 (4), pp. 165 - 177 (1478-4629).

Zivanovic, S., Pavic, A. and Reynolds, P., 2005b. Vibration serviceability of footbridges under human-induced excitation: a literature review. *Journal of Sound and Vibration*, 279(1–2), pp.1-74. ISSN 0022-460X. <http://dx.doi.org/10.1016/j.jsv.2004.01.019>.

- Zivanovic S., 2006. Probability-based estimation of vibration for pedestrian structures due to walking, PhD Thesis, Department of Civil and Structural Engineering, University of Sheffield.
- Zivanovic, S., Pavic, A. and Reynolds, P., 2007. Probability-based prediction of multi-mode vibration response to walking excitation. *Engineering Structures* 29(6), pp.942–54.
- Živanović, S., Diaz, I.M. and Pavić, A., 2009. Influence of walking and standing crowds on structural dynamic properties. *Proceeding of Conference & Exposition on Structural Dynamics (IMAC XXVII)*.
- Živanović, S. and Pavic, A., 2009. Probabilistic modelling of walking excitation for building floors. *Journal of Performance of Constructed Facilities* 23 (3), pp.132 – 143.
- Živanović, S., Pavic, A. and Ingolfsson, E. T., 2010. Modeling spatially unrestricted pedestrian traffic on footbridges. *Journal of Structural Engineering* 136 (10), pp.1296 – 1308.
- Živanović, S. and Pavic, A., 2011. Quantification of dynamic excitation potential of pedestrian population crossing footbridges. *Shock & Vibration* 18 (4), pp.563 – 577.
- Živanović, S., 2012. Benchmark footbridge for vibration serviceability assessment under vertical component of pedestrian load. *Journal of Structural Engineering*, 138 (10), pp.1193 – 1202.

Appendix I

The below table shows the relation between the tests being referred to in Chapters 6-10.

No.	Mode of structure	Location of peds	Number of peds	Test reference Chapter 6	Test reference Chapter 7	Test reference Chapter 8	Test reference Chapter 10
Mode 1 tests							
1	1	All-over	0	1.1	-	-	-
2	1	All-over	0	1.2	-	-	-
3	1	All-over	2	1.3	1.1	1.1	-
4	1	All-over	3	1.4	1.2	1.2	-
5	1	All-over	4	1.5	1.3	1.3	-
6	1	All-over	6	1.6	1.4	1.4	-
7	1	All-over	6	1.7	1.5	1.5	-
8	1	All-over	10	1.8	1.6	1.6	-
9	1	All-over	10	1.9	1.7	1.7	-
10	1	All-over	15	1.10	1.8	1.8	-
11	1	Mid-span	3	1.11	1.1C	-	-
12	1	Mid-span	6	1.12	1.2C	-	-
13	1	Mid-span	10	1.13	1.3C	-	-
14	1	3/8 span	6	1.14	1.4C	-	-
15	1	¼ span	6	1.15	1.5C	-	-
16	1	All-over	3	-	-	-	Test 1
17	1	All-over	6	-	-	-	Test 2
18	1	All-over	10	-	-	-	Test 3
Mode 2 tests							
19	2	All-over	0	2.1	-	-	-
20	2	All-over	0	2.2	-	-	-
21	2	All-over	3	2.3	2.1	2.1	-
22	2	All-over	6	2.4	2.2	-	-
23	2	All-over	6	2.5	2.3	2.2	-
24	2	All-over	8	2.6	2.4	-	-
25	2	All-over	10	2.7	2.5	-	-
26	2	All-over	10	2.8	2.6	2.3	-
27	2	All-over	15	2.9	2.7	-	-
28	2	¼ span	3	2.10	2.1C	-	-
29	2	¼ span	6	2.11	2.2C	-	-
30	2	¼ span	10	2.12	2.3C	-	-